NUREG/CR-5745
EGG-2650

Assessment of ISLOCA Risk-Methodology and Application to a Combustion Engineering Plant

Prepared by
D. T. Kelly, J. L. Auflick, L. N. Haney

Idaho National Engineering Laboratory
EG&G Idaho, Inc.

Prepared for
U.S. Nuclear Regulatory Commission

AVAILABILITY NOTICE

Availability of Reference Materials Cited in NRC Publications

Most documents cited in NRC publications will be available from one of the following sources:

1. The NRC Public Document Room, 2120 L Street, NW., Lower Level, Washington, D.C. 20555

2. The Superintendent of Documents, U.S. Government Printing Office, P.O. Box 37082, Washington, DC 20013-7082

3. The National Technical Information Service, Springfield, VA 22161

Although the listing that follows represents the majority of documents cited in NRC publications, it is not intended to be exhaustive.

Referenced documents available for inspection and copying for a fee from the NRC Public Document Room include NRC correspondence and internal NRC memoranda; NRC bulletins, circulars, information notices, inspection and investigation notices; licensee event reports; vendor reports and correspondence; Commission papers; and applicant and licensee documents and correspondence.

The following documents in the NUREG series are available for purchase from the GPO Sales Program: formal NRC staff and contractor reports, NRC-sponsored conference proceedings, international agreement reports, grant publications, and NRC booklets and brochures. Also available are regulatory guides, NRC regulations in the *Code of Federal Regulations*, and *Nuclear Regulatory Commission Issuances*.

Documents available from the National Technical Information Service include NUREG-series reports and technical reports prepared by other Federal agencies and reports prepared by the Atomic Energy Commission, forerunner agency to the Nuclear Regulatory Commission.

Documents available from public and special technical libraries include all open literature items, such as books, journal articles, and transactions. *Federal Register* notices, Federal and State legislation, and congressional reports can usually be obtained from these libraries.

Documents such as theses, dissertations, foreign reports and translations, and non-NRC conference proceedings are available for purchase from the organization sponsoring the publication cited.

Single copies of NRC draft reports are available free, to the extent of supply, upon written request to the Office of Administration, Distribution and Mail Services Section, U.S. Nuclear Regulatory Commission, Washington, DC 20555.

Copies of industry codes and standards used in a substantive manner in the NRC regulatory process are maintained at the NRC Library, 7920 Norfolk Avenue, Bethesda, Maryland, for use by the public. Codes and standards are usually copyrighted and may be purchased from the originating organization or, if they are American National Standards, from the American National Standards Institute, 1430 Broadway, New York, NY 10018.

DISCLAIMER NOTICE

NUREG/CR-5745
EGG-2650
RG, 1S, 9L

Assessment of ISLOCA Risk-Methodology and Application to a Combustion Engineering Plant

Manuscript Completed: March 1992
Date Published: April 1992

Prepared by
D. L. Kelly, J. L. Auflick, L. N. Haney

Idaho National Engineering Laboratory
Managed by the U.S. Department of Energy

EG&G Idaho, Inc.
Idaho Falls, ID 83415

Prepared for
Division of Safety Issue Resolution
Office of Nuclear Regulatory Research
U.S. Nuclear Regulatory Commission
Washington, DC 20555
NRC FIN B5699
Under DOE Contract No. DE-AC7-76ID01570

ABSTRACT

Inter-system loss-of-coolant accidents (ISLOCAs) have been identified as important contributors to offsite risk for some nuclear power plants. A methodology has been developed for identifying and evaluating plant-specific hardware designs, human factors issues, and accident consequence factors relevant to the estimation of ISLOCA core damage frequency and risk. This report presents a detailed description of the application of this analysis methodology to a Combustion Engineering plant.

CONTENTS

LIST OF FIGURES

LIST OF TABLES

EXECUTIVE SUMMARY

Inter-system loss-of-coolant accidents (ISLOCAs) have been identified in some probabilistic risk assessments (PRAs) as major contributors to offsite risk at nuclear power plants (NPPs). They have the potential to result in core damage and containment bypass, which may lead to the early release of large quantities of fission products to the offsite environment. Recent events at several operating reactors have been identified as ISLOCA precursors. These events have raised concerns over the frequency of occurrence, plausible initiators, and means of identifying and mitigating this potential accident. In response to these concerns, a June 7, 1989, memorandum, "Request for Office of Nuclear Regulatory Research (RES) Support for Resolution of the ISLOCA Issue," was transmitted from Dr. Thomas E. Murley to Dr. Eric S. Beckjord. The ISLOCA research program described in this report was initiated in response to this memorandum.

The objective of the ISLOCA research program is to provide the U.S. Nuclear Regulatory Commission with qualitative and quantitative information on the hardware, human factors, and accident consequence issues that contribute to ISLOCA risk. To meet this objective, a methodology has been developed to estimate the core damage frequency (CDF) and offsite consequences associated with an ISLOCA, and this methodology is being applied to individual NPPs. This report describes the ISLOCA methodology and the results of its application to a Combustion Engineering (CE) NPP.

An eight-step methodology was developed to evaluate the ISLOCA issue qualitatively and quantitatively. These steps and their relationships to one another are shown in Figure ES-1. This methodology was applied to a CE plant by a team of PRA and human factors specialists. The important results, *specific to this plant*, are

1. Human errors that could occur during startup and shutdown of the plant were not found to be significant contributors to ISLOCA CDF and risk.

2. ISLOCA sequences initiated by hardware failures were the dominant contributors to CDF and risk.

3. Isolation of the break would be an important recovery action during an ISLOCA. Refueling water storage pool makeup capacity is insufficient to maintain an adequate reactor coolant inventory for breaks outside the containment that are larger than approximately 1 inch in diameter. The analysis indicates that hardware would be available to isolate these ISLOCA breaks; however, post-break procedures are not available to ensure that this hardware is used in all sequences.

4. At the time of the plant visit, a general survey was made of the interfacing system flow paths to qualitatively estimate the impact on equipment of ruptures in various locations. This survey could not verify that the emergency core cooling systems (ECCS) are adequately separated such that any postulated rupture would not affect redundant ECCS trains. This issue is still under study at the Idaho National Engineering Laboratory.

5. It appears that relatively simple changes to procedures and training could reduce ISLOCA risk substantially by reducing the initiator frequency and increasing the likelihood of successfully isolating an intersystem break.

6. The ISLOCA methodology has been successful in providing important insights on the relative contribution of both hardware faults and human actions to ISLOCA CDF and risk. In particular, the extensive task analysis performed as part of the human reliability analysis provided many valuable insights that would have been missed in a less detailed analysis.

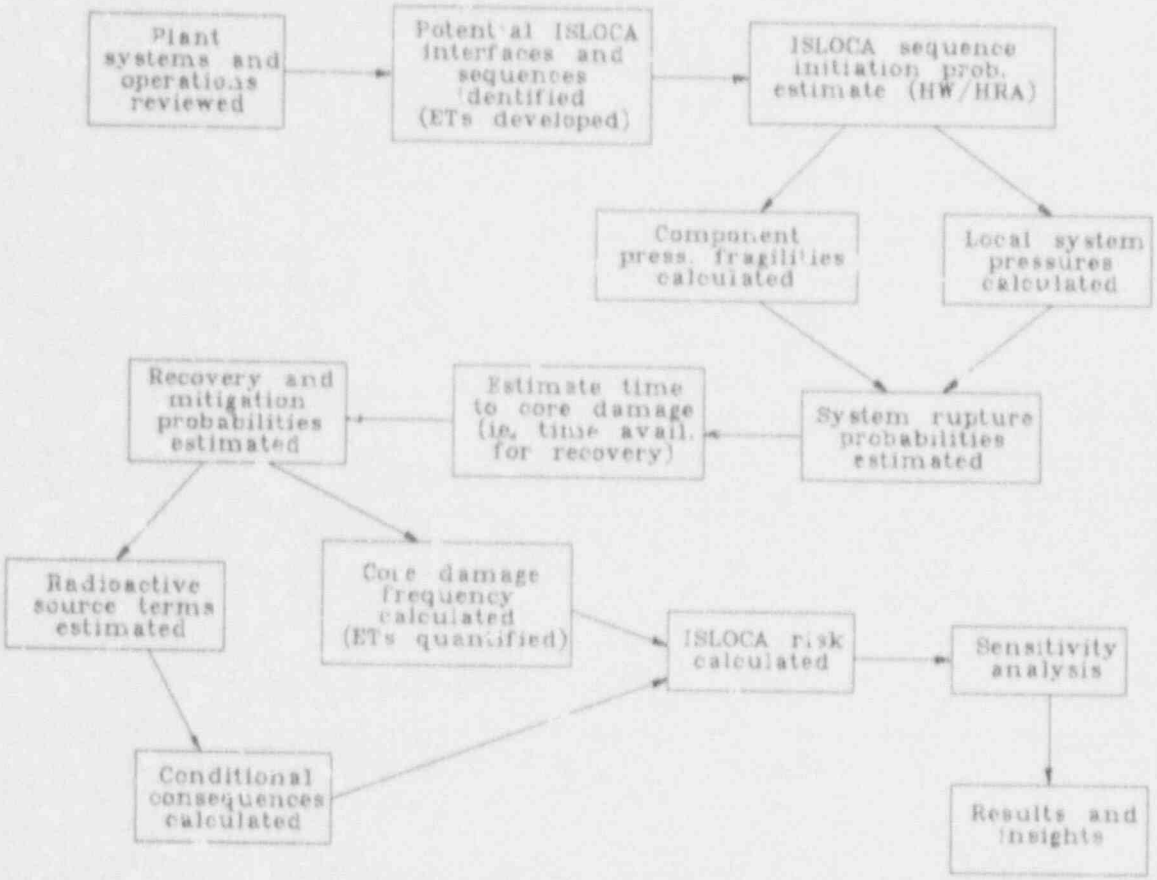

Figure ES-1. Approach for plant-specific evaluation of ISLOCA.

While caution must be exercised when using these results to draw general conclusions about the ISLOCA risk at other NPPs, the perspective provided by the aforementioned important insights, along with suitable sensitivity studies and companion PRAs, provide additional technical bases upon which a regulatory decision for resolution of ISLOCA as a generic issue can be considered.

ACKNOWLEDGMENTS

We would like to thank all of the plant personnel who assisted in the data-gathering visits. Without their assistance, this analysis could not have been completed.

At the Idaho National Engineering Laboratory, thanks are due to John Schroeder, who assisted in the rupture probability calculations, to Craig Kullberg, who provided the core uncovery time estimates, and to Curtis Smith, who assisted in the sequence screening analysis and developed the simplified system flow diagrams. Special thanks go to operator examiner Mark Jones for his invaluable assistance in interpreting the plant operating procedures and developing the sequence progression. Bob Richards aided in programming the software used in the human reliability analysis.

Finally, we would like to thank all the members of the inter-system loss-of-coolant accident inspection team for their aid in gathering and interpreting plant data.

ACRONYMS

ACI	Auto-closure interlock
AFW	Auxiliary feedwater
ARP	Annunciator response procedure
BNL	Brookhaven National Laboratory
CDF	Core damage frequency
CE	Combustion Engineering
CR	Control room
CRS	Control room supervisor
CVCS	Chemical and volume control system
DF	Decontamination factor
DHR	Decay heat removal
ECCS	Emergency core cooling systems
EPRI	Electric Power Research Institute
GLP	Gross leak pressure
HCR	Human cognitive reliability
HEP	Human error probability
HOV	Hydraulically operated valve
HPSI	High-pressure safety injection
HRA	Human reliability analysis
INEL	Idaho National Engineering Laboratory
ISLOCA	Inter-system loss-of-coolant accident
IST	In-service testing
LER	Licensee Event Report
LOCA	Loss-of-coolant accident
LPSI	Low-pressure safety injection
MAAP	Modular Accident Analysis Program
MACCS	MELCOR Accident Consequence Code System
MOV	Motor-operated valve
NPP	Nuclear power plant
NRC	Nuclear Regulatory Commission
NSSS	Nuclear steam supply system
P&ID	Piping and instrumentation diagram
PIV	Pressure isolation valve
PRA	Probabilistic risk assessment
PSF	Performance shaping factor
PWR	Pressurized water reactor
PZR	Pressurizer
RCS	Reactor coolant system
RO	Reactor operator
RPV	Reactor pressure vessel
RWSP	Refueling water storage pool
SDC	Shutdown cooling
SHARP	Systematic Human Action Reliability Procedure
SI	Safety injection
SIT	Safety injection tank (accumulator)
TALENT	Task Analysis-Linked Evaluation Technique
THERP	Technique for human error rate prediction

Assessment of ISLOCA Risks—Methodology and Application to a Combustion Engineering Plant

1. INTRODUCTION

The *Reactor Safety Study—An Assessment of Accident Risks in U.S. Commercial Nuclear Power Plants* (WASH-1400)[1] identified a class of accidents that can result in overpressurization and rupture of systems that interface with the reactor coolant system (RCS). These events were postulated to be caused by failure of the check valves and motor-operated valves (MOVs) normally used for system isolation. In a subset of these inter-system loss-of-coolant accidents (ISLOCAs), called V-sequences or event V, the system rupture occurred outside of the containment building. In cases where the rupture led to severe core damage, ISLOCAs were found to be significant contributors to risk because fission products released from the RCS bypassed the containment and were discharged directly to the environment. Subsequent probabilistic risk assessments (PRAs), including the NUREG-1150[2] results for Surry and Sequoyah, have identified ISLOCAs as important contributors to public health risk. Researchers at Brookhaven National Laboratory (BNL) have evaluated the vulnerability of several reactor designs to an ISLOCA and identified improvements that could reduce ISLOCA frequency.[3,4]

Recent events at several operating reactors have been identified as precursors to an ISLOCA. These events have raised concerns over the frequency of occurrence, potential initiators, and means of identifying and mitigating this potential accident. In response to these concerns, a June 7, 1989, memorandum, "Request for Office of Nuclear Regulatory Research (RES) Support for Resolution of the ISLOCA Issue," was transmitted from Dr. Thomas E. Murley to Dr. Eric S. Beckjord. The ISLOCA research program described in this report was initiated in response to this memorandum.

The objective of the ISLOCA research program is to provide the U.S. Nuclear Regulatory Commission (NRC) with qualitative and quantitative information on the hardware, human factors, and accident consequence issues that contribute to ISLOCA risk. This information is to be used to

- Developing a PRA framework for evaluating the ISLOCA issue and identifying insights with respect to the risk contribution from both hardware and human factors, along with recommendations for reducing the ISLOCA risk.
- Highlighting the effects of specific types of human errors and their root causes on ISLOCA risk, along with recommendations for risk reduction.
- Evaluating the fragility of low-pressure systems exposed to high-pressure, high-temperature reactor coolant. This evaluation will include identification of likely failure locations and failure probabilities.
- Identifying and describing potential ISLOCA sequences with respect to timing, possible accident management strategies, and effects on other plant equipment and systems.
- Estimating the fission product source terms and offsite consequences for postulated ISLOCAs. Again, important issues will be identified and recommendations will be made on possible consequence reduction actions.

To meet the above program objectives, a methodology has been developed to estimate the ISLOCA core damage frequency (CDF) and offsite risk, and this methodology is being applied to a limited sample of nuclear power plants (NPPs) of different design. This report describes the ISLOCA methodology and documents the results from its application to a Combustion Engineering

(CE) plant. These results emphasize the effect of hardware failures and human actions on the ISLOCA CDF. The offsite risk measures are considered useful in comparing results from the sensitivity studies. Major uncertainties in this estimate are also identified.

Section 2 of this report describes the methodology developed to evaluate ISLOCAs, the approach taken for its application to a specific plant, and a description of the plant systems that were identified as potential ISLOCA flow paths. Section 3 describes the interfacing systems and the possible ISLOCA scenarios. Section 4 describes the plant-specific results and Section 5 contains the conclusions and recommendations from this assessment. Appendices A–H are used to document the details of the separate analyses.

2. APPROACH

The general approach that is being used to evaluate ISLOCA risk and plant vulnerabilities to ISLOCA is to perform a detailed analysis for a small but diverse sample of plants and, to the extent possible, extrapolate and generalize these results for additional plants. A detailed plant analysis methodology was developed to meet the program objectives discussed in the previous section. The steps in this individual plant methodology are illustrated in Figure 1. Subsections 2.1 through 2.7 discuss each of these steps briefly.

Before beginning the individual plant evaluations, historical plant operating information was reviewed to provide insights on potential ISLOCA issues. The major emphasis of this evaluation was identification and evaluation of Licensee Event Reports (LERs) that (a) involved valve failures resulting from either hardware failures or human errors or (b) indicated that an ISLOCA had occurred. The results from this search provided information on the causes and frequencies of valve failures and provided important insights on the systems involved and the potential causes of those ISLOCAs that have occurred. This information was used during the plant visits to help identify systems to be reviewed, develop the event trees, and quantify the failure rates of some interfacing system valves. Appendix A to *Assessment of ISLOCA Risks—Methodology and Application to a Babcock and Wilcox Plant* summarizes the results of this evaluation.[5]

2.1 Assessment of ISLOCA Potential

The first step in the individual plant evaluation approach is a preliminary assessment of the potential for an ISLOCA to occur. Plant-specific

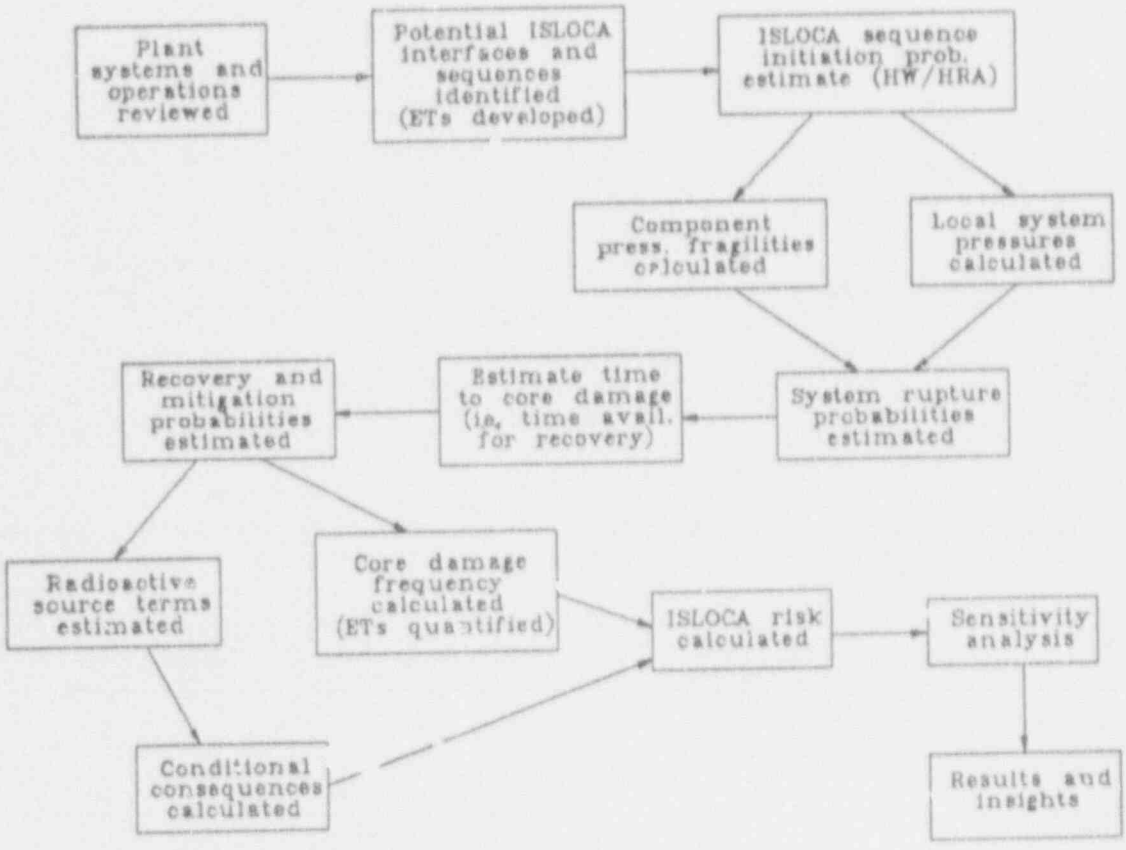

Figure 1. Approach for plant-specific evaluation of ISLOCA.

information on the systems that could be involved in an ISLOCA is obtained during a short data-gathering visit to the plant. Detailed information is obtained on the hardware and operation of a range of low- and high-pressure interfacing systems. Examples of information collected include plant procedures, piping and instrumentation diagrams (P&IDs), isometric drawings, and training manuals. This information is then reviewed by a team of PRA and human factors specialists to familiarize them with the systems and operations that have the potential to initiate, prevent, or mitigate an ISLOCA. All systems that interface with the RCS are identified during this preliminary assessment. A determination is then made of the maximum interfacing system break size that would not be expected to result in core damage. The systems are screened to identify those with interfacing pipe sizes larger than this maximum value with the potential to bypass containment. The systems that meet this screening criterion are analyzed further to identify specific ISLOCA initiators and scenarios. The identified scenarios are developed in sufficient detail to guide the team in obtaining detailed information during a subsequent extended plant visit.

2.2 Gathering of Detailed Plant-Specific Information

An extended visit to the plant allowed the analysts to gather the information needed to complete the above reviews and to develop and analyze the candidate ISLOCA scenarios. Members of the team that developed the candidate scenarios obtained information by interviewing plant personnel and walking down the systems of interest. This task was performed in conjunction with an ISLOCA inspection conducted by the NRC Office of Nuclear Reactor Regulation. The types of information that were obtained during this visit include detailed information on

- Hardware that would be involved in an ISLOCA. For example, data were collected on control valves, relief valves, piping, flanges, pumps, and heat exchangers.

- Procedures, guidelines, and practices followed by plant personnel during startup, normal power operation, and shutdown of the plant, as well as detailed information on maintenance and in-service testing.

- Factors that could influence performance of plant personnel as related to initiation, detection, diagnosis, prevention, or mitigation of an ISLOCA.

2.3 Development of Event Trees

After the plant-specific information was collected, a final list of low-pressure interfaces and scenarios was compiled and the detailed accident sequence analysis begun. This analysis was a joint effort of the PRA and human factors specialists. The scenarios were modeled using (primarily) component level event trees combining the hardware faults and the human errors that constitute each sequence in the scenario. In general, each event tree comprised three phases:

1. The initiating events, which are those combinations of failures, both hardware and human-related, that result in a failure of the RCS pressure isolation boundary and expose the low-pressure interfacing system to the RCS.

2. The rupture events, which model a break in the interfacing system, its size, and location.

3. The post-rupture events, which model the performance of the control room and auxiliary operators in recovering from or mitigating the consequences of an ISLOCA. The list of possible ISLOCA sequences contains both hardware-based sequences (as found in typical PRAs) and sequences initiated by human error. The potential human errors in both types of sequence comprised errors of omission, commission, and pre-existing or latent errors.

2.4 Estimation of Rupture Potential

It is important to realistically assess the performance of those components designed for low-pressure conditions that are exposed to the beyond-design pressures associated with an ISLOCA. The basic approach for performing this assessment is

- The failure probability of each piece of equipment in the interfacing system is described by a lognormal distribution with a specified median failure pressure and logarithmic standard deviation
- Thermal-hydraulic response of the systems is simulated, if necessary, to estimate the pressure distribution in the system based on the expected initiating event, initial primary system conditions, and the expected performance of relief valves designed to protect the systems from overpressurization
- The failure pressure of each component is compared with the calculated pressure at that point in the system to estimate the component failure probability (see Appendix F for details)
- The individual component failure probabilities are combined to give an estimate of the system rupture probability.

The component and piping failure pressures and distributions used in the rupture calculations were developed from an independent structural analysis performed by Impell Corporation (see Appendix H). Not only were failure pressures calculated, but likely leak rates and leak areas, also. In this respect, flanges are somewhat unique in that there are actually two failure pressures of interest. First, there is the estimated gross leak pressure (GLP) at which a measurable leak area develops. At lower pressures, leakage is possible but only at very small rates (measured in mg/s) caused by seepage around the flange gasket. Once the GLP is exceeded, the flange bolts begin to stretch (elastic deformation) and the flange surfaces begin to separate. At some yet higher pressure (P_o), the bolts begin to undergo plastic deformation. At this point, large leak areas begin to develop with correspondingly large leak rates. These three pressure regions (below GLP, between GLP and P_o, and greater than P_o), are associated with three leak sizes, respectively: spray leaks, small leaks, and large leaks.

2.5 Human Reliability Analysis

The predominant human errors for each scenario in the ISLOCA PRA were modeled using the techniques of human reliability analysis (HRA). HRA is a methodological tool used for prediction, evaluation, and quantitative analysis of work-oriented human performance. As a diagnostic tool, HRA can estimate the error rate anticipated for individual tasks and can identify where errors are likely to be most frequent.

The general methodological framework for the ISLOCA HRA was based on guidelines (under development) from the NRC-sponsored Task Analysis-Linked Evaluation Technique (TALENT) Program,[6] which recommends the use of task analyses, time-line analyses, and interface analyses in a detailed HRA. NUREG/CR-1278, *Handbook of Human Reliability Analysis with Emphasis on Nuclear Power Plant Applications* [which discusses the technique for human error rate prediction (THERP)],[7] recommends similar techniques and, in addition, provides a data base that can be used for estimating human error probabilities (HEPs). Finally, the ISLOCA HRA integrated the steps from the *Systematic Human Action Reliability Procedure* (SHARP)[8] and *A Guide for General Principles of Human Action Reliability Analysis for Nuclear Power Generation Stations* (IEEE Standard P1082/D7).[9]

From this combination of approaches, the analysts identified 11 basic steps to be followed in performing the HRA:

1. Select the analysis team and train them on relevant plant functions and systems (IEEE P1082).[9]

2. Familiarize the team with the plant through the use of system walkdowns, simulator observations, etc. (IEEE P1082).[9]

3. Ensure that the full range of potential human actions and interactions is considered in the analysis (SHARP) (IEEE P1082).[8,9]

4. Construct the initial model of the relevant systems and interactions (IEEE P1082).[9]

5. Identify and screen specific human actions that are significant contributors to safe operation of the plant. This was accomplished through detailed task analyses, timeline analyses, observations of operator performance in the plant and in the simulator, and evaluations of the human/machine interface (SHARP and IEEE P1082).[8,9]

6. Develop a *detailed* description of the important human interactions and associated key factors necessary to complete the plant model. This description should include the key failure modes, an identification of errors of omission/commission, and a review of relevant performance shaping factors (SHARP) (IEEE P1082).[8,9]

7. Select and apply the appropriate HRA techniques for modeling the important human actions (SHARP).[8]

8. Evaluate the impact on ISLOCA of significant human actions identified in Step 6 (SHARP).[8]

9. Estimate error probabilities for the various human actions and interactions, determine sensitivities, and establish uncertainty ranges (SHARP and IEEE P1082).[8,9]

10. Review results for completeness and relevance (IEEE P1082).[9]

11. Document all information necessary to provide an audit trail and to make the information understandable (SHARP).[8]

Because most of the human actions in this HRA involved the use of various written normal, abnormal, and emergency operating procedures, THERP-type HRA event trees were used to model most of the human actions in the detailed analyses.[7] However, not all ISLOCA scenarios were best represented by THERP event trees alone. In those cases, HRA fault trees were used in conjunction with the THERP event trees. The fault trees and THERP event trees were used in a detailed analysis to estimate the probability of human error for each of the dominant human actions.

Traditionally, human reliability analysts model human performance through the use of an event tree like that shown in Figure 2, with operator error generally placed along the descending right branches of the event tree, and successful operator actions sequenced on the left side of the tree. For example, on the top left, event a, [RO (reactor operator) detects decreasing pressurizer (PZR) level and pressure] is the success path. Failure to accomplish this task is modeled as event A, (RO fails to detect decreasing pressurizer level and pressure). When a second operator, or group of operators, is involved, such as in event B, [control room (CR) fails to detect PZR Hi-Lo alarm], the action of this second operator may be modeled in a recovery branch, as shown in Figure 2. Event b models how the control room also has an opportunity to detect the PZR Hi-Lo alarm. If the control room does detect the alarm, this becomes a recovery action because it would bring the model back to the success path (via the dotted lines in Figure 2).

The basic, or unmodified, HEPs for branches in the HRA event trees were estimated using techniques from THERP and human cognitive reliability (HCR).[10] These basic HEP estimates were then revised by using performance shaping factors (PSFs) to more realistically model the work process at the plant. Each PSF was either positive or negative and, accordingly, either decreased or increased the likelihood of a given human error. For example, an analog meter, such as a pressure gauge, if it does not have easily seen limit marks, would be judged to be a negative PSF. Thus, there would be a higher-than-normal probability for

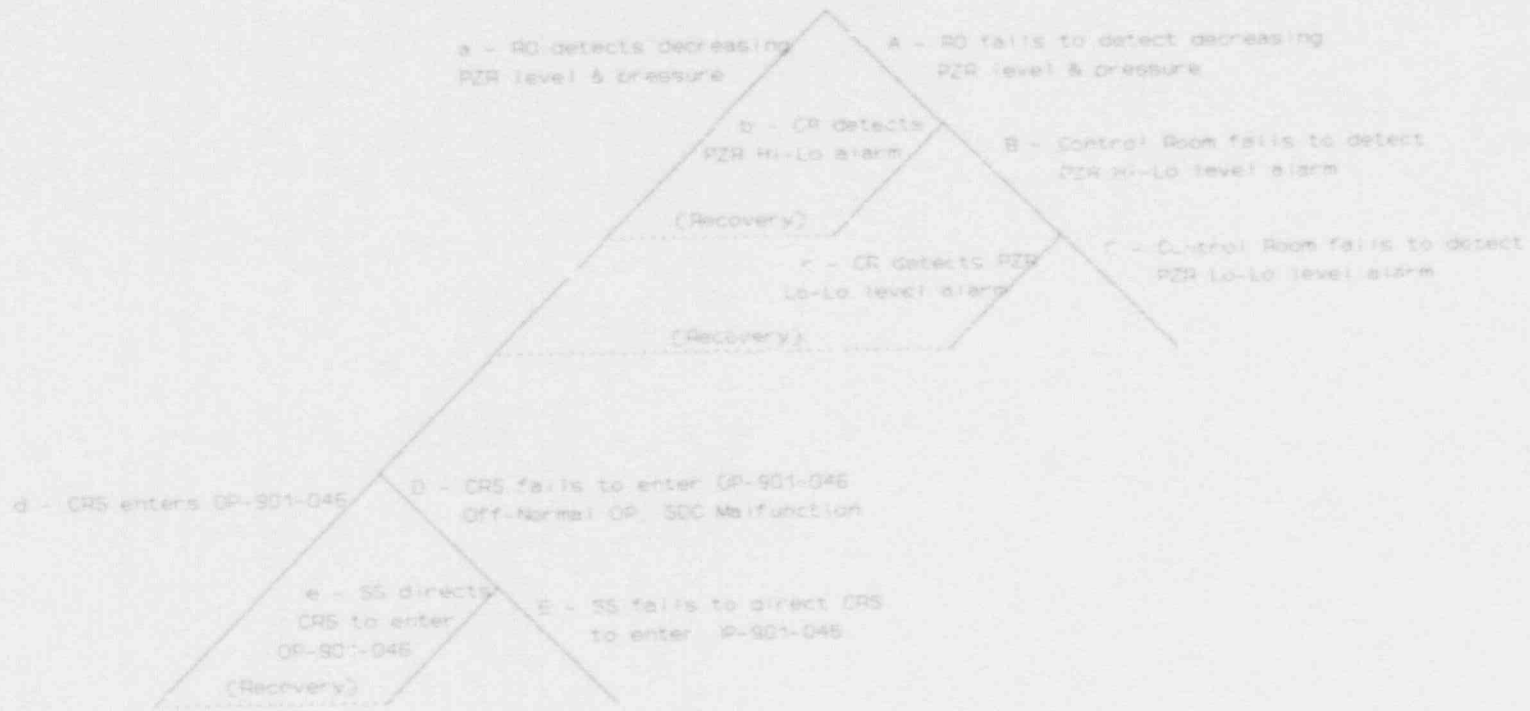

Figure 2. Example of HRA event tree.

error in reading the gauge. Individual PSFs were derived from task analyses, time-line analyses, evaluation of the human/machine interface, and direct observations of operator performance. They are presented as part of the *ISLOCA Inspection Report*.[11]

Specific PSFs that were investigated include

- Quality of the human/machine interface
- Written procedures (emergency, abnormal, maintenance, etc.)
- P&IDs
- Response times for systems and personnel
- Communication requirements
- Determination of whether the operator actions were skill-, rule-, or knowledge-based
- Crew experience
- Levels of operator stress in different scenarios
- Feedback from the systems in the plant
- Task dependence and operator dependence
- Location of the task (control room, auxiliary building, etc.)
- Training for individual operator actions including those required in ISLOCA situations.

Finally, the combination of all identified failure paths (i.e., sequences that included either single or multiple human errors leading to a failure of the action modeled by the HRA tree) gave the failure probability for the action modeled in the HRA tree. The guidelines of THERP were followed in identifying the individual error paths. As depicted by Figure 2, each human error event tree may have several unique error paths. For example, event A, event B, and event C together constitute an error path in which the reactor operator fails to detect decreasing PZR level and pressure, followed by individual failures of the control room to detect two PZR level alarms. In a similar manner, failure path A-b-D-E models a sequence where the reactor operator fails to detect decreasing PZR level and pressure, then recovers (e.g., the control room detects the PZR Hi-Lo alarm) from this first failure (event b), only to have both the control room supervisor (CRS) and shift supervisor (SS) fail to enter Procedure OP-901-046, "Shutdown Cooling Malfunction." Probabilities for each unique error path were calculated by multiplying each HEP on a given error path by other HEPs on the same path. For example, the error rate for path A-B-C would be calculated by multiplying the HEP of failure A by that for failure B and then by the HEP for failure C, resulting in a nominal HEP for that specific path. Other error paths for this event tree include A-B-c-D-E and a-D-E. The individual error path failure probabilities were then summed to give the total event tree failure probability. Comprehensive details of this process are provided in Appendix C for each event, and the results are summarized in Section 4.2.

A detailed HRA was conducted for each of the significant scenarios identified in the ISLOCA PRA. See Section 4.2 or Appendix C for details of the results of these analyses. (The tables in Section 4 summarize the results.) These tables provide the identifier and description for each significant human error, as well as both nominal and mean HEPs. Nominal HEPs in these tables are assumed to be *median point estimates from a lognormal distribution* (using guidelines from *Handbook of Human Reliability Analysis with Emphasis on Nuclear Power Plant Applications*),[8] while mean values are *mean HEPs from a lognormal distribution*, which were derived using the following formula:

$$\text{mean } HEP = exp\left(\mu + \frac{\sigma^2}{2}\right)$$

where

$$\mu = \ln\hat{x}$$

$$\hat{x} = \text{the median HEP}$$

$$\sigma = \frac{ln(error\ factor)}{1.645}$$

The conversions to mean values were carried out as a result of mathematical concerns where median values from a lognormal distribution should not be multiplied by mean values in estimating the mean CDF, a process that has been followed in some past HRAs.

2.6 Quantification of Event Trees

The top events on the ISLOCA accident sequence event trees are quantified by separate calculations that generate the conditional probabilities of occurrence of each event for each path through the tree. The means of obtaining the rupture event probabilities and the probabilities relating to failure of plant personnel have already been discussed. Hardware failure probabilities were developed using the data base documented in Appendix B of *Assessment of ISLOCA Risks—Methodology and Application to a Babcock and Wilcox Plant*.[5] The ISLOCA event trees were constructed using the ETA-II personal computer code.[12]

2.7 Consequence Evaluation

The ISLOCA CDFs are multiplied by the corresponding consequences (conditional on the occurrence of core damage) calculated using the MELCOR Accident Consequence Code System (MACCS) code to obtain the ISLOCA annual risk estimates.[13] The conditional consequences were generated with MACCS using a hybrid input deck. The fission product source terms were obtained from the SEQSOR parametric source term generation code.[14] The source terms generated are the ones identified with the containment bypass V-sequence in NUREG-1150.[2] The site information was taken from the Surry MACCS input deck used in the NUREG-1150 program. The Surry site was chosen by reviewing *Technical Guidance for Siting Criteria Development*[15] and calculating an average site based on weather-weighted population density. This average population density was then compared to the five NUREG-1150 sites and Surry was chosen because it most closely matched the calculated average population density. Further details of the consequence calculations can be found in Appendix G.

3. DESCRIPTION OF THE INTERFACING SYSTEMS

The unit analyzed is a 3,390 MWt pressurized water reactor (PWR), with a two-by-four loop (two hot legs and four cold legs) CE nuclear steam supply system (NSSS). It is equipped with a large, dry, atmospheric-pressure containment and a separate reactor auxiliary building and turbine building. An overview of the interfacing systems is presented in the following section. For more details on the interfacing systems, see Appendix A.

3.1 Interfacing Systems

All interfacing systems were screened to identify those systems that required further evaluation. The first criterion used in screening was that any system with an interfacing pipe diameter larger than 1 inch should be evaluated. The 1-inch pipe size was selected based on an estimation of the discharge from a 1 inch high-pressure pipe break, which was about 200 gpm. A 200-gpm leak rate outside of the containment is considered to be critical based on the capacity of the refueling water storage pool (RWSP) (minimum Technical Specification volume of 443,000 gal), the capacity of the three charging pumps (132 gpm), and the normal makeup rate to the RWSP (~150 gpm). Based on these considerations and the number of hours it would take for the plant to achieve cold shutdown (conservatively assumed to be about 10 hours), leak rates of 200 gpm or less were judged not to be risk significant. The second criterion was that systems whose low-pressure portions were isolated from reactor pressure by three or more normally closed valves or periodically leak-tested check valves in series would not be analyzed. The basis for screening out such systems is the low expected frequency of [illegible] dure of the pressure isolation boundary.

The initial screening resulted in the selection of the safety injection (SI) system for further analysis, including the high- and low-pressure safety injection pumps and the shutdown cooling (SDC) lines. Figures 3 through [illegible] show simplified flow diagrams of the [illegible] hardware configuration. Additional details on these systems are provided in Appendix A. The SI system interface comprises 12 separate reactor pressure vessel (RPV) injection lines, eight high pressure and four low pressure. Starting from the RPV, each injection line contains two check valves in series, a normally closed motor-operated flow control valve and the SI pump discharge check valve. The SDC interface consists of four low-pressure injection lines to each of the RCS cold legs, two high-pressure recirculation lines to the RCS hot legs, and two suction lines from the RCS hot legs used for shutdown cooling.

3.2 Potential ISLOCA Scenarios

Potential scenarios were developed by examining the system interfaces and plant operational information. A team of PRA and human factors specialists was involved in the scenario development. In some cases (e.g., the SI system injection lines), the sequences are hardware-driven; that is, the ISLOCA potential is a function of the hardware failure rates of the pressure isolation boundary valves. In other cases (e.g., the SDC suction lines), human errors can initiate an ISLOCA. Table 1 summarizes the ISLOCA scenarios identified.

3.2.1 SDC Suction Lines During Shutdown. During the plant shutdown process, the operators will open MOVs SI-401 and SI-407 and hydraulically operated valve (HOV) SI-405 to allow for the removal of decay heat. Sequence 1A investigates the likelihood that the valves (that will be opened by the operators) are opened prematurely, that is, at an RCS pressure greater than the procedural limit of 396 psig.

3.2.2 SDC Suction Lines During Startup. Sequence 1B is similar to Sequence 1A, except that the plant is undergoing a startup. Thus, failure to close MOVs SI-401 and HOVs SI-405 is modeled, as opposed to Sequence 1A where the failure mode for valves SI-401 and SI-405 was premature opening.

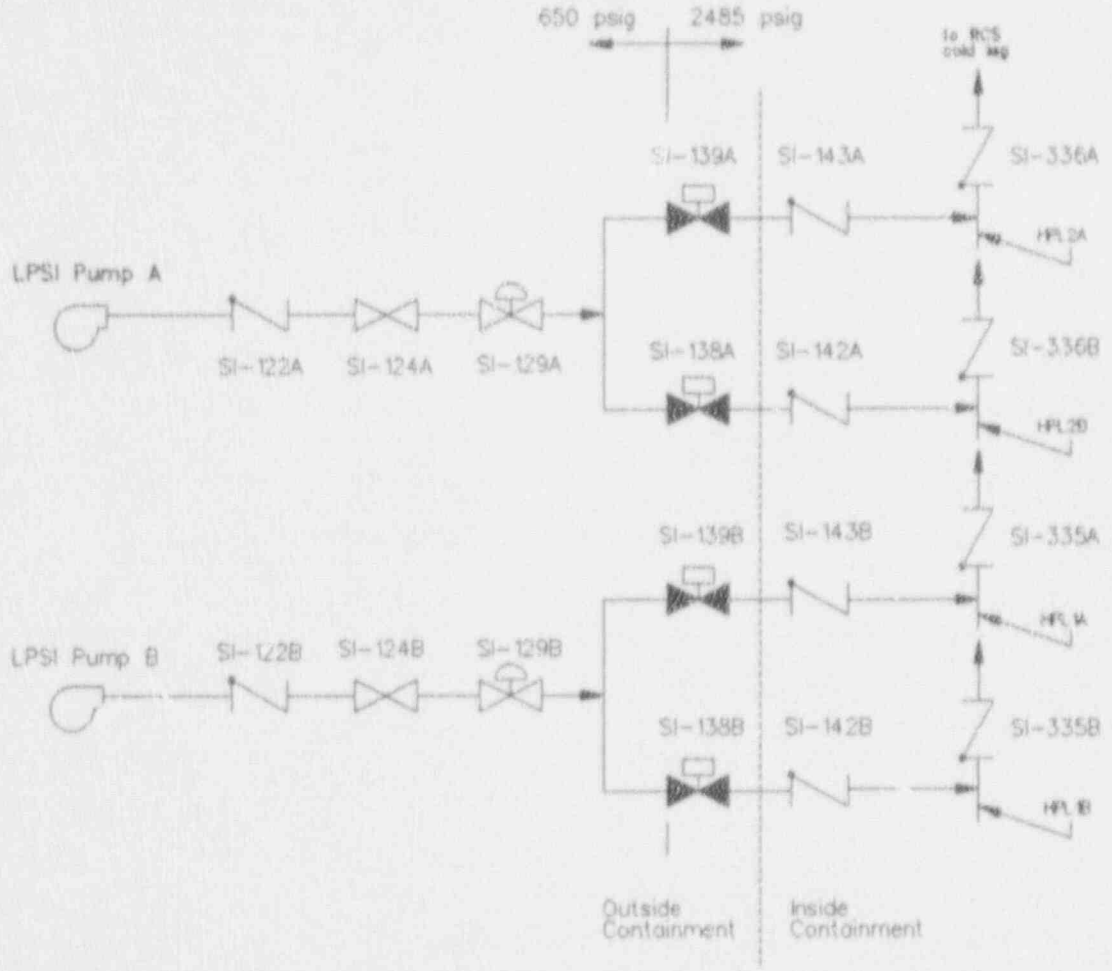

Figure 3. Flow diagram of RCS cold legs to low-pressure safety injection (LPSI) pump discharge.

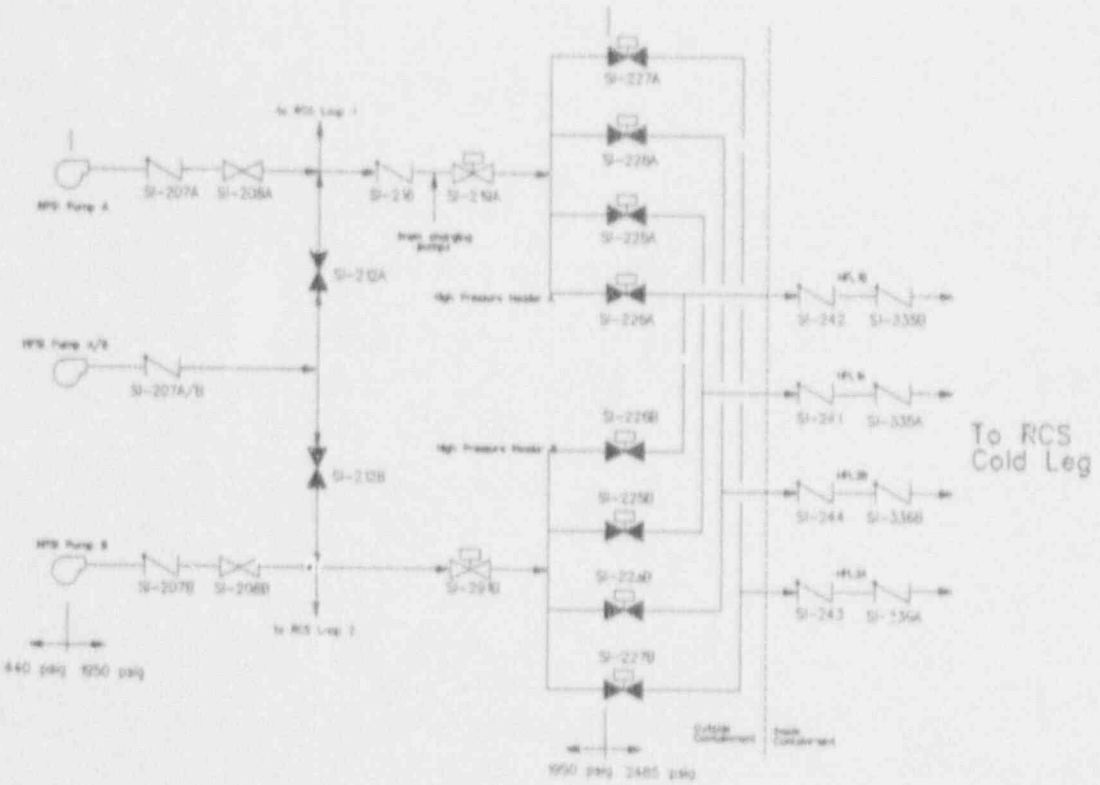

Figure 4. Flow diagram of RCS cold legs to high-pressure safety injection (HPSI) pump discharge.

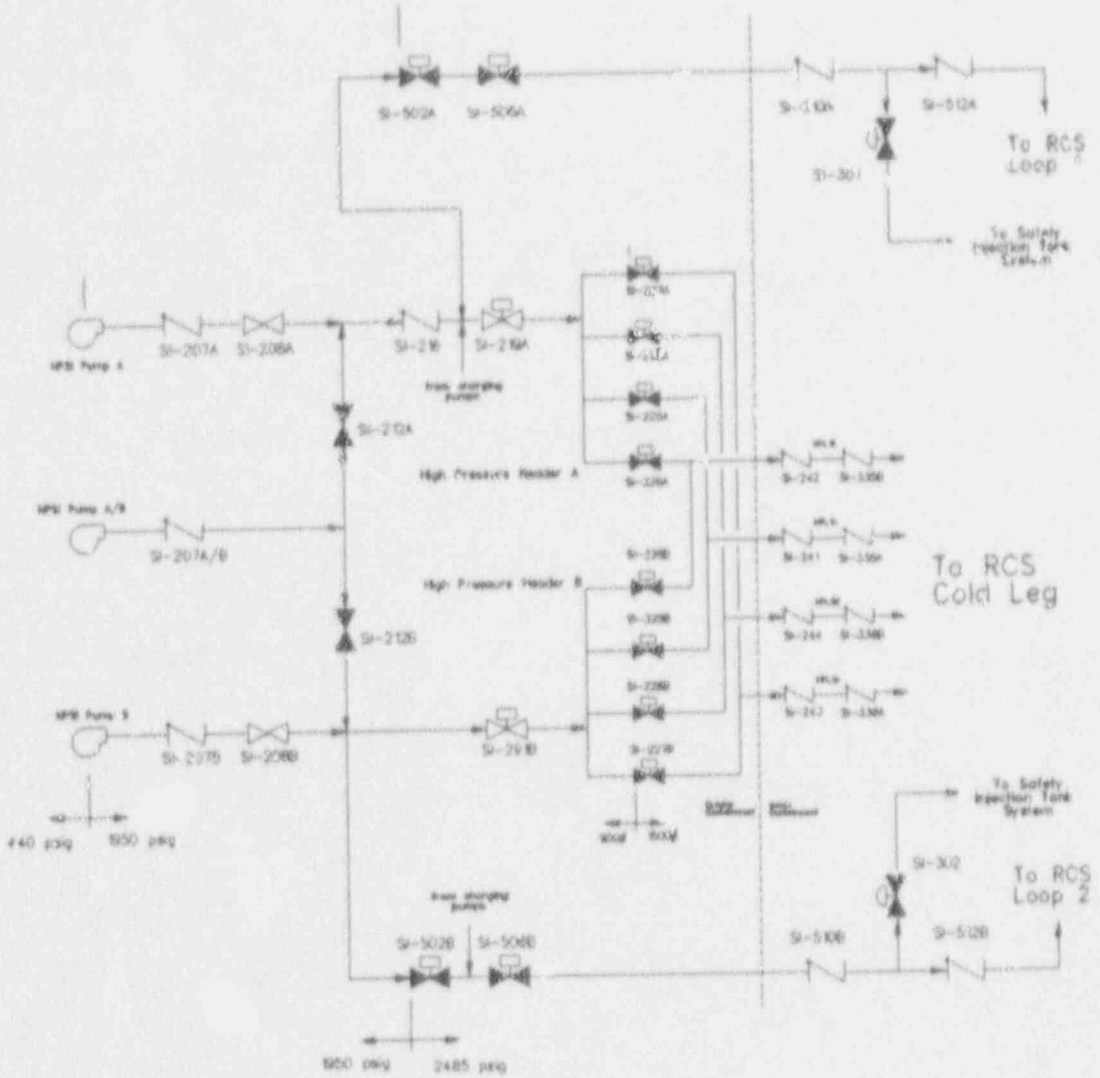

Figure 5. Flow diagram of RCS hot legs to HPSI pump discharge.

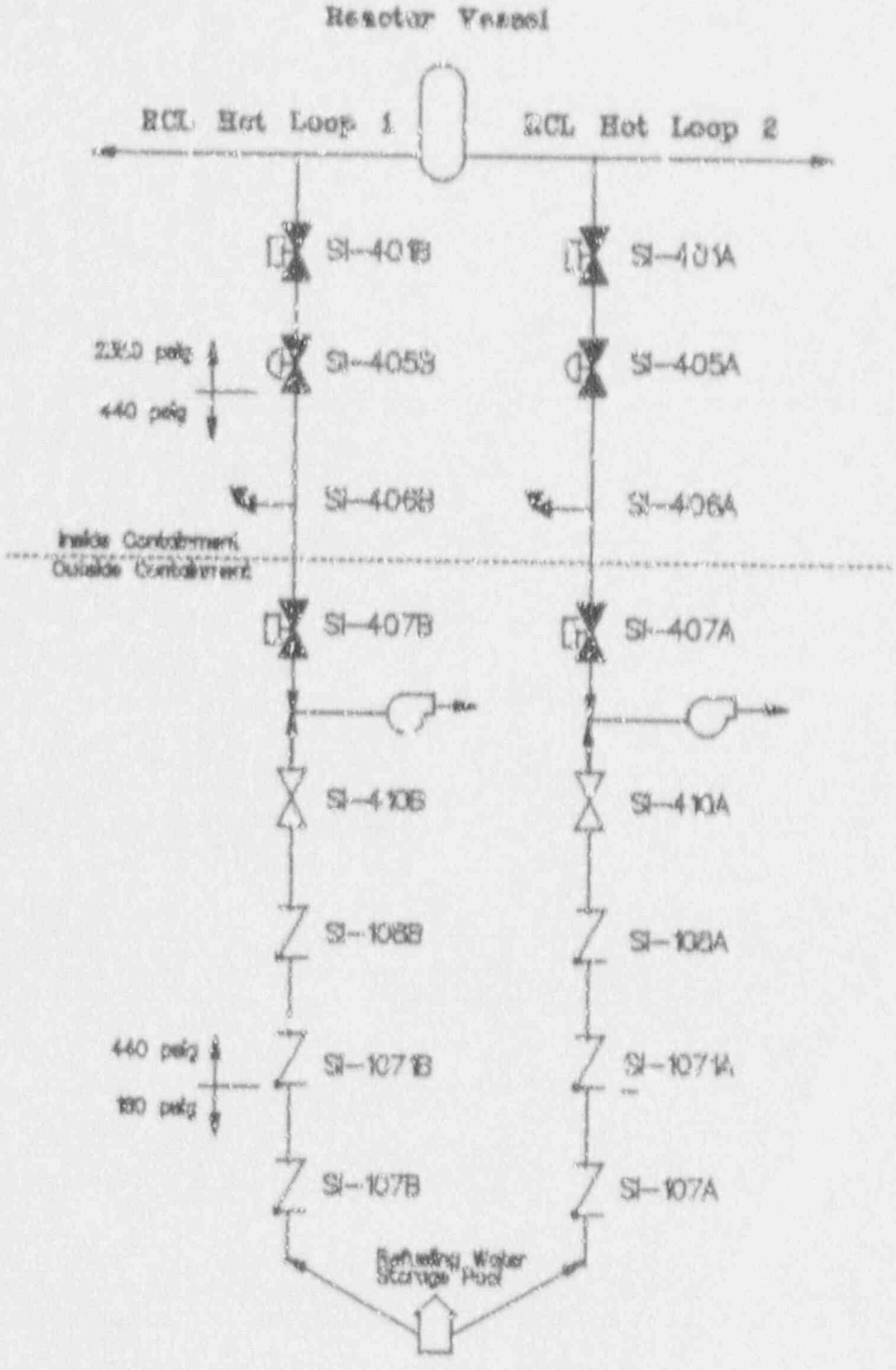

Figure 6. Flow diagram of RCS hot legs to the RWSP via the LPSI system.

Table 1. List of potential ISLOCA scenarios.

Interface	Description	Notes
SDC suction lines	Failure to close valves during startup or premature opening during shutdown	Two scenarios investigated: one startup and one shutdown (SEQs-1A and 1B)
LPSI cold leg injection lines	Failure of two check valves with stroke-testing of normally closed MOV	Initiated by hardware failures in conjunction with MOV stroke testing (SEQ-2)
HPSI cold leg interface	Failure of two pressure isolation check valves and stroke test of normally closed MOV, plus failure of safety injection pump discharge check valve	Only hardware failures considered (SEQs-3A and 3B)
HPSI hot leg interface	Failure of two pressure isolation check valves and stroke test of normally closed MOV, plus failure of safety injection pump discharge check valve	Only hardware failures considered (SEQs-4A and 4B)
SDC suction lines	Failure of two check valves	Sequence initiated during normal shutdown (SEQ-5)

3.2.3 LPSI Cold Leg Injection Lines to RCS. Through the normal reactor operating year, MOVs SI-138 (A/B) and SI-139 (A/B) are stroke-tested quarterly. Thus, the accident sequence for the LPSI pump discharge is based upon the fact that the MOVs will be opened once each quarter.

3.2.4 HPSI Cold Leg Interface. These scenarios are similar to Sequence 2. Once each quarter, MOVs SI-225 through SI-228 (A/B) are stroke-tested while the plant is operating at normal power. Thus, the accident sequence path for the HPSI pump cold leg discharge is based upon the fact that the MOVs will be opened once each quarter. Note that Sequence 3B is similar to Sequence 3A, but there is one less check valve to protect the low-pressure portions of the SI system.

3.2.5 HPSI Hot Leg ... ce. Once every quarter, MOVs SI-502A and SI-506A are stroke tested. Therefore, Sequence 4A is based on the opening of MOV SI-502A. Since valve SI-502A is opened and closed before valve SI-506A is opened, the opening of SI-502A is defined as the initiating event for the sequence. Once again, the assumption of no prior knowledge of the condition of the system is used. Sequence 4B is similar to Sequence 4A except that check valve SI-216 is missing from piping header B.

3.2.6 SDC Suction Lines During Normal Shutdown. When the CE plant enters the shutdown mode, the operators rely on check valves SI-108 and SI-1071 closing when the RCS pressure exceeds the interfacing system design pressure. Thus, Sequence 5 is based upon failure of the two check valves.

4. RESULTS

Because of the unique nature of the ISLOCA sequence, a detailed understanding of the capabilities of the plant hardware and personnel is needed to accurately analyze the ISLOCA challenge. For this report, an ISLOCA is considered to involve a loss of reactor coolant outside containment. Since the supply of water available for makeup to the RCS is essentially limited to the available inventory in the RWSP, a high-priority item for the control room operators should be to isolate the break expeditiously and terminate the loss of reactor coolant. If the break were isolated in a timely manner and the loss of RCS inventory terminated, the plant could be cooled down safely using the auxiliary feedwater (AFW) system (secondary cooldown) or SDC (primary cooldown).

Before discussing the detailed results, some general comments can be made that are applicable to all the postulated ISLOCA scenarios. During the course of the plant visit, particular attention was paid to the issue of local environmental effects resulting from ruptures in the interfacing systems. At the time of the plant visit, the probabilistic system rupture calculations had not been completed, so a general survey was made of the interfacing system flow paths to *qualitatively* estimate the impact of ruptures on equipment in various locations. This survey included walkdowns of the emergency core cooling systems (ECCS) to examine likely break locations. For example, the assumption was made for this analysis that all equipment in the compartment where a break occurs will be rendered unavailable for use in isolating/mitigating the ISLOCA. Therefore, equipment in compartments judged to be candidate locations for an ISLOCA break was inventoried. This survey could not verify that the ECCS are adequately separated such that any postulated rupture would not affect redundant ECCS trains. If there were a piping break and blowdown of steam from the RCS into one of the safeguards pump rooms, the plant configuration may not ensure that at least one train of ECCS would still be available after a rupture had occurred. However, we stress that these conclusions are not based on mechanistic heat and mass transfer calculations and are therefore qualitative in nature. This issue is still under investigation at the INEL.

4.1 Event Trees

The following sections describe the event trees developed for the postulated ISLOCA scenarios. The event trees are quantified on a yearly or quarterly basis, as reflected in the frequency of the initiating event. The event trees are constructed such that the downward branch depicts the failure event listed at the top of the event tree and the upward branch denotes the complement of the event (i.e., typically success). The top events are a combination of individual component failures, human errors, and functional failures that describe the progression of the ISLOCA from initiation to core damage or recovery.

All event tree quantification is performed using mean failure probabilities. The derivations of the event tree split fractions are presented in Appendices B and C. Note that detailed (i.e., nonscreening) failure probabilities were calculated only for Sequences 2 and 5; all of the other sequences had CDFs $<10^{-8}$/year in the screening analysis and were not developed further.

Finally, each event tree end state was assigned to one of the source term bins listed below:

- **OK**—No overpressurization of the low-pressure system occurred (no fission product release).
- **OK-op**—Scenario results in overpressurization of the interfacing system but the system does not rupture or leak (no fission product release).
- **LK-ncd**—Scenario results in RCS leakage from the interfacing system, through either a break or an open relief valve, but severe core damage (sufficient to cause offsite health effects) does not occur because the leak is either isolated before core uncovery or the leak is too small to interfere with core cooling (no fission product release).

- **LOCA-ic**—Identifies scenarios that produce a loss-of-coolant accident (LOCA) inside containment. Because these sequences are enveloped by the design basis analysis of the plant, they are not fully developed on the event trees and are not considered to be core damage events for the purposes of this analysis.

- **PEL-mit**—An ISLOCA with core damage occurs but the radioactive fission product release is mitigated through some means, such as scrubbing through an overlying water pool or general area fire sprays in the auxiliary building.

- **REL-ig**—An ISLOCA with core damage occurs and results in a large unmitigated radioactive release. Note that this does not necessarily mean that the break size is large.

4.1.1 Premature Entry Into Shutdown Cooling—SEQ-1A. A risk-significant scenario at the Babcock and Wilcox plant[5] involved premature entry into shutdown cooling, with RCS pressure and temperature above the open permissive set point of the decay heat removal (DHR) system suction isolation valves. This scenario was considered credible at the Babcock and Wilcox plant because the plant procedures allowed operators to bypass the open permissive interlock for one of the two shutdown cooling isolation valves. This allowed an error of commission to be postulated in which, once a decision is made to enter shutdown cooling, the operators will be led to bypass the interlock for the other valve, also, even though the procedure does not instruct them to do so. For the CE plant the HRA did not reveal any circumstances that would lead to an analogous scenario. Therefore, this scenario was not developed further.

4.1.2 Shutdown Cooling System/Reactor Coolant System ISLOCA During Startup—SEQ-1B. Figure 7 shows the event tree used to model an intersystem LOCA between the RCS and SDC system during startup. The SDC suction isolation valves from the RCS are open initially because the SDC system is being used to remove decay heat from the reactor. Since startup is a "low-pressure" procedure compared to normal full RCS pressure, it is assumed that any overpressurization that causes the relief valve to open will not cause an ISLOCA. The event tree models one flow line (out of two) on a mission time of one year.

4.1.3 RCS To LPSI Cold Leg Discharge—SEQ-2. Through the normal reactor operating year, MOVs SI-138 (A/B) and SI-139 (A/B) are stroke-tested quarterly. Thus, the accident sequence path for the LPSI pump discharge is based upon the fact that the MOVs will be opened once each quarter. Figure 8 shows the event tree used to model this sequence.

Obviously, if the two isolation check valves [SI-335/336 (A/B) and SI-142/143 (A/B)] protecting the MOVs had failed, it would not be desirable to open the MOVs. But, for analyzing this sequence, it is assumed that no prior information (for example, a high-pressure reading on the pressure indicator between the two isolation check valves) is known for the system. This assumption is made because the stroke-testing procedure does not direct the operators to check pressure between the PIV check valves before performing the stroke test. In addition, the annunciator card for this pressure indicator was found to be deactivated during the plant inspection,[11] so no credit was given for this annunciator. Therefore, for the model, it is postulated that internal failure of the two isolation check valves will automatically lead to an overpressurization of the interfacing system when the MOV is stroke tested. Note that the event tree evaluates one flow path (out of four possible) for a mission time of one quarter. Thus, to get the failure frequency for the complete system based on a one year mission time, the sequence end state frequencies must be multiplied by 16.

4.1.4 RCS Cold Legs to HPSI (Header A)—SEQ-3A. This scenario is similar to Sequence 2. Once each quarter, MOVs SI-225 through SI-228 (A/B) are stroke tested while the plant is operating. Thus, the accident sequence path for the HPSI pump discharge is based upon

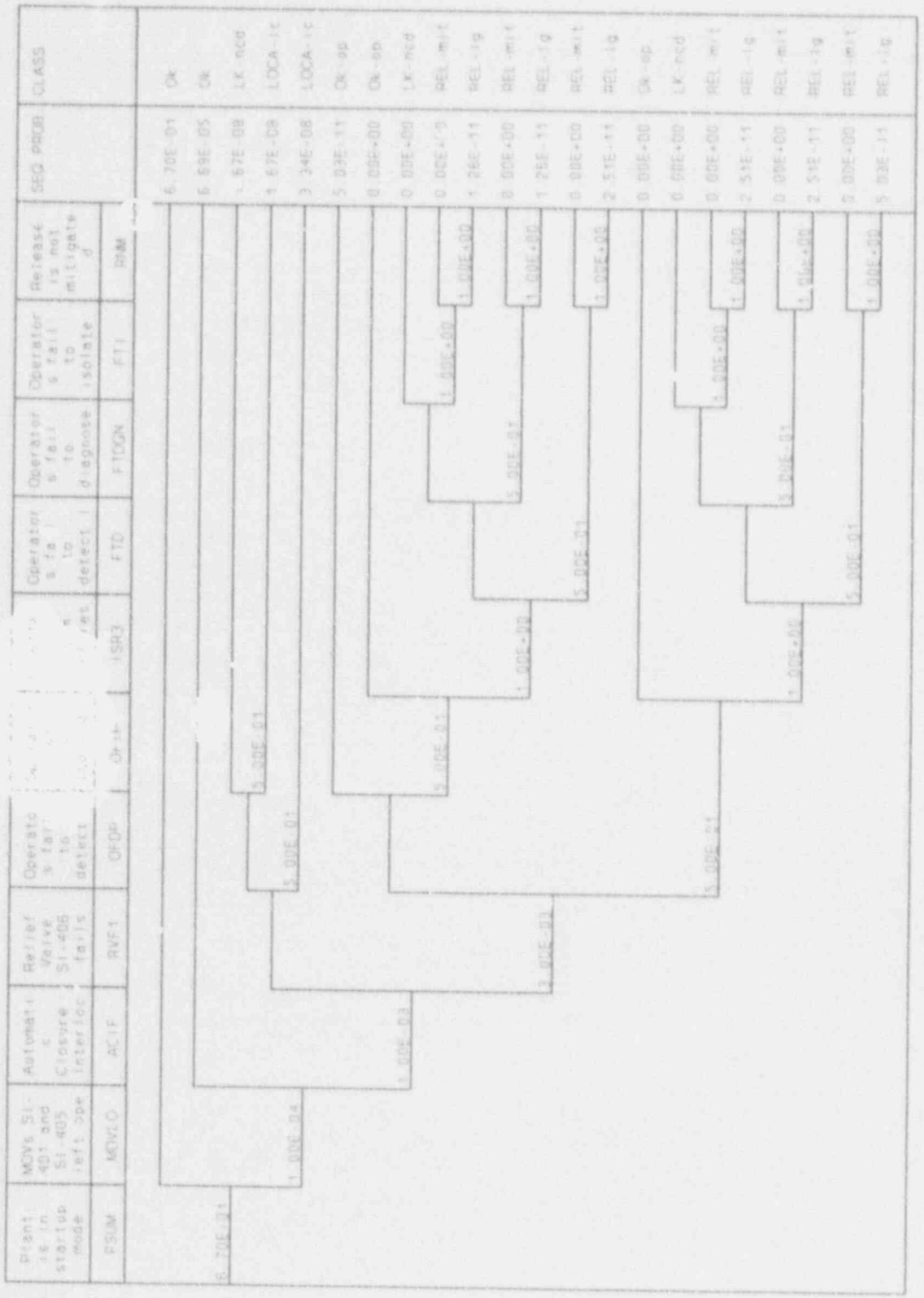

Figure 7. SDC system ISLOCA during startup (SEQ-1B).

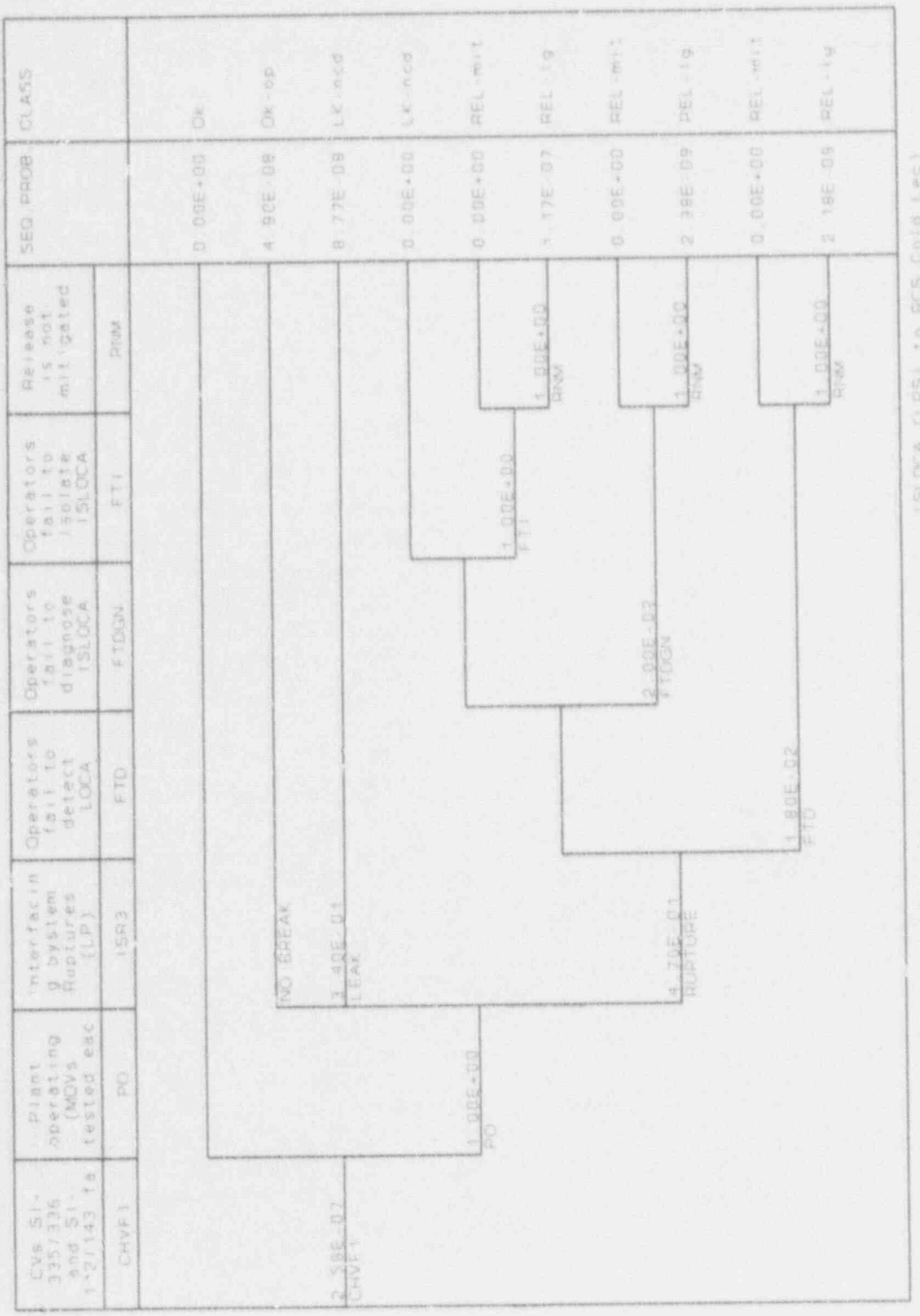

Figure 8. Event tree for LPSI cold leg discharge to RCS (SEQ-2).

the fact that the MOVs will be opened once each quarter.

Once again, if the isolation check valves protecting the MOVs had failed, it would not be desirable to open the MOVs. But, for this analysis, no prior knowledge for the system is assumed (see discussion in Section 4.1.3). Thus, for the model, random failure of the two isolation check valves is assumed to lead automatically to a demand on check valve SI-216. Figure 9 shows the event tree for this sequence.

4.1.5 RCS Cold Legs to HPSI (Header B)—SEQ-3B. Sequence 3B is comparable to Sequence 3A with the exception that Sequence 3B has one less check valve to protect the interfacing system. Whereas header A has check valve SI-216, header B does not have the corresponding check valve in the piping design. Figure 10 shows the event tree for this sequence.

4.1.6 RCS Hot Legs to HPSI (Header A)—SEQ-4A. Once every quarter MOVs SI-502A and SI-506A are stroke-tested. Therefore, Sequence 4A is based on the opening of MOV SI-502A. Since valve SI-502A is opened and closed before valve SI-506A is opened, the opening of SI-502A is defined as the initiating event for the sequence. Once again, the assumption of no prior knowledge of the condition of the system is used. Figure 11 shows the event tree for this sequence.

4.1.7 RCS Hot Legs to HPSI (Header B)—SEQ-4B. Sequence 4B is similar to Sequence 4A except that check valve SI-216 is missing from piping header B. The initiating event for Sequence 4B is the opening of MOV SI-502B. The initiating event probability is identical to that of Sequence 4A and is assumed to be 1.0. Figure 12 shows the event tree for this sequence.

4.1.8 RCS to LPSI During Shutdown—SEQ-5. When the analyzed plant enters shutdown cooling, the operators rely on check valves SI-108 and SI-1071 closing when the RCS pressure exceeds the interfacing system design pressure. Thus, Sequence 5 is based upon failure of the two check valves. Figure 13 shows the event tree for this sequence.

4.2 Human Reliability Analysis

This section summarizes the results of the ISLOCA HRA efforts. Appendix C provides detailed information regarding HRA fault trees, event trees, tabulated HEP values, and discussions of the HRA process. The HEPs presented as part of the HRA are estimates based upon the best contemporary models and quantitative techniques. As in any HRA, these HEPs must be considered in light of hardware failure information contained within this report and should not be used in isolation.

HRA was used to model the predominant human errors for each significant scenario in the ISLOCA PRA. As discussed in Section 2.5, HRA is a methodological tool that involves the quantitative analysis, prediction, and evaluation of work-oriented human performance. The ISLOCA HRA diagnosed those factors within the plant's systems that could lead to less than optimal human performance in the initiation, detection, diagnosis, and mitigation of ISLOCA scenarios. HRA was used as a diagnostic tool to isolate the error rate anticipated for individual tasks and to determine where errors were likely to be most frequent.

Because most of the human actions in this HRA involved the use of various written normal, abnormal, and emergency operating procedures, THERP-type HRA event trees were chosen for modeling most of the human actions in the detailed analysis. However, in several ISLOCA scenarios, HRA fault trees were used in conjunction with the typical THERP event trees to provide the best representation of the modeled events. Detailed analyses were conducted using the fault trees and/or THERP event trees to estimate the error probabilities and uncertainty ranges of the dominant human actions.

Individual error branches for each of the HRA event trees (see Section 2.5 or Appendix C for details) were quantified using techniques from

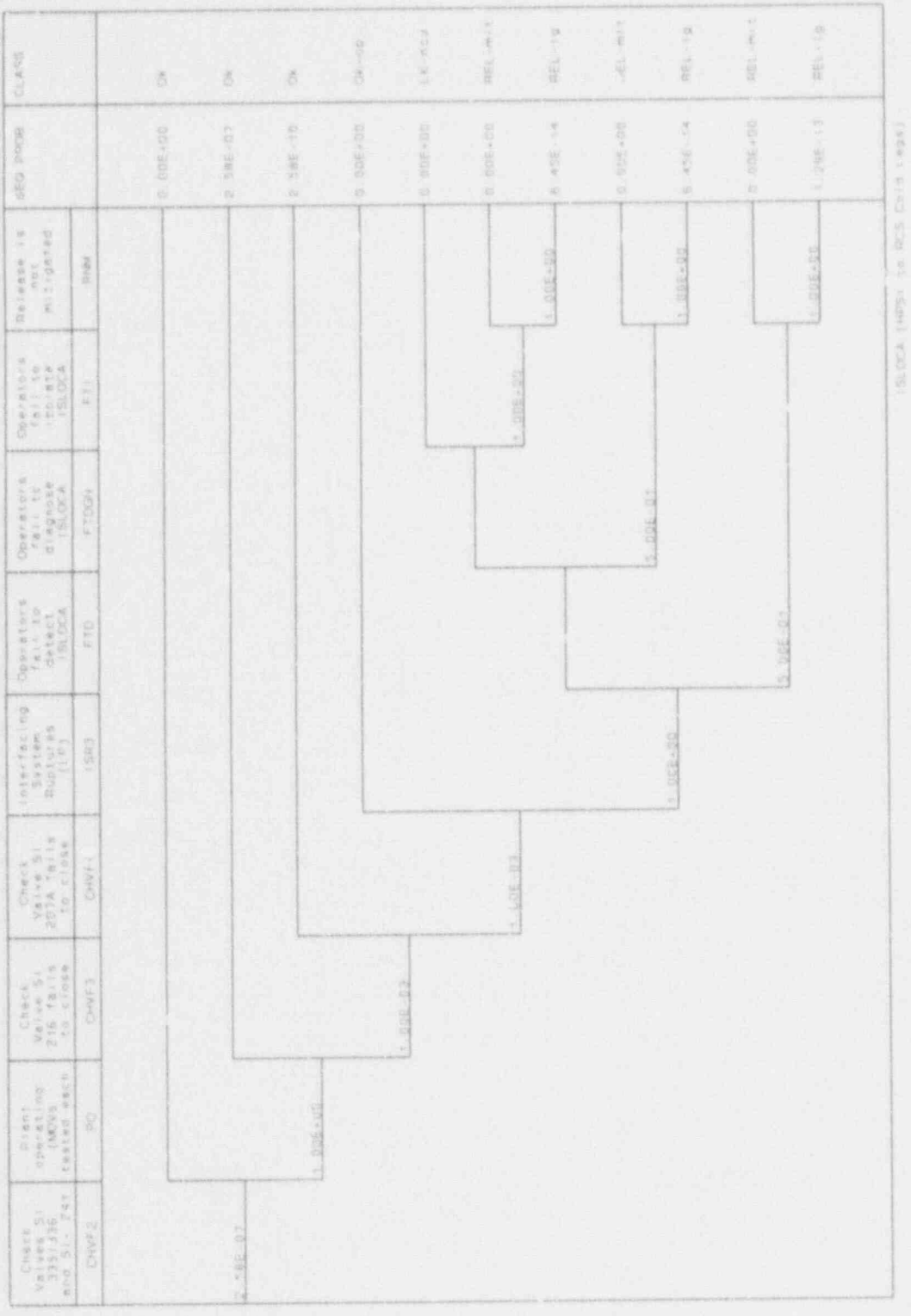

Figure 9. Event tree for HPSI header A cold leg discharge to RCS (SEQ-3A).

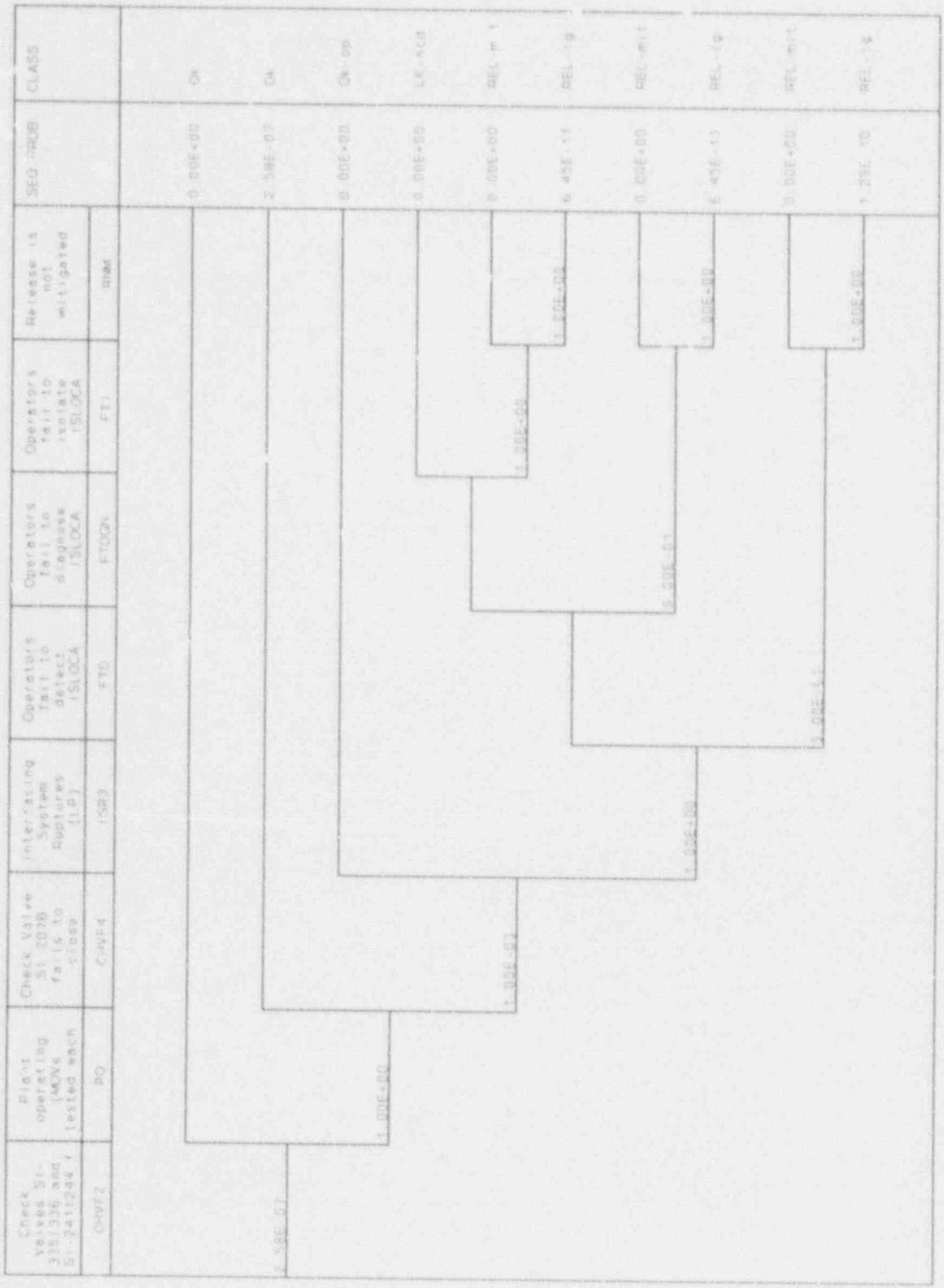

Figure 10. Event tree for HPSI header B discharge to RCS cold legs (SEQ-3B).

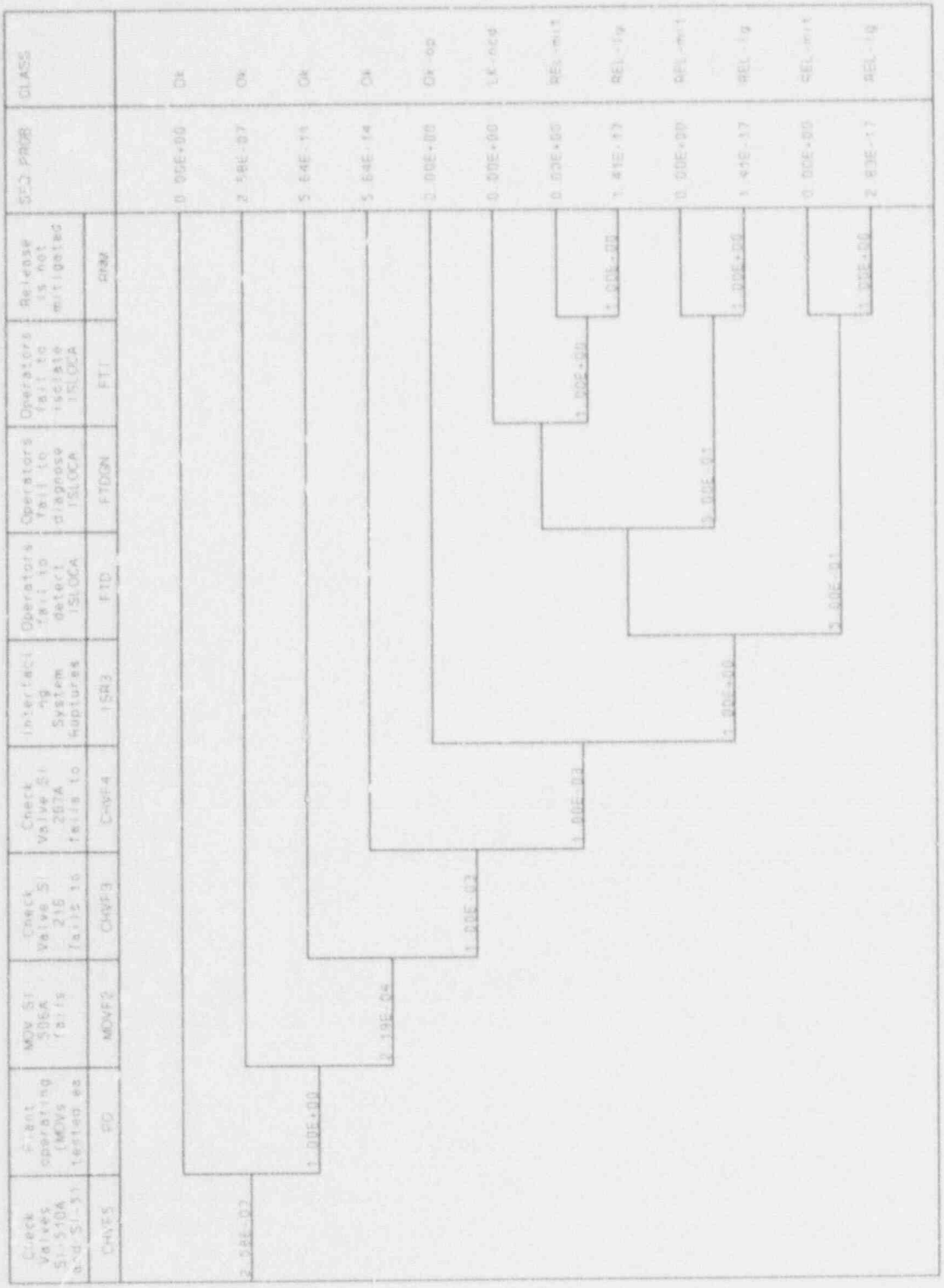

Figure 11. Event tree for HPSI header A discharge to RCS hot legs (SEQ-4A).

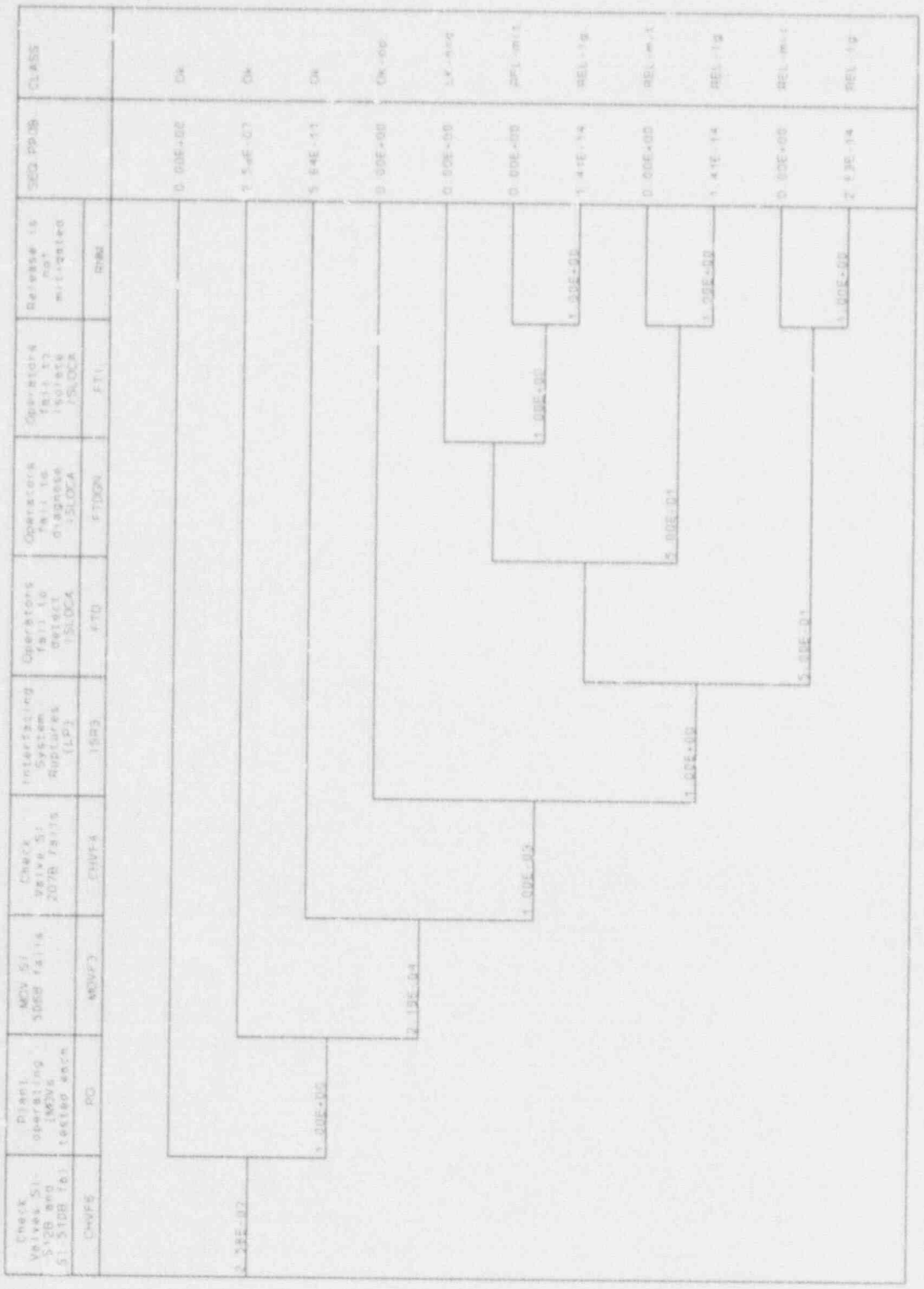

Figure 12. Event tree for HPSI header B discharge to RCS hot legs (SEQ-4B).

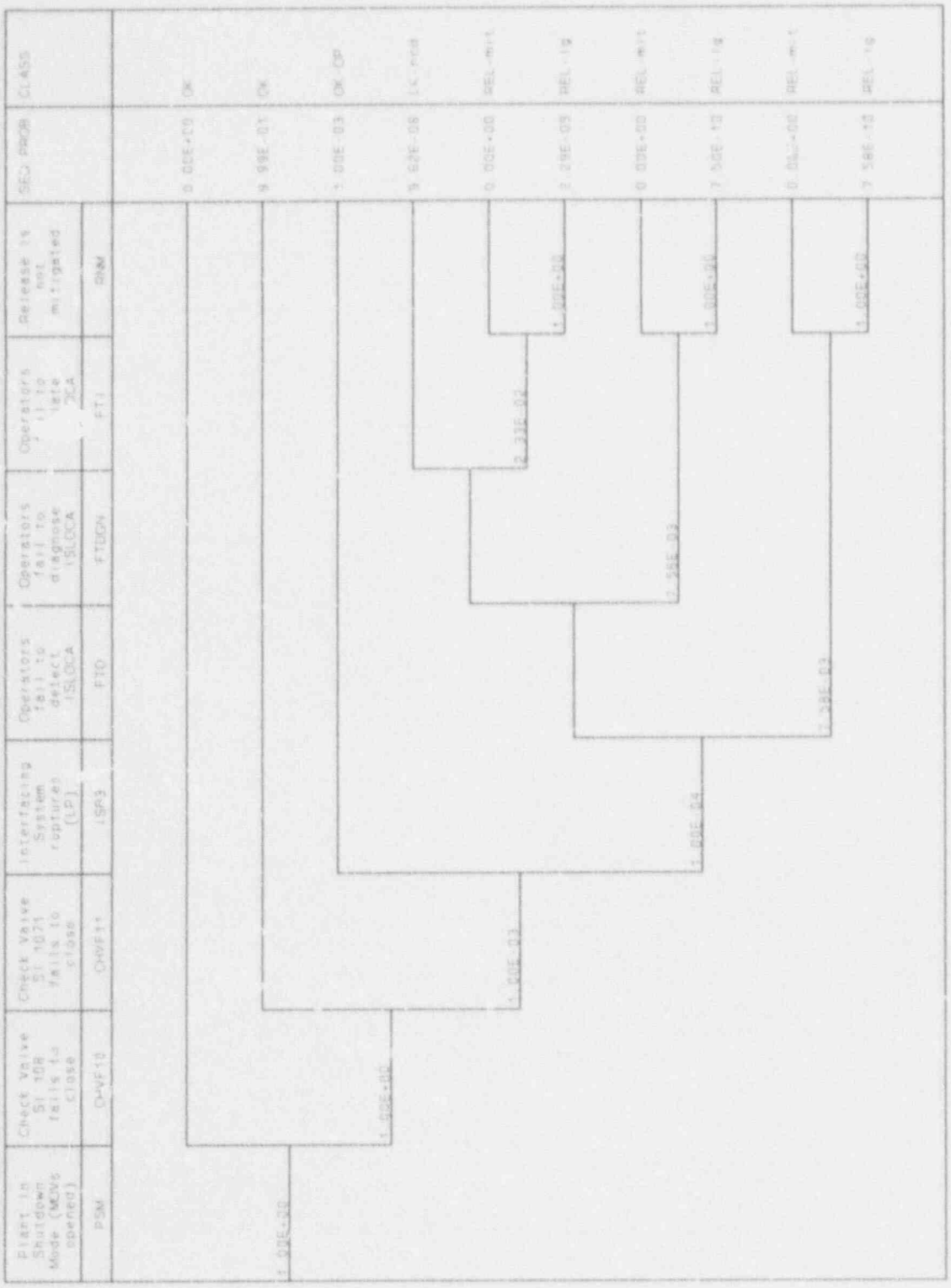

Figure 13. Event tree for RCS to LPSI during shutdown (SEQ-5).

THERP and HCR. Specific human actions on each error branch were assigned an estimate of the basic HEP. These basic HEP estimates were then modified using PSFs to realistically describe the work process at the plant. Finally, possible failure paths (i.e., sequences that included either single or multiple human errors leading to a failure of the action modeled by the HRA tree) were identified and combined to estimate the total failure probability for the HRA tree, in accordance with the THERP guidelines. Individual PSFs were derived from task analyses, time-line analyses, evaluation of the human/machine interface, and direct observations of operator performance. The majority of these PSFs were presented in the *ISLOCA Inspection Report* for the analyzed plant.[11] Each PSF was seen as casting either a positive or negative influence on the basic HEP, that is, as either decreasing or increasing the probability of failure for a given human action. For example, some of the positive PSFs in evaluations of the CE plant included the following.

- "The team did not identify any significant deficiencies in the man-machine interface that might significantly increase the probability of an operator error initiating an ISLOCA."[11]

- "The team found emergency operating procedures to be well written although they lacked some human factors considerations (see the second item in the negative PSFs listed below)."[11]

- "Although training specific to ISLOCAs was not part of the licensee's training program, operators indicated, during walkthroughs and simulator exercises, that they were *generally* well prepared to cope with losses of RCS inventory."[11]

Examples of negative PSFs were

- "The team identified weaknesses in the man-machine interface that could adversely affect the ability of the operators to mitigate an ISLOCA because of poor equipment labeling and the inaccessibility of some equipment."[11]

- Even though emergency operating procedures were generally well written, the RCS leak procedure, OP-902-002, does not provide relevant guidance with respect to requisite actions for the isolation of ISLOCAs. As a result, operators and supervisory personnel would be required to rely on knowledge-based actions, outside of normal procedures.

- Within the context of the prior training, operator training (based on Three Mile Island scenarios) emphasized that operators should not override a safety injection signal occurring in conjunction with an unisolated RCS leak (see Sequence 2). This training could lead control room personnel away from the actions necessary in Sequence 2 to isolate a break in the safety injection lines (e.g., operators would have to sequentially close each HPSI and LPSI safety injection valve on the affected SI train).

- Operators' ISLOCA diagnostic abilities were centered on Attachment 1 of GP-902-002, which verifies a LOCA outside containment but directs operators to a procedure (OP-902-002) that does not provide relevant guidance for the isolation of an ISLOCA.

A detailed HRA was conducted for each of the significant scenarios identified in the ISLOCA PRA. Tables 2 and 3 summarize the results of these analyses, which are extensively described in Appendix C. These tables provide the identifier and description for each significant human error, as well as the mean HEPs.

Inspection of these tables reveals that HEPs increase with time following an interfacing system rupture. These increasing error rates reflect the following circumstances identified for the CE plant. First, procedures may not effectively lead operators to the control room indications that are most relevant for detection of an ISLOCA, and do not provide definitive guidance for necessary and sufficient actions to isolate an ISLOCA in the two sequences that were modeled in detail.

Table 2. Estimated mean HEPs for Sequence 2.

Identifier	Human error	Mean HEP
FTD-LOCA	Control room fails to detect LOCA	0.018
FTDGN	Control room fails to diagnose ISLOCA	0.02
FTI	Control room fails to isolate ISLOCA	1.00

Table 3. Estimated mean HEPs for Sequence 5.

Identifier	Human error	Mean HEP
FTD	Operators fail to detect loss-of-coolant	0.0076
FTDGN	Operators fail to diagnose system leakage	0.0076
FTI-A	Fail to isolate (1 SDC in service)	0.0233
FTI-B	Fail to isolate (both SDC in service)	0.0233

Second, diagnostic abilities in the control room (e.g., procedures and training) rely on the diagnostic flow chart in Attachment 1 of OP-902-002, the RCS leak procedure. That flow chart can successfully diagnose a LOCA outside of containment, but also directs operators to use OP-902-002, with the drawbacks mentioned above. Therefore, operator workload is increased and significant stress (threat level) is likely to be experienced by the operators at the time when ISLOCA isolation actions are required.

4.3 Quantification of ISLOCA Model

Based on the event trees described in Section 4.1 (and in more detail in Appendix B), the total mean ISLOCA CDF for the plant is estimated to be 2.0×10^{-6} per reactor-year of operation. Table 4 provides a breakdown of this frequency by sequence and release category. The dominant scenario is hardware dominated, involving failure of the pressure isolation check valves in the LPSI cold leg discharge to the RCS (SEQ-2). This scenario is equivalent to the classical event-V category of core damage sequences that has been examined in some past PRAs. Note, however, that this sequence could be eliminated by modifying the stroke test procedure to require the operators to check for pressurization of the header between the discharge check valves prior to performing the stroke test. The relative insignificance of the human error-initiated sequences is due to the excellent administrative controls and safety culture present at the plant, for example, the practice of not defeating (jumpering out) equipment interlocks during normal operations and the tight control of keys needed to restore power to isolation valves.

The likely failure locations for Sequence 2 are the schedule 40 piping and the 10-inch, 300-psi flange at the discharge flow element. The flange failure probability was relatively high (0.69) because of the "soft" SA 193-B8 bolts that are used. Upgrading these bolts to SA 564 grade 630 would eliminate flange failure from consideration in this sequence. [As discussed in Appendix F, the probability of flange failure was partitioned into small leaks and large failures. The large failure probability of 0.12 was used in calculating the split fraction used in the event tree for this

Table 4. ISLOCA CDF (per reactor-year).

Scenario	CDF	REL-lg	REL-mit	LOCA-ic	LK-ncd	OK-op
1A	ε[a]	ε	0.0	ε	ε	ε
1B	ε	ε	0.0	ε	ε	ε
2	2.0E−06	2.0E−06	0.0	0.0	1.4E−06	7.8E−07
3A	ε	ε	0.0	0.0	ε	0.0
3B	ε	ε	0.0	0.0	ε	0.0
4A	ε	ε	0.0	0.0	ε	0.0
4B	ε	ε	0.0	0.0	ε	0.0
5	ε	ε	0.0	0.0	9.6E−08	1.0E−03
Totals	2.0E−06	2.0E−06	0.0	ε	1.5E−06	1.0E−03

a. ε $<10^{-8}$/year.

sequence. Small leaks were judged to be recoverable by the operator (see Appendix C for more details) and were binned into the LK-ncd end state on the event tree.]

Sequence 5 was the major contributor to ISLOCA risk in the initial screening analysis because the frequency of pressurizing the low-pressure system beyond its design pressure was approximately 10^{-3}/year; however, detailed analysis of the component pressure fragility showed that small flange leaks are the only credible overpressure failure modes for this sequence, and the probability of even these small leaks is extremely small ($<10^{-4}$/flange). The components contributing to the rupture probability are the 150-psi flanges at check valves SI-107 (suction from RWSP) and SI-407 (suction from containment sump). (Refer to Appendix H for the details of the component pressure fragility analysis.) This sequence would also appear to be driven by hardware failures; however, the hardware failure of concern is the demand failure of check valves SI-108 A and B. A demand failure probability of 1.0 was assumed for these valves, based on their as-found condition at the plant and the complete lack of testing or maintenance on these valves at the time of the inspection. Were these valves to receive regular leak-testing and some form of periodic maintenance (e.g., disassembly to inspect for boric acid precipitation and corrosion), a generic demand failure probability of 10^{-3} could be justified. The Impelh analysis of these flanges also showed that the leak rates would be far too small to threaten core cooling. However, the HRA for this sequence was done before these results were available, so operator response to a small break was modeled. Even with this additional conservatism, the CDF from this sequence is $<10^{-8}$/year. Had the flange failure probability been higher, the probability that the failure results in a leak large enough to threaten core cooling would have had to be factored into the CDF calculation.

4.4 Risk Assessment

As described in Section 2.6, the offsite consequences of ISLOCA core damage sequences were estimated using the V-sequence source term from the June 1989, NUREG-1150 analysis of Sequoyah (see Appendix G for details of the consequence analysis). The conditional consequences for the base case analysis are listed in Table 5. Based on information from the NUREG-1150 program that estimated decontamination factors (DFs) for both dry and wet containment bypass releases, a DF of 1 (no decontamination) is assumed for the release from the auxiliary building (large dry release) in the base case. Additional work on estimating DFs for the auxiliary building has been sponsored by the Electric Power Research Institute (EPRI) using the Modular Accident Analysis Program (MAAP) code.[a] This work would seem to support DFs for a dry release in the range of 3 to 80, depending on the specific configuration of the auxiliary building. Wet release DFs, either due to a flooded break location or scrubbing by general area fire sprays in the auxiliary building, ranged from 40 on up. However, the MAAP code, when the core flow blockage feature is used (as it was for the EPRI work), tends to predict relatively little hydrogen generation in-vessel. Hydrogen generated in-vessel, if released into the auxiliary building, could burn, potentially opening pathways for free convective exchange with the outside environment, thus reducing the effective auxiliary building DF. The effect of a credible range of DFs on the offsite consequences is examined in Section 4.5.

When reviewing the ISLOCA consequence and risk estimates, several aspects of this calculation should be kept in mind. Many measures of risk are available and have been used in recent studies. However, to produce these estimates, many sequence-specific and site-specific assumptions must be made, from the cost of land to the warning time available to activate the offsite emergency response plan before a release occurs. These assumptions can have significant effects on the consequences calculated with MACCS. The base case ISLOCA risks are shown in Table 6.

4.5 Uncertainty and Sensitivity Study Results

No uncertainty analysis was performed for the dominant ISLOCA scenarios because the best-estimate CDF is relatively low and almost all of the uncertainty is contained in the initiating event of Sequence 2, failure of the two series check valves. The error factor on this initiating event is 100; therefore, the CDF distribution will have a

a. Electric Power Research Insutute, *Evaluation of the Consequences of Containment Bypass Scenarios*, EPRI-NP-6586-L, November 1989. This report contains proprietary information that is not available to the general public; however, the results of this study were made available to the INEL analysts for review.

Table 5. Base case ISLOCA consequences conditional upon severe core damage.

Mean early fatalities	Mean latent fatalities	Mean 50-mi dose (person-rem)
9.99E+1	5.36E+3	6.12E+6

Table 6. Base case ISLOCA risk (per reactor-year).

Mean early fatalities	Mean latent fatalities	Mean 50-mi dose (person-rem)
2.0E−4	1.1E−2	1.22E+1

large, positive skewness coefficient, indicating that the reported mean CDF will be close to the 95th percentile value.

Based on similar results obtained for the Westinghouse plant,[16] the uncertainty in CDF should span approximately four orders of magnitude.

4.5.1 Component Rupture Pressure Uncertainty. The base case analysis used a logarithmic standard deviation of 0.36 for the pipe rupture pressure distribution (which was modeled as lognormal). As discussed in Appendix H, this value is derived by assuming that the probability of component failure is 10^{-3} when applied stress equals yield stress. This may be an overly conservative assumption; however, sensitivity cases were examined in References 5 and 16 in which the probability of component failure at yield stress was taken to be 10^{-4} and 10^{-5}. These values correspond to a logarithmic standard deviation for the pipe rupture pressure of 0.30 and 0.26, respectively. The rupture probabilities were recalculated, with the result that there was not a significant effect on CDF. Because the piping materials are the same in the CE plant as in the Babcock and Wilcox and Westinghouse plants, this result should apply to the CE plant, also. Therefore, no detailed calculations were performed.

4.5.2 Auxiliary Building DF Uncertainty. Uncertainty due to lack of knowledge was treated via a sensitivity analysis that examined the effects of a range of credible auxiliary building DFs on fission product source terms and offsite consequences. The details of this analysis can be found in Appendix G. The important aspects and results of this analysis are summarized below.

For the dry ISLOCA sequences, the base case DF for all release classes had a uniform value of 1 and the release was at ground-level. The sensitivity analysis involved calculating new fission product source terms with uniform-valued DFs of 5, 10, 50, and 100 for all release classes except the noble gases, for which the base case DF of 1 was retained. For the first two calculations, with DFs of 5 and 10, a ground-level release was assumed. For the last two calculations, with DFs of 50 and 100, the release elevation was specified as 10 m. The reason for the change in release elevation is that industry-sponsored analyses of auxiliary building DFs show that higher DFs, in the absence of water-scrubbing, are produced when there is a lack of free convective exchange with the outside environment. This generally corresponds to having an opening high up in the auxiliary building, with a release from the reactor coolant system in the lower elevations of the building.

Sensitivity cases also were run to examine the potential effects of auxiliary building fire sprays on the release (there are no such sprays at the plant analyzed in this report). In these so-called wet ISLOCA sequences, the base case DF was specified as a distribution that was sampled upon, as in the NUREG-1150 analysis of Sequoyah. The distribution is shown in Table 7 for the base

Table 7. Distribution of DF for the base case analysis of the wet ISLOCA sequences as specified in the SEQSOR input.

Distribution of DF (%)	DF
0	5.1E+03
1	4.5E+03
5	4.1E+03
25	1.3E+02
50	6.2E+00
75	3.0E+00
95	1.8E+00
99	1.7E+00
100	1.6E+00

case analysis of the wet sequences. As was done for the dry sequences, sensitivity analyses were performed with uniform-valued DFs of 5, 10, 50, and 100 for all release classes except the noble gases, for which the DF remained at the base case value of 1. For the first two sensitivity calculations, with DFs of 5 and 10, a ground-level release was assumed. For the calculations with DFs of 50 and 100, calculations were performed with the release elevation specified both at ground level and 10 m.

Tables 8 and 9 present the mean conditional consequence results for the dry and wet ISLOCA sequence sensitivity cases, respectively. These results are also presented graphically in Figures 14 through 19. Comparisons of the dry and wet sequence consequence results are also presented graphically in Figures 20 through 22.

Table 8. Mean MACCS consequence results for each dry ISLOCA sequence sensitivity.

Sensitivity Case				
DF	Release elevation	Mean early fatalities	Mean latent fatalities	Mean 50-mi dose (person-rem)
1	0.0	9.99E+01	5.36E+03	6.12E+06
5	0.0	1.63E+00	1.82E+03	2.15E+06
10	0.0	4.03E−01	1.17E+03	1.55E+06
50	10.0	7.12E−02	5.16E+02	8.83E+05
100	10.0	6.10E−02	3.97E+02	7.24E+05

Table 9. Mean MACCS consequence results for each wet ISLOCA sequence sensitivity.

Sensitivity case				
DF	Release elevation	Mean early fatalities	Mean latent fatalities	Mean 50-mi dose (person-rem)
Base[a]	0.0	3.69E+00	1.71E+03	2.08E+06
5	0.0	9.92E−01	1.49E+03	1.79E+06
10	0.0	4.01E−01	9.85E+02	1.37E+06
50	0.0	1.76E−01	4.43E+02	7.78E+05
50	10.0	1.18E−01	4.51E+02	7.86E+05
100	0.0	1.59E−01	3.51E+02	6.40E+05
100	10.0	1.06E−01	3.56E+02	6.46E+05

a. Wet sequence base case DF is a sampled distribution as given in Table 7.

Figure 14. Mean early fatality consequence results as a function of DF for the dry ISLOCA sequences.

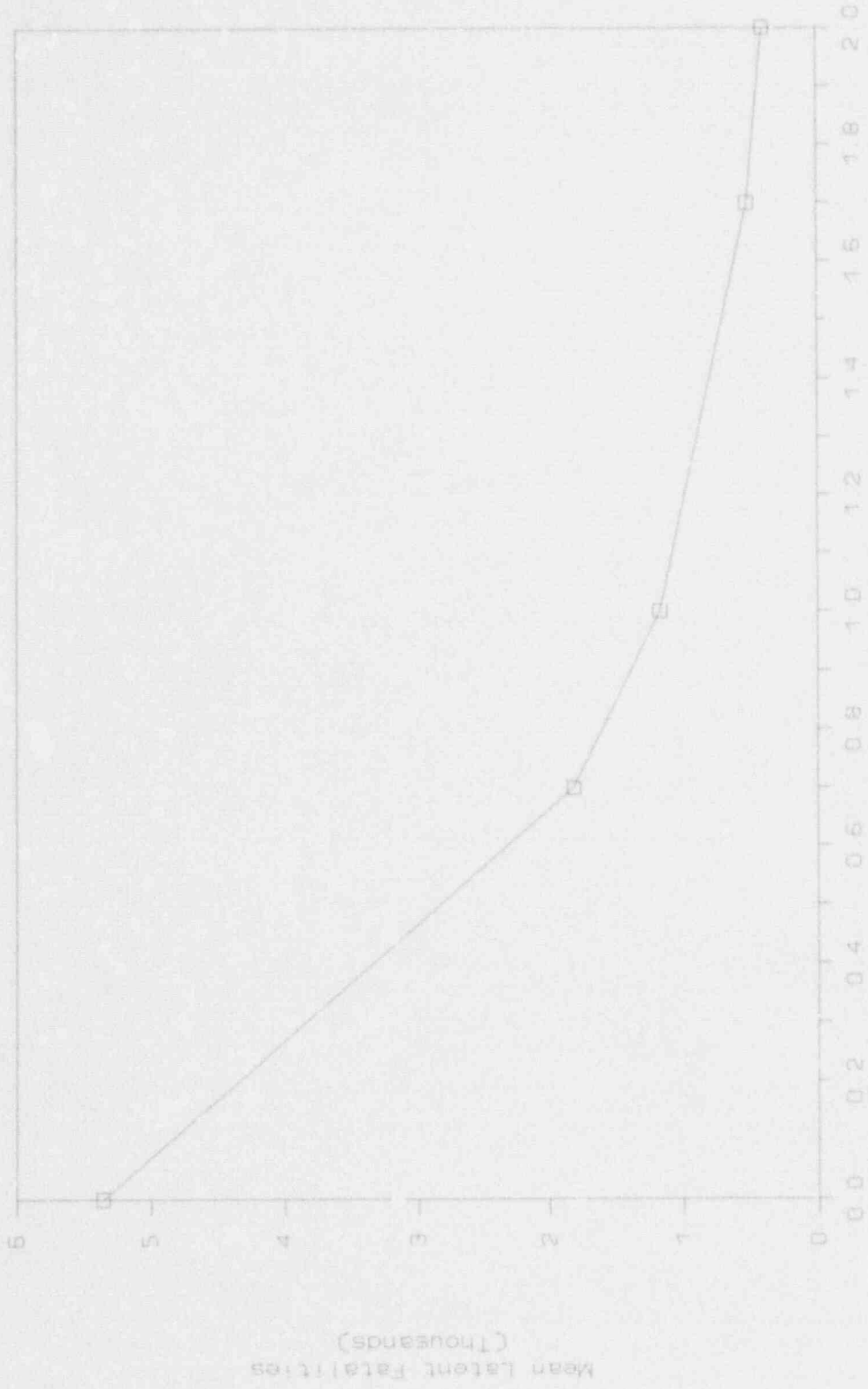

Figure 15. Mean latent fatality consequence results as a function of DF for the dry ISLOCA sequences.

Figure 16. Mean 50-mi population dose consequence results as a function of DF for the dry ISLOCA sequences.

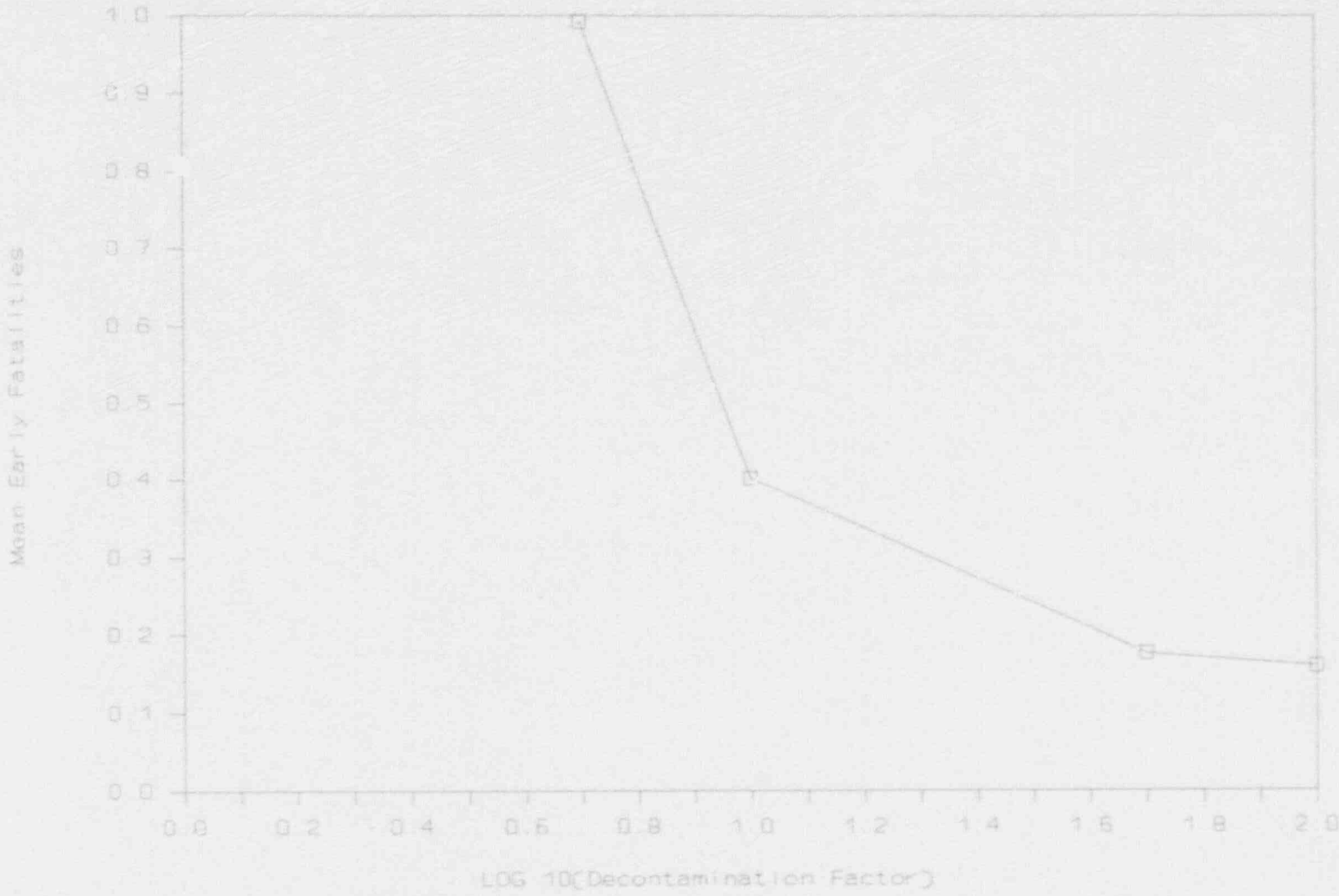

Figure 17. Mean early fatality consequence results as a function of DF for the wet ISLOCA sequences (all release elevations are 0.0 m).

Figure 18. Mean latent fatality consequence results as a function of DF for the wet ISLOCA sequences (all release elevations are 0.0 m).

Figure 19. Mean 50-mi population dose consequence results as a function of DF for the wet ISLOCA sequences (all release elevations are 0.0 m).

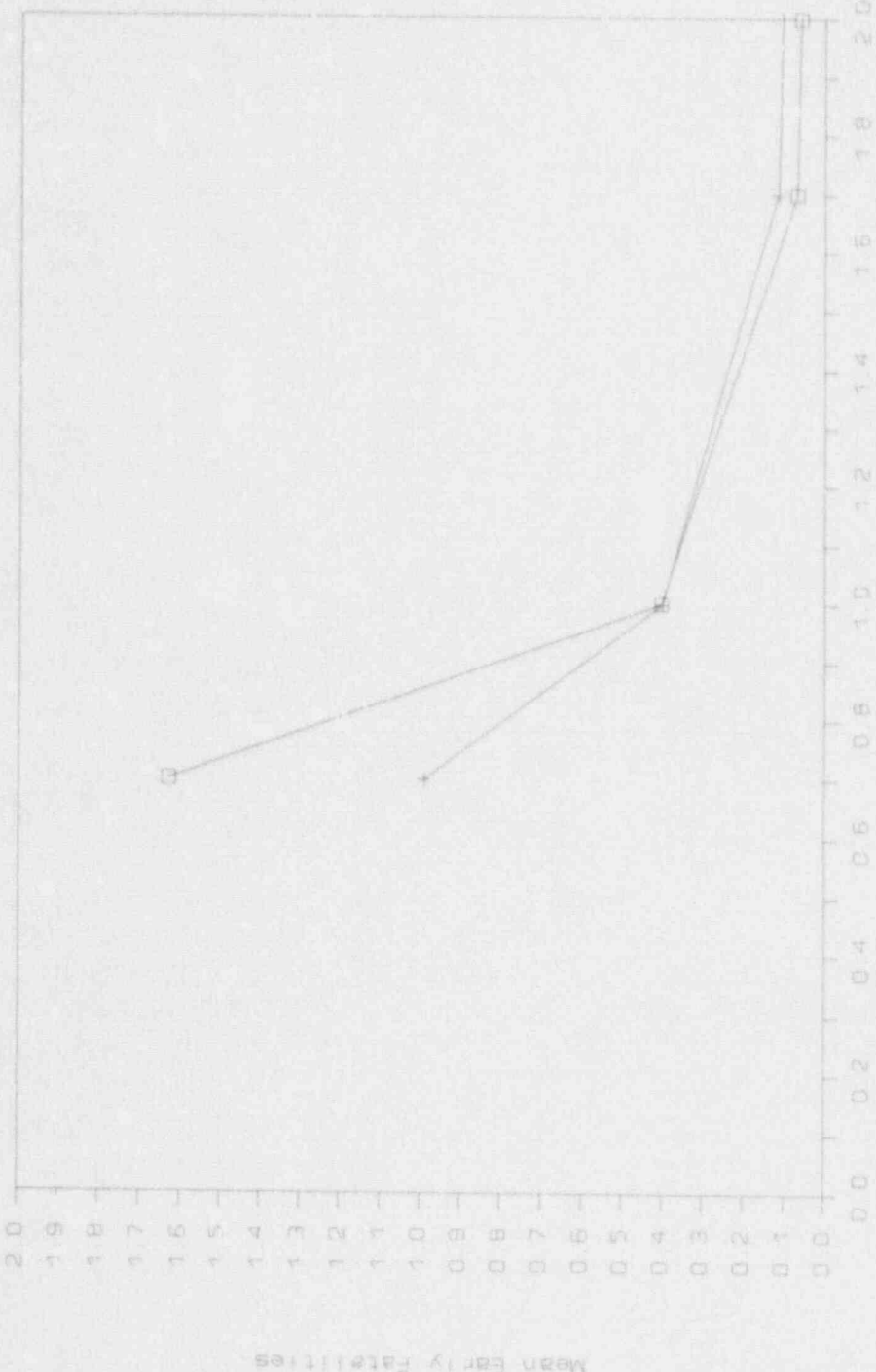

Figure 20. Comparison of dry and wet ISLOCA sequence mean early fatality consequence results as a function of DF (release elevation is 100 m for DFs of 50.0 and 100.0, otherwise elevation is 0.0 m).

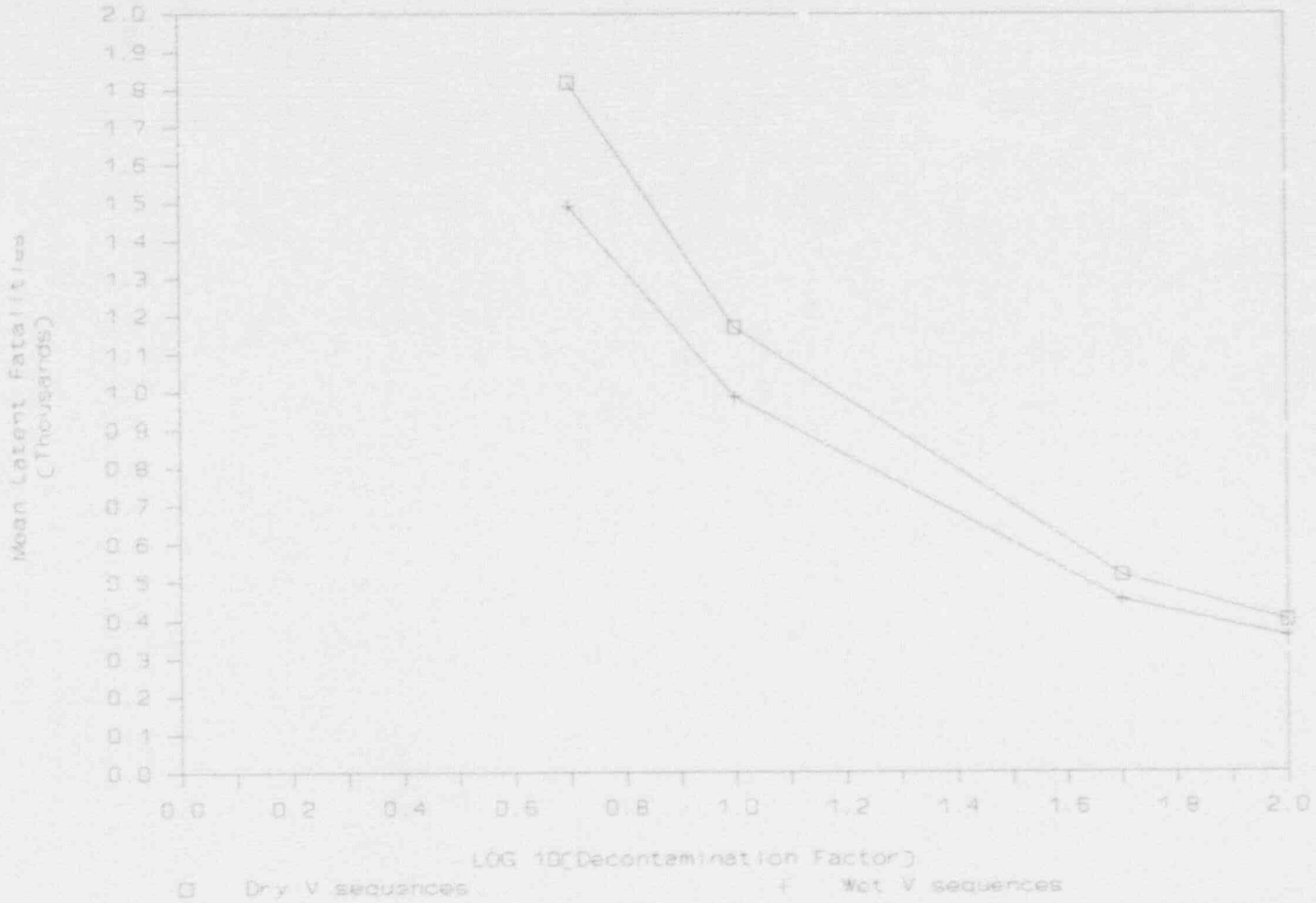

Figure 21. Comparison of dry and wet ISLOCA sequence mean latent fatality consequence results as a function of LF (release elevation is 10.0 m for DFs of 50.0 and 100.0, otherwise elevation is 0.0 m).

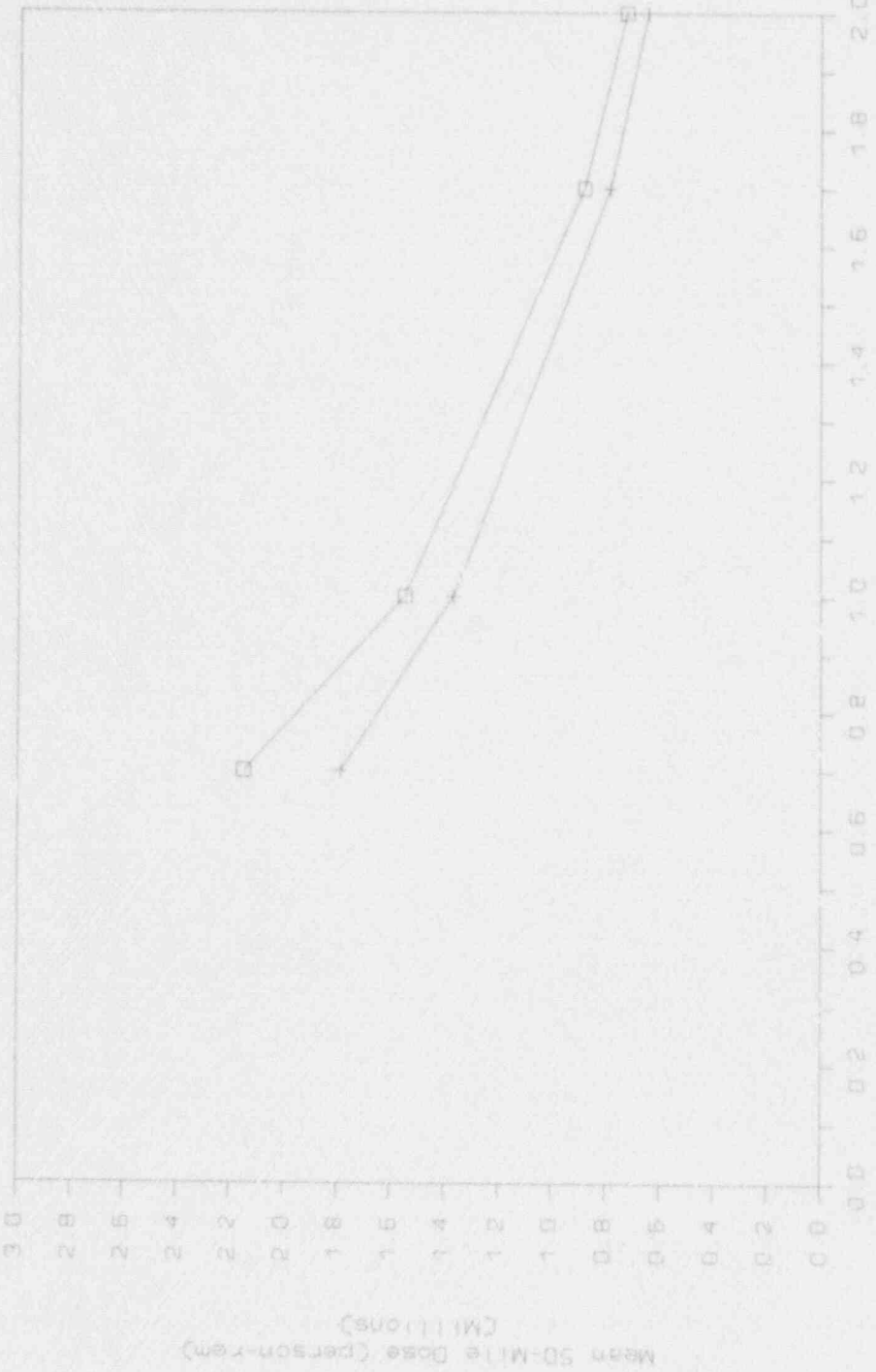

Figure 22. Comparison of dry and wet ISLOCA sequence mean 50-mi population dose consequences as a function of DF (release elevation is 10.0 m for DFs of 50.0 and 100.0, otherwise elevation is 0.0 m).

5. CONCLUSIONS

The methodology for evaluating ISLOCA risk that was developed in *Assessment of ISLOCA Risks—Methodology and Application to a Babcock and Wilcox Plant*[5] has been applied to a CE plant with a dry, atmospheric-pressure containment. This methodology has been successful in providing insights regarding the *relative* contributions of both hardware faults and human actions to ISLOCA CDF. The results indicate that human errors of commission, latent faults of equipment, and normal procedural tasks can combine in an ISLOCA sequence. However, the methodology also was used to identify potential means of reducing these contributions to risk. Conclusions are presented below, followed by a preliminary discussion of the relationship of these results to the general population of NPPs.

5.1 Plant-Specific Conclusions

A publicly available PRA of the analyzed plant has not yet been completed by the licensee. Therefore, no comparison could be made of the results of this analysis with results obtained by the licensee.

In the pressure fragility analysis of the interfacing systems, existing relief valves were found to provide very little protection against the dominant ISLOCA initiator (SEQ-2). Typically, relief valves in the interfacing systems are designed to mitigate the occasional pressure transient associated with routine valve realignments and pump starts and stops. The pressures generated in ISLOCA events simply overwhelm the relatively small relief capacity of these valves.

The Idaho National Engineering Laboratory HRA found that operator error could contribute to ISLOCA initiators. However, risk-significant human error initiators were judged unlikely during operations involving interfacing systems. This is due, in part, to the existence of significant administrative procedures and related operator training, as well as the presence of well-controlled interlocks that prevent the inadvertent operation of those pressure isolation valves under operator control. The HRA found a higher probability for operator error during detection, diagnosis, and isolation of an ISLOCA. This results from an interaction of the following variables:

- A limited number of clear control room indications for ISLOCA
- Emergency procedures that do not address isolation of a break outside containment
- Limited amount of time in the dominant scenario for the detection, diagnosis, and isolation of ISLOCA before core uncovery
- Operator exposure to high workload and threat stress at the time when actions to isolate an ISLOCA are needed.

5.2 General Conclusions

Extreme caution should be exercised when attempting to extrapolate the results of a single analysis to estimate the performance of the entire commercial nuclear power industry. The analysis of the CE plant in this report has identified some potential ISLOCA issues, but the completeness and typicality of the results, even for other CE plants, has not been determined. The analysis of this plant indicates that the most important concern regarding ISLOCA risk centers on the lack of procedural guidance for responding to an ISLOCA, rather than on the plant personnel. However, it is imprudent to conclude that human errors, while not important ISLOCA initiators at the plant analyzed in this report, will not dominate the ISLOCA risk for other plants. Therefore, a major emphasis in any evaluation of ISLOCA should be the assessment of the potential for human error initiators. Specifically, this involves judging the adequacy of plant procedures and personnel training and awareness of the potential for and consequences of an ISLOCA. To generalize, the plant personnel's understanding of the importance of maintaining the pressure isolation

boundary, and recognizing the potential for an ISLOCA and its consequences, can have a dramatic impact on ISLOCA risk. In the case of the CE plant analyzed in this report, the detailed HRA considering these effects eliminated human error-initiated ISLOCAs from detailed consideration, whereas at the Babcock and Wilcox plant,[5] the effect was just the opposite; the dominant ISLOCA sequence was initiated by a human error of commission.

6. REFERENCES

1. U.S. Nuclear Regulatory Commission, *Reactor Safety Study—An Assessment of Accident Risks in U.S. Commercial Nuclear Power Plants*, WASH-1400, October 1975.

2. U.S. Nuclear Regulatory Commission, *Severe Accident Risks: An Assessment for Five U.S. Nuclear Power Plants*, NUREG-1150, June 1989.

3. G. Bozoki et, al., *Interfacing Systems LOCA: Pressurized Water Reactors*, NUREG/CR-5102, BNL-NUREG-52135, February 1989.

4. T-L. Chu, S. Stoyanov, and R. Fitzpatrick, *Interfacing Systems LOCA: Boiling Water Reactors*, NUREG/CR-5124, BNL-NUREG-52141, EGG-2608, February 1989.

5. W. J. Galyean and D. I. Gertman, *Assessment of ISLOCA Risks—Methodology and Application to a Babcock and Wilcox Nuclear Power Plant*, NUREG/CR-5604, EGG-2608, April 1992.

6. T. G. Ryan, "A Task Analysis Linked Approach for Integrating the Human Factor in Reliability Assessment of NPP," *Reliability Engineering and System Safety*, 22, 1988.

7. A. Swain and H. Gutman, *Handbook of Human Reliability Analysis with Emphasis on Nuclear Power Plant Applications*, NUREG/CR-1278, August 1983.

8. G. Hannaman and A. Spurgin, *Systematic Human Action Reliability Procedure (SHARP)*, EPRI NP-3583, Electric Power Research Institute, 1984.

9. Institute of Electrical and Electronics Engineers, *A Guide for General Principles of Human Action Reliability Analysis for Nuclear Power Generation Stations*, IEEE Draft Standard P1082/D7, August 1989.

10. G. W. Hannaman, A. Spurgin, and Y. Lukic, *Human Cognitive Reliability Model for PRA Analysis*, NUS-4531, Electric Power Research Institute, 1984.

11. J. Ball, *ISLOCA Inspection Report 50-382/90-200*, U.S. Nuclear Regulatory Commission, Washington D.C., September 14, 1990.

12. Science Applications International Corporation, *ETA-II, Version 2.0*, Los Altos, California, 1990.

13. D. I. Chanin, et al., *MELCOR Accident Consequence Code System (MACCS)*, NUREG/CR-4691, February 1990.

14. J. Gregory, et al., *Evaluation of Severe Accident Risks: Sequoyah Unit 1*, NUREG/CR-4551, Vol. 5, Rev. 1, draft report for comment, June 1990 (available from Public Document Room Washington D.C.).

15. D. C. Aldrich, et al., *Technical Guidance for Siting Criteria Development*, NUREG/CR-2239, SAND81-1549, 1982.

16. D. L. Kelly, J. L. Auflick, and L. N. Haney, *Assessment of ISLOCA Risks—Methodology and Application to a Westinghouse Four-Loop Ice Condenser Plant*, NUREG/CR-5744, EGG-2649, April 1992.

Appendix A

System Descriptions

Appendix A
System Descriptions

The plant analyzed for this report is a single-unit site. The unit is a 3390 Mwt pressurized water reactor (PWR), with an NSSS supplied by Combustion Engineering (CE). The unit has a large dry containment that is maintained at atmospheric pressure and a separate reactor auxiliary building and turbine building.

The plant is similar to other CE plants in the number and type of charging and safety injection pumps.

A.1 Reactor Coolant System

The reactor coolant system (RCS) transfers energy from the reactor core to the secondary water in the steam generators. The RCS pressure boundary acts as a barrier (one of several) against the uncontrolled release of radioactive material from the reactor core and primary coolant.

During power operation, primary coolant in the RCS is circulated by one reactor coolant pump in each of the four cold legs. Pressure is maintained within a prescribed band by the combined action of the pressurizer heaters and sprays. RCS inventory is maintained within a prescribed band by the chemical and volume control system (CVCS), otherwise known as the charging system.

Component Information

A. RCS
   1. Volume: 10,300 ft^3 excluding pressurizer and surge line
   2. Nominal operating pressure: 2235 psig

B. Steam generators (2)
   1. Type: vertical shell and U-tube
   2. Model: CE

A.2 Interfacing Systems

All interfacing systems were screened to identify those systems that needed further evaluation. The criterion used in screening was that any system with an interfacing pipe diameter larger than one inch should be evaluated. The one-inch pipe size was selected based on an estimation of the discharge from a one-inch high pressure pipe break, which was about 200 gpm. A 200-gpm leak rate outside of the containment is considered to be critical based on: the capacity of the RWSP (Technical Specification minimum volume of 443,000 gal), the capacity of three charging pumps (132 gpm), and the normal makeup rate to the RWSP (~150 gpm). Based on these considerations and the number of hours it would take for the plant to achieve cold shutdown (conservatively assumed to be about 10 hours), leak rates of 200 gpm or less were judged not to be risk-significant.

The initial screening resulted in the selection of the safety injection (SI) system, including the low pressure safety injection system, and the shutdown cooling system. Figures A.1 through A.6 are schematic diagrams showing the hardware configuration of the safety injection system.

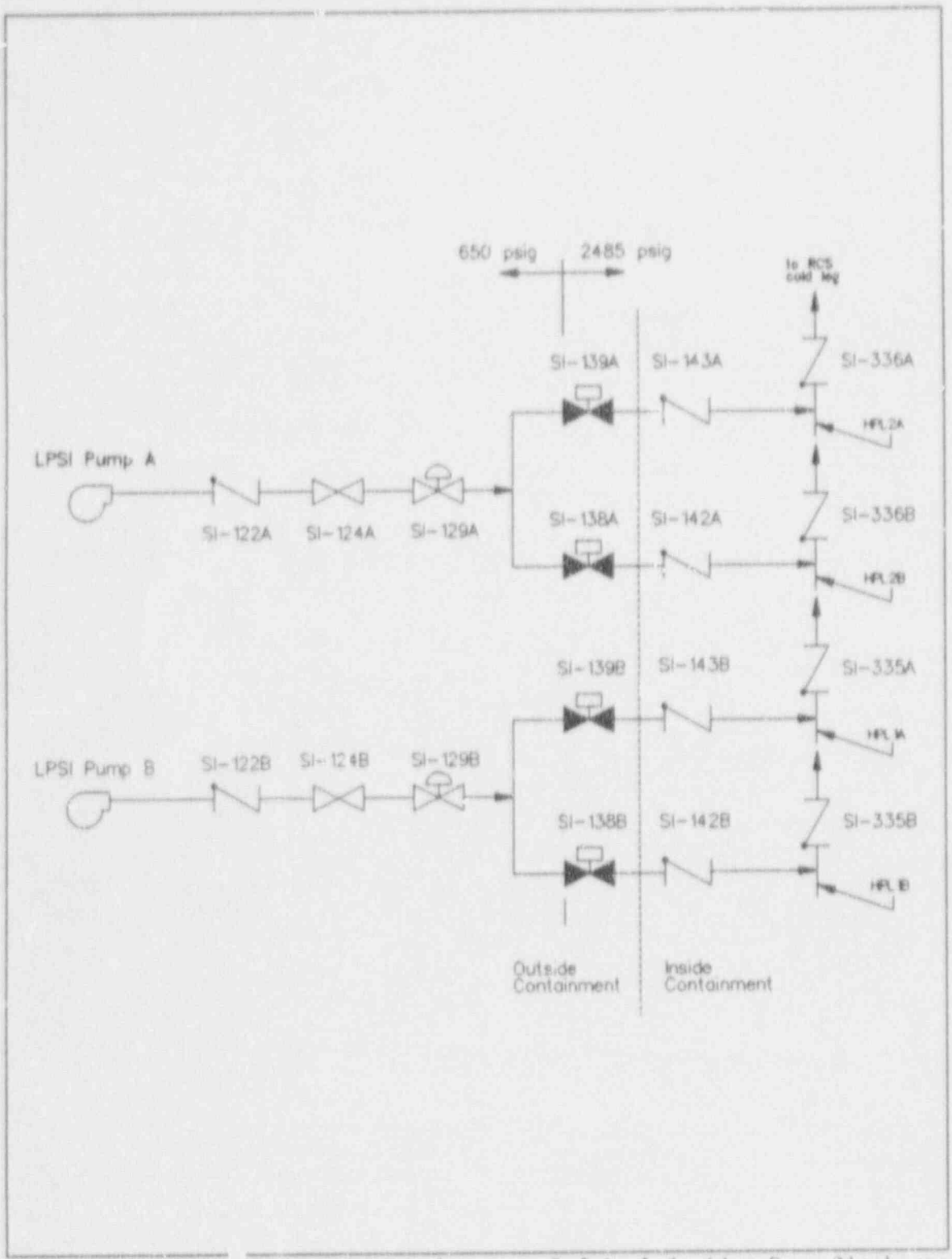

Figure A.1 : RCS Cold Legs to Low Pressure Safety Injection Pump Discharge Schematic.

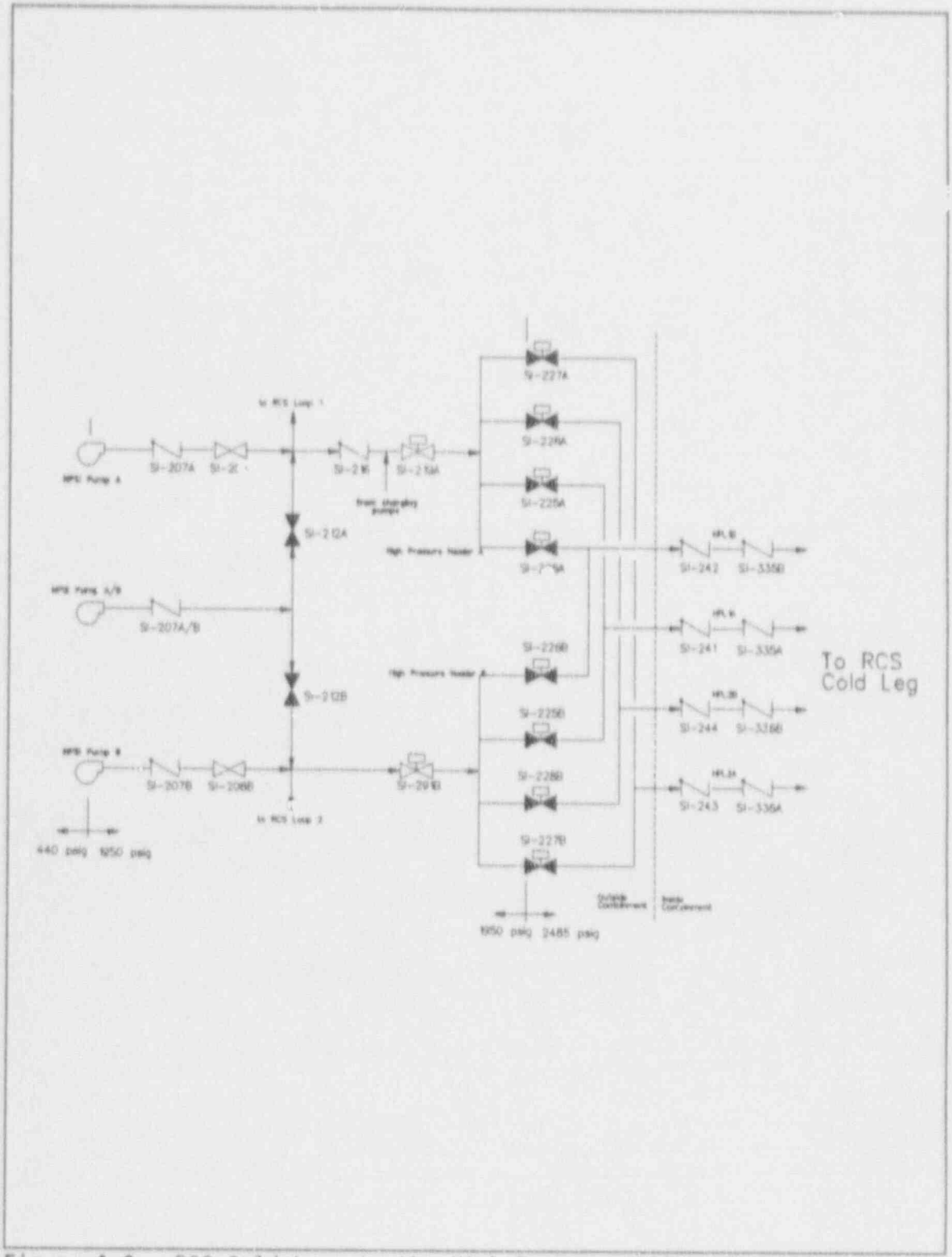

Figure A.2 : RCS Cold Legs to the High Pressure Safety Injection Pump Discharge Flow Diagram.

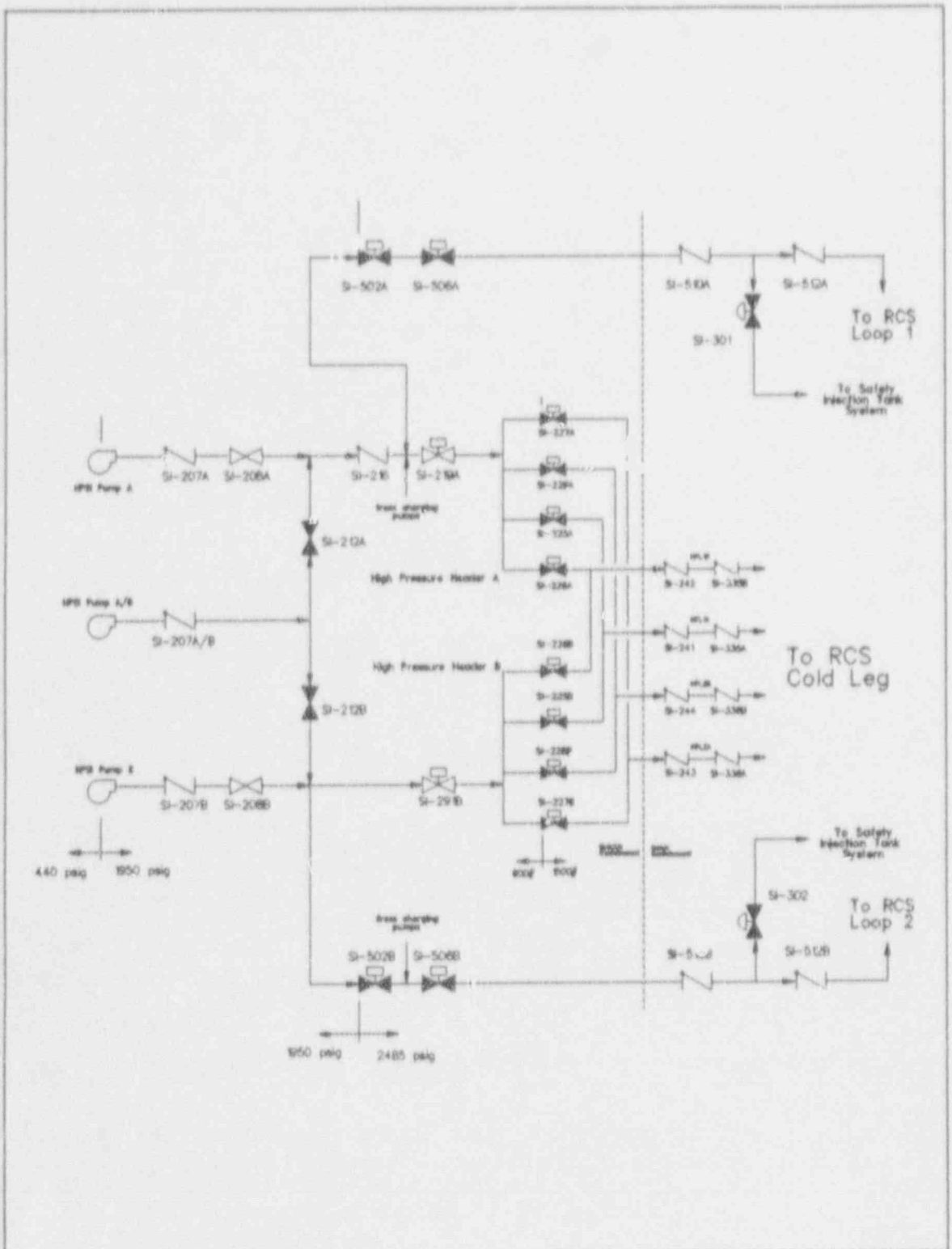

Figure A.3 : RCS Hot Legs to High Pressure Safety Injection Pump Discharge Line Schematic

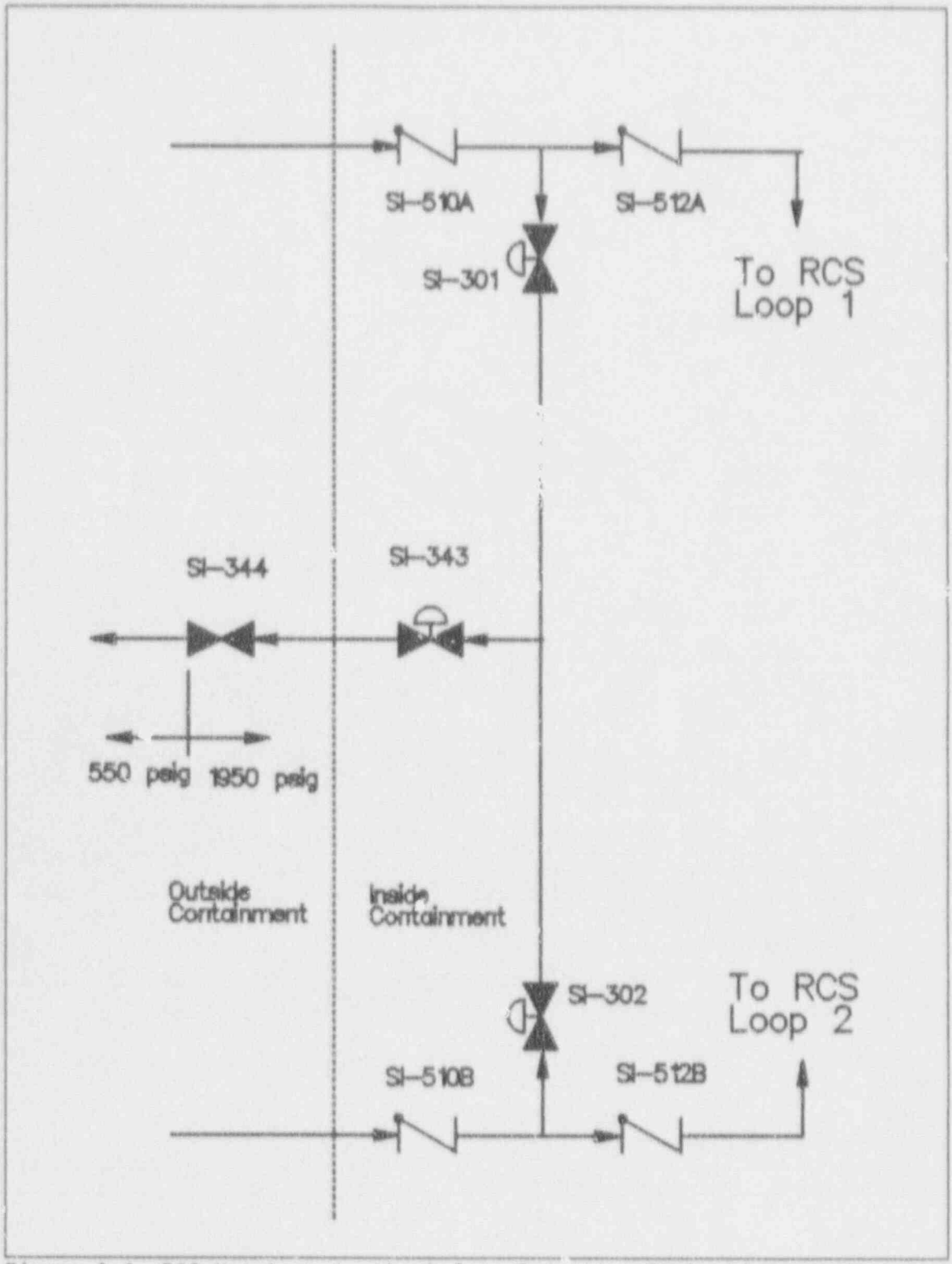

Figure A.4 RCS Hot Legs to the Safety Injection Tanks Line Diagram

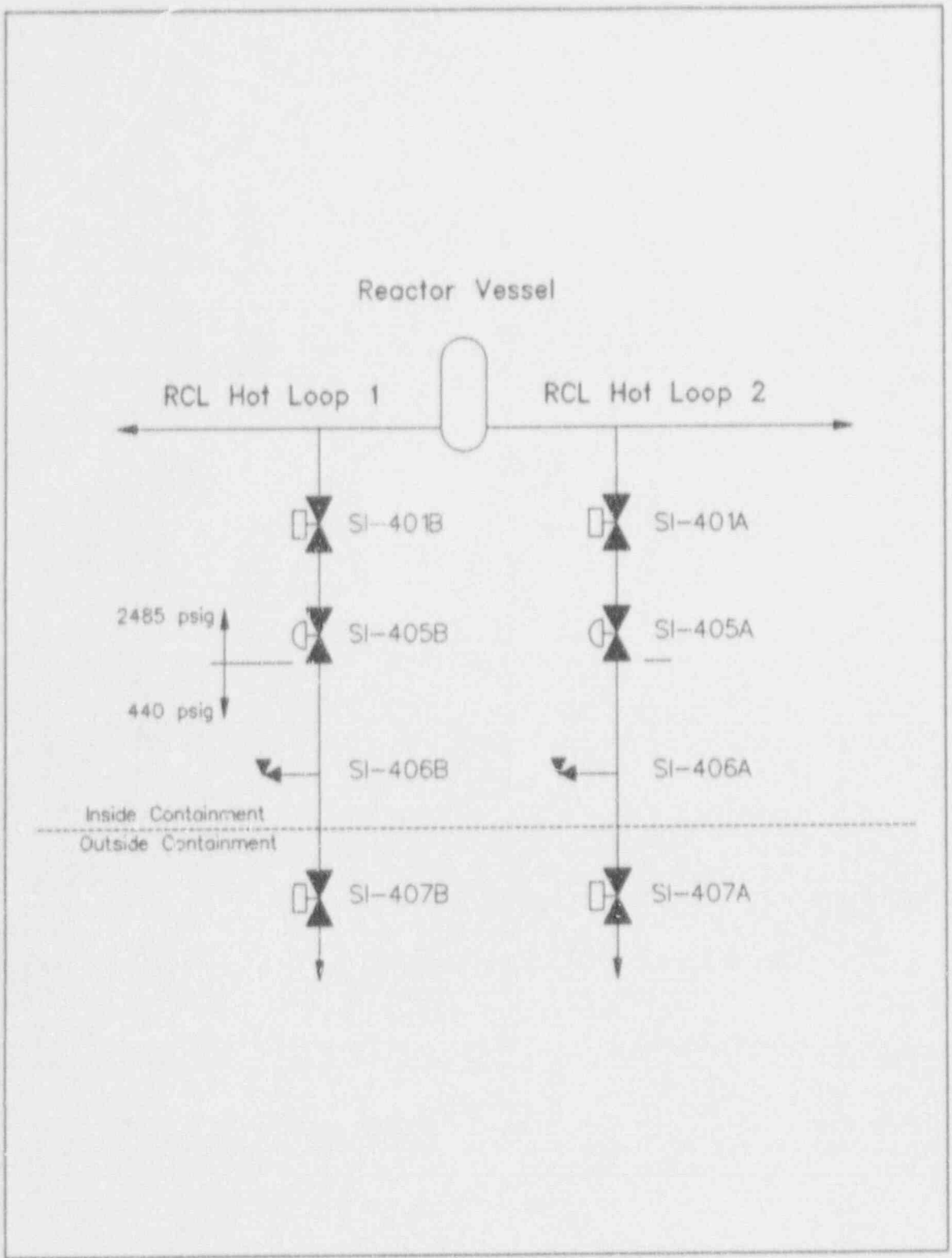

Figure A.[illegible] Shutdown Cooling Suction Line Schematic.

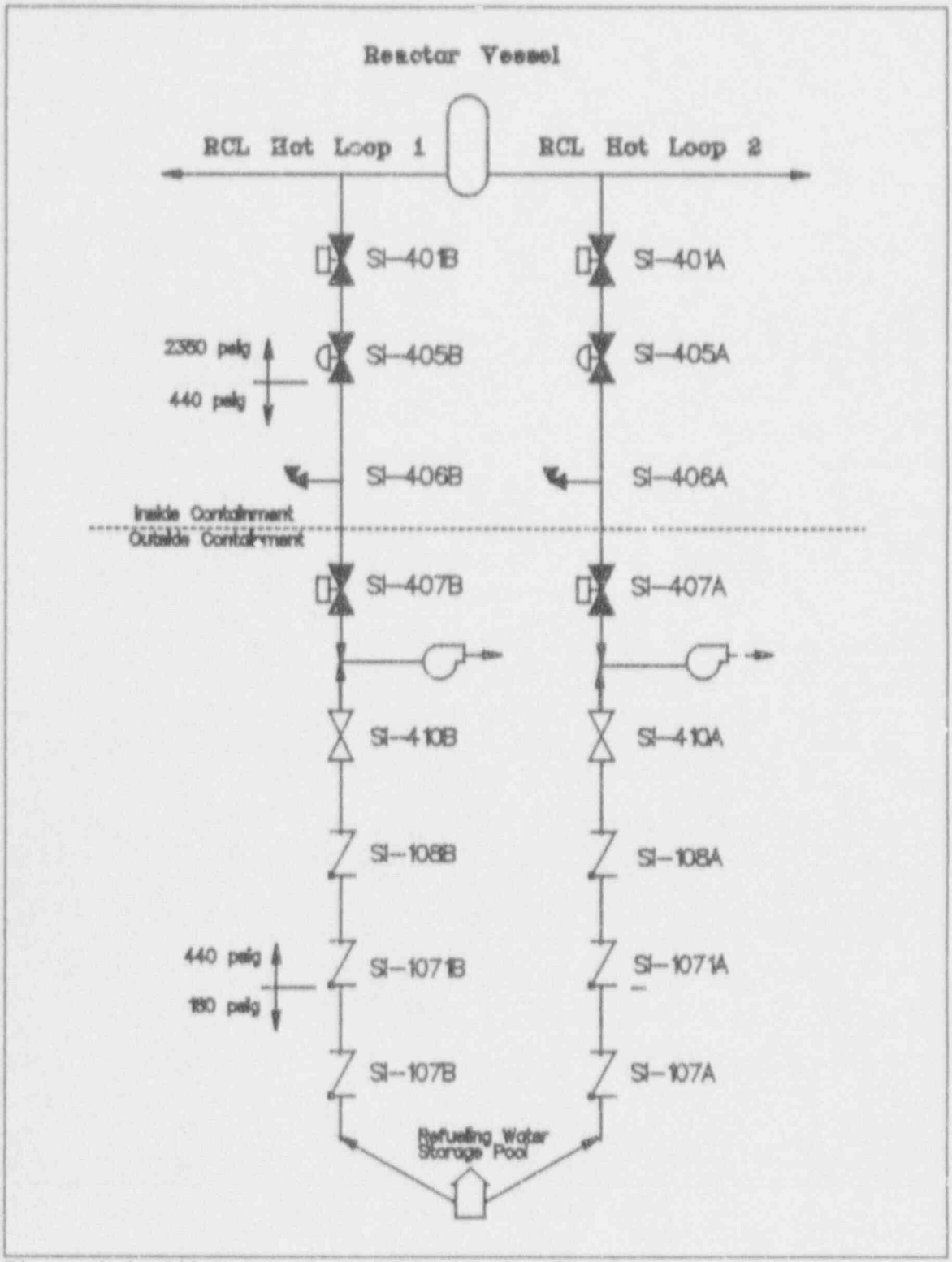

Figure A.6 RCS Hot Legs to RWSP via the LPSI System

A.2.1 Safety Injection System

The safety injection system provides high and low pressure coolant injection capability, as well as the ability to remove residual heat from the reactor core when the plant is shutdown and at low pressures. There are two low pressure safety injection system trains, each with one safety injection pump, and two high pressure trains with three pumps. The safety injection pumps are normally aligned for cold leg injection (to all four RCS cold legs), but are capable of supplying flow to the hot legs, also. The pumps start automatically upon receipt of a safety injection actuation signal. During injection, the RWSP supplies borated water which the safety injection pumps deliver to the cold legs via a common discharge header that branches into four lines, one for each RCS loop.

The low pressure safety injection pumps also provide the motive force for shutdown cooling flow. In this mode of operation they take suction from the RCS hot legs and discharge to the cold legs through the shutdown cooling heat exchangers.

The safety injection system also contains four cold leg safety injection tanks (SITs). Each SIT contains borated water with a pressurized cover gas. The borated water is forced into the respective cold legs when RCS pressure decreases below the cover gas pressure.

Testing of the safety injection system is specified in the plant Technical Specifications and in the in-service testing (IST) program. The pumps are flow-tested on a quarterly basis. The normally closed discharge MOVs are stroke-tested quarterly. Functional actuation tests of the safety injection system are performed during cold shutdown.

Table A.1 Low Pressure Safety Injection Pump Data

Type	Single-stage, vertical, centrifugal
Design pressure	650 psig

Design temperature	400° F.
Design flow	4050 gpm
Maximum flow	5500 gpm
Design head	342 ft
Head at maximum flow	265 ft

Table A.2 High Pressure Safety Injection Pump Data

Type	Multi-stage, horizontal, centrifugal
Design pressure	1950 psig
Design temperature	400° F.
Design flow	380 gpm
Maximum flow	910 gpm
Design head	2830 ft
Head at maximum flow	1275 ft

Appendix B

ISLOCA Event Trees

Appendix B
ISLOCA Event Trees

This appendix describes in detail the ISLOCA scenarios developed for the CE plant and the event trees used to calculate the core damage frequency. The event trees are quantified on a yearly basis. The downward branch at each node depicts the failure event listed at the top of the event tree and the upward branch denotes the complement of the event (typically success). The top events represent a combination of individual component failures, human errors, and functional failures that describe the ISLOCA progression.

All event tree quantification is performed using mean failure probabilities. An uncertainty analysis of core damage frequency is presented in Section 4.5 of the main report. In addition, sensitivity studies were performed for selected issues that are believed to dominate the risk or about which there is significant uncertainty.

Note that only screening failure probabilities are shown for Sequences 1B, 3A, 3B, 4A, and 4B. Sequences 2 and 5 were analyzed in detail, so the failure probabilities shown in the event trees for these sequences are the mean values calculated in the detailed analysis.

Finally, each event tree end state was assigned to one of the consequence bins listed below.

OK - No overpressurization of the low pressure system occurred.

OK-op - Scenario results in overpressurization of the interfacing system but the system does not rupture or leak.

LK-ncd - Scenario results in RCS leakage from the interfacing system, through either a break or an open relief valve, but no severe core damage (sufficient to cause offsite health effects) occurs because the leak is either isolated before core uncovery or the leak is too small to interfere with core cooling.

LOCA-ic - Identifies scenarios that produce a LOCA inside containment. Because these sequences are enveloped by the design basis analysis of the plant, they are not fully developed on the event trees and these scenarios are not considered to be core damage events.

REL-mit - An ISLOCA with core damage occurs but the radioactive release is mitigated through some means, such as scrubbing through an overlying water pool or general area fire sprays in the auxiliary building.

REL-lg - An ISLOCA with core damage occurs and results in a large unmitigated radioactive release. Note that this does not necessarily imply that the break size is large.

B.1 Premature Entry Into Shutdown Cooling - SEQ1A

A risk-significant scenario at the Babcock and Wilcox (B&W) plant (see [B-1]) involved premature entry into shutdown cooling, with RCS pressure and temperature above the open permissive set point of the decay heat removal (DHR) system suction isolation valves. This scenario was considered credible at the B&W plant because the plant procedures allowed operators to bypass the open permissive interlock for one of the two shutdown cooling isolation valves. This allowed an error of commission to be postulated in which, once the decision is made to enter shutdown cooling early, the operators will be led to bypass the interlock for the other valve, also, even though the procedure does not instruct them to do so. For the CE plant, the HRA did not reveal any circumstances that would lead to an analogous scenario. Therefore, this scenario was not developed further.

B.2 RCS To SI System ISLOCA During Plant Startup - SEQ1B

In Sequence 1B the plant is undergoing a startup from cold shutdown. Thus, failure to close MOVs SI-401 and HOVs SI-405 prior to raising RCS pressure above 396 psig is the initiating event. The event tree for this sequence is contained in Figure B.2, while the corresponding flow diagram is displayed in Figure B.1. Since startup is a "low-pressure" procedure compared

to normal full RCS pressure, it is assumed that any overpressurization that causes the relief valve to open will not cause an ISLOCA. The event tree models one flow line (out of two) on a mission time of one year.

PSUM. The initiating event for this sequence is a startup from cold shutdown. Such a startup is estimated to occur once every 18 months (cold shutdown does not necessarily occur at every shut down), the frequency of event PSUM is assumed to be 0.67/year.

MOVLO. Once the plant is in a startup mode, MOV SI-401 (A/B) and HOV SI-405 (A/B) must both be left open after the RCS pressure exceeds 396 psig for an ISLOCA to occur. Thus, event MOVLO represents the probability that both SI-401 and SI-405 are left open. The screening probability assumed for MOVLO was 1.0×10^{-4}.

ACIF. If both valves SI-401 and SI-405 are left open, the automatic closure interlock (ACI) is designed to shut both valves automatically when the RCS pressure exceeds 700 psig. Event ACIF models the probability that the ACI fails. Compounding the evaluation of this event is the fact that the analyzed plant is petitioning the NRC for permission to remove the ACI (this is being done because of concerns about losing SDC inadvertently due to valve closure). Thus, two separate probabilities for this event were used. With the ACI in place, the screening probability was assumed to be 1.0×10^{-3}. For the case of removal of the ACI, the probability of failure for this event would obviously be 1.0. The Sequence 1B event tree shows the sequence with the ACI in place.

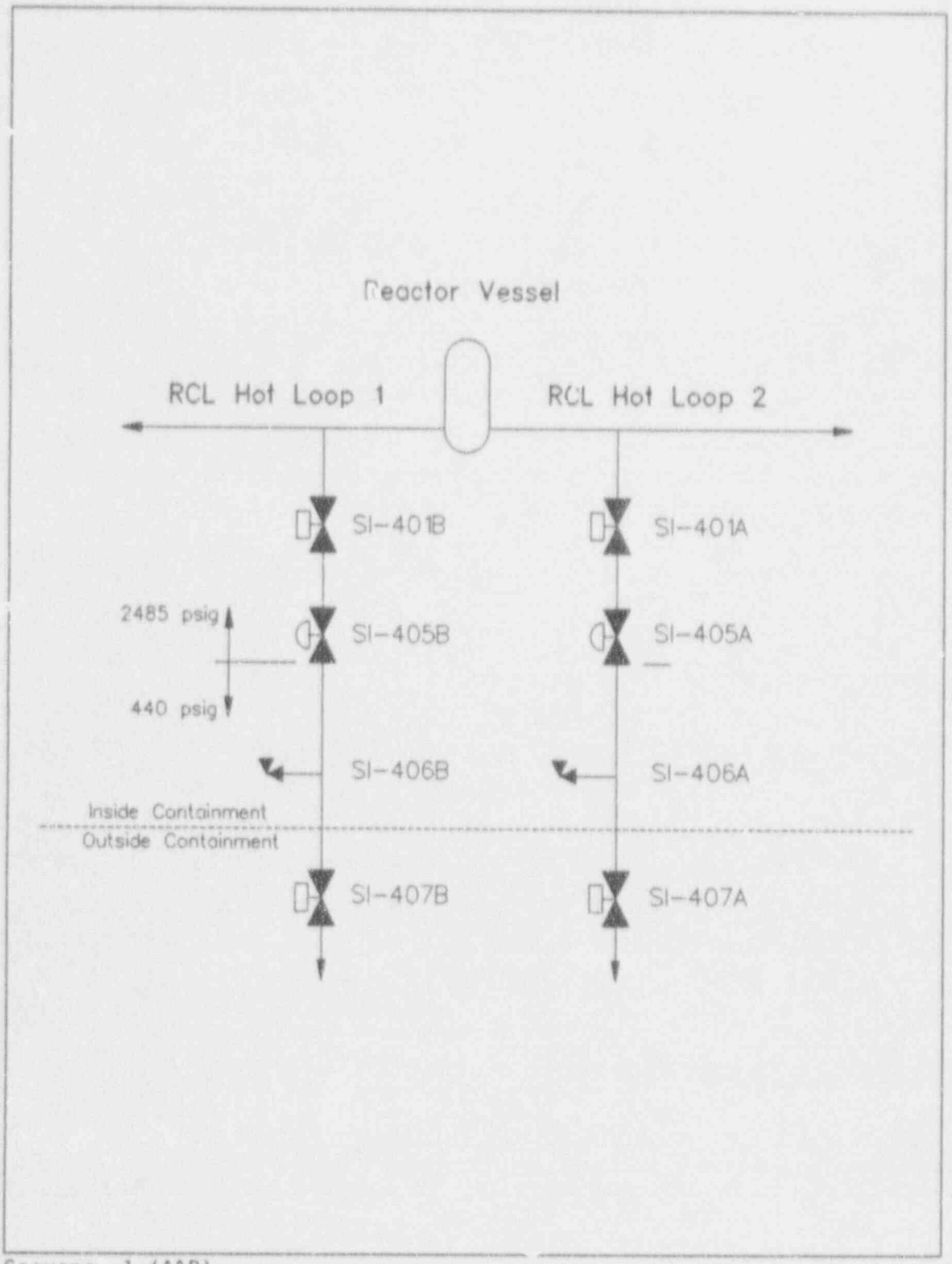

Sequence 1 (A&B)

Figure B.1 : Shutdown Cooling Suction Line Schematic.

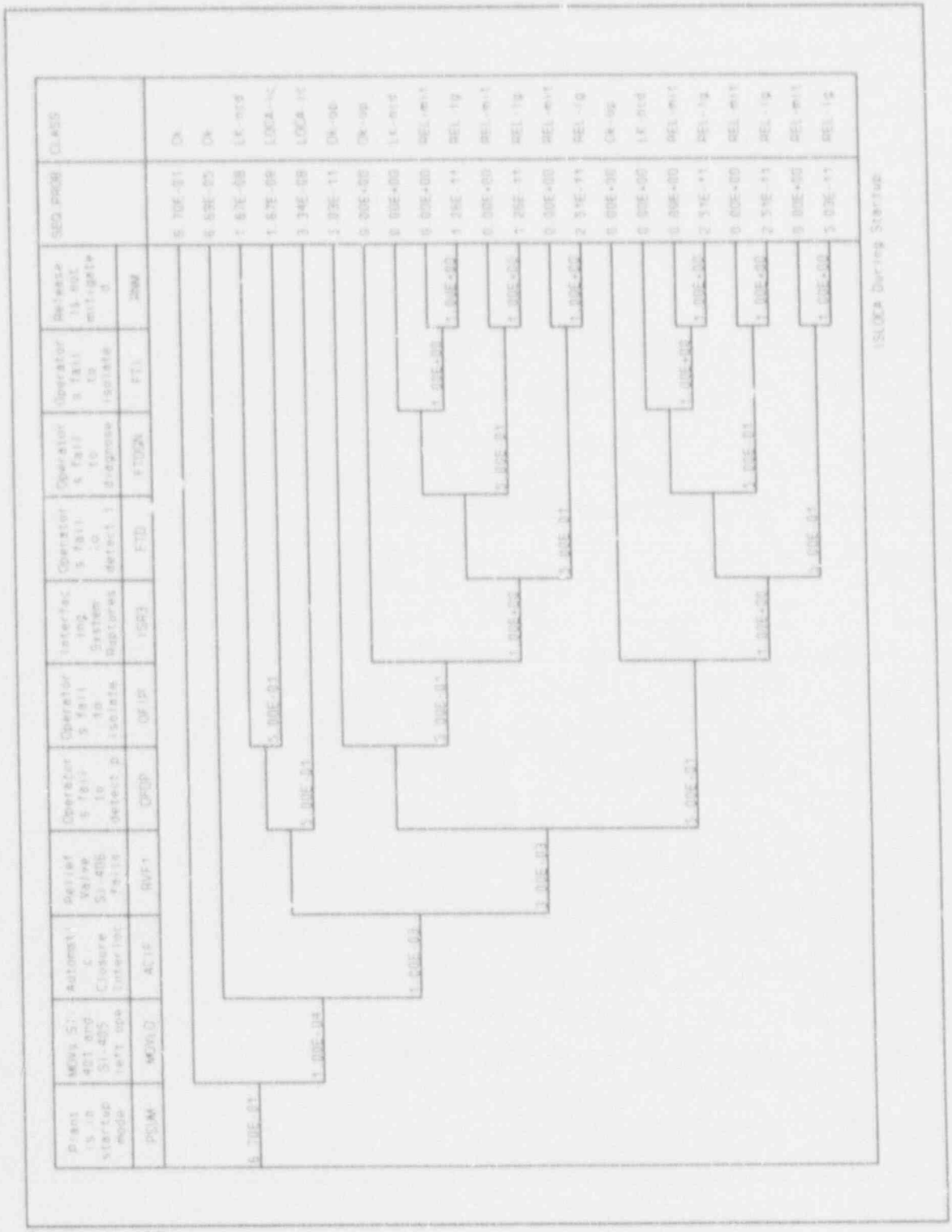

Sequence 1B

Figure B.2 : Shutdown Cooling Suction Line ISLOCA Sequence Event Tree (plant in startup mode).

RVF1. This event models failure of relief valve SI-406 to open on demand. The failure probability was taken to be 1.0×10^{-3}.

OFOP. This event models failure of the operators to detect the overpressure condition in time to prevent damage. A screening probability of 0.5 was used for this and all other human error probabilities in this sequence.

OFIP. This event models operator failure to isolate the SDC system from the RCS prior to damage. A screening failure probability of 1.0 was used.

ISR3. Event ISR3 models a break in the low pressure portion of the SDC system outside containment. The conditional probability of a break is taken to be 1.0 for the screening analysis.

FTD. Event FTD models failure of the operators to detect the loss of coolant and enter the correct emergency procedure. A screening failure probability of 1.0 was used.

FTDGN. This event models failure of the operators to diagnose that the break is outside containment. A screening failure probability of 1.0 was used.

FTI. This event models operator failure to isolate the break given that it has been detected and diagnosed. A screening failure probability of 1.0 was used.

RNM. Based on the walkdowns performed during the plant visit, the probability that the release would not be mitigated by flooding or auxiliary building fire sprays was judged to be 1.0.

B.3 RCS To LPSI Cold Discharge - SEQ2

Through the normal reactor operating year, MOVs SI-138 (A/B) and SI-139 (A/B) are stroke-tested quarterly. Thus, the accident sequence path for the

low pressure safety injection (LPSI) pump discharge is based upon the fact that the MOVs will be opened once each quarter. Figure B.3 illustrates the simplified flow diagram for the LPSI pumping path. The corresponding event tree for this sequence is contained in Figure B.4. The event tree evaluates one flow path (out of four possible) for a mission time of one quarter. Thus, to get the failure frequency estimate for the complete system based on a one-year mission time, the sequence end state frequencies must be multiplied by 16.

Obviously, if the two isolation check valves (SI-335/336 (A/B) and SI-142/143 (A/B)) protecting the MOVs had failed, it would not be desirable to open the MOVs. But, for analyzing this sequence, it is assumed that no prior information (for example, a high pressure reading between the two isolation check valves) is known for the system. This assumption is made because the stroke-testing procedure does not direct the operators to check pressure between the PIV check valves before performing the stroke test. Therefore, for the model, it is postulated that internal failure of the two isolation check valves will automatically lead to an overpressurization of the interfacing system when the MOV is stroke-tested.

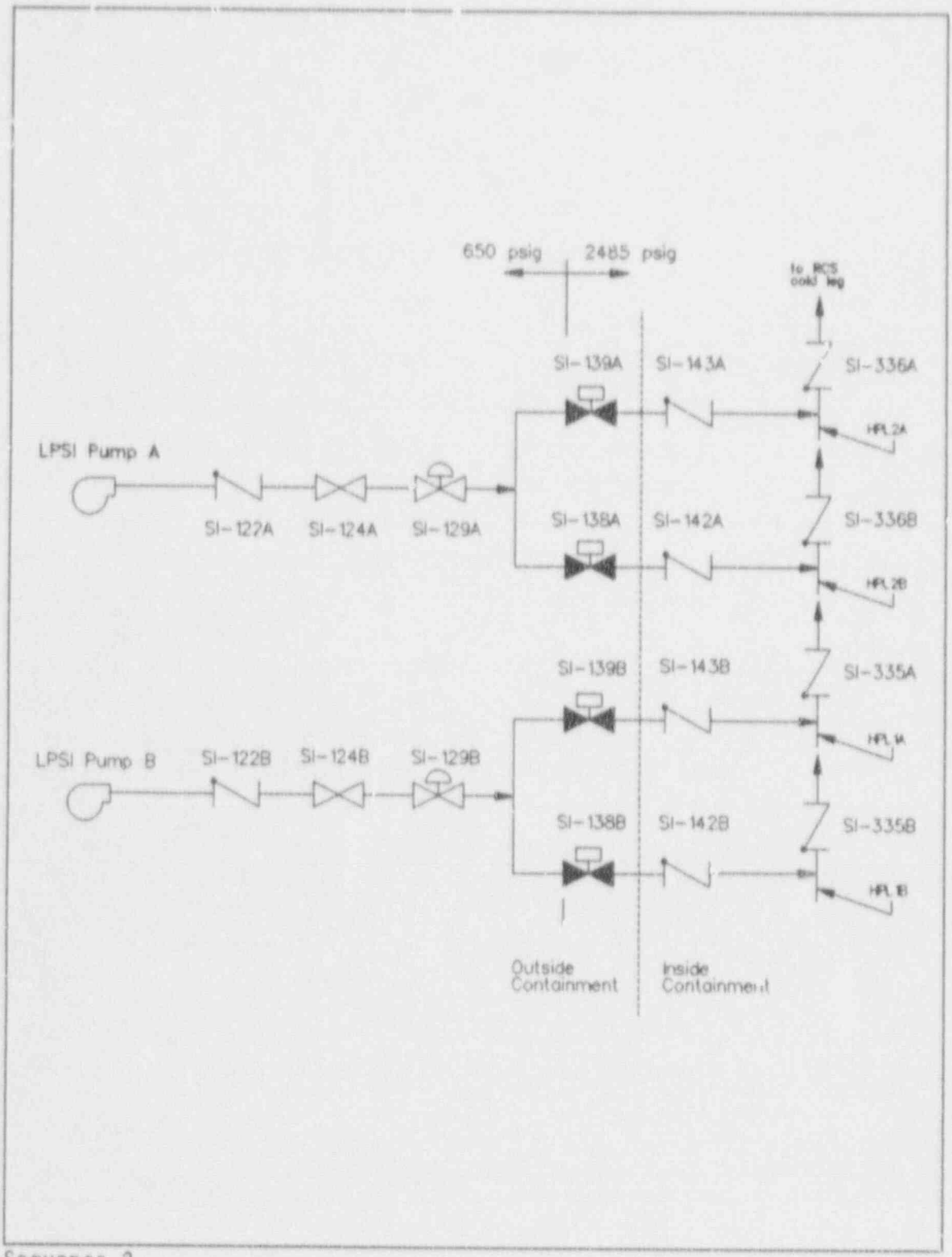

Sequence 2

Figure B.3 : RCS Cold Legs to Low Pressure Safety Injection Pump Discharge Schematic.

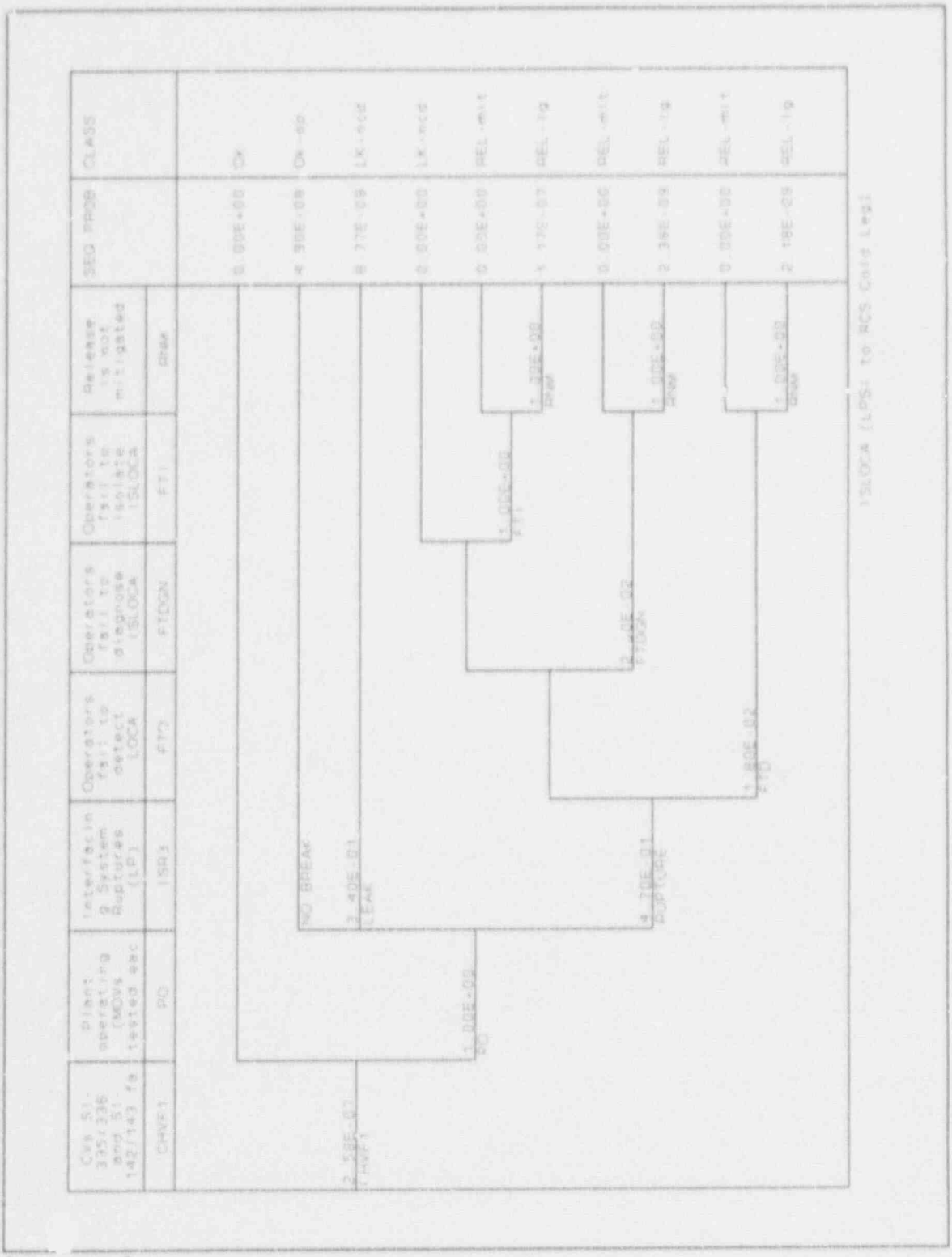

Sequence 2

Figure B.4 : RCS Cold Legs to Low Pressure Safety Injection Discharge ISLOCA Sequence Event Tree.

CHVF1. The failure of the two isolation check valves (SI-335/336 (A/B) and SI-143/144 (A/B)) is modeled as the initiating event. Since it is assumed that both valves are closed and in a non-failed state at the beginning of the mission time, only a time-dependent failure mode is presumed.

Even though the two check valves are not the same size (SI-335/336 are 12-inch valves, while SI-143/144 are 8-inch valves) and the environmental conditions are not identical for the two check valves, an assumption is made that the failure rate λ is constant and the same for the two valves. This is a conservative assumption that reflects the lack of detail available in the valve failure rate database. The failure rate is assumed to be lognormally distributed, with a mean value of 8.7×10^{-8}/h and error factor of 10. The probability that one of the check valves fails in a time T is defined as

$$P(T \le \tau) = \int_0^{\tau} \lambda e^{-\lambda t} dt$$

$$= 1 - e^{-\lambda \tau}$$

$$\approx \lambda \tau \quad (for\ \lambda \tau \ll 1)$$

Since the model for CHVF1 assumes both check valves failure rates are identical, the underlying probability failure distributions for the two valves must be interchangeable, which leads to the assumption that the valves need to be treated as if the failures were correlated. Thus, for the two check valves in series, the probability that they both fail in the mission time is given by the probability of the first check valve failing intersected with the probability of the second check valve failing, or

$$E(CHVF1) = E\left[(CHVF)_1 \bigcap (CHVF)_2\right]$$

$$= \tau^2 E(\lambda^2)$$

$$\approx \tau^2([E(\lambda)]^2 + Var(\lambda))$$

Given that the mission time is 2190 hours, the probability of failure for the two check valves is calculated to be 2.58×10^{-7}. This probability is multiplied by 16 (four quarters per year times four injection lines) in calculating the end state frequencies for this sequence.

PO. This event models the opening of MOVs SI-138 (A/B) and SI-139 (A/B). Since the MOVs are opened once each quarter for stroke-testing, the probability of event PO in the mission time is assumed to be 1.0.

ISR3. Event ISR3 models a break in the low pressure portion of the LPSI system outside containment. This probability is calculated in Appendix F. The conditional probability of a break is found to be 1.0.

FTD. Event FTD models failure of the operators to detect the loss of coolant and enter the correct emergency procedure. The quantification of this event can be found in Appendix C. The mean failure probability is estimated to be 1.8×10^{-2}.

FTDGN. This event models failure of the operators to diagnose that the break is outside containment. The quantification of this event is presented in Appendix C. The mean failure probability is estimated to be 2.0×10^{-2}.

FTI. This event models operator failure to isolate the break given that it has been detected and diagnosed. In quantifying this event (see Appendix C for details), the flow of the plant's existing emergency procedures was strictly modeled. Because the emergency procedures do not contain steps that would direct the operators to isolate the break (by terminating LPSI flow), and because the operators have received post-TMI training that cautions against overriding a valid safety injection signal, the failure probability of this event is 1.0. It is possible that the operators could take knowledge-based actions outside of the emergency procedures, but such actions were not modeled in the base case analysis.

RNM. Based on the walkdowns performed during the plant visit, the probability that the release would not be mitigated by flooding or auxiliary building fire sprays was judged to be 1.0.

B.4 RCS Cold Legs to High Pressure Safety Injection (Header A) - SEQ-3A

This scenario is similar to Sequence 2. Once each quarter, MOVs SI-225 through SI-228 (A/B) are stroke-tested while the plant is operating. Thus, the accident sequence path for the high pressure safety injection (HPSI) pump discharge is based upon the fact that the MOVs will be opened once each quarter. Figure B.5 depicts the simplified flow diagram for the HPSI pumping path. The matching event tree for this sequence is in Figure B.6. The event tree models one flow path (out of four) on a mission time of one quarter.

Once again, if the isolation check valves in the sequence protecting the MOVs had failed, it would not be desirable to open the MOVs. But, for this analysis, it is assumed that there is no prior knowledge for the system. Thus, for the model, it is assumed that random failure of the two isolation check valves will automatically lead to a demand on check valve SI-216.

CHVF2. The initiating event for this sequence is the failure of the two isolation check valves (SI-335/336 (A/B) and SI-241 through SI-244 (A/B)). The event is modeled as a single event, similar to event CHVF1. It is assumed that both valves are closed and in a non-failed state at the beginning of the mission time, leading to only a time-dependent failure mode for the check valves.

Although the two check valves are not the same size (SI-335/336 are 12-inch valves, while SI-241 through SI-244 are 8-inch valves) and the

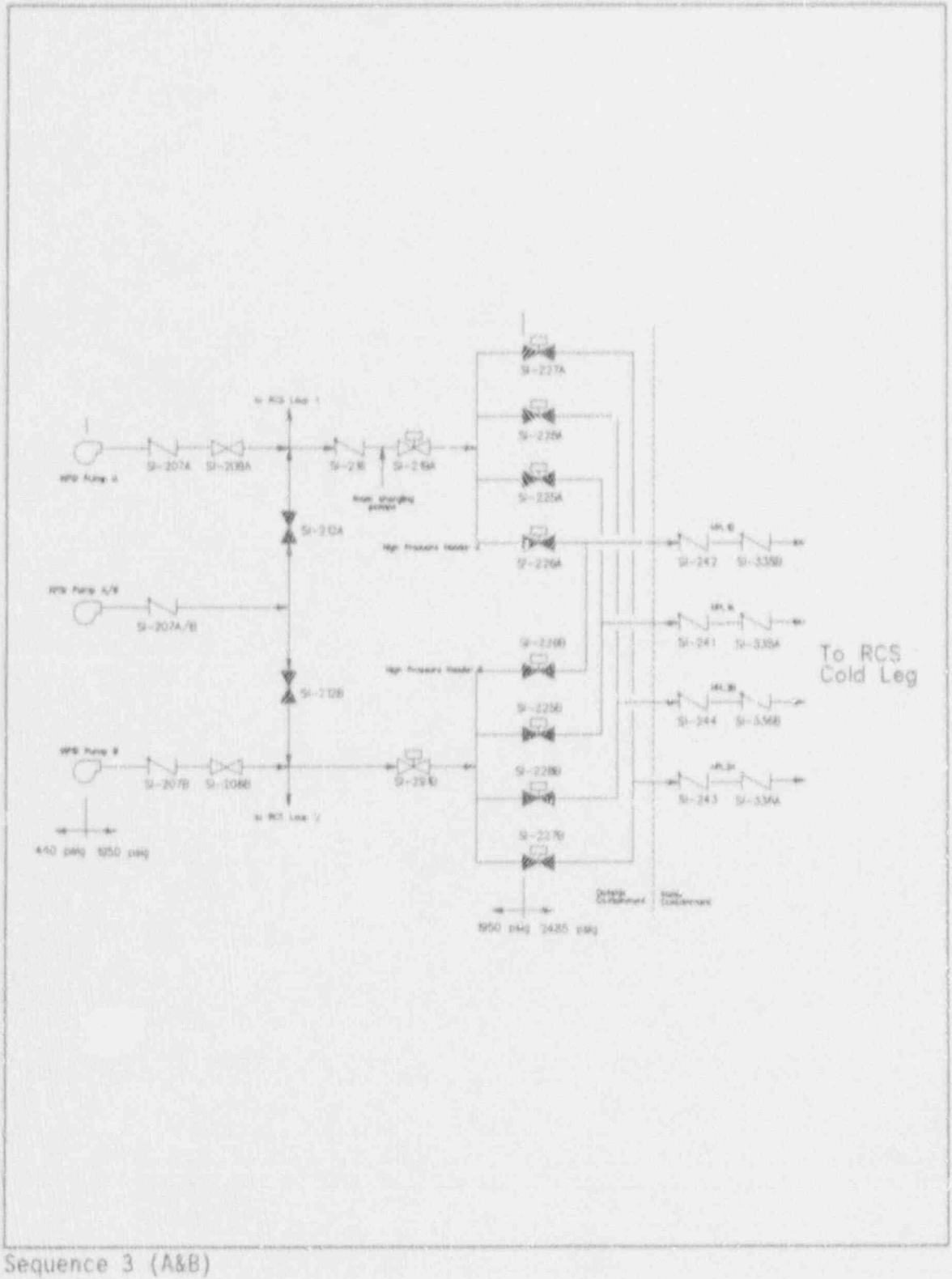

Sequence 3 (A&B)

Figure B.5 : RCS Cold Legs to the High Pressure Safety Injection Pump Discharge Flow Diagram.

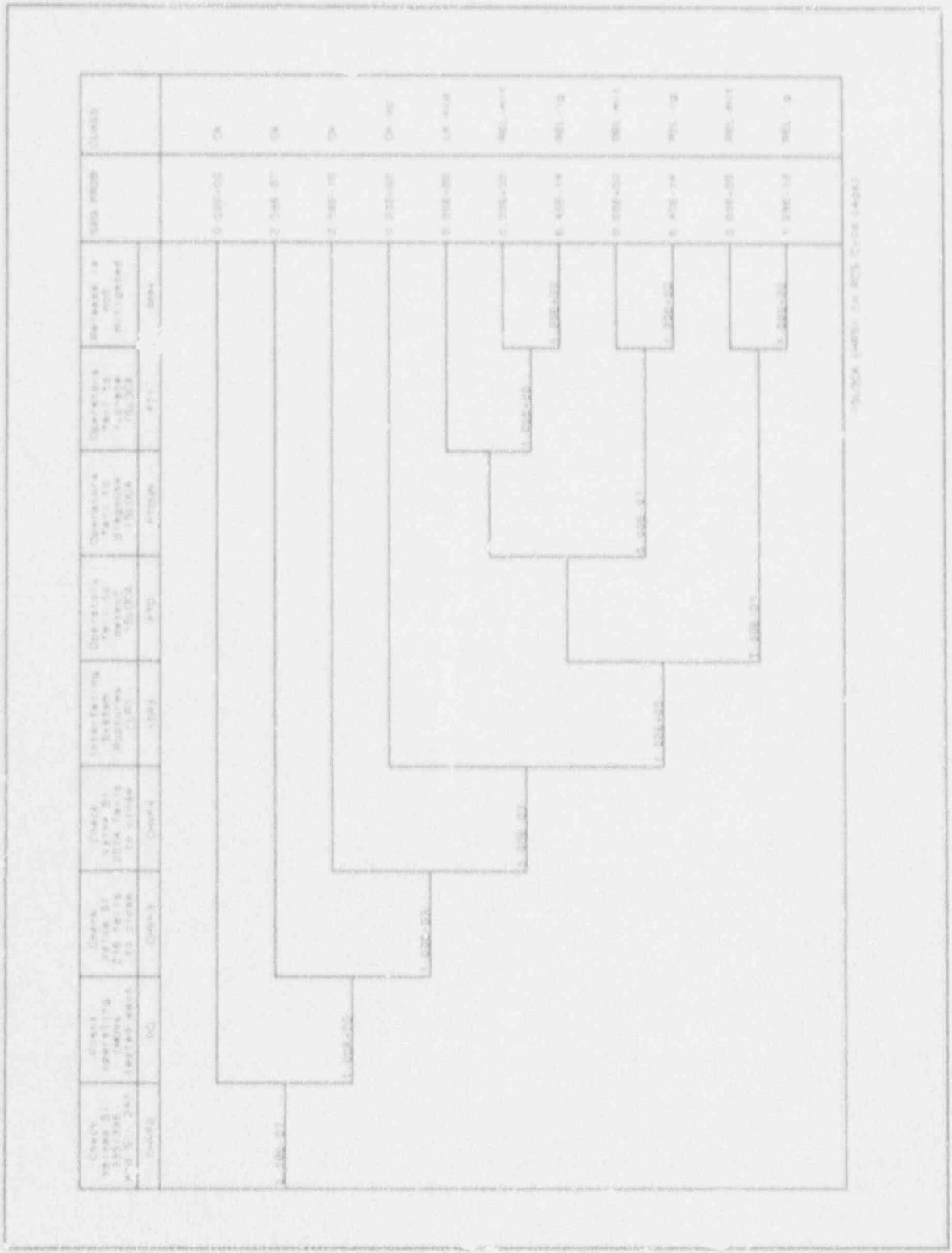

Sequence 3A

Figure 8.6 : RCS Cold Legs to the High Pressure Safety Injection (Header A) ISLOCA Event Tree

environmental conditions are not identical for the two check valves, it is assumed that the failure rate λ is constant and the same for the two valv' The failure rate is assumed to be lognormally distributed, with a mea of 8.7×10^{-8}/h and an error factor of 10. Using the analysis from Sequence 2, the quarterly failure probability of event CHVF2 is found to be 2.58×10^{-7}.

PO. Event PO is similar to that for Sequence 2, except the MOVs that are opened during stroke-testing are SI-225 through SI-228 (A/B). Since the MOVs are opened once each quarter, the event probability for one mission time is assumed to be 1.0.

CHVF3. Once the two isolation check valves fail, the interfacing system will become pressurized, putting a demand on check valve SI-216. Thus, event CHVF3 models the probability of the check valve SI-216 failing to close upon demand. This failure probability is taken to be 1.0×10^{-3}/demand.

CHVF4. This event is the same as CHVF4 except that check valv' SI-207A must close. The failure rate of CHVF5 is taken to be 1.0×10^{-3}/demand, also.

B.5 RCS Cold Legs to HPSI (Header B) - SEQ-3B

Sequence 3B is comparable to Sequence 3A with the exception that Sequence 3B has one less check valve to protect the interfacing system. Whereas header A has check valve SI-216, header B does not have the corresponding check valve in the piping design.

The piping diagram for this sequence is shown in Figure B.5, the event tree in Figure B.7. The only difference between the event tree for Sequence 3A and that for Sequence 3B is that event CHVF3 has been deleted in sequence 3B. As in Sequence 3A, the event tree analyzes one flow path (out of four possible) on a mission time of one quarter.

After the deletion of event CHVF3, the remaining events in the event tree are identical for the two sequences.

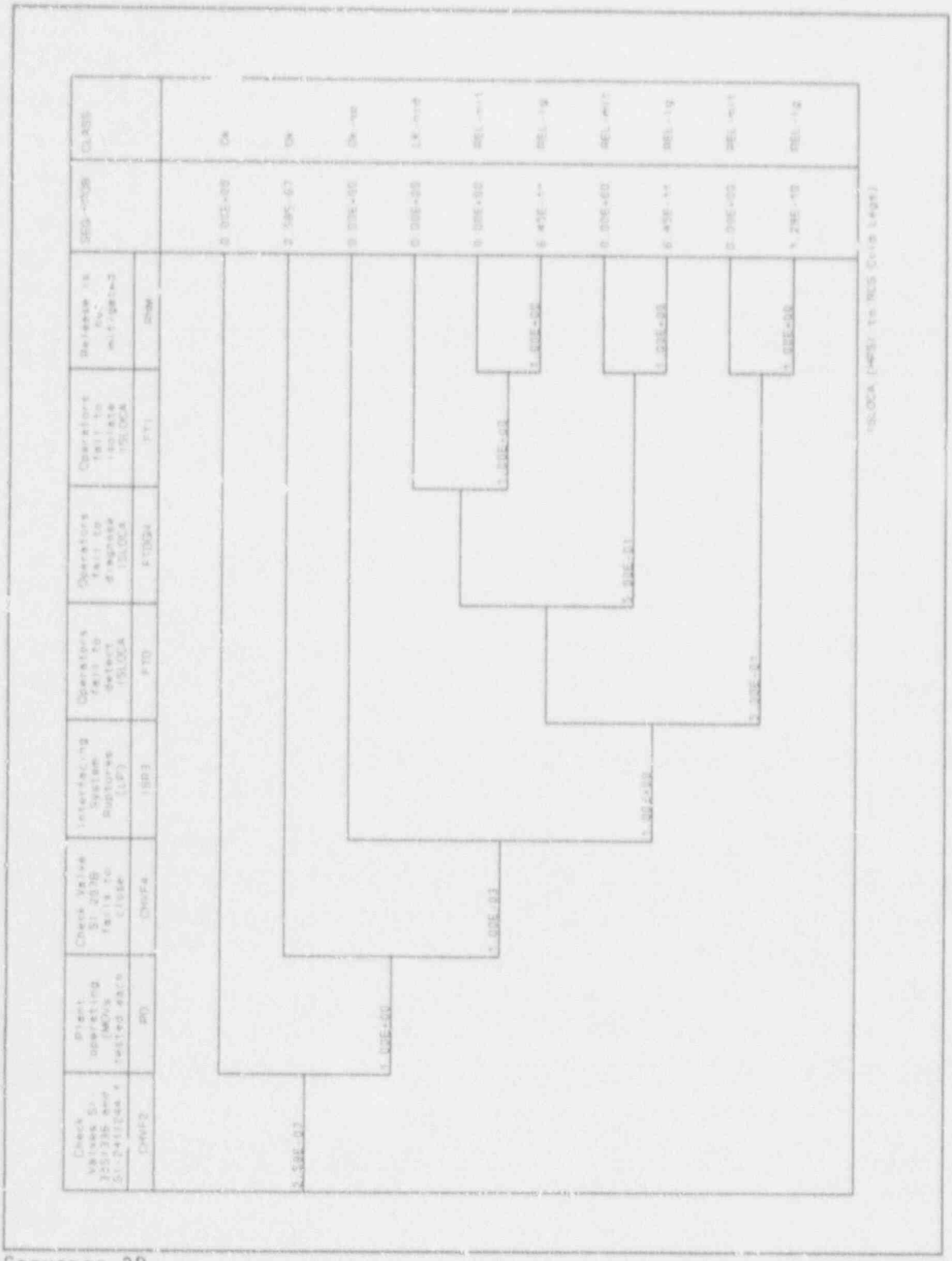

Sequence 3B

Figure B.7 : RCS Cold Legs to High Pressure Safety Injection (Header B) ISLOCA Event Tree

B.6 RCS Hot Legs to HPSI (Header A) - SEQ-4A

Once every quarter MOVs SI-502A and SI-506A are stroke-tested. Therefore, Sequence 4A is based on the opening of MOV SI-502A. Since valve SI-502A is opened and closed before valve SI-506A is opened, the opening of SI-502A is defined as the initiating event for the sequence. Once again, the assumption of no prior knowledge of the condition of the system is used. The system flow diagram in shown in Figure B.8. The event tree for Sequence 4A is shown in Figure B.9. The event tree analyzes one flow path (out of four) on a mission time of one quarter.

CHVF5. The initiating event is similar to event CHVF1 from Sequence 2, except the two check valves that are modeled are SI-512A and SI-510A. The modeling of the two check valves results in a quarterly failure probability of 2.58×10^{-7}.

PO. Event PO models the plant operating at normal power and the MOV SI-502A being opened for stroke-testing. Since valve SI-502A is stroke-tested once a quarter, the probability of event PO is assumed to be 1.0.

MOVF2. Event MOVF2 models the internal random failure of MOV SI-506A. The failure rate is assumed to be 1.0×10^{-7}/hr. Thus, for a mission time of 2190 hours, the probability of failure for the closed MOV is 2.19×10^{-4}.

The remaining events are the same as for Sequences 3A and 3B.

B.7 RCS Hot Legs to HPSI (Header B) - SEQ-4B

Sequence 4B is similar to Sequence 4A except that check valve SI-216 is absent from piping header B. The flow diagram is contained in Figure B.8, while the event tree is contained in Figure B.10. As in Sequence 4A, the event tree models one flow path (out of four) on a mission time of one quarter.

The initiating event for Sequence 4B is the opening of MOV SI-502B. The initiating event probability is identical to that of Sequence 4A, and is assumed to be 1.0.

CHVF6. This event is similar to event CHVF5, except the two check valves that are modeled are SI-512B and SI-510B. The quarterly failure probability is found to be 2.58×10^{-7}.

PO. Event PO models the plant operating and valve SI-502B opening. Since SI-502B is tested every quarter, the probability of this event is assumed to be 1.0.

MOVF3. Event MOVF3 is like event MOVF2, except that the valve that is modeled is SI-506B. The probability of failure for this event is 2.19×10^{-4}.

The remaining sequence events and event probabilities have previously been defined.

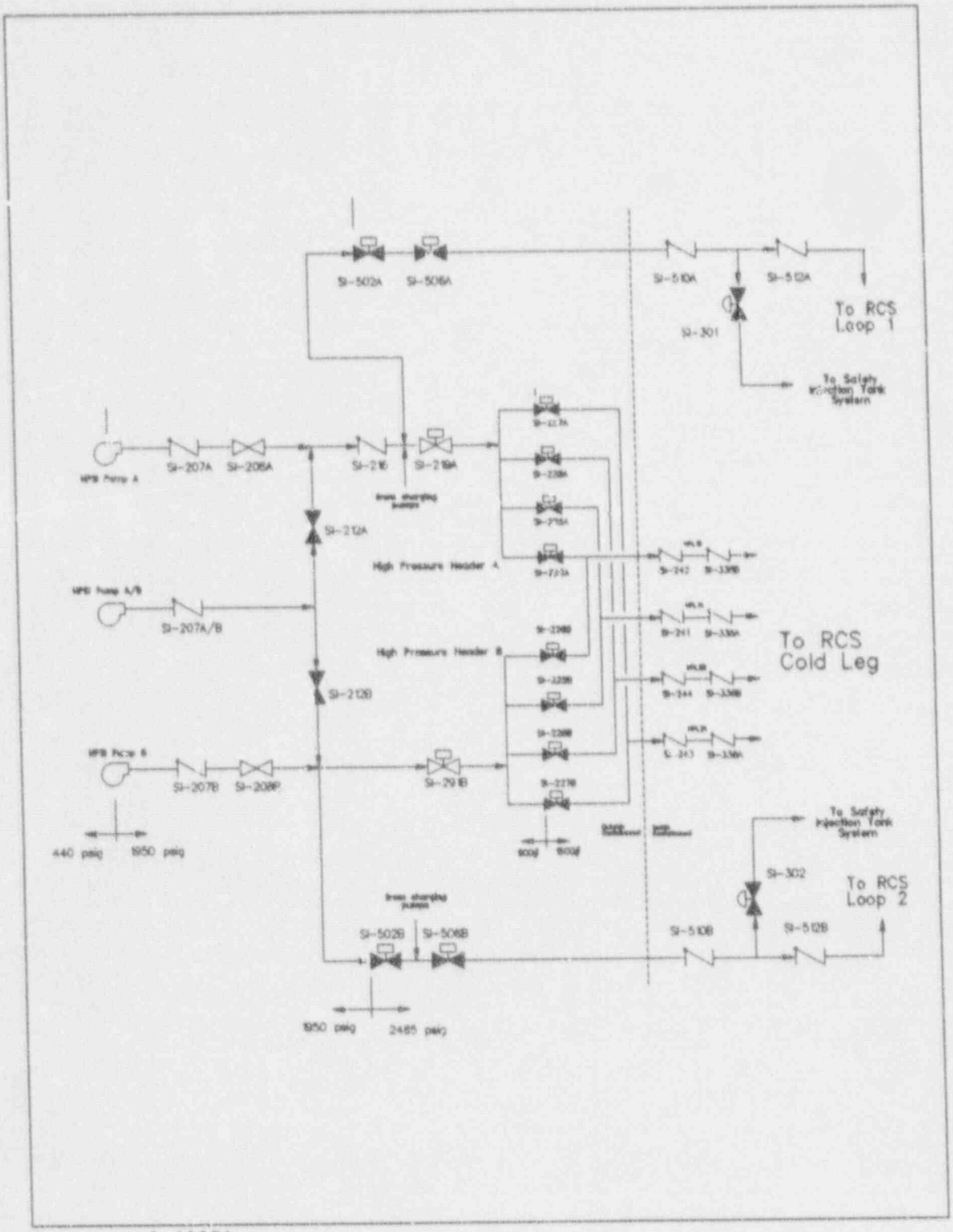

Sequence 4 (A&B)

Figure B.8 : RCS Hot Legs to High Pressure Safety Injection Pump Discharge Line Schematic

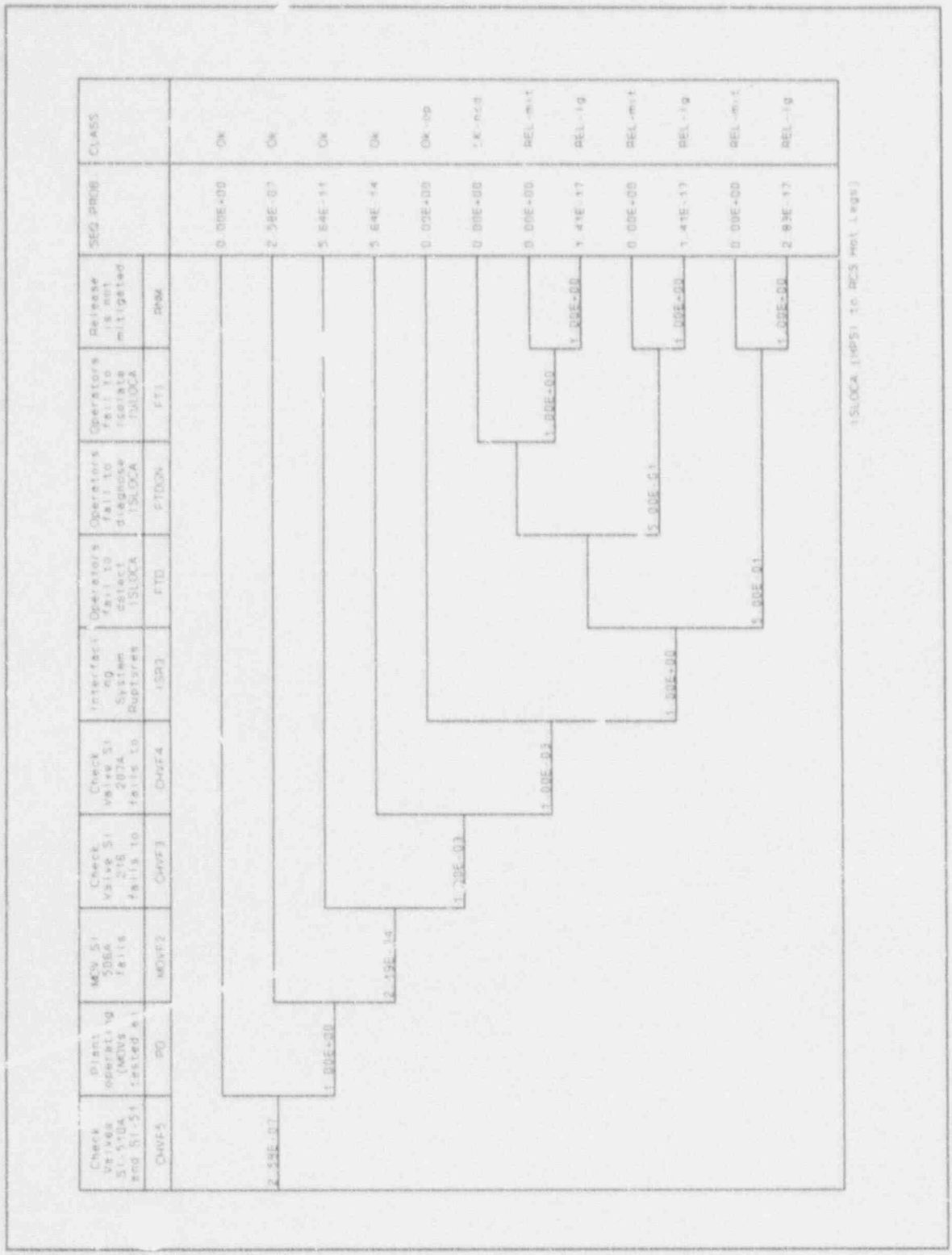

Sequence 4A

Figure B.9 : RCS Hot Legs to High Pressure Safety Injection Discharge (Header A) ISLOCA Event Tree.

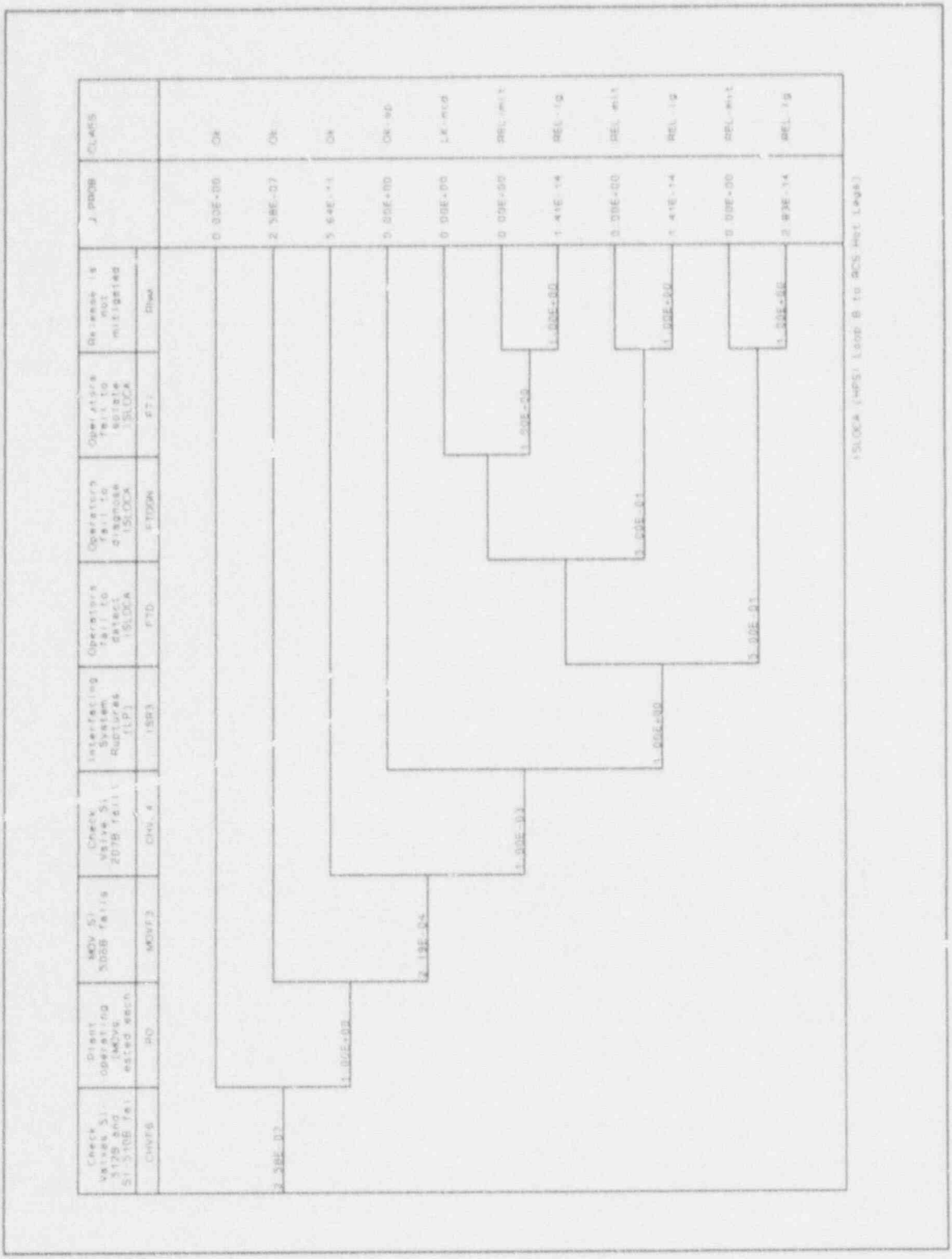

Sequence 4B

Figure B.10 : RCS Hot Legs to High Pressure Safety Injection Discharge (Header B) ISLOCA Event Tree

B.8 RCS Hot Legs to the LPSI System During Shutdown - SEQ-5

When the analyzed plant enters shutdown cooling, the operators rely on check valves SI-108 and SI-1071 closing when the RCS pressure exceeds the interfacing system design pressure. Thus, Sequence 5 is based upon failure of the two check valves. The simplified flow diagram for this sequence is contained in Figure B.11. The ISLOCA event tree is contained in Figure B.12.

PSM. The plant is assumed to enter shutdown cooling using the LPSI system once a year on average. During the shutdown, MOVs SI-401, SI-405, and SI-407 (A/B) are opened. Therefore, the probability of one initiating event in the mission time is assumed to be 1.0.

CHVF10. This event models the failure of check valve SI-108. Due to the as-found degraded condition of valve SI-108, no credit is taken for this valve. Thus, the demand failure probability of event CHVF10 is assumed to be 1.0.

CHVF11. Event CHVF11 models the failure of check valve SI-1071 to close on demand. The demand probability is assumed to be $1x10^{-3}$.

The remaining events have already been defined. The human error probabilities were calculated in Appendix C. The probability of a break in the interfacing system was calculated in Appendix F.

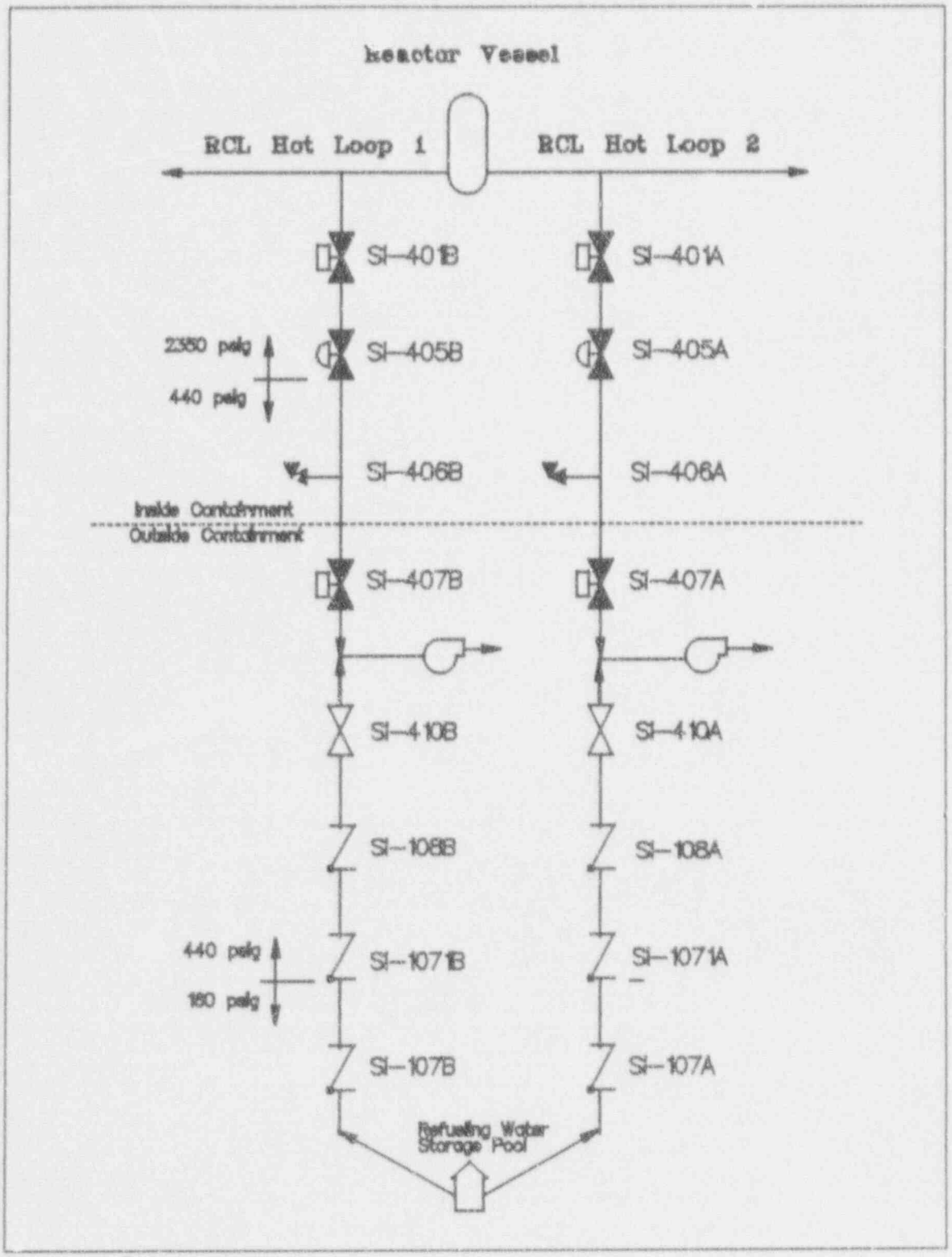

Sequence 5

Figure B.11 : RCS Hot Legs to RWSP via the LPSI System

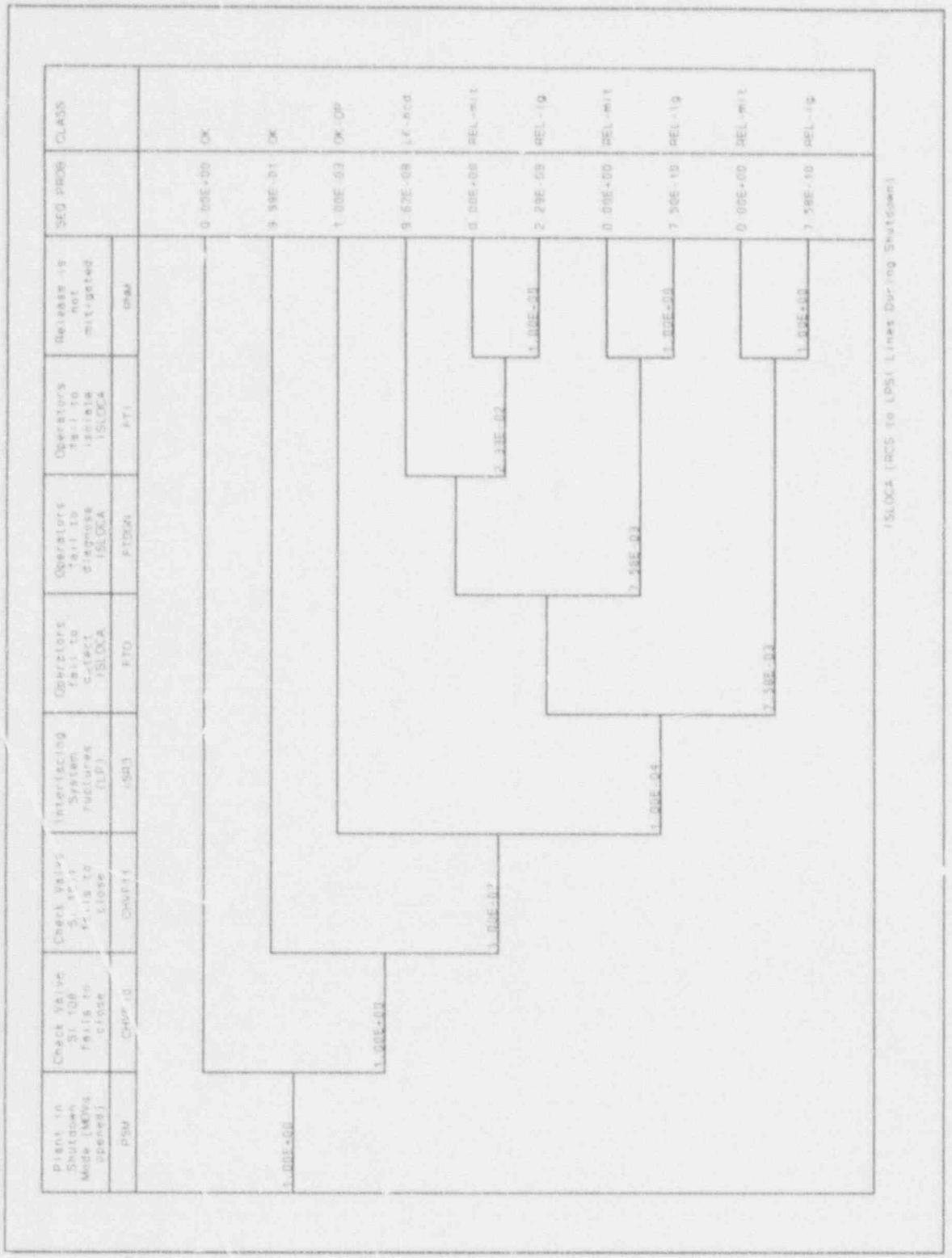

Sequence 5

Figure B.12 : RCS Hot Legs to RWSP via the LPSI System ISLOCA Event Tree

References

B-1. W. J. Galyean, et al., *Assessment of ISLOCA Risks - Methodology and Application: Babcock and Wilcox Plant*, NUREG/CR-5604, to be published.

Appendix C

Human Reliability Analysis for the Combustion Engineering ISLOCA Probabilistic Risk Assessment

CONTENTS

Figures and Related Tables

CE ISLOCA Human Reliability Analysis

This appendix describes in detail the methodology and results of the human reliability analysis (HRA) for the third ISLOCA probabilistic risk assessment (PRA). HRA was used to model the predominant human errors for each significant scenario in the PRA. HRA is a methodological tool for analyzing, predicting, and evaluating work-oriented human performance in quantitative, that is, probabilistic terms. As a diagnostic tool, HRA can be used to identify those factors in the system which lead to less than optimal human performance and can estimate the error rate anticipated for individual tasks. In a given system, or sub-system, HRA can also be utilized to determine where human errors are likely to be most frequent. Traditionally, HRA analysts model human performance through the use of event trees like those found later in this appendix.

The general methodological framework for this ISLOCA HRA was based on guidelines (under development) from the NRC-sponsored Task Analysis-Linked Evaluation Technique (TALENT) Program [C-1] which recommends the use of task analyses, time line analyses, and interface analyses in a detailed HRA. NUREG/CR-1278, the Handbook of Human Reliability Analysis with Emphasis on Nuclear Power Plant Applications (THERP) [C-2], recommends similar techniques and, in addition, provides a data base that can be used for estimating human error probabilities (HEPs). Finally, this ISLOCA HRA integrated the steps from the Systematic Human Action Reliability Procedure (SHARP) [C-3], and A Guide for General Principles of Human Action Reliability Analysis for Nuclear Power Generation Stations (draft IEEE standard P1082/D7 [C-4]).

From this combination of approaches, the analysts identified 11 basic steps, summarized below, which were used as guidelines for this HRA. Following this brief summation of the 11 steps is a detailed explanation of how each step was applied to the HRA process. The 11 basic steps are as follows:

1. Select the team and train them on relevant plant functions and systems. (IEEE P1082)

2. Familiarize the team with the plant through the use of system walkdowns, simulator observations, etc. (IEEE P1082)
3. Ensure that the full range of potential human actions and interactions is considered in the analysis. (SHARP) (IEEE P1082)
4. Construct the initial model of the relevant systems and interactions. (IEEE P1082)
5. Identify and screen specific human actions that are significant contributors to the safe operation of the plant. This was accomplished through detailed task analyses, time line analyses, observations of operator performance in the plant and in the simulator, and evaluations of the human-machine interface. (SHARP and IEEE P1082)
6. Develop a *detailed* description of the important human interactions and associated key factors necessary to complete the plant model. This description should include the key failure modes, an identification of errors of omission/commission, and a review of relevant performance shaping factors. (SHARP) (IEEE P1082)
7. Select and apply appropriate HRA techniques for modeling the important human actions. (SHARP)
8. Evaluate the impact on ISLOCA of significant human actions identified in Step 6. (SHARP)
9. Estimate error probabilities for the various human actions and interactions, determine sensitivities, and establish uncertainty ranges. (SHARP) (IEEE P1082)
10. Review results (for completeness and relevance). (IEEE P1082)
11. Document all information necessary to provide an audit trail and to make information understandable. (SHARP)

The following paragraphs explain in detail how each of the preceding steps was completed. Since the PRA/HRA process is iterative in nature, the reader should note that several sections of this 11 step method were repeated to refine the analysis.

The first two steps in this process required the selection of a PRA/HRA team and their subsequent training on the plant and its relevant systems. The PRA/HRA team from the INEL was composed of three members: a nuclear engineer (for the PRA), a human factors engineer (for the HRA), and an electrical engineer (with extensive experience in both the PRA and HRA approaches). To familiarize, or train themselves, the team members reviewed the following:

- mechanical and electrical system descriptions (e.g., the reactor coolant, residual heat removal, safety injection, and chemical and volume control systems),
- a sourcebook of plant systems and schematic drawings (NRC-03-87-029, FIN D-1763 [C-5]),
- the plant's Final Safety Analysis Report (FSAR),
- the plant's Technical Specifications [C-6],
- plant procedures (operating, abnormal, emergency, maintenance, administrative, etc.), station directives, and operational practices,
- piping and instrumentation diagrams (P&IDs),
- the types, capacities, and locations of check valves/motor-operated valves identified as being pressure isolation valves,
- training materials such as flow charts, lesson plans, etc.,
- crew composition (for control room and auxiliary building operators) and level of training/experience,
- significant precursor information from general ISLOCA-related LERs, as well as a plant-specific ISLOCA-related LER (NRC Inspection Report 50-412/90-10 and 50-414/90-10 [C-7]).

This training/familiarization process for the plant's systems was enhanced by a two-week visit to the plant.

Step #3 required that significant human actions and interactions be incorporated into the ISLOCA PRA analysis. This was accomplished through an extensive data collection process during the plant visit. As part of the data collection, the utility provided written procedures, training materials, and P&ID drawings. This data was supplemented by interviews and detailed task

analyses with both licensed and non-licensed nuclear operators in the plant. Observations of control room personnel, the use of the utility's simulator, and system walkdowns with licensed and non-licensed operators supplied additional information. Further information was supplied through interviews and walkthroughs with a former shift supervisor (with over 10 years experience) from this particular plant.

The initial plant models were constructed in the fourth step. Using the plant-specific data gathered in Step #3, the HRA analysts worked with the PRA analyst and systems engineering personnel to specify human actions related to the postulated ISLOCA scenarios. As a consequence of several findings from the earlier ISLOCA PRA of the B&W plant, significant attention was given to latent, or precursor, human errors during normal operations which could lead to inoperable equipment or misaligned valves. Examples of these precursor actions included: jumpering of valves to defeat protective interlocks, maintenance procedures, in-service testing practices, and administrative procedures governing the generation and completion of work packages.

The HRA analysts also examined active, or initiator, failures which could lead to an ISLOCA, and post-initiating human errors during responses to abnormal situations. Examples of initiator failures included violations of Technical Specifications, procedural violations (such as early entry into decay heat removal), selection of the incorrect vent path, and reconfiguring plant equipment. For post-initiating errors, the HRA team examined operator responses following a significant break outside containment. Specifically, the HRA analysts looked at operator actions entailing detection, diagnosis, recovery, and isolation.

The fifth step required the HRA analysts to identify those human actions which are significant contributors to the effective operation and safety of the plant. Using the data collected in Step #3, in conjunction with a review of operational procedures and training materials, the HRA team screened the various human actions, identifying those which had a significant impact on plant operations and/or safety with respect to ISLOCA. These significant

human actions were included in the PRA event trees, and they helped guide the activities in the next step.

The output from the preceding step (i.e., Step #5) was a group of important human actions, for specific ISLOCA scenarios, which were described in generic, functional terms (e.g., operators recover system). In the sixth step, the analysts expanded the description of each of these key human actions from a functional description into specific operator tasks and subtasks (e.g., operator opens valve SI-401A, or operator closes valve SI-407B). By breaking down the human actions into specific tasks and subtasks associated with individual equipment and procedures, the analysts began to identify specific failure modes, root causes, and failure effects. The description of each task/subtask was enhanced by referencing significant performance shaping factors (PSFs) which affected a given task. These PSFs were derived from the task analyses, time line analyses, evaluation of the human-machine interface, and direct observations of operator performance. Examples of PSFs included:

1 - the quality of the human-machine interface,
2 - written procedures (emergency, abnormal, maintenance, etc.),
3 - P&IDs,
4 - response times for systems and personnel,
5 - communication requirements,
6 - whether the operator actions were skill, rule, or knowledge-based,
7 - crew experience,
8 - levels of operator stress in different scenarios,
9 - feedback from the systems in the plant,
10 - task dependence and operator dependence,
11 - location of the task (e.g., control room, auxiliary building, etc.),
12 - training for individual operator actions, including ISLOCA situations.

Each PSF was seen as casting either a positive or negative influence on the basic HEP, that is, as either decreasing or increasing the probability of

failure for a given human action. For example, some of the positive PSFs found at the plant included the following:

1 - "The team did not identify any significant deficiencies in the man-machine interface that might significantly increase the probability of an operator error initiating an ISLOCA." [C-7]

2 - "The team found emergency operating procedures to be well written although they lacked some human factors considerations (see #2, negative PSFs)." [C-7]

3 - "Although training specific to ISLOCAs was not part of the licensee's training program, operators indicated, during walkthroughs and simulator exercises, that they were generally well prepared to cope with losses of RCS inventory."[C-7]

Examples of negative PSFs were:

1 - "...the team identified weaknesses in the man-machine interface that could adversely affect the ability of the operators to mitigate an ISLOCA because of poor equipment labeling and the inaccessibility of some equipment." [C-7]

2 - Even though EOPs were generally well-written, the RCS Leak Procedure, OP-902-002, does not provide relevant guidance with respect to requisite actions for the isolation of ISLOCAs. As a result, operators and supervisory personnel would have to rely on knowledge-based actions, outside of normal procedures.

3 - Within the context of the prior finding, operator training (based on Three Mile Island scenarios) emphasized that operators should not override a safety injection occurring in conjunction with an unisolated RCS leak (see Sequence 2). This training could lead control room personnel away from the necessary actions in Sequence 2 to isolate a break in the safety injection lines (e.g., operators would have to sequentially close each HPSI and LPSI safety injection valve on the affected SI train).

4 - Operators' ISLOCA diagnostic abilities were focused on Attachment 1 of OP-902-002, which verifies a LOCA outside containment but directs operators to a procedure (OP-902-002) which does not provide relevant guidance for the isolation of an ISLOCA.

For this HRA analysis, the majority of influences from specific PSFs were implicitly modeled as each HEP was identified and quantified using various THERP tables. A careful examination of these tables will show how

individual basic HEPs can only be identified after associated PSFs are specified. Stress and dependence were explicitly modeled (using THERP) as two of the more significant PSFs. From a human performance perspective, high levels of stress lead to higher probabilities of human error. Generally, a person's short-term memory (STM) can retain from five to nine items of information for brief periods. However, as stress increases, this capacity shrinks to levels where STM can only hold three to five items. This well documented finding interacts with a phenomenon called cognitive tunnel vision where high levels of stress cause an operator's visual and perceptual abilities to begin shrinking into a limited focus so that only one or two salient aspects of his environment are featured. Also, as stress continues to increase, the operator begins to retreat from current conditions, relying on previously learned (perhaps incorrect) patterns of behavior. In Sequence 2, for operator actions FTD-LOCA (fail to detect LOCA) and FTDGN (fail to diagnose ISLOCA), stress levels were modeled as moderately high due to required procedural responses during a reactor trip and/or safety injection. For Sequence 5, FTD (fail to detect loss of coolant) stress was initially modeled as optimal until entry into OP-901-046, the Shutdown Cooling Malfunction procedure, when it increased to moderately high. For FTDGN in Sequence 2, stress remained at moderately high levels, but was increased slightly (e.g., a PSF modifier of 3) in FTI-A/FTI-B. This slight increase was modeled to reflect this plant's concern about a loss of shutdown cooling (based on a significant past LER.

In several of the ISLOCA scenarios, low (LD), moderate (MD), and high (HD) levels of dependence were assigned between the control room supervisor (CRS) or shift supervisor (SS) and the licensed reactor operator (RO). As used in THERP, dependence refers to the level of interaction between two or more workers. Dependence is usually modeled on a scale which ranges from complete dependence (where a second worker fails on a given task because of the failure of a primary worker on the same task) to complete independence (zero dependence or ZD).

A detailed data collection form (see Figures #1 and #2 in this appendix) was developed as an aid in the HRA data collection, task analyses, and the

decomposition and description activity just mentioned. This data form served as a template which guided the collection of the requisite information, in sufficient detail, for each task or subtask in the dominant ISLOCA sequences. Additional items of information, for each human action, were added to these forms as new details surfaced (i.e., details from follow-up telephone conversations with plant personnel, the ISLOCA inspection report for this plant, and a comparison of procedural steps to P&IDs).

The output from the preceding step (#6) is an extensive list of operator tasks and subtasks (with their associated PSFs) for each human action in the dominant PRA sequences. These detailed tasks are the required input for the seventh step, where appropriate HRA techniques for modeling the significant human actions were selected and applied. For each human action, the analysts selected an appropriate technique for task modeling and quantification. Because most of the human actions in this HRA involved the use of various written procedures, THERP-type HRA event trees were used in modeling a majority of the human actions in the detailed analysis. However, not all ISLOCA scenarios were best represented by THERP event trees alone. In those cases, HRA fault trees were used in conjunction with the typical THERP event trees. The fault trees and THERP event trees were used in a detailed analysis to estimate the probability of human error for each of the dominant human actions. Quantification techniques included THERP and Human Cognitive Reliability (HCR) [C-8]. For each human failure, basic HEPs were calculated using THERP or HCR and were then modified using performance shaping factors (PSFs) to realistically describe the work processes at the utility.

Prior to the quantification, or estimation of human error probabilities, the PRA and HRA specialists reviewed and evaluated the significant human actions, and their associated PSFs, for each of the dominant ISLOCA sequences (Step #8). After this evaluation, the HRA analysts developed the HRA event trees and fault trees used to model the significant human actions, and their associated PSFs, for each of the dominant ISLOCA sequences (Step #8). After this evaluation, the HRA analysts developed the HRA event trees and fault trees used to model the significant human actions in each sequence. According to the SHARP method, the development and use of these HRA fault and event

p 1

Sequence ID _____ Task ID _____ Subtask ID _____

Crew size & composition _____

Who does task/subtask? _____

Crew experience: Low_____ Optimal_____ Moderate_____ High_____

Is time limit important for this task/subtask? Yes or No

Time to perform task/subtask (after diagnosis/decision) _____

Median response time for whole task_____ Std Dev _____

Plant/system time available _____

If task not successfully completed, what is next action? _____

_____

_____

_____

and type of alarms competing for attention _____

_____

Quality of plant interface: Excellent___ Good___ Fair___ Poor___ Very Poor

Operators' Stress: Low___ Optimal___ Moderate___ High____

Type of instrument/control _____

HF notes on controls _____

_____

Consequence of improper performance: High___ Medium___ Low___

Explain: _____

Feedback/system response to operator action _____

_____

Operation routine: Yes or No Operation/transient understood: Yes or No

Proc Reqd: Yes or No Proc covers case: Yes or No

Proc well written: Yes or No Proc understood: Yes or No

Proc practiced: Yes or No How much practice/training on task? _____

Cognitive Behavior: Skill_____ Rule_____ Knowledge_____

Tagging: Yes or No Describe: _____

Recovery Actions: Checklists_____ Inspections_____ 2nd Person_____

Feedback from Annunciators_____ Alarms_____ Displays_____

_____

Figure 1: ISLOCA Data Collection Form, page 1

p 2

Local or Remote operation? Explain: _____

Type of clothing during action: _____

_____

Tasks or subtasks done step-by-step_____ or Dynamic_____

Dependence: Is the order of the tasks critical Yes or No

Does the success/failure of one action affect the success/failure of the next

Yes or No Explain:_____

If 2 men do the job, does the action of either one affect the success/failure

of the next? Yes or No Explain:_____

Is the job done with rest stops_____ or continuous performance_____?

Is there any radiation safety or caution for this job? Yes or No

If yes, what dosage?_____ mrem

HF comments of plant-specific PSF's: _____

_____

_____

_____

Additional Comments/observations: _____

_____

_____

_____

_____

_____

_____

_____

_____

_____

_____

_____

_____

_____

_____

_____

_____

Figure 2: ISLOCA Data Form, page 2

trees "provides a disciplined approach for explicitly evaluating alternative actions and, if properly interpreted, may provide the rationale for including some human errors known as acts of commission in the event trees." This HRA modeled errors of commission and omission, which are identified on specific branches of the event trees seen later in this appendix.

Assigning HEP estimates to each of the subtasks was the major activity in Step #9 - Quantification. Traditionally, HRA analysts model human performance through the use of an event tree like Figure 3, which represents "FTD," fail to detect LOCA for Sequence 2. Operator error was generally placed along the descending right branches of the event tree. Successful operator actions were sequenced on the left side of the tree. For example, on the top left, Event "a" - Control Room (CR) Detects Dropping Pressurizer (PZR) Pressure, is the success path. Failure to accomplish this task is modeled as Event "A" - CR Fails to Detect Pressurizer (PZR) Pressure Dropping. When a second operator, or group of operators, is involved, such as in Event "B" - Control Room Fails to Detect PZR Low Pressure Alarms, the action of this second operator, or group, may be modeled in a recovery branch, as shown in Figure 3. Event "b" models the opportunity for the control room to detect the pressurizer low pressure alarms. If the control room does detect the alarm, this becomes a recovery action because it would bring the model back to the success path (via the dotted lines in Figure 3).

Basic HEPs for each individual failure were calculated using THERP or HCR. These basic HEPs were then modified using PSFs to realistically describe the work process. Each PSF either increased or reduced the likelihood of a given human error action. For the event tree in Figure 3, the following PSFs were used to modify the basic HEPs:

- The control room is assumed to be in Mode 1 operations with one RO performing a quarterly stroke test on the safety injection (SI) valves. It is assumed that two PIV check valves have failed and that, as the RO opens the associated SI valve, there is an immediate overpressurization and break, which results in a reactor trip and safety injection actuation signal.

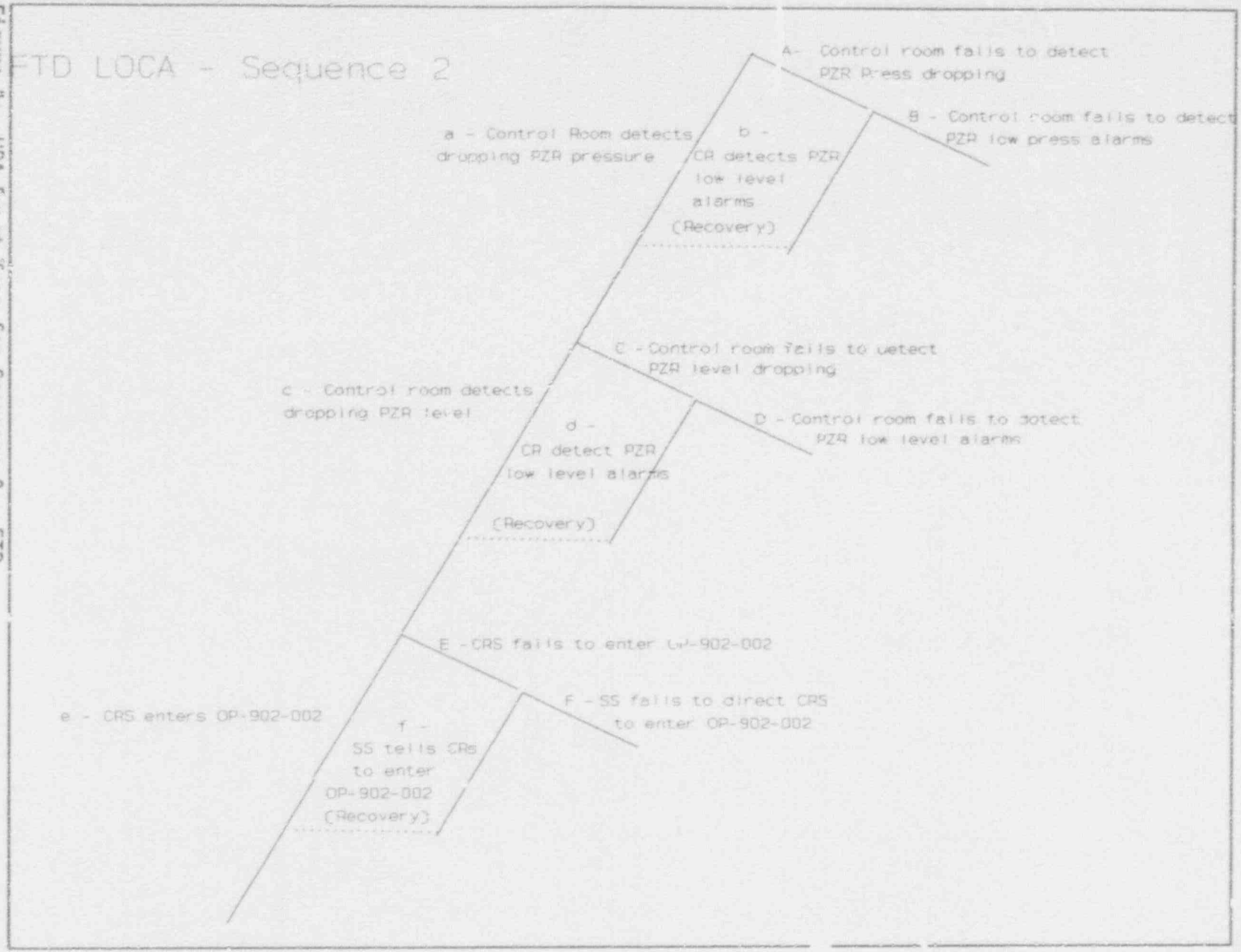

Figure 3: HRA Event Tree for Sequence 2 - FTD

- Stress levels were modeled as being moderately high following the break.
- The crew was judged to be experienced.
- High dependency (HD) was used to model the relationship between the CR's ability to detect decreasing pressurizer pressure (or level) and the CR's ability to detect the subsequent pressurizer alarms. High dependence was also modeled between the CRS and SS as they decide to enter OP-902-002, the RCS Leak Reduction Procedure.

Individual error paths were identified and failure probabilities were estimated using the HEPs and tables from THERP or estimates from HCR. (The probabilistic values in the THERP tables are to be considered as median values from a lognormal distribution. The estimates from HCR are assumed to be point estimates). For example, path "A" in Figure 3 leads to failure by the CR to detect pressurizer pressure dropping (the first branch on the right side of the tree). This particular failure had a basic median HEP of 0.006 (from Table C1) and an error factor of 3. This information came from THERP Table 20-10 #3, item #2, and was modified by a PSF of 2, for moderately high stress. The basic median HEP is converted to a basic mean HEP which is modified by the same PSFs. This results in a nominal mean HEP of 0.015 and an error factor of 3.

Each event tree has several unique error paths. For example, event "A" and event "B" together constitute an error path wherein the CR fails to detect dropping pressurizer pressure and the same CR crew fails to detect the subsequent alarms. In a similar manner, failure path "A-b-C-D" models a sequence of events in which the CR fails to detect dropping pressurizer pressure, then detects the subsequent low pressurizer pressure alarms, but fails to detect decreasing pressurizer level and the subsequent low level alarms. Probabilities for each unique error path were calculated by multiplying each nominal mean HEP on a given error path by any other nominal mean HEP on the same error path (see Table C2). For example, the error rate for path "A-B" would be calculated by multiplying the HEP of failure "A" (0.015) by the HEP for failure "B" (0.279), resulting in a nominal HEP for

that path equaling 0.004 (0.015 x 0.279 = 0.004). NOTE: the 6-digit accuracy for numerical values in the following tables is an artifact of the software used for quantification and does not imply 6-digit precision for the HEP estimates. Other examples of error paths for this event tree include: "A-b-C-D", "a-c-E-F", and "A-b-C-d-E-F." The failure probabilities for individual error paths were summed to give the total failure probability for that event tree. The resulting error factor for the total failure probability was calculated from an uncertainty analysis using IRRAS (the Integrated Reliability and Risk Analysis System [C-9]).

Table C1 lists the basic median HEPs and nominal mean HEPs for the event tree depicted in Figure 3 (FTD-LOCA, Sequence 2). This table enumerates the basic human actions/errors, the basic or unmodified HEPs (median and mean), their sources from the table and item number in THERP, whether the action was modeled as being performed in a step-by-step mode or dynamically, PSF modifier values and the related THERP source, level of dependency, and finally, the nominal, or modified, mean HEP with its error factor (derived from THERP HEPs or THERP Table 20-20).

Table C1: HEPS for Sequence 2 ; FTD LOCA - Sequence 2

	Human Action / Error	Basic Median HEP	Error Factor	Source/ THERP Table #	Step-by-Step or Dynamic	Modifier for PSFs	Modifier Source	THERP Dependency	Basic Mean HEP	Nominal Mean HEP	Error Factor
A	Control room fails to detect dropping PZR pressure	0.006	3.0	T20-10 #3	SBS	2	T20-16 #4a	ZD	0.007499	0.014998	3.0
B	Control room fails to detect PZR low pressure alarms	0.0001	10.0	T20-23 #1a	SBS	2	T20-16 #4a	HD	0.000266	0.500266	5.0
										# 0.278928	2.5
C	Control room fails to detect dropping PZR level	0.006	3.0	T20-10 #3	SBS	2	T20-16 #4a	ZD	0.007499	0.014998	3.0
D	Control room fails to detect PZR low level alarms	0.0001	10.0	T20-25 #1	SBS	2	T20-16 #4a	HD	0.000266	0.500266	5.0
										# 0.278928	2.5
E	CRS fails to enter OP-902-002	0.005	10.0	T20-6 #4	SBS	2	T20-16 #4a	ZD	0.013317	0.026635	10.0
F	SS fails to direct CRS to enter OP-902-002	0.1	5.0	T20-22 #1	SBS	2	T20-16 #2a	HD	0.161383	0.661383	5.0
										# 0.33097	2.3

Table C2: Failure Paths and Total Failure Probabilities (Seq. 2, FTD)

Table C2 : Failure Paths and Total Failure Probabilities

FTD LOCA - Sequence 2

	Failure Path	Calculations	Results
1	AB	0.014998 x 0.278928	0.004183
2	AbCD	0.014998 x 0.014998 x 0.278928	0.000062
3	AbCdEF	0.014998 x 0.014998 x 0.026635 x 0.33097	0.000001
4	AbcEF	0.014998 x 0.026635 x 0.33097	0.000132
5	aCD	0.014998 x 0.278928	0.004183
6	aCdEF	0.014998 x 0.026635 x 0.33097	0.000132
7	acEF	0.026635 x 0.33097	0.00881
		Total Failure Probability	0.018
		Error Factor	4.26

Table C2 lists the individual failure paths for Figure 3, FTD-LOCA, and the resulting failure probabilities for each path, including how the failure probabilities were calculated (again, digit numbers do not imply 6-digit precision for HEP estimates). (As a note for subsequent tables, failure probabilities of "*" on the tables signify negligible error rates which were less than 10^{-6}.) Table C2 also lists a total failure probability for each event tree, which is simply the sum of the failure probabilities from the individual failure paths. As indicated in Table C2, the total failure probability for the FTD-LOCA event tree in Figure 3 is estimated to be about 0.018. As a point estimate, given the PSFs discussed earlier, an RO, or group in the CR, can be expected not to enter the correct procedure after detecting a loss of coolant, about 18 times out of a thousand.

As discussed in Section 4.2 of the main report, the estimates of human error probabilities obtained from THERP are generally treated as point estimates with a given error factor. The authors of THERP indicate that there is insufficient data, at this time, to accurately determine the true shape of the underlying probability distribution associated with these point estimates and that these distributions are unimportant. Quoting from THERP (pages 7-6 through 7-8):

> "Although we would like to have data clearly showing the distributions of human performance for various NPP (nuclear power plant) tasks, there is ample evidence that the outcomes of HRAs are relatively insensitive to assumptions about such distributions...."

The authors then provide several examples to support a general conclusion:

> "the assumption of normal, lognormal, or other similar distributions will make no material difference in the results of HRA analyses for NPP operations. In some cases, this insensitivity may result from a well designed system that has so many recovery factors that the effect of any one human error on the system is not substantial.... For computational convenience, one might wish to assume the same distribution for

probabilities of human failure as the one used for probabilities of equipment failure, as was used in WASH-1400."

To summarize, the authors of THERP "suggest" that HRA analysts "assume" the point estimates from THERP are medians from a lognormal distribution, even though such an assumption is "speculative" at best.

While the THERP approach (treating the HEPs as median values from a lognormal distribution) has certain computational and interpretational advantages, it has one distinct drawback, with respect to PRAs. In most PRAs, hardware failure probabilities are assumed to be lognormally distributed. The HEPs are multiplied by hardware failure probabilities when calculating core damage frequencies. This requires a median to be multiplied by a mean, a procedure which does not result in a mean value of the core damage frequency. A mean core damage frequency can be obtained by converting the median HEP values (from an assumed lognormal distribution) to mean HEP values, thereby allowing the necessary multiplications.

This HRA adopted THERP's recommendation to treat each HEP as a median value from a lognormal distribution. Detailed HRA analyses were conducted for each of the significant scenarios identified in this ISLOCA PRA. Tables C1 and C2 summarize the results of these analyses, i.e., by converting the median HEPs to mean HEPs using the following formulas:

$$Mean\ HEP = \exp\left(\mu + \frac{\sigma^2}{2}\right);$$

$$where\ \hat{x} = the\ Median\ HEP;$$

$$\mu = \ln\hat{x};\ and,$$

$$\sigma = \frac{\ln(ErrorFactor)}{1.645}$$

Converting median HEPs (from an assumed lognormal distribution) to mean HEPs allowed uncertainties in human error to be included in calculations of the uncertainty in core damage frequency. The actual conversions to mean HEPs were accomplished by inserting the basic, median HEPs in each event tree into the equations above. The resulting mean HEPs were then modified by appropriate PSFs and used in the appropriate error branch on specific event trees to calculate error path and total failure probabilities for each event tree.

A careful review of Table C1 will show that the conversion from median to mean HEPs can cause problems with the resulting confidence interval. The reader may recall that individual HEPs are considered a point estimate with some uncertainty, e.g., a confidence interval, surrounding it. Generally, this confidence interval is defined by calculating the upper bound (95th percentile) and lower bound (5th percentile) for each HEP. The upper bound is found by multiplying the nominal (modified-median) HEP by its associated error factor (EF) and the lower bound results by dividing the nominal (modified-median) HEP by the same EF. For example, when the basic median HEP for event "A" (Table C1) is modified, it becomes a value of 0.012 (the nominal mean HEP equals 0.015), the resulting upper bound is 0.036 (0.012 x an EF of 3). Likewise, the lower bound is 0.004 (0.012 divided by the EF of 3).

However, when a basic HEP is modified by several PSFs, including dependency, problems with the confidence interval begin to arise. For example, examine event "B" on Table C1. The basic median HEP for this event is 0.001 with an EF of 10. When this HEP is converted to a mean value and modified for stress and high dependence, the resulting nominal mean HEP is 0.5 with an EF of 5 (from THERP Table 20-20, #5). If one calculates the upper bound for this HEP by multiplying this value by the EF (or more correctly by multiplying the modified median value, 0.5, by the EF) the result is a value of 2.5; this value is an anomaly, because the maximum value for a probability is constrained to be less than or equal to one (i.e., unity). To correct this difficulty, the nominal mean HEP and EF were adjusted using a constrained lognormal distribution (see Appendix D for details). The resulting revised nominal mean HEP and EF are shown in Table C1 as the values with a "#", just

below the old values for event "B". The revised mean HEP is 0.279 with an EF of 2.5. Similar adjustments have been made for other events in Sequence 2, as well as for several human actions in Sequence 5. Table C3 lists all of the HEP revisions for each sequence and individual actions in this HRA. This table lists the sequence number and associated HRA tree, the human action from that tree, and the following numerical values:

1 - basic median HEP with its EF,
2 - modified median HEP (using associated PSFs) with suggested EF,
3 - Mean HEP and its EF (from lognormal distribution),
4 - Revised mean HEP and EF (from constrained lognormal distribution),
5 - 50th percentile value (constrained lognormal distribution), and
6 - 95th percentile value (constrained lognormal distribution).

This example focused on the event tree for Sequence 2, event FTD-LOCA; a similar process was followed for each of the remaining human actions in the HRA. Specific details, including event trees and HEP tables are provided in the following section.

In the final two steps (#9 and #10) of the HRA process, the analysts reviewed the results of the HRA and documented all of the information needed to provide an audit trail. As final HRA failure probabilities were generated for each ISLOCA sequence, the HRA analysts consulted with the PRA analyst and a systems engineer regarding the validity, completeness, and relevance of the results. During these reviews, several questions arose which required more information. Several telephone calls were placed to operations personnel at the plant and detailed interviews or walkthroughs were conducted with a past shift supervisor from the plant.

The last step necessitated the documentation of the data, methodology, and results from this HRA to provide an audit trail. This was accomplished by creating a data notebook containing the completed data forms, pertinent procedures, working notes from the ISLOCA inspection, and the NRC ISLOCA inspection report.

Table C3: Revised HEPs for the CE ISLOCA HRA

HEP Revisions Using a Constrained Lognormal Distribution

Seq. #	Human Action	Median HEP (EF)	Modified Med. (EF)	Mean HEP(EF)	Revised Mean(EF)	50 %ile	95 %ile
2-FTD	B-CR fails to detect PZR low press alarms	0.0001(10)	0.5 (5)	0.5 (5)	0.279(2.5)	0.237	0.608
	D-CR fails to detect PZR low level alarms	0.0001(10)	0.5 (5)	0.5 (5)	0.279(2.5)	0.237	0.608
	F-SS fails to direct CRS to enter OP-902-002	0.1 (5)	0.6 (5)	0.661(5)	0.331(2.3)	0.291	0.672
2-FTDGN	B-SS fails to determine if SG pressure low/dropping	0.1 (5)	0.6 (5)	0.661(5)	0.331(2.3)	0.291	0.672
	D-SS fails to determine contain. press. not rising	0.1 (5)	0.6 (5)	0.661(5)	0.331(2.3)	0.291	0.672
	F-SS fails to detect no activity in steam plant	0.1 (5)	0.6 (5)	0.661(5)	0.331(2.3)	0.291	0.672
	H-SS fails to verify entry into OP-902-002	0.1 (5)	0.6 (5)	0.661(5)	0.331(2.3)	0.291	0.672
6-FTD	C-CR fails to detect PZR Lo-Lo level alarm	0.001(10)	0.5 (5)	0.5 (5)	0.279(2.5)	0.237	0.608
	E-SS fails to direct CRS to enter OP-901-046	0.005(10)	0.51 (5)	0.51(5)	0.284(2.5)	0.241	0.614
6-FTDGN	E-SS fails to direct CRS to enter Sec. 6.1(Op-901-046)	0.005(10)	0.51 (5)	0.51(5)	0.284(5)	0.241	0.614
6-FTI-A	B-RO fails to remind CRS to close SI401(A/B)	0.1 (5)	0.65 (5)	0.74(5)	0.354(2.2)	0.315	0.697
	D-CRS fails to remind RO to close SI401(A/B)	0.1 (5)	0.4 (5)	0.56(5)	0.299(2.4)	0.257	0.633
	F-RO fails to remind CRS to check RCS not stabilizing	0.1 (5)	0.65 (5)	0.74(5)	0.354(2.2)	0.315	0.697
	H-CRS fails to tell Ro to check RCS not stabilizing	0.1 (5)	0.4 (5)	0.56(5)	0.299(2.4)	0.257	0.633
	J-Ro fails to remind CRS to place standby SDC...	0.1 (5)	0.65 (5)	0.74(5)	0.354(2.2)	0.315	0.697
	L-CRS fails to verify RO placed Standby SDC...	0.1 (5)	0.4 (5)	0.56(5)	0.299(2.4)	0.257	0.633
	N-RO fails to remind CRS to close SI401(A/B) on...	0.1 (5)	0.65 (5)	0.74(5)	0.354(2.2)	0.315	0.697
	P-CRS fails to verify RO closed correct SI401...	0.1 (5)	0.4 (5)	0.56(5)	0.299(2.4)	0.257	0.633
6-FTI-B	B-RO fails to remind CRS to close SI401(A/B)	0.1 (5)	0.65 (5)	0.74(5)	0.354(2.2)	0.315	0.697
	D-CRS fails to remind RO to close SI401(A/B)	0.1 (5)	0.4 (5)	0.56(5)	0.299(2.4)	0.257	0.633
	F-RO fails to remind CRS to check RCS not stabilizing	0.1 (5)	0.65 (5)	0.74(5)	0.354(2.2)	0.315	0.697
	H-CRS fails to tell Ro to check RCS not stabilizing	0.1 (5)	0.4 (5)	0.56(5)	0.299(2.4)	0.257	0.633
	J-Ro fails to remind CRS to place standby SDC...	0.1 (5)	0.65 (5)	0.74(5)	0.354(2.2)	0.315	0.697
	L-CRS fails to verify RO placed Standby SDC...	0.1 (5)	0.4 (5)	0.56(5)	0.299(2.4)	0.257	0.633
	N-RO fails to remind CRS to close SI401(A/B) on...	0.1 (5)	0.65 (5)	0.74(5)	0.354(2.2)	0.315	0.697
	P-CRS fails to verify RO closed correct SI401...	0.1 (5)	0.4 (5)	0.56(5)	0.299(2.4)	0.257	0.633

Scenarios and Human Actions for the CE ISLOCA HRA

This section describes the scenarios and summarizes the human actions analyzed in the CE ISLOCA HRA. Human actions for the sequences were initially identified in a cooperative effort by PRA and HRA analysts based on plant-specific information. The sequences were selected for analysis by using screening HEPs in the PRA modeling to determine likely scenarios in terms of ISLOCA risk (i.e., core damage frequencies greater than 10^{-8}/yr). A screening HEP of 0.5 was used, except in some cases where a screening HEP of 1.0 was judged appropriate. Following are brief descriptions of the selected scenarios from an HRA perspective and specific tables of the human actions relevant to the scenarios.

Sequence 1A: Premature Entry Into Shutdown Cooling (SDC)

During the plant shutdown process, the operators will open MOVs SI-401 (A&B) and SI-407 (A&B) and HOV SI-405 (A&B) to place both trains of SDC into service. Sequence 1A investigates the likelihood that the operators prematurely open these valves when RCS pressure is above SDC entry procedural limits (396 psig and 350° F). To open the valves, operators would have to override interlock permissives, disregard administrative barriers, and take actions beyond those specified by operating procedures. Further human actions for this scenario were not analyzed in the HRA, as premature opening of the SDC system suction isolation valves (the scenario initiator) was estimated by the HRA to be not credible, having a negligible probability.

Sequence 1B: Startup with Shutdown Cooling Valves Open

Sequence 1B is similar to Sequence 1A, except that the plant is undergoing a startup. In this sequence operators must fail to close MOVs SI-401 (A&B) and SI-407 (A&B) and HOV SI-405 (A&B) leaving one, or both trains of SDC in service. An extensive review of administrative barriers, operating procedures, and plant systems indicated that the plant has well defined procedural guidance, in conjunction with redundant systems and multiple alarms which would warn operators about any of the MOVs or HOVs being left open

during plant startup and pressurization. In addition, the auto-closure interlocks on the SI-401 and SI-405 valves (a feature which the utility wants to remove) would automatically close both valves when RCS pressure exceeded 700 psia. Further human actions for this scenario were not analyzed in the HRA, since startup of the plant with these valves left open was estimated by the HRA to be not credible, having a negligible probability.

Sequence 2: RCS Cold Leg/LPSI Discharge Interfacing LOCA

In this scenario the reactor is operating at power and a quarterly stroke test is being performed on the LPSI discharge motor-operated flow control valves [SI-138 (A&B) and SI-139 (A&B)]. Two check valves protecting one of the four MOVs are assumed to have failed. When the MOV is cycled open during the stroke test, the LPSI piping is exposed to RCS operating pressure. This results in overpressurization of one LPSI train and a rupture of the system in one of the reactor auxiliary building (RAB) safeguard pump rooms, creating a large RCS leak outside of containment. A reactor trip and safety injection automatically occur upon low pressurizer level before the MOV is stroked shut. LPSI components in either the overpressurized or remaining train may be adversely affected and fail due to their proximity to the leak. The leak may be isolated by closing the MOV that was stroked open (which created the overpressurization). Operator failure to detect, diagnose, and isolate the leak may result in core damage.

Sequence 5 (A&B): LPSI/RWSP Suction Interfacing LOCA During Shutdown

In this scenario, the reactor is shut down and SDC is being brought into service to remove decay heat. Low pressure piping from the refueling water storage pool (RWSP) is protected from higher pressure in the LPSI piping (used during SDC) by two check valves in each line. Failure of both check valves in one line is assumed to result in overpressurization and rupture of the RWSP suction piping, thus creating a reactor coolant leak in the RAB, outside of containment. Version A of the scenario begins with one SDC train in service and one in standby. Version B of the scenario begins with both SDC trains in service. The RCS leak can be isolated by shutting one of the suction

isolation valves (MOVs SI-401, SI-407, or HOV SI-405) in the affected SDC train. Failure of the operators to detect, diagnose, and isolate the break will lead to core damage.

Human Actions For this ISLOCA HRA

The following table lists the PRA identifier and a brief description of each relevant human action identified for analysis in this HRA.

Table C4: Human Actions for the CE HRA

Seq. #	IDENTIFIER	DESCRIPTION
2	FTD	Control room (or operators) fail to detect LOCA
2	FTDGN	Control room fails to diagnose ISLOCA
2	FTI	Control room/operators fail to isolate break
5	FTD	Control room/operators fail to detect LOCA
5	FTDGN	Control room/operators fail to diagnose ISLOCA
5	FTI-A	Control room fails to isolate break with one train of shut down cooling in service
5	FTI-B	Control room fails to isolate break with both trains of shut down cooling in service

Modeling Of Human Actions And Estimated Human Error Probabilities

This section describes the HRA event trees and the HEP estimates for the human actions identified as significant for this ISLOCA HRA. An HRA event tree (with any associated fault trees), subtask HEP tables documenting HEP estimation for each subtask branch on the tree, and tables providing failure path calculations and total failure probability estimates are presented for each human action. Each set of trees and tables for a human action is preceded by a brief discussion relevant to the modeling and HEP estimation for that action.

FTD: Sequence 2

Event FTD for Sequence 2 models operator or control room failure to detect significant indications for a loss of coolant and enter OP-902-002, the Loss of Coolant Accident Recovery Procedure. The critical subtasks, detecting symptoms of a LOCA, i.e., decreasing pressurizer level and pressure, for FTD are modeled according to step B.2 of this procedure. The HRA modelir assumes that the control room is in Mode 1 operation with one RO performing a quarterly stroke test on the safety injection (SI) valves. It also assumes that two PIV check valves have failed and that as the RO opens the associated SI valve, there is an immediate overpressurization and break, resulting in a reactor trip and safety injection actuation signal (SIAS). Furthermor stress levels were modeled as being moderately high and the crew was judged to be experienced. High dependency (HD) was used to model the relationship between the CR's ability to detect decreasing pressurizer pressure (or level) and the CR's ability to detect the subsequent pressurizer alarms. High dependence was also modeled between the CRS and SS as they decide to enter OP-902-002. The HRA event tree, subtask quantifications, and total failure probabilities for this event have already been presented in Figure 3 and Tables C1 and C2. As listed in Table C2, the total mean failure probability for event FTD in this sequence is 0.0175 with an EF of 4.26. No credit was given to the CR for an alarmed pressure indicator (PI) between the two check valves because the CR generally disabled this annunciator by pulling its card,

and because the stroke test procedure does not direct operators to check the pressure on this PI before stroking the valve open.

FTDGN: Sequence 2 (Using Procedure Only)

Event FTDGN for Sequence 2 models failure of the control room to correctly diagnose an ISLOCA using the diagnostic flow chart from OP-902-000 (and Attachment 1 of OP-902-002), the Emergency Entry Procedure. The critical subtasks for event FTDGN are modeled according to the requisite actions for the CRS and SS to correctly diagnose an ISLOCA. HRA modeling includes critical procedural steps from the diagnostic flow chart and verification of entry into OP-902-002, the Loss of Coolant Accident Recovery Procedure. Recovery paths are also modeled. Stress was assigned a PSF value of 2, i.e., moderately high, and high dependence was assessed between the SS and CRS during diagnosis of the event. The HRA event tree, subtask quantifications, and total failure probabilities are presented in Figure 4 and Tables C5 and C6. As listed in Table C6 the total mean failure probability for event FTDGN (Using procedure only) is 0.02 with an EF of 3.96.

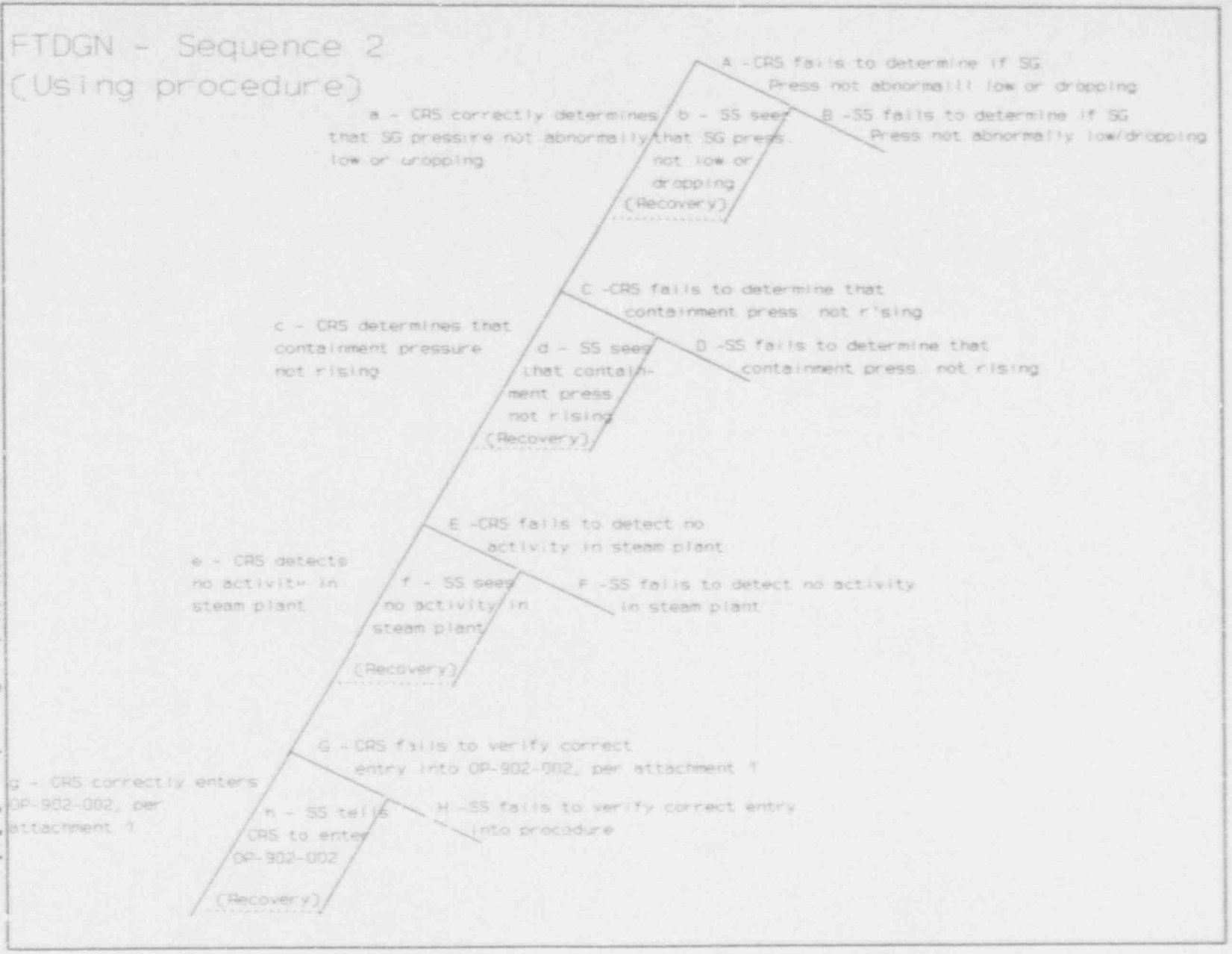

Figure 4: HRA Event Tree for Sequence 2 - FTDGN (Using Procedure Only)

Table C5: HEPs for Sequence 2, FTDGN (Using Procedure Only)

Table C5: HEPS for Sequence 2 ; FTDGN (using procedure only)

	Human Action / Error	Basic Median HEP	Error Factor	Source/ THERP Table #	Step-by-Step or Dynamic	Modifier for PSFs	Modifier Source	THERP Dependency	Basic Mean HEP	Nominal Mean HEP	Error Factor
A	CRS fails to determine SG pressure not abnormally low or dropping	0.006	3.0	T20-10 #3	SBS	2	T20-16 #4a	ZD	0.007499	0.014998	3.0
B	SS fails to determine if SG pressure not abnormally low or dropping	0.1	5.0	T20-22 #1	SBS	2	T20-16 #4a	HD	0.161383	0.661383	5.0
										# 0.33097	2.3
C	CRS fails to determine that containment pressure not rising	0.006	3.0	T20-10 #3	SBS	2	T20-16 #4a	ZD	0.007499	0.014998	3.0
D	SS fails to determine containment pressure not rising	0.1	5.0	T20-22 #1	SBS	2	T20-16 #4a	HD	0.161383	0.661383	5.0
										# 0.33097	2.3
E	CRS fails to detect no activity in steam plant	0.006	3.0	T20-10 #3	SBS	2	T20-16 #4a	ZD	0.007499	0.014998	3.0
F	SS fails to detect no activity in steam plant	0.1	5.0	T20-22 #1	SBS	2	T20-16 #4a	HD	0.161383	0.661383	5.0
										# 0.33097	2.3
G	CRS fails to enter OP-902-002 per attachment #1	0.006	3.0	T20-10 #3	SBS	2	T20-16 #4a	ZD	0.007499	0.014998	3.0
H	SS fails to verify entry into OP-902-002 per attachment #1	0.1	5.0	T20-22 #1	SBS	2	T20-16 #4a	HD	0.161383	0.661383	5.0
										# 0.33097	2.3

Table C6: Failure Paths and Total Failure Probabilities (Seq. 2, FTDGN)

Table C6: Failure Paths and Total Failure Probabilities

FTDGN (using procedure only) - Sequence 2

	Failure Path	Calculations	Results
1	AB	0.014998 x 0.33097	0.004963
2	AbCD	0.014998 x 0.014998 x 0.33097	0.000074
3	AbCdEF	0.014998 x 0.014998 x 0.014998 x 0.33097	0.000001
4	AbCdEfGH	0.014998 x 0.014998 x 0.014998 x 0.014998 x 0.33097	*
5	AbCdeGH	0.014998 x 0.014998 x 0.014998 x 0.33097	0.000001
6	AbcEF	0.014998 x 0.014998 x 0.33097	0.000074
7	AbcEfGH	0.014998 x 0.014998 x 0.014998 x 0.33097	0.000001
8	AbceGH	0.014998 x 0.014998 x 0.33097	0.000074
9	aCD	0.014998 x 0.33097	0.004963
10	aCdEF	0.014998 x 0.014998 x 0.33097	0.000074
11	aCdEfGH	0.014998 x 0.014998 x 0.014998 x 0.33097	0.000001
12	aCdeGH	0.014998 x 0.014998 x 0.33097	0.000074
13	acEF	0.014998 x 0.33097	0.004963
14	acEfGH	0.014998 x 0.014998 x 0.33097	0.000074
15	aceGH	0.014998 x 0.33097	0.004963
		Total Failure Probability	0.02
		Error Factor	3.96

FTI: Sequence 2 (Using Procedure)

An extensive review of OP-902-002, the Loss of Coolant Accident Recovery Procedure, and multiple interviews with a past SS from this utility indicate that this scenario is beyond the scope of the appropriate procedure (which was written to cover a design basis LOCA only). As a result, there are no actions within this procedure that would guide operators to isolate the leak in this scenario (FTI - Sequence 2). Therefore, HRA modeling only included one subtask, "Control Room Fails to Isolate Break," with a failure probability of 1.0.

Since procedure OP-902-002 does not provide guidance pertaining to the isolation of an ISLOCA, the question becomes: "What will an average Control Room (SS, CRS, Shift Technical Advisor, and Technical Support Center) do to isolate this ISLOCA break?" Figures 6 and 7 and Tables C-9 - C-12, (following Table C-8) present a sensitivity analysis for Sequence 2 actions: events FTDGN and FTI. The sensitivity analysis is based on interviews with a past shift supervisor from the CE plant. It attempts to model the "average" CRS, SS, and Control Room response using the diagnostic flow chart from OP-902-002 and knowledge-based behavior, which lies outside of procedural guidance.

Figure 5: HRA Event Tree for Sequence 2 - FTI (Using Procedure Only)

Table C7: HEPs for FTI - Sequence 2 (Using Procedure Only)

Table C7: HEPS for Sequence 2 ; FTI (Following Procedure Only)

Human Action / Error	Basic Median HEP	Error Factor	Source/ THERP Table,[4]	Step-by-Step or Dynamic	Modifier for PSFs	Modifier Source	THERP Dependency	Basic Mean HEP	Nominal Mean HEP	Error Factor
A Control room fails to isolate ISLOCA following OP-902-002	1.0	1.0		SBS				1.0	1.0	1.0

Table C8: Failure Path and Total Failure Probability (Seq. 2, FII-Procedure)

Table C8: Failure Paths and Total Failure Probabilities

FII (Following Procedure Only)

Failure Path		Calculations	Results
1	A	1.0	1.0
		Total Failure Probability	1.0
		Error Factor	1.0

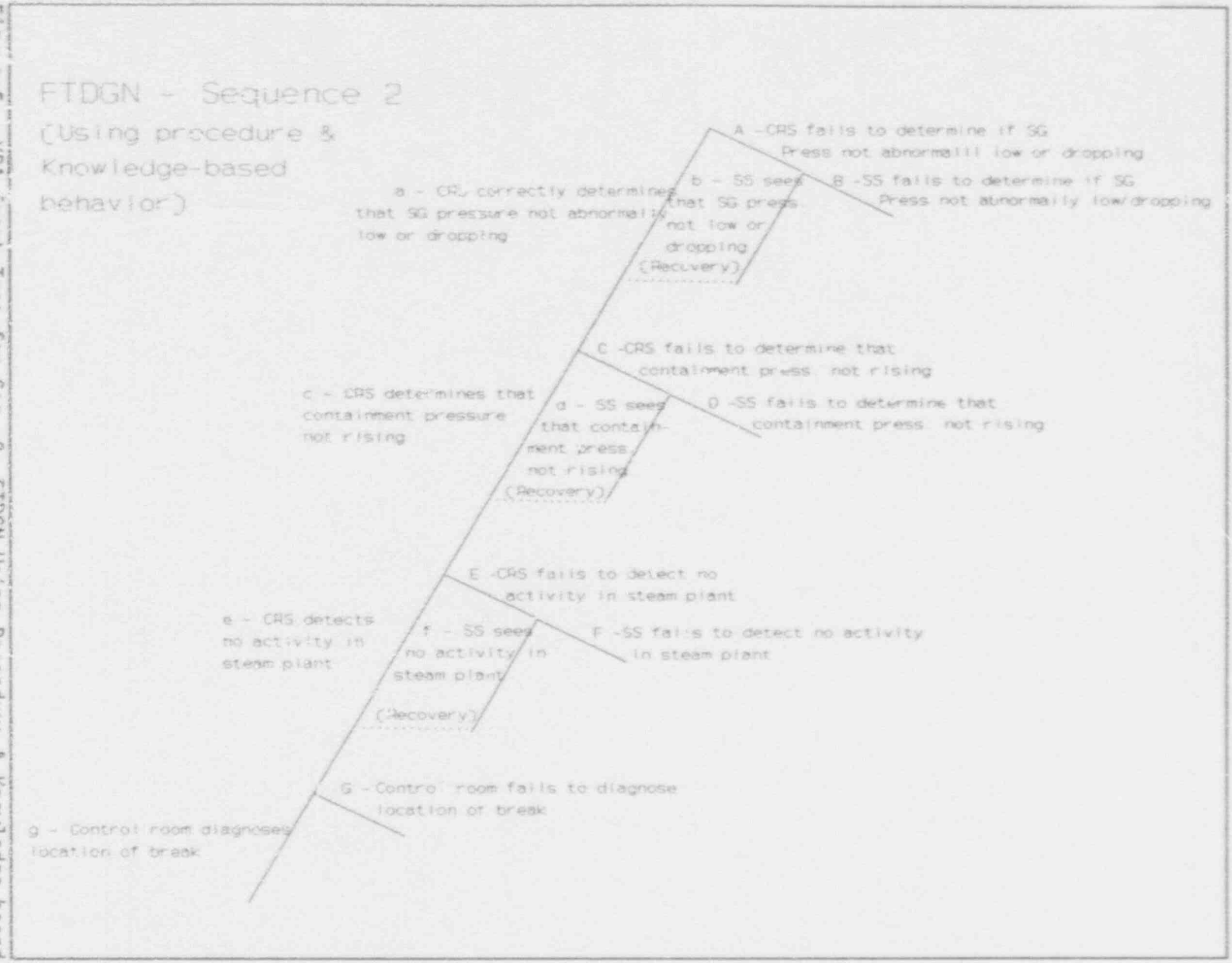

Figure 6: HRA Event Tree for Seq. 2, FTDGN-Using Procedure & Knowledge-based Behavior

Table C9: HEPS for Sequence 2 ; FTDGN (using proc. & knowledge-based behavior)

	Human Action / Error	Basic Median HEP	Error Factor	Source/ THERP Table #	Step-by-Step or Dynamic	Modifier for PSFs	Modifier Source	THERP Dependency	Basic Mean HEP	Nominal Mean HEP	Error Factor
A	CRS fails to determine SG pressure not abnormally low or dropping	0.006	3.0	T20-10 #3	SBS	2	T20-16 #4a	ZD	0.007499	0.014998	3.0
B	SS fails to determine if SG pressure not abnormally low or dropping	0.1	5.0	T20-22 #1	SBS	2	T20-16 #4a	HD	0.161383	0.661383	5.0
										# 0.33097	2.3
C	CRS fails to determine that containment pressure not rising	0.006	3.0	T20-10 #3	SBS	2	T20-16 #4a	ZD	0.007499	0.014998	3.0
D	SS fails to determine containment pressure not rising	0.1	5.0	T20-22 #1	SBS	2	T20-16 #4a	HD	0.161383	0.661383	5.0
										# 0.33097	2.3
E	CRS fails to detect no activity in steam plant	0.006	3.0	T20-10 #3	SBS	2	T20-16 #4a	ZD	0.007499	0.014998	3.0
F	SS fails to detect no activity in steam plant	0.1	5.0	T20-22 #1	SBS	2	T20-16 #4a	HD	0.161383	0.661383	5.0
										# 0.33097	2.3
G	Control room fails to diagnose correct location of break	0.48	5.0	HCR-knowledge	SBS	1		ZD	0.774642	0.774642	5.0
										# 0.362672	2.1

Table C10: Failure Path & Total Failure Probability (Seq. 2, FTDGN-Knowledge-based)

Table C10: Failure Paths and Total Failure Probabilities

FTDGN (using proc. & knowledge-based behavior) - Sequence 2

Failure Path		Calculations	Results
1	AB	0.014998 x 0.33097	0.004963
2	AbCD	0.014998 x 0.014998 x 0.33097	0.000074
3	AbCdEF	0.014998 x 0.014998 x 0.014998 x 0.33097	0.000001
4	AbCdEfG	0.014998 x 0.014998 x 0.014998 x 0.362672	0.000001
5	AbCdeG	0.014998 x 0.014998 x 0.362672	0.000081
6	AbcEF	0.014998 x 0.014998 x 0.33097	0.000074
7	AbcEfG	0.014998 x 0.014998 x 0.362672	0.000081
8	AbceG	0.014998 x 0.362672	0.005439
9	aCD	0.014998 x 0.33097	0.004963
10	aCdEF	0.014998 x 0.014998 x 0.33097	0.000074
11	aCdEfG	0.014998 x 0.014998 x 0.362672	0.000081
12	aCdeG	0.014998 x 0.362672	0.005439
13	acEF	0.014998 x 0.33097	0.004963
14	acEfG	0.014998 x 0.362672	0.005439
15	aceG	0.362672	0.362672
		Total Failure Probability	0.39
		Error Factor	2.02

FTI: Sequence 2 (Using Knowledge-based Behavior)

For event FTI, Sequence 2, using knowledge-based behavior, outside of procedures, entry into this action assumes successful diagnosis of an ISLOCA (using Attachment 1 of OP-902-002), successful diagnosis of the break's most probable location (i.e., the safeguards pump room on the minus 35-foot level of the RAB), AND an understanding that the break occurred when the RO opened one of the LPSI flow control valves (FCVs) on the affected safety injection train during a quarterly stroke test. Successful isolation of the break depends on the operators going outside of procedures, overriding their training (to not terminate SI without meeting SI termination criteria) and closing the correct LPSI FCV [SI-138, SI-139 (A or B)]. This could be done by successively closing individual LPSI FCVs, then monitoring the pressurizer to see if level and pressure are stabilizing.

Figure 7 shows an HRA fault tree which models this sequential closing of the four LPSI FCVs. FP#1 (failure path #1) models the probability of an RO failing to close the correct FCV valve by sequentially opening and closing each one: FCV1 is the probability of an RO failing to select the correct FCV on the first try (1 chance in 4 of being correct); FCV2 is the probability of an RO failing to select the correct FCV on the second try (1 chance in 3 of being correct); FCV3 is the probability of an RO failing to select the correct FCV on the third try (1 chance in 2 of being correct); and HEP, which is the probability of selecting the correct valve on the fourth try but incorrectly activating the controls for that valve. FP#2 models correctly selecting the proper FCV on the first attempt (/FCV1, i.e., the complement, or probability of success, for FCV1) and the human error probability (HEP) for incorrectly activating the FCV controls. FP#3 models the probability of an RO failing to select the correct FCV on the first try (FCV1), correctly selecting the valve on the second attempt (/FCV2, the complement of FCV2), and the human error probability (HEP). FP#4 models the probability of an RO failing to select the correct FCV on the first try, the failure of an RO to select the correct valve on the second attempt, selecting the correct valve of the third attempt (/FCV3 - the complement of FCV3) and the human error probability (HEP). The total failure probability for this action is 0.019 with an EF of 2.97.

Small Break FTDGN: Sequence 2 (Using Knowledge-based Behavior)

For a small break ISLOCA (flange failure), event FTDGN is modeled in the same manner as before with the addition of subtask "G" - Control Room Fails to Diagnose Location of Break. This particular subtask was re-quantified using the HCR technique assuming that the operators had 26970 seconds available and it would take 1830 seconds to complete the task; the crew had average (nominal) training; the situation was a potential emergency; and the quality of the man-machine interface was fair. The knowledge-based non-response probability for this subtask was estimated to be 0.001. The resulting total failure probability was estimated to be 0.016.

Small Break FTI: Sequence 2 (Using Knowledge-based Behavior)

For event FTI (small break), Sequence 2, using knowledge-based behavior, outside of procedures, entry into this action once again assumes successful diagnosis of an ISLOCA (using Attachment 1 of OP-902-002), successful diagnosis of the break's most probable location (i.e., the safeguards pump room on the minus 35-foot level of the RAB), AND an understanding that the break occurred when the RO opened one of the LPSI flow control valves (FCVs) on the affected safety injection train during a quarterly stroke test. As before, successful isolation of the break depends on the operators going outside of procedures, overriding their training (to not terminate SI without meeting SI termination criteria) and closing the correct LPSI FCV [SI-138, SI-139 (A or B)]. This could be done by successively closing individual LPSI FCVs, then monitoring the pressurizer to see if level and pressure are stabilizing. The HRA event trees and total failure probability (0.019) for this action have already been presented in Figure 7 and Tables C-11 and C-12.

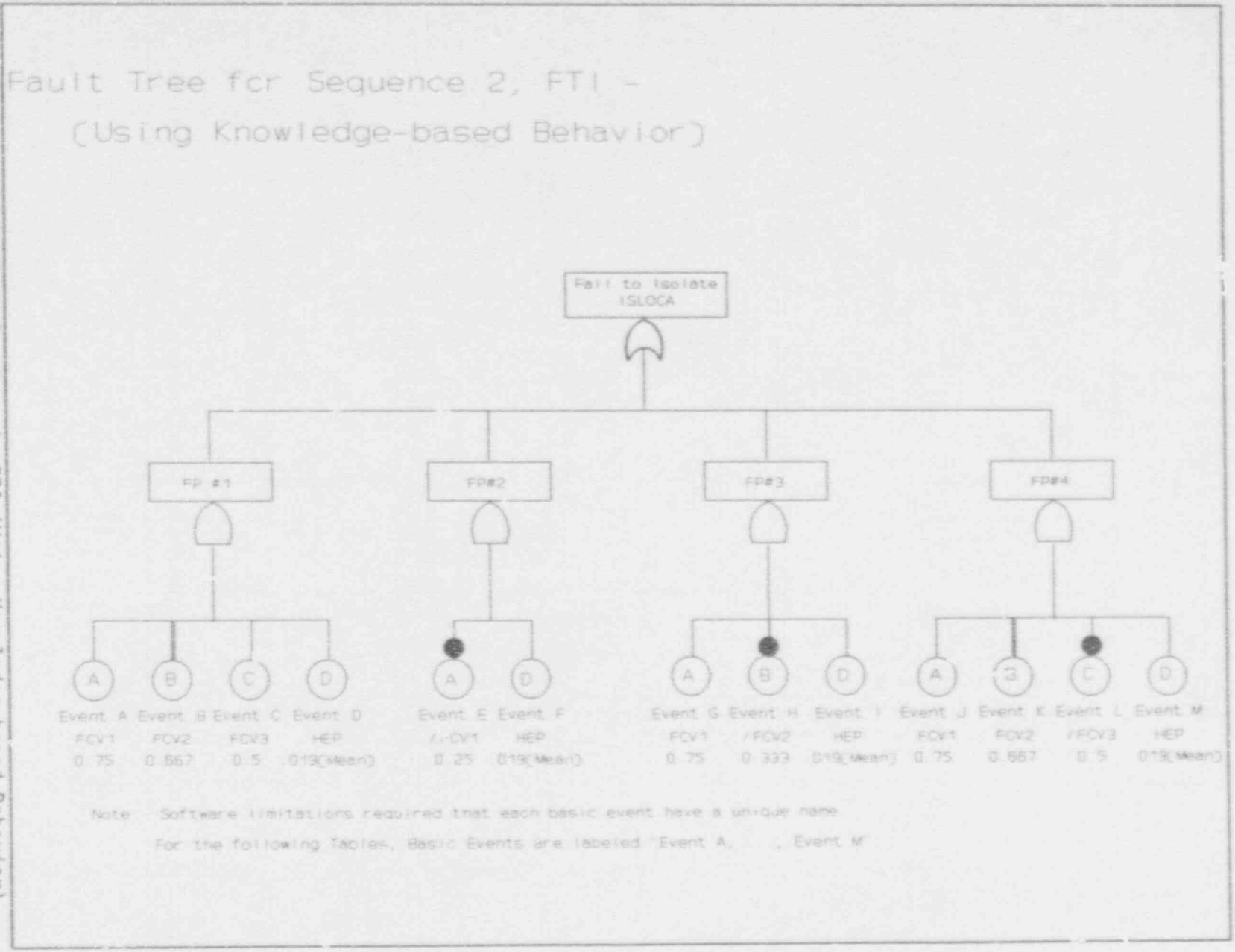

Figure 7: HRA Fault Tree for Seq. 2, FTI (Using Knowledge-based Behavior)

Table C11: HEPS for Sequence 2 ; FTI-Using Knowledge-based Behavio

	Human Action / Error	Basic Median HEP	Error Factor	Source/ THERP Table #	Step-by-Step or Dynamic	Modifier for PSFs	Modifier Source	THERP Dependency	Basic Mean HEP	Nominal Mean HEP	Error Factor
A	FCV1-Operators fail to select correct FCV on 1st try	0.75	1.0						0.75	0.75	1.0
B	FCV2-Operators fail to select correct FCV on 2nd try	0.667	1.0						0.667	0.667	1.0
C	FCV3-Operators fail to select correct FCV on 3rd try	0.5	1.0						0.5	0.5	1.0
D	HEP-Operators incorrectly activate FCV control	0.003	3.0	T20-12 #10	SBS	5	T20-16 #5	ZD	0.0037499	0.018747	3.0
E	/FCV1- e.g. the complement of "A"	0.25	1.0						0.25	0.25	1.0
F	HEP-Operators incorrectly activate control	0.003	3.0	T-3-12 #10	SBS	5	T20-16 #5	ZD	0.0037499	0.018747	3.0
G	FCV1-Operators fail to select correct FCV...	0.75	1.0						0.75	0.75	1.0
H	/FCV2-Complement of "E"	0.333	1.0						0.333	0.333	1.0
I	HEP-Operators incorrectly activate control	0.003	3.0	T20-12 #10	SBS	5	T20-16 #5	ZD	0.0037499	0.018747	3.0
J	FCV1-Operators fail to select correct FCV...	0.75	1.0						0.75	0.75	1.0
K	FCV2-Operators fail to select correct FCV...	0.667	1.0						0.667	0.667	1.0
L	/FCV3-Complement of "C"	0.5	1.0						0.5	0.5	1.0
M	HEP-Operators incorrectly activate control	0.003	3.0	T20-12 #10	SBS	5	T20-16 #5	ZD	0.0037499	0.018747	3.0

Table C12: Failure Paths & Total Failure Probability (Seq.2, FTI-Knowledge-based)

Table C12: Failure Paths and Total Failure Probabilities

FTI-Using Knowledge-based Behavior

	Failure Path	Calculations	Results
1	ABCD	0.75 x 0.667 x 0.5 x 0.018747	0.0046689
2	aEF	0.25 x 0.018747	0.0046936
3	acGH	0.75 x 0.333 x 0.018747	0.0046682
4	acgIKLM	0.75 x 0.667 x 0.5 x 0.018747	0.0046689
		Total Failure Probability	0.019
		Error Factor	2.37

FTD: Sequence 5

Event FTD for Sequence 5 represents operator failure to detect a reactor coolant leak resulting from failure of low pressure flanges in a suction line from the RWSP. The leak results from a failure of two check valves protecting RWSP piping from higher pressure in the LPSI lines used during shutdown cooling. HRA modeling includes detection by the RO of decreasing pressurizer level and pressure, and subsequent entry into procedure OP-901-046 (Shutdown Cooling Malfunction) at the direction of the control room supervisor (CRS). Control room (CR) personnel are given recovery credit for detecting decreasing pressurizer level (Hi-Lo and Lo-Lo PZR level alarms). Recovery credit for entering OP-901-046 is given for the shift supervisor (SS) advising the CRS to enter the procedure. The HRA event tree, subtask quantifications, and total failure probability are presented in Figure 8, Table C13, and Table C14, respectively. Table C14 lists the total mean failure probability for this event tree as 0.00758.

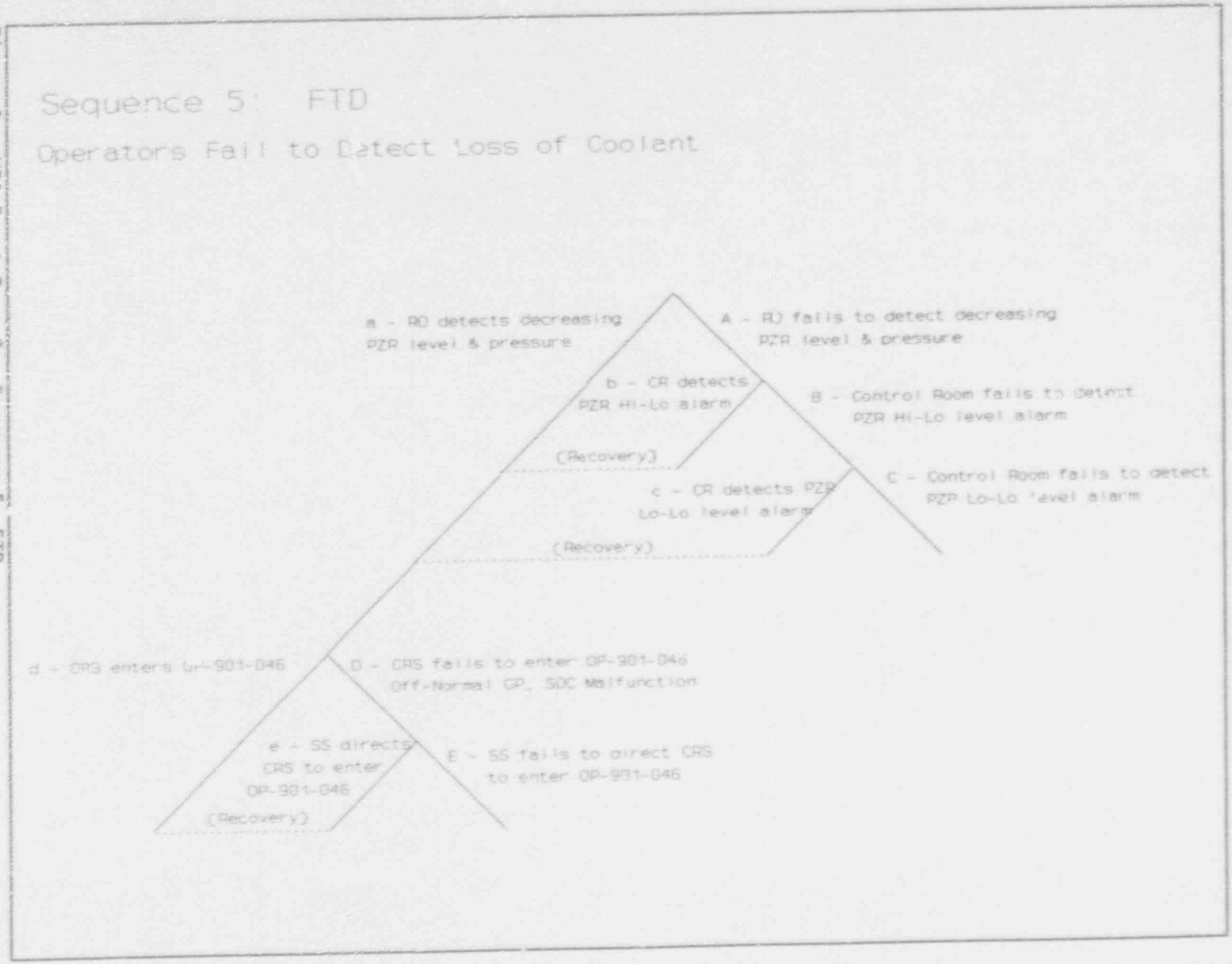

Figure 8: HRA Event Tree For Sequence 5, FTD

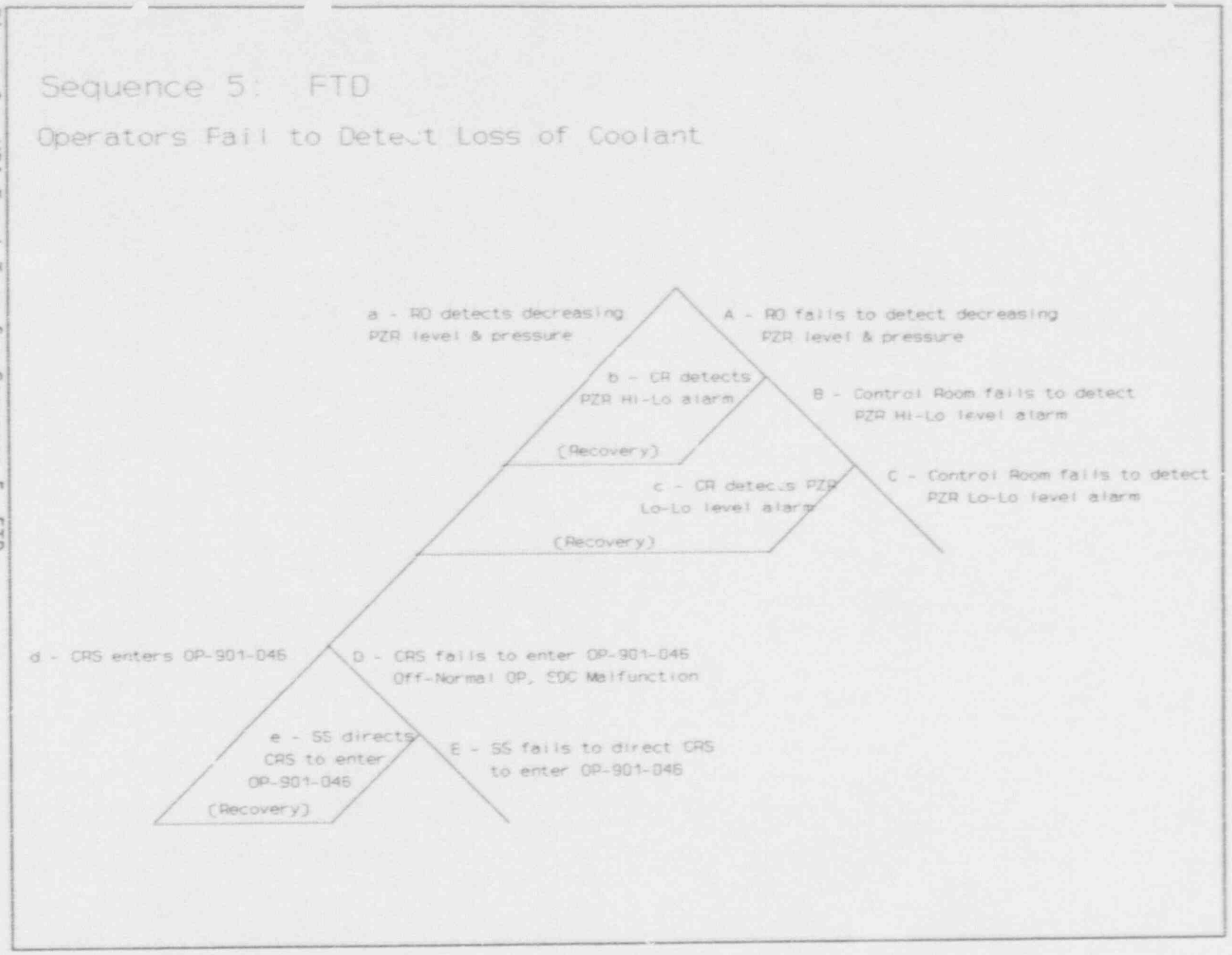

Figure 8: HRA Event Tree for Sequence 5, FTD

Table C13: HEPS for Sequence 5, FTD-Operators Fail to Detect Loss of Coolant

	Human Action / Error	Basic Median HEP	Error Factor	Source/ THERP Table #	Step-by-Step or Dynamic	Modifier for PSFs	Modifier Source	THERP Dependency	Basic Mean HEP	Nominal Mean HEP	Error Factor
A	RO fails to detect decreasing PZR level & pressure	0.003	3.0	T20-9 #4	SBS	1	T20-16 #2a	ZD	0.003749	0.003749	3.0
B	Control room fails to detect PZR Hi-Lo level alarm	0.0001	10.0	T20-23 #2a	SBS	1	T20-16 #2a	ZD	0.000266	0.000266	10.0
C	Control room fails to detect PZR Lo-Lo level alarm	0.001	10.0	T20-23 #2b	SBS	1	T20-16 #2a	HD	0.002663	0.501331	5.0
										# 0.279364	2.5
D	CRS fails to enter OP-901-046 - SDC Malfunction	0.005	10.0	T20-6 #3	SBS	2	T20-16 #4	ZD	0.013317	0.026635	10.0
E	SS fails to direct CRS to enter OP-901-046	0.005	10.0	T20-6 #3	SBS	2	T20-16 #4	HD	0.013317	0.513317	5.0
										# 0.283505	2.5

Table C14: Failure Paths & Total Failure Probability (Seq. 5, FTD)

Table C14: Failure Paths and Total Failure Probabilities

Sequence 5: FTD-Operators Fail to Detect Loss of Coolant

	Failure Path	Calculations	Results
1	ABC	0.003749 x 0.000266 x 0.279304	*
2	ABcDE	0.003749 x 0.000266 x 0.826635 x 0.283505	*
3	AbDE	0.003749 x 0.026635 x 0.283505	0.000028
4	aDE	0.826635 x 0.283565	0.007551
		Total Failure Probability	0.008
		Error Factor	11.68

FTDGN: Sequence 5

Event FTDGN for Sequence 5 represents operator failure to diagnose that the reactor coolant leak is outside of containment (in the RAB) and enter the section of procedure OP-901-046 (Shutdown Cooling Malfunction) relevant to the isolation of the leak. HRA modeling includes detection of the safeguards room flooding alarm by control room (CR) personnel, with recovery credit for detection of RAB radiation alarm(s) and increasing waste tank level by CR personnel. Step 2 of SUBSEQUENT OPERATOR ACTIONS (OP-901-046) directs operators to Attachment 6.1, System Leakage, based on relevant CR indications. Sequence 5 HRA modeling for event FTDGN includes entry into Attachment 6.1 on the direction of the control room supervisor (CRS) and recovery credit for the shift supervisor (SS) advising the CRS to do so. The HRA event tree, subtask quantifications, and total failure probability are presented in Figure 9 and Tables C15 and C16, respectively. Table C16 also lists the total mean failure probability for this event tree as 0.00755.

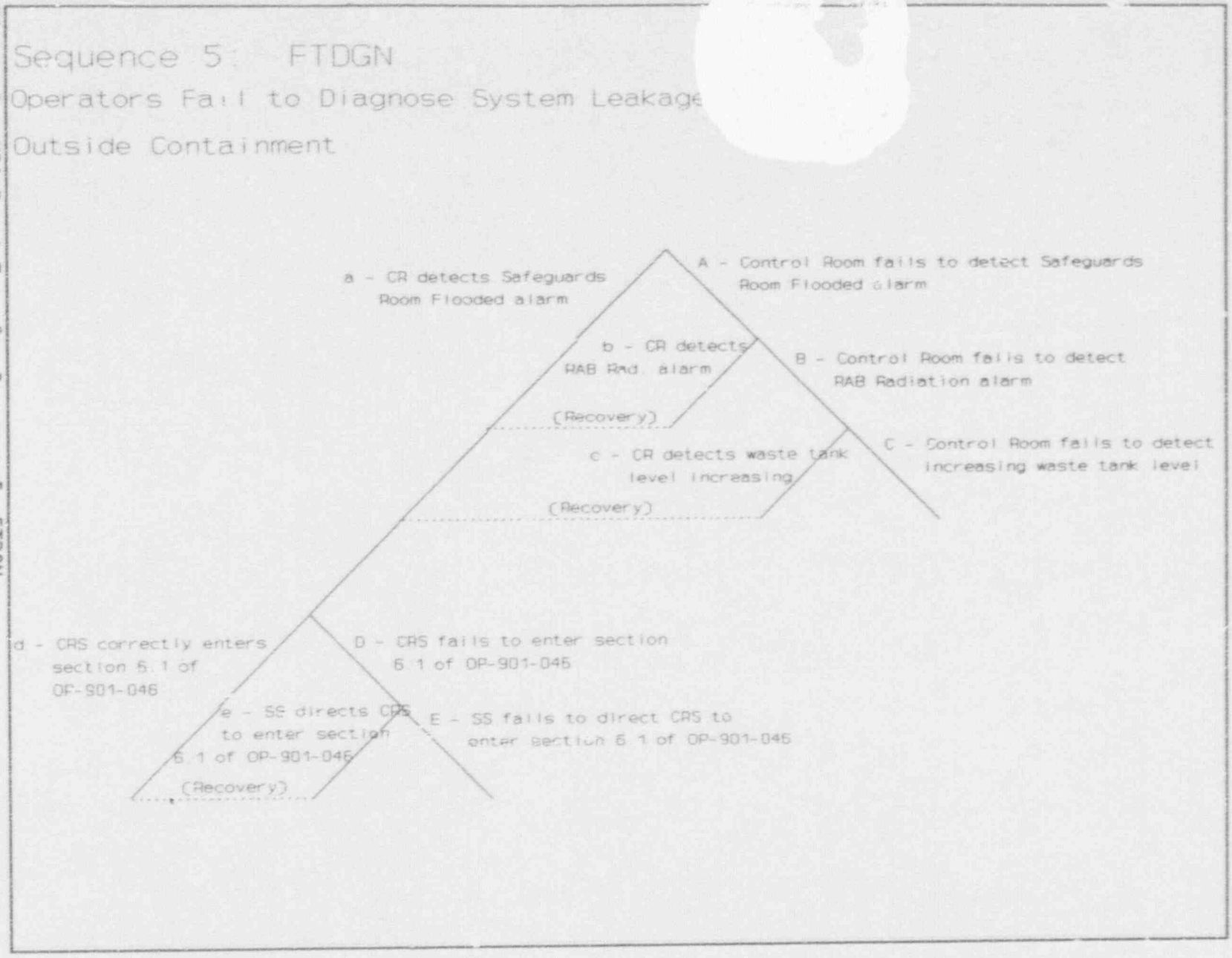

Figure 9: HRA Event Tree for Sequence 5, FTDGN

Table C15: HEPS for Sequence 5, FTDGN-Operators Fail to Diagnose ISLOCA

	Human Action / Error	Basic Median HEP	Error Factor	Source/ THERP Table #	Step-by-Step or Dynamic	Modifier for PSFs	Modifier Source	THERP Dependency	Basic Mean HEP	Nominal Mean HEP	Error Factor
A	Control room fails to detect Safeguards Room Flooded alarm	0.0001	10.0	T20-23 #2a	SBS	2	T20-16 #4	ZD	0.000756	0.000532	10.0
B	Control room fails to detect RAB radiation alarm	0.0001	10.0	T20-23 #2a	SBS	2	T20-16 #4	ZD	0.000266	0.000532	10.0
C	Control room fails to detect increasing waste tank level	0.003	3.0	T20-9 #4	SBS	2	T20-16 #4	ZD	0.003745	0.007499	3.0
D	CRS fails to enter section 6.1 of OP-901-046 - SDC Malfunction	0.005	10.0	T20-6 #3	SBS	2	T20-16 #4	ZD	0.013317	0.026635	10.0
E	SS fails to direct CRS to enter section 6.1 of OP-901-046	0.005	10.0	T20-6 #3	SBS	2	T20-16 #4	HD	0.013317	0.513317	5.0
										# 0.283505	2.5

Table C16: Failure Paths & Total Failure Probability (Seq. 5, FTDGN)

Table C16: Failure Paths and Total Failure Probabilities

Sequence 5: FTDGN Operators Fail to Diagnose ISLOCA

	Failure Path	Calculations	Results
1	ABC	0.000532 x 0.000532 x 0.007499	*
2	ABcDE	0.000532 x 0.000532 x 0.026635 x 0.283505	*
3	AbDE	0.000532 x 0.026635 x 0.283505	0.000604
4	aDE	0.026635 x 0.283505	0.007554
		Total Failure Probability	0.008
		Error Factor	12.11

FTI-A: Sequence 5 (1 Train of SDC)

Event FTI-A for Sequence 5 represents operator failure to isolate the leak (see Sequence 5 description in Sequences and Human Actions section) by performing the relevant steps of Attachment 6.1 (System Leakage) of procedure OP-901-046 (Shutdown Cooling Malfunction), when one SDC train is in service and one is in standby. The HRA event tree for event FTI-A models the critical steps, substeps, and actions represented in steps 9 and 10 of Attachment 6.1 related to isolation of the leak. Steps/substeps modeled include: closing the SDC suction isolation valve on the train in standby, observation of RCS level for stabilization, placing the isolated SDC train in service (referencing OP-009-005, system operating procedure, Shutdown Cooling System), and closing the SDC suction isolation valve on the initially operating SDC train. The HRA modeling conservatively assumes that the leak is in the second train isolated. Omission and commission errors are modeled for each step/substep. Omission errors are modeled as errors by the control room supervisor (CRS), with recovery credit for the reactor operator (RO). A high level of dependence was modeled between the two (CRS & RO), when the CRS was directing RO actions. Commission errors are modeled as errors by the RO, with recovery credit for the CRS. For these actions, a moderate level of dependence was modeled between the RO performing the action and the CRS who would be concurrently performing other dynamic actions. The HRA event tree, subtask quantifications, and total failure probability are presented in Figure 10, Table C17, and Table C18, respectively. Table C18 also lists the total mean failure probability for this event tree as 0.0233.

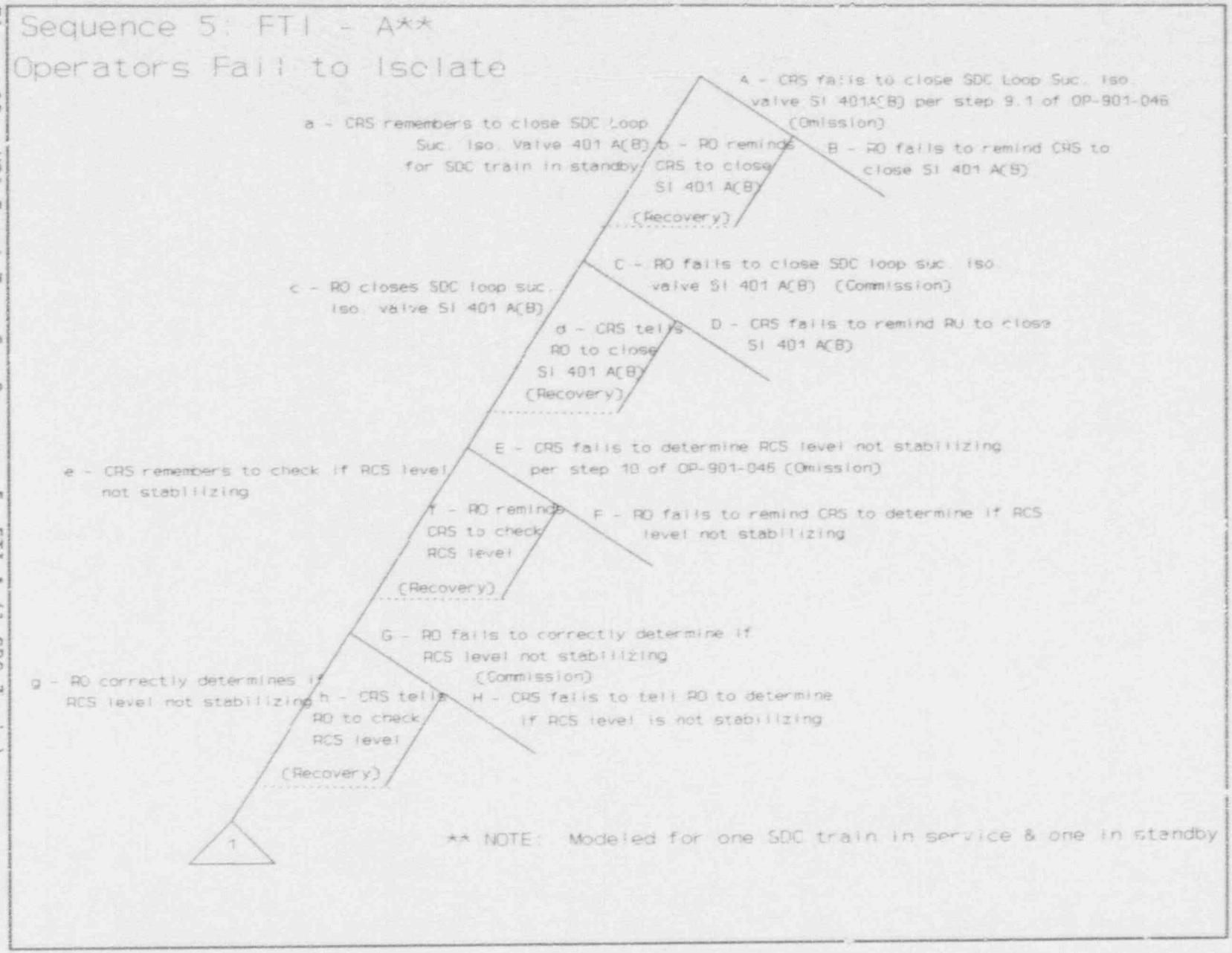

Figure 10: HRA Event Tree for Sequence 5, FTI-A (1 SDC Train)

Figure 10 (cont.):

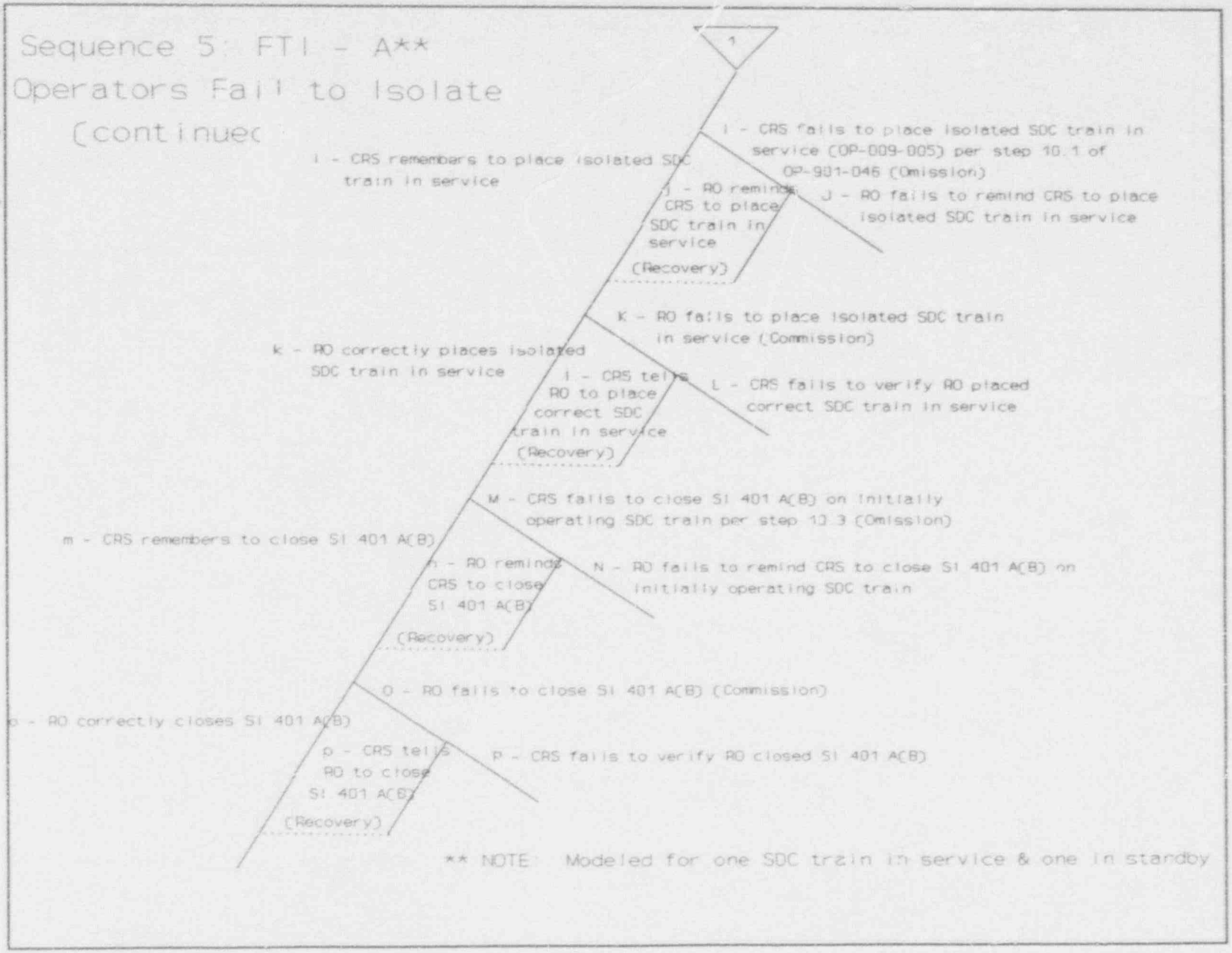

Table C17: HEPS for Sequence 5, FTI-A; Fail to Isolate (1 SDC Train)

	Human Action / Error	Basic Median HEP	Error Factor	Source/ THERP Table #	Step-by-Step or Dynamic	Modifier for PSFs	Modifier Source	THERP Dependency	Basic Mean HEP	Nominal Mean HEP	Error Factor
A	CRS fails to close SDC loop Suc. Isa. valve SI-401 A(B) (Omission)	0.003	3.0	T20-7 #3	SBS	3	T20-16 #2	ZD	0.003749	0.011248	3.0
B	RO fails to remind CRS to close SI-401 A(B)	0.1	5.0	T20-22 #1	SBS	3	T20-16 #2	HD	0.161383	0.742075	5.0
										# 0.353909	2.2
C	RO fails to close SI-401 A(B) (Commission)	0.001	3.0	T20-12 #3	SBS	3	T20-16 #2	ZD	0.001249	0.003749	3.0
D	CRS fails to remind RO to close SI-401 A(B)	0.1	5.0	T20-22 #1	SBS	3	T20-16 #2	MD	0.161383	0.557844	5.0
										# 0.298605	2.4
E	CRS fails to determine in RCS level not stabilizing (Omission)	0.003	3.0	T20-7 #3	SBS	3	T20-16 #2	ZD	0.003749	0.011248	3.0
F	RO fails to remind CRS to determine if RCS level not stabilizing	0.1	5.0	T20-22 #1	SBS	3	T20-16 #2	HD	0.161383	0.742075	5.0
										# 0.353909	2.2
G	RO fails to correctly determine if RCS level not stabilizing (Commission)	0.003	3.0	T20-19 #1	SBS	3	T20-16 #2	ZD	0.003749	0.011248	3.0
H	CRS fails to tell RO to determine if RCS level not stabilizing	0.1	5.0	T20-22 #1	SBS	3	T20-16 #2	MD	0.161383	0.557844	5.0
										# 0.298605	2.4
I	CRS fails to place isolated train in service	0.003	3.0	T20-7 #3	SBS	3	T20-16 #2	ZD	0.003749	0.011248	3.0

Table C17: HEPS for Sequence 5, FTI-A; Fail to Isolate (1 SDC Train)

	Human Action / Error	Basic Median HEP	Error Factor	Source/ THERP Table #	Step-by-Step or Dynamic	Modifier for PSFs	Modifier Source	THERP Dependency	Basic Mean HEP	Nominal Mean HEP	Error Factor
J	RO fails to remind CRS to place standby SDC train in service	0.1	5.0	T20-22 #1	SBS	3	T20-16 #2	HD	0.161383	0.742075	5.0
										# 0.353909	2.2
K	RO fails to place isolated SDC train in service	0.001	3.0	T20-12 #3	SBS	3	T20-16 #2	ZD	0.001249	0.003749	3.0
L	CRS fails to verify RO placed correct SDC train in service	0.1	5.0	T20-22 #1	SBS	3	T20-16 #2	MD	0.161383	0.557844	5.0
										# 0.298605	2.4
M	CRS fails to close SI-401 A(B) on initially operating SDC train	0.003	3.0	T20-7 #3	SBS	3	T20-16 #2	ZD	0.003749	0.011248	3.0
N	RO fails to remind CRS to close SI-401 A(B) on initially operating SDC train	0.1	5.0	T20-22 #1	SBS	3	T20-16 #2	HD	0.161383	0.742075	5.0
										# 0.353909	2.2
O	RO fails to close correct SI-401 A(B) valve (Commission)	0.001	3.0	T20-12 #3	SBS	3	T20-16 #2	ZD	0.001249	0.003749	3.0
P	CRS fails to verify RO closed correct SI-401 A(B) valve	0.1	5.0	T20-22 #1	SBS	3	T20-16 #2	MD	0.161383	0.557844	5.0
										# 0.298605	2.4

Table C18: Failure Paths and Total Failure Probabilities

Sequence 5: FTi-A; Fail to Isolate (1 SDC Train)

	Failure Path	Calculations	Results
1	AB	0.011248 x 0.353909	0.00398
2	AbCD	0.011248 x 0.003749 x 0.298605	0.0000 12
3	AbCdEF	0.011248 x 0.003749 x 0.011248 x 0.353909	*
4	AbCdEfGH	0.011248 x 0.003749 x 0.011248 x 0.011248 x 0.298605	*
5	AbCdEfGhIJ	0.011248 x 0.003749 x 0.011248 x 0.011248 x 0.011248 x 0.353909	*
6	AbCdEfGhIjKL	0.011248 x 0.003749 x 0.011248 x 0.011248 x 0.011248 x 0.003749 x 0.298605	*
7	AbCdEfGhIjKlMN	0.011248 x 0.003749 x 0.011248 x 0.011248 x 0.011248 x 0.003749 x 0.011248 x 0.353909	*
8	AbCdEfGhIjKlMnOP	0.011248 x 0.003749 x 0.011248 x 0.011248 x 0.011248 x 0.003749 x 0.011248 x 0.003749 x 0.298605	*
9	AbCdEfGhIjKlmOP	0.011248 x 0.003749 x 0.011248 x 0.011248 x 0.011248 x 0.003749 x 0.003749 x 0.298605	*
10	AbCdEfGhIjkMN	0.011248 x 0.003749 x 0.011248 x 0.011248 x 0.011248 x 0.011248 x 0.353909	*
11	AbCdEfGhIjkMnOP	0.011248 x 0.003749 x 0.011248 x 0.011248 x 0.011248 x 0.011248 x 0.003749 x 0.298605	*
12	AbCdEfGhIjkmOP	0.011248 x 0.003749 x 0.011248 x 0.011248 x 0.011248 x 0.003749 x 0.298605	*
13	AbCdEfGhIKL	0.011248 x 0.003749 x 0.011248 x 0.011248 x 0.003749 x 0.298605	*
14	AbCdEfGhIKlMN	0.011248 x 0.003749 x 0.011248 x 0.011248 x 0.003749 x 0.011248 x 0.353909	*
15	AbCdEfGhIKlMnOP	0.011248 x 0.003749 x 0.011248 x 0.011248 x 0.003749 x 0.011248 x 0.003749 x 0.298605	*
16	AbCdEfGhIKlmOP	0.011248 x 0.003749 x 0.011248 x 0.011248 x 0.003749 x 0.003749 x 0.298605	*
17	AbCdEfGhIkMN	0.011248 x 0.003749 x 0.011248 x 0.011248 x 0.011248 x 0.353909	*
18	AbCdEfGhIkMnOP	0.011248 x 0.003749 x 0.011248 x 0.011248 x 0.011248 x 0.003749 x 0.298605	*
19	AbCdEfGhIkmOP	0.011248 x 0.003749 x 0.011248 x 0.011248 x 0.003749 x 0.298605	*
20	AbCdEfgIJ	0.011248 x 0.003749 x 0.011248 x 0.011248 x 0.353909	*

Table C18 (cont.):

Table C18: Failure Paths and Total Failure Probabilities

Sequence 5: FTI-A; Fail to Isolate (1 SDC Train)

	Failure Path	Calculations	Results
21	AbCdEfgIjKL	0.011248 x 0.003749 x 0.011248 x 0.011248 x 0.003749 x 0.298605	*
22	AbCdEfgIjKlMN	0.011248 x 0.003749 x 0.011248 x 0.011248 x 0.003749 x 0.011248 x 0.353909	*
23	AbCdEfgIjKlMnOP	0.011248 x 0.003749 x 0.011248 x 0.011248 x 0.003749 x 0.011248 x 0.003749 x 0.298605	*
24	AbCdEfgIjKlmOP	0.011248 x 0.003749 x 0.011248 x 0.011248 x 0.003749 x 0.003749 x 0.298605	*
25	AbCdEfgIjkMN	0.011248 x 0.003749 x 0.011248 x 0.011248 x 0.011248 x 0.353909	*
26	AbCdEfgIjkMnOP	0.011248 x 0.003749 x 0.011248 x 0.011248 x 0.011248 x 0.003749 x 0.298605	*
27	AbCdEfgIjkmOP	.011248 x 0.003749 x 0.011248 x 0.011248 x 0.003749 x 0.298605	*
28	AbCdEfgIKL	0.011248 x 0.003749 x 0.011248 x 0.003749 x 0.298605	*
29	AbCdEfgIKlMN	0.011248 x 0.003749 x 0.011248 x 0.003749 x 0.011248 x 0.353909	*
30	AbCdEfgIKlMnOP	0.011248 x 0.003749 x 0.011248 x 0.003749 x 0.011248 x 0.003749 x 0.298605	*
31	AbCdEfgIKlmOP	0.011248 0.003749 x 0.011248 x 0.003749 x 0.003749 x 0.298605	*
32	AbCdEfgIkMN	0.011248 x 0.003749 x 0.011248 x 0.011248 x 0.353909	*
33	AbCdEfgIkMnOP	0.011248 x 0.003749 x 0.011248 x 0.011248 x 0.003749 x 0.298605	*
34	AbCdEfgIkmOP	0.011248 x 0.003749 x 0.011248 x 0.003749 x 0.298605	*
35	AbCdeGH	0.011248 x 0.003749 x 0.011248 x 0.298605	*
36	AbCdeGhIJ	0.011248 x 0.003749 x 0.011248 x 0.011248 x 0.353909	*
37	AbCdeGhIjKL	0.011248 x 0.003749 x 0.011248 x 0.011248 x 0.003749 x 0.298605	*
38	AbCdeGhIjKlMN	0.011248 x 0.003749 x 0.011248 x 0.011248 x 0.003749 x 0.011248 x 0.353909	*
39	AbCdeGhIjKlMnOP	0.011248 x 0.003749 x 0.011248 x 0.011248 x 0.003749 x 0.011248 x 0.003749 x 0.298605	*
40	AbCdeGhIjKlmOP	0.011248 x 0.003749 x 0.011248 x 0.011248 x 0.003749 x 0.003749 x 0.298605	*
41	AbCdeGhIjkMN	0.011248 x 0.003749 x 0.011248 x 0.011248 x 0.011248 x 0.353909	*
42	AbCdeGhIjkMnOP	0.011248 x 0.003749 x 0.011248 x 0.011248 x 0.011248 x 0.003749 x 0.298605	*

Table C18 (cont.):

Table C18: Failure Paths and Total Failure Probabilities

Sequence 5: FTI-A; Fail to Isolate (1 SDC Train)

	Failure Path	Calculations	Results
43	AbCdeGhIJkmOP	0.011248 x 0.003749 x 0.011248 x 0.011248 x 0.903749 x 0.298605	*
44	AbCdeGhIKL	0.011248 x 0.903749 x 0.011248 x 0.003749 x 0.298605	*
45	AbCdeGhIKlMN	0.011248 x 0.003749 x 0.011248 x 0.003749 x 0.011248 x 0.353909	*
46	AbCdeGhIKlMnOP	0.011248 x 0.003749 x 0.011248 x 0.003749 x 0.011248 x 0.003749 x 0.298605	*
47	AbCdeGhIKlmOP	0.011248 x 0.003749 x 0.011248 x 0.003749 x 0.003749 x 0.298605	*
48	AbCdeGhikMN	0.011248 x 0.003749 x 0.011248 x 0.011248 x 0.353909	*
49	AbCdeGhikMnOP	0.011248 x 0.003749 x 0.011248 x 0.011248 x 0.003749 x 0.298605	*
50	AbCdeGhikmOP	0.011248 x 0.003749 x 0.011248 x 0.903749 x 0.298605	*
51	AbCdegIJ	0.011248 x 0.003749 x 0.011248 x 0.353909	*
52	AbCdegIJKL	0.011248 x 0.003749 x 0.011248 x 0.003749 x 0.298605	*
53	AbCdegIJKlMN	0.011248 x 0.003749 x 0.011248 x 0.003749 x 0.011248 x 0.353909	*
54	AbCdegIjKlMnOP	0.011248 x 0.003749 x 0.011248 x 0.003749 x 0.011248 x 0.003749 x 0.298605	*
55	AbCdegIJKlmOP	0.011248 x 0.003749 x 0.011248 x 0.003749 x 0.003749 x 0.298605	*
56	AbCdegIjkMN	0.011248 x 0.003749 x 0.011248 x 0.011248 x 0.353909	*
57	AbCdegIjkMnOP	0.011248 x 0.003749 x 0.011248 x 0.011248 x 0.003749 x 0.298605	*
58	AbCdegIjkmOP	0.011248 x 0.003749 x 0.011248 x 0.003749 x 0.298605	*
59	AbCdegIKL	0.011248 x 0.003749 x 0.003749 x 0.298605	*
60	AbCdegIKlMN	0.011248 x 0.003749 x 0.003749 x 0.011248 x 0.353909	*
61	AbCdegIKlMnOP	0.011248 x 0.003749 x 0.003749 x 0.011248 x 0.003749 x 0.298605	*
62	AbCdegIKlmOP	0.011248 x 0.003749 x 0.003749 x 0.003749 x 0.298605	*
63	AbCdegIkMN	0.011248 x 0.003749 x 0.011248 x 0.353909	*
64	AbCdegIkMnOP	0.011248 x 0.003749 x 0.011248 x 0.003749 x 0.298605	*

Table C18 (cont.):

Table C18: Failure Paths and Total Failure Probabilities

Sequence 5: FTI-A; Fail to Isolate (1 SDC Train)

	Failure Path	Calculations	Results
65	AbCdegikmOP	0.011248 x 0.003749 x 0.003749 x 0.298605	*
66	AbcEF	0.011248 x 0.011248 x 0.353909	0.000044
67	AbcEfGH	0.011248 x 0.011248 x 0.011248 x 0.298605	*
68	AbcEfGhIJ	0.011248 x 0.011248 x 0.011248 x 0.011248 x 0.353909	*
69	AbcEfGhIJKL	0.011248 x 0.011248 x 0.011248 x 0.011248 x 0.003749 x 0.298605	*
70	AbcEfGhIJKlMN	0.011248 x 0.011248 x 0.011248 x 0.011248 x 0.003749 x 0.011248 x 0.353909	*
71	AbcEfGhIJKlMnOP	0.011248 x 0.011248 x 0.011248 x 0.011248 x 0.003749 x 0.011248 x 0.003749 x 0.298605	*
72	AbcEfGhIJKlmOP	0.011248 x 0.011248 x 0.011248 x 0.011248 x 0.003749 x 0.003749 x 0.298605	*
73	AbcEfGhIJkMN	0.011248 x 0.011248 x 0.011248 x 0.011248 x 0.011248 x 0.353909	*
74	AbcEfGhIJkMnOP	0.011248 x 0.011248 x 0.011248 x 0.011248 x 0.011248 x 0.003749 x 0.298605	*
75	AbcEfGhIJkmOP	0.011248 x 0.011248 x 0.011248 x 0.011248 x 0.003749 x 0.298605	*
76	AbcEfGhIKL	0.011248 x 0.011248 x 0.011248 x 0.003749 x 0.298605	*
77	AbcEfGhIKlMN	0.011248 x 0.011248 x 0.011248 x 0.003749 x 0.011248 x 0.353909	*
78	AbcEfGhIKlMnOP	0.011248 x 0.011248 x 0.011248 x 0.003749 x 0.011248 x 0.003749 x 0.298605	*
79	AbcEfGhIKlmOP	0.011248 x 0.011248 x 0.011248 x 0.003749 x 0.003749 x 0.298605	*
80	AbcEfGhIkMN	0.011248 x 0.011248 x 0.011248 x 0.011248 x 0.353909	*
81	AbcEfGhIkMnOP	0.011248 x 0.011248 x 0.011248 x 0.011248 x 0.003749 x 0.298605	*
82	AbcEfGhIkmOP	0.011248 x 0.011248 x 0.011248 x 0.003749 x 0.298605	*
83	AbcEfgIJ	0.011248 x 0.011248 x 0.011248 x 0.353909	*
84	AbcEfgIJKL	0.011248 x 0.011248 x 0.011248 x 0.003749 x 0.298605	*
85	AbcEfgIJKlMN	0.011248 x 0.011248 x 0.011248 x 0.003749 x 0.011248 x 0.353909	*
86	AbcEfgIJKlMnOP	0.011248 x 0.011248 x 0.011248 x 0.003749 x 0.011248 x 0.003749 x 0.298605	*

Table C18 (cont.):

Table C18: Failure Paths and Total Failure Probabilities

Sequence 5: FTI-A; Fail to Isolate (1 SDC Train)

	Failure Path	Calculations	Results
87	AbcEfgIjKlmOP	0.011248 x 0.011248 x 0.011248 x 0.003749 x 0.003749 x 0.298605	*
88	AbcEfgIjkMN	0.011248 x 0.011248 x 0.011248 x 0.011248 x 0.353909	*
89	AbcEfgIjkMnOP	0.011248 x 0.011248 x 0.011248 x 0.011248 x 0.003749 x 0.298605	*
90	AbcEfgIjkmOP	0.011248 x 0.011248 x 0.011248 x 0.003749 x 0.298605	*
91	AbcEfgIKL	0.011248 x 0.011248 x 0.003749 x 0.298605	*
92	AbcEfgIKlMN	0.011248 x 0.011248 x 0.003749 x 0.011248 x 0.353909	*
93	AbcEfgIKlMnOP	0.011248 x 0.011248 x 0.003749 x 0.011248 x 0.003749 x 0.298605	*
94	AbcEfgIKlmOP	0.011248 x 0.011248 x 0.003749 x 0.003749 x 0.298605	*
95	AbcEfgIkMN	0.011248 x 0.011248 x 0.011248 x 0.353909	*
96	AbcEfgIkMnOP	0.011248 x 0.011248 x 0.011248 x 0.003749 x 0.298605	*
97	AbcEfgIkmOP	0.011248 x 0.011248 x 0.003749 x 0.298605	*
98	AbceGH	0.011248 x 0.011248 x 0.298605	0.000037
99	AbceGhIJ	0.011248 x 0.011248 x 0.011248 x 0.353909	*
100	AbceGhIJKL	0.011248 x 0.011248 x 0.011248 x 0.003749 x 0.298605	*
101	AbceGhIJKlMN	0.011248 x 0.011248 x 0.011248 x 0.003749 x 0.011248 x 0.353909	*
102	AbceGhIJKlMnOP	0.011248 x 0.011248 x 0.011248 x 0.003749 x 0.011248 x 0.003749 x 0.298605	*
103	AbceGhIJKlmOP	0.011248 x 0.011248 x 0.011248 x 0.003749 x 0.003749 x 0.298605	*
104	AbceGhIJkMN	0.011248 x 0.011248 x 0.011248 x 0.011248 x 0.353909	*
105	AbceGhIJkMnOP	0.011248 x 0.011248 x 0.011248 x 0.011248 x 0.003749 x 0.298605	*
106	AbceGhIJkmOP	0.011248 x 0.011248 x 0.011248 x 0.003749 x 0.298605	*
107	AbceGhIKL	0.011248 x 0.011248 x 0.003749 x 0.298605	*
108	AbceGhIKlMN	0.011248 x 0.011248 x 0.003749 x 0.011248 x 0.353909	*

Table C18: Failure Paths and Total Failure Probabilities

Sequence 5: FTI-A; Fail to Isolate (1 SDC Train)

	Failure Path	Calculations	Results
109	AbceGhiKlMnOP	0.011248 x 0.011248 x 0.003749 x 0.011248 x 0.003749 x 0.298605	*
110	AbceGhiKlm...	0.011248 x 0.011248 x 0.003749 x 0.003749 x 0.298605	*
111	AbCeGhiKMN	0.011248 x 0.011248 x 0.011248 x 0.353909	*
112	AbceGhiKMnOP	0.011248 x 0.011248 x 0.011248 x 0.003749 x 0.298605	*
113	AbceGhiKmOP	0.011248 x 0.011248 x 0.003749 x 0.298605	*
114	AbcegIJ	0.011248 x 0.011248 x 0.353909	0.000044
115	AbcegIJKL	0.011248 x 0.011248 x 0.003749 x 0.298505	*
116	AbcegIjKIMN	0.011248 x 0.011248 x 0.003749 x 0.011248 x 0.353909	*
117	AbcegIjKIMnOP	0.011248 x 0.011248 x 0.003749 x 0.011248 x 0.003749 x 0.298605	*
118	AbcegIjKImOP	0.011248 x 0.011248 x 0.003749 x 0.003749 x 0.298605	*
119	AbcegIjkMN	0.011248 x 0.011248 x 0.011248 x 0.353909	*
120	AbcegIjkMnOP	0.011248 x 0.011248 x 0.011248 x 0.003749 x 0.298605	*
121	AbcegIjkmOP	0.011248 x 0.011248 x 0.003749 x 0.298605	*
122	AbcegtKL	0.011248 x 0.003749 x 0.298605	0.000012
123	AbcegtKIMN	0.011248 x 0.003749 x 0.011248 x 0.353909	*
124	AbcegtKIMnOP	0.011248 x 0.003749 x 0.011248 x 0.003749 x 0.298605	*
125	AbcegtKImOP	0.011248 x 0.003749 x 0.003749 x 0.298605	*
126	AbcegtkMN	0.011248 x 0.011248 x 0.353909	0.000044
127	AbcegtkMnOP	0.011248 x 0.011248 x 0.003749 x 0.298605	*
128	AbcegtkmOP	0.011248 x 0.003749 x 0.298605	0.000012
129	aCD	0.003749 x 0.298605	0.001119
130	aCdEF	0.003749 x 0.011248 x 0.353909	0.000014

Table C18 (cont.):

Table C18: Failure Paths and Total Failure Probabilities

Sequence 5: FTI-A; Fail to Isolate (1 SDC Train)

Failure Path		Calculations	Results
131	aCdEfGhI	0.003749 x 0.011248 x 0.011248 x 0.298605	*
132	aCdEfGhIJ	0.003749 x 0.011248 x 0.011248 x 0.011248 x 0.353909	*
133	aCdEfGhIjKL	0.003749 x 0.011248 x 0.011248 x 0.011248 x 0.003749 x 0.298605	*
134	aCdEfGhIjKlMN	0.003749 x 0.011248 x 0.011248 x 0.011248 x 0.003749 x 0.011248 x 0.353909	*
135	aCdEfGhIjKlMnOP	0.003749 x 0.011248 x 0.011248 x 0.011248 x 0.003749 x 0.011248 x 0.003749 x 0.298605	*
136	aCdEfGhIjKlmOP	0.003749 x 0.011248 x 0.011248 x 0.011248 x 0.003749 x 0.003749 x 0.298605	*
137	aCdEfGhIjkMN	0.003749 x 0.011248 x 0.011248 x 0.011248 x 0.011248 x 0.353909	*
138	aCdEfGhIjkMnOP	0.003749 x 0.011248 x 0.011248 x 0.011248 x 0.011248 x 0.003749 x 0.298605	*
139	aCdEfGhIjkmOP	0.003749 x 0.011248 x 0.011248 x 0.011248 x 0.003749 x 0.298605	*
140	aCdEfGhIKL	0.003749 x 0.011248 x 0.011248 x 0.003749 x 0.298605	*
141	aCdEfGhIKlMN	0.003749 x 0.011248 x 0.011248 x 0.003749 x 0.011248 x 0.353909	*
142	aCdEfGhIKlMnOP	0.003749 x 0.011248 x 0.011248 x 0.003749 x 0.011248 x 0.003749 x 0.298605	*
143	aCdEfGhIKlmOP	0.003749 x 0.011248 x 0.011248 x 0.003749 x 0.003749 x 0.298605	*
144	aCdEfGhIkMN	0.003749 x 0.011248 x 0.011248 x 0.011248 x 0.353909	*
145	aCdEfGhIkMnOP	0.003749 x 0.011248 x 0.011248 x 0.011248 x 0.003749 x 0.298605	*
146	aCdEfGhIkmOP	0.003749 x 0.011248 x 0.011248 x 0.003749 x 0.298605	*
147	aCdEfgIJ	0.003749 x 0.011248 x 0.011248 x 0.353909	*
148	aCdEfgIJKL	0.003749 x 0.011248 x 0.011248 x 0.003749 x 0.298605	*
149	aCdEfgIJKlMN	0.003749 x 0.011248 x 0.011248 x 0.003749 x 0.011248 x 0.353909	*
150	aCdEfgIJKlMnOP	0.003749 x 0.011248 x 0.011248 x 0.003749 x 0.011248 x 0.003749 x 0.298605	*
151	aCdEfgIJKlmOP	0.003749 x 0.011248 x 0.011248 x 0.003749 x 0.003749 x 0.298605	*
152	aCdEfgIjkMN	0.003749 x 0.011248 x 0.011248 x 0.011248 x 0.353909	*

Table C18 (cont.):

Table C18: Failure Paths and Total Failure Probabilities

Sequence 5: FTI-A; Fail to Isolate (1 SDC Train)

	Failure Path	Calculations	Results
153	aCdEfgIjkMnOP	0.003749 x 0.011248 x 0.011248 x 0.011248 x 0.003749 x 0.298605	*
154	aCdEfgIjkmOP	0.003749 x 0.011248 x 0.011248 x 0.003749 x 0.298605	*
155	aCdEfgIKL	0.003749 x 0.011248 x 0.003749 x 0.298605	*
156	aCdEfgIKlMN	0.003749 x 0.011248 x 0.003749 x 0.011248 x 0.353909	*
157	aCdEfgIKlMnOP	0.003749 x 0.011248 x 0.003749 x 0.011248 x 0.003749 x 0.298605	*
158	aCdEfgIKlmOP	0.003749 x 0.011248 x 0.003749 x 0.003749 x 0.298605	*
159	aCdEfgikMN	0.003749 x 0.011248 x 0.011248 x 0.353909	*
160	aCdEfgikMnOP	0.003749 x 0.011248 x 0.011248 x 0.003749 x 0.298605	*
161	aCdEfgikmOP	0.003749 x 0.011248 x 0.003749 x 0.298605	*
162	aCdeGH	0.003749 x 0.011248 x 0.298605	0.000012
163	aCdeGhIJ	0.003749 x 0.011248 x 0.011248 x 0.353909	*
164	aCdeGhIJKL	0.003749 x 0.011248 x 0.011248 x 0.003749 x 0.298605	*
165	aCdeGhIJKlMN	0.003749 x 0.011248 x 0.011248 x 0.003749 x 0.011248 x 0.353909	*
166	aCdeGhIJKlMnOP	0.003749 x 0.011248 x 0.011248 x 0.003749 x 0.011248 x 0.003749 x 0.298605	*
167	aCdeGhIJKlmOP	0.003749 x 0.011248 x 0.011248 x 0.003749 x 0.003749 x 0.298605	*
168	aCdeGhIjkMN	0.003749 x 0.011248 x 0.011248 x 0.011248 x 0.353909	*
169	aCdeGhIjkMnOP	0.003749 x 0.011248 x 0.011248 x 0.011248 x 0.003749 x 0.298605	*
170	aCdeGhIjkmOP	0.003749 x 0.011248 x 0.011248 x 0.003749 x 0.298605	*
171	aCdeGhIKL	0.003749 x 0.011248 x 0.003749 x 0.298605	*
172	aCdeGhIKlMN	0.003749 x 0.011248 x 0.003749 x 0.011248 x 0.353909	*
173	aCdeGhIKlMnOP	0.003749 x 0.011248 x 0.003749 x 0.011248 x 0.003749 x 0.298605	*
174	aCdeGhIKlmOP	0.003749 x 0.011248 x 0.003749 x 0.003749 x 0.298605	*

Table C18 (cont.):

Table C18: Failure Paths and Total Failure Probabilities

Sequence 5: FTI-A; Fail to Isolate (1 SDC Train)

Failure Path	Calculations	Results
175 aCdeGhikMN	0.003749 x 0.011248 x 0.011248 x 0.353909	*
176 aCdeGhikMnOP	0.003749 x 0.011248 x 0.011248 x 0.003749 x 0.298605	*
177 aCdeGhikmOP	0.003749 x 0.011248 x 0.003749 x 0.298605	*
178 aCdegIJ	0.003749 x 0.011248 x 0.353909	0.000014
179 aCdegIJKL	0.003749 x 0.011248 x 0.003749 x 0.298605	*
180 aCdegIjKlMN	0.003749 x 0.011248 x 0.003749 x 0.011248 x 0.353909	*
181 aCdegIjKlMnOP	0.003749 x 0.011248 x 0.003749 x 0.011248 x 0.003749 x 0.298605	*
182 aCdegIjKlmOP	0.003749 x 0.011248 x 0.003749 x 0.003749 x 0.298605	*
183 aCdegIjkMN	0.003749 x 0.011248 x 0.011248 x 0.353909	*
184 aCdegIjkMnOP	0.003749 x 0.011248 x 0.011248 x 0.003749 x 0.298605	*
185 aCdegIjkmOP	0.003749 x 0.011248 x 0.003749 x 0.298605	*
186 aCdegIKL	0.003749 x 0.003749 x 0.298605	0.000004
187 aCdegiKlMN	0.003749 x 0.003749 x 0.011248 x 0.353909	*
188 aCdegiKlMnOP	0.003749 x 0.003749 x 0.011248 x 0.003749 x 0.298605	*
189 aCdegiKlmOP	0.003749 x 0.003749 x 0.003749 x 0.298605	*
190 aCdegIkMN	0.003749 x 0.011248 x 0.353909	0.000014
191 aCdegIkMnOP	0.003749 x 0.011248 x 0.003749 x 0.298605	*
192 aCdegIkmOP	0.003749 x 0.003749 x 0.298605	0.000004
193 acEF	0.011248 x 0.353909	0.00398
194 acEFGH	0.011248 x 0.011248 x 0.298605	0.000037
195 acEFGhIJ	0.011248 x 0.011248 x 0.011248 x 0.353909	*
196 acEFGhIjKL	0.011248 x 0.011248 x 0.011248 x 0.003749 x 0.298605	*

Table C18 (cont.):

Table C18: Failure Paths and Total Failure Probabilities

Sequence 5: FTI-A; Fail to Isolate (1 SDC Train)

	Failure Path	Calculations	Results
197	acEfGhIjK1MN	0.011248 x 0.011248 x 0.011248 x 0.003749 x 0.011248 x 0.353909	*
198	acEfGhIjKlMnOP	0.011248 x 0.011248 x 0.011248 x 0.003749 x 0.011248 x 0.003749 x 0.298605	*
199	acEfGhIjKlmOP	0.011248 x 0.011248 x 0.011248 x 0.003749 x 0.003749 x 0.298605	*
200	acEfGhIjkMN	0.011248 x 0.011248 x 0.011248 x 0.011248 x 0.353909	*
201	acEfGhIjkMnOP	0.011248 x 0.011248 x 0.011248 x 0.011248 x 0.003749 x 0.298605	*
202	acEfGhIjkmOP	0.011248 x 0.011248 x 0.011248 x 0.003749 x 0.298605	*
203	acEfGhIKL	0.011248 x 0.011248 x 0.003749 x 0.298605	*
204	acEfGhIKlMN	0.011248 x 0.011248 x 0.003749 x 0.011248 x 0.353909	*
205	acEfGhIKlMnOP	0.011248 x 0.011248 x 0.003749 x 0.011248 x 0.003749 x 0.298605	*
206	acEfGhIKlmOP	0.011248 x 0.011248 x 0.003749 x 0.003749 x 0.298605	*
207	acEfGhIkMN	0.011248 x 0.011248 x 0.011248 x 0.353909	*
208	acEfGhIkMnOP	0.011248 x 0.011248 x 0.011248 x 0.003749 x 0.298605	*
209	acEfGhIkmOP	0.011248 x 0.011248 x 0.003749 x 0.298605	*
210	acEfgIJ	0.011248 x 0.011248 x 0.353909	0.000044
211	acEfgIJKL	0.011248 x 0.011248 x 0.003749 x 0.298605	*
212	acEfgIJKlMN	0.011248 x 0.011248 x 0.003749 x 0.011248 x 0.353909	*
213	acEfgIJKlMnOP	0.011248 x 0.011248 x 0.003749 x 0.011248 x 0.003749 x 0.298605	*
214	acEfgIJKlmOP	0.011248 x 0.011248 x 0.003749 x 0.003749 x 0.298605	*
215	acEfgIJkMN	0.011248 x 0.011248 x 0.011248 x 0.353909	*
216	acEfgIJkMnOP	0.011248 x 0.011248 x 0.011248 x 0.003749 x 0.298605	*
217	acEfgIJkmOP	0.011248 x 0.011248 x 0.003749 x 0.298605	*
218	acEfgIKL	0.011248 x 0.003749 x 0.298605	0.000012

Table C18 (cont.):

Table C18: Failure Paths and Total Failure Probabilities

Sequence 5: FTI-A; Fail to Isolate (1 SDC Train)

Failure Path	Calculations	Results
219 acEfgIKlMN	0.011248 x 0.003749 x 0.011248 x 0.353909	*
220 acEfgIKlMnOP	0.011248 x 0.003749 x 0.011248 x 0.003749 x 0.298605	*
221 acEfgIKlmOP	0.011248 x 0.003749 x 0.003749 x 0.298605	*
222 acEfgIkMN	0.011248 x 0.011248 x 0.353909	0.000044
223 acEfgIkMnOP	0.011248 x 0.011248 x 0.003749 x 0.298605	*
224 acEfgIkmOP	0.011248 x 0.003749 x 0.298605	0.000012
225 aceGH	0.011248 x 0.298605	0.003358
226 aceGhIJ	0.011248 x 0.011248 x 0.353909	0.000044
227 aceGhIJKL	0.011248 x 0.011248 x 0.003749 x 0.298605	*
228 aceGhIJKlMN	0.011248 x 0.011248 x 0.003749 x 0.011248 x 0.353909	*
229 aceGhIJKlMnOP	0.011248 x 0.011248 x 0.003749 x 0.011248 x 0.003749 x 0.298605	*
230 aceGhIJKlmOP	0.011248 x 0.011248 x 0.003749 x 0.003749 x 0.298605	*
231 aceGhIJkMN	0.011248 x 0.011248 x 0.011248 x 0.353909	*
232 aceGhIJkMnOP	0.011248 x 0.011248 x 0.011248 x 0.003749 x 0.298605	*
233 aceGhIJkmOP	0.011248 x 0.011248 x 0.003749 x 0.298605	*
234 aceGhIKL	0.011248 x 0.003749 x 0.298605	0.000012
235 aceGhIKlMN	0.011248 x 0.003749 x 0.011248 x 0.353909	*
236 aceGhIKlMnOP	0.011248 x 0.003749 x 0.011248 x 0.003749 x 0.298605	*
237 aceGhIKlmOP	0.011248 x 0.003749 x 0.003749 x 0.298605	*
238 aceGhIkMN	0.011248 x 0.011248 x 0.353909	0.000044
239 aceGhIkMnOP	0.011248 x 0.011248 x 0.003749 x 0.298605	*
240 aceGhIkmOP	0.011248 x 0.003749 x 0.298605	0.000012

Table C18 (cont.):

Table C18: Failure Paths and Total Failure Probabilities

Sequence 5: FTI-A; Fail to Isolate (1 SDC Train)

	Failure Path	Calculations	Results
241	acegIJ	0.011248 x 0.353909	0.00398
242	acegIjKL	0.011248 x 0.003749 x 0.298605	0.000012
243	acegIjKlMN	0.011248 x 0.003749 x 0.011248 x 0.353909	*
244	acegIjKlMnOP	0.011248 x 0.003749 x 0.011248 x 0.003749 x 0.298605	*
245	acegIjKlmOP	0.011248 x 0.003749 x 0.003749 x 0.298605	*
246	acegIjkMN	0.011248 x 0.011248 x 0.353909	0.000044
247	acegIjkMnOP	0.011248 x 0.011248 x 0.003749 x 0.298605	*
248	acegIjkmOP	0.011248 x 0.003749 x 0.298605	0.000012
249	acegiKL	0.003749 x 0.298605	0.001119
250	acegiKlMN	0.003749 x 0.011248 x 0.353909	0.000015
251	acegiKlMnOP	0.003749 x 0.011248 x 0.003749 x 0.298605	*
252	acegiKlmOP	0.003749 x 0.003749 x 0.298605	0.000004
253	acegikMN	0.011248 x 0.353909	0.00398
254	acegikMnOP	0.011248 x 0.003749 x 0.298605	0.000012
255	acegikmOP	0.003749 x 0.298605	0.001119
		Total Failure Probability	0.4 [illegible]
		Error Factor	2.77

FTI-B: Sequence 5 (2 Trains of SDC)

Event FTI-B for Sequence 5 represents operator failure to isolate the leak (see Sequence 5 description in Sequences and Human Actions section) by performing the relevant steps of Attachment 6.1 (System Leakage) of procedure OP-901-046 (Shutdown Cooling Malfunction), when both SDC trains are in service. The HRA event tree for FTI-B models the critical steps, substeps, and actions represented in steps 11 and 12 of Attachment 6.1 relating to isolation of the leak. Steps and substeps modeled include closing the SDC suction isolation valve on one SDC train, observing RCS level for stabilization, placing the isolated SDC train in service (referencing OP-009-005: system operating procedure, Shutdown Cooling System), and closing the suction isolation valve on the opposite SDC train. The HRA modeling conservatively assumes that the leak is in the second train isolated. Omission and commission errors are modeled for each step/substep. Omission errors are modeled as errors by the control room supervisor (CRS), with recovery credit for the reactor operator (RO). A high level of dependence was modeled between the two, when the CRS was directing RO actions. Commission errors are modeled as errors by the RO, with recovery credit for the CRS. For these actions, a moderate level of dependence was modeled between the RO performing the action and the CRS who would be concurrently performing other dynamic actions. The HRA event tree, subtask quantifications, and total failure probability are presented in Figure 11, Table C19, and Table C20, respectively. Table C20 also lists the total mean failure probability for this event tree as 0.0233.

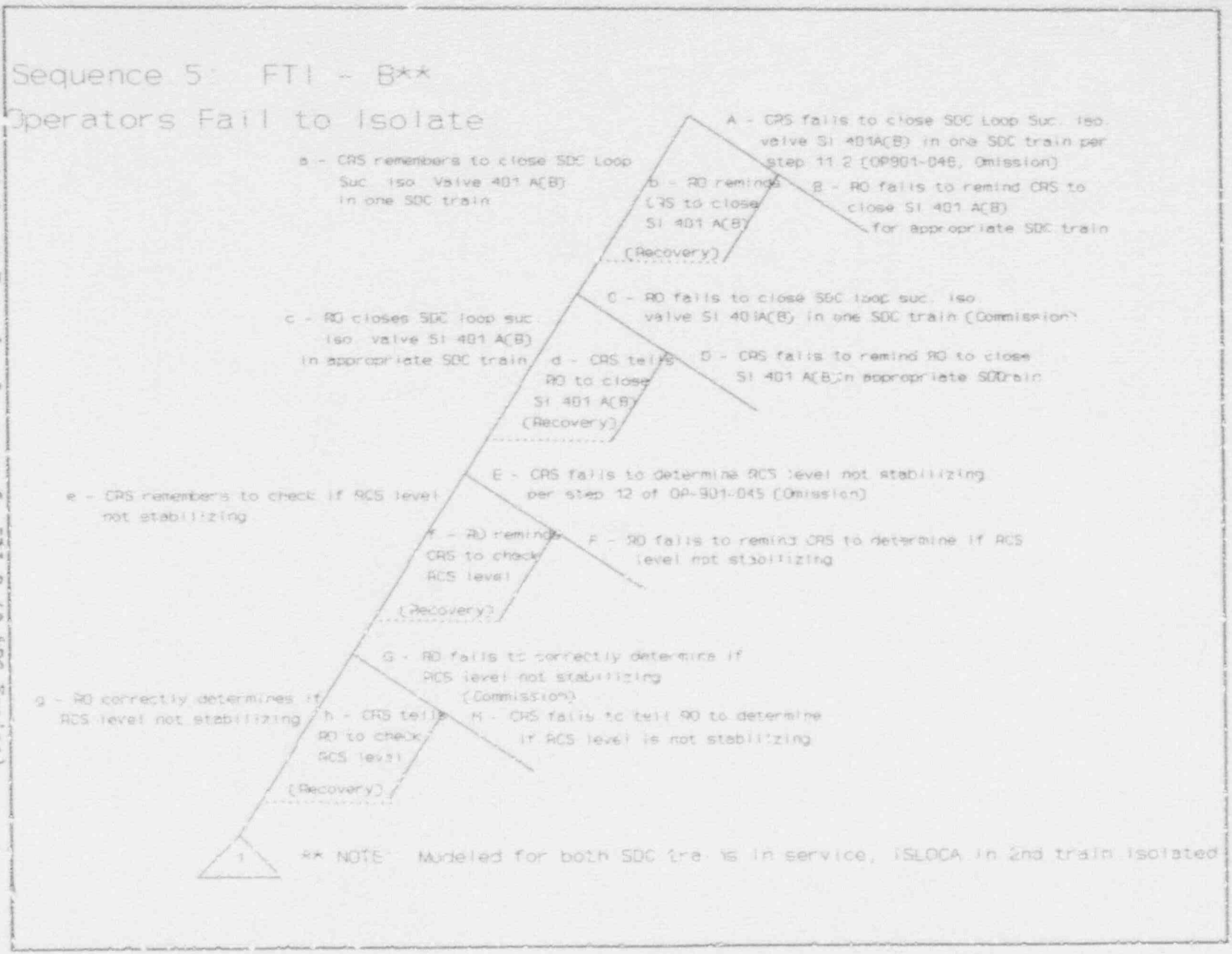

Figure 11: HRA Event Tree for Sequence 5, FTI-B (2 SDC Trains)

Figure 11 (cont.):

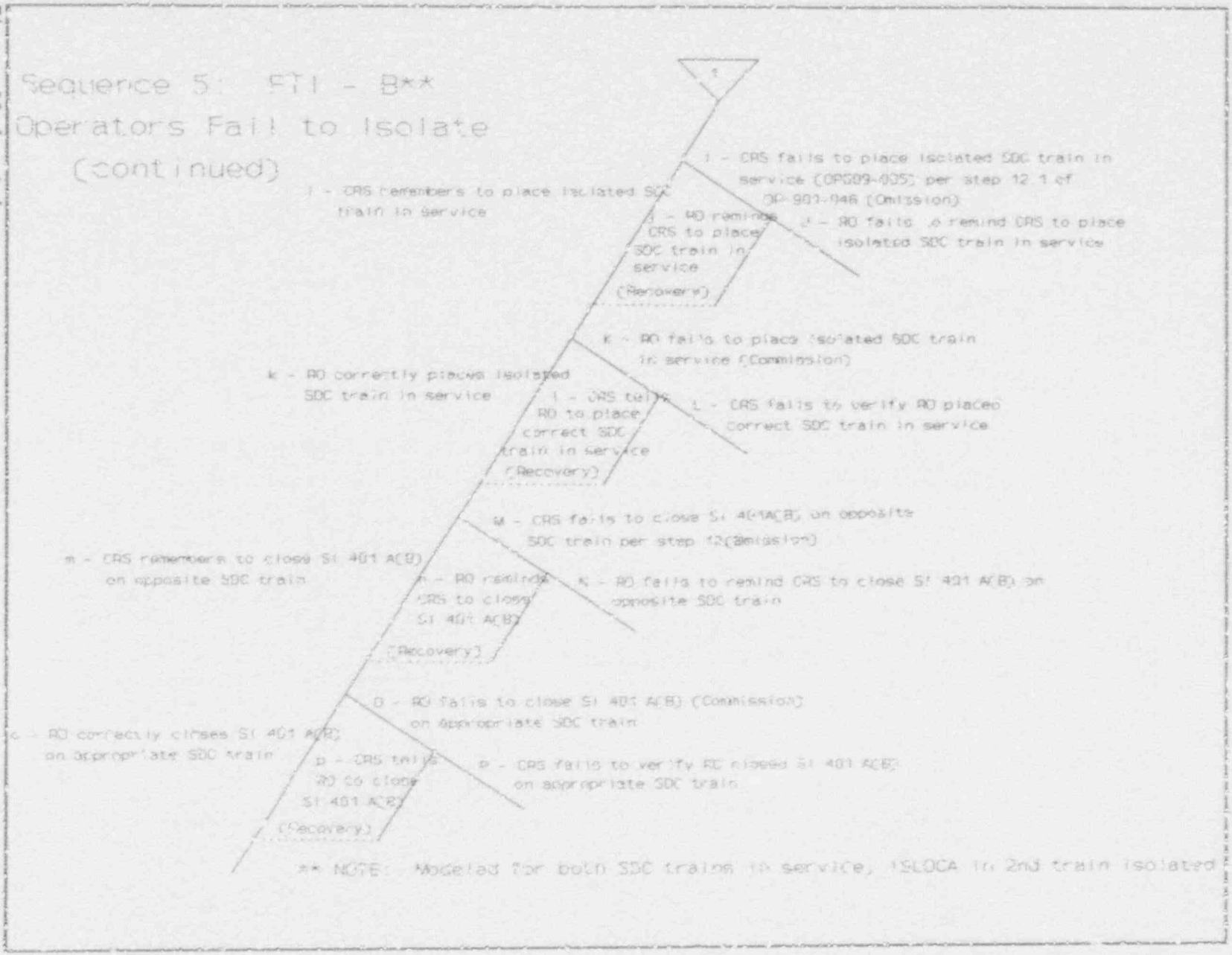

Table C19: HEPs for Sequence 5, FTI-B (2 SDC Trains)

Table C19: HEPS for Sequence 5, FTI-B; Fail to Isolate (2 SDC Trains)

	Human Action / Error	Basic Median HEP	Error Factor	Source/ T&ERP Table #	Step-by-Step or Dynamic	Modifier for PSFs	Modifier Source	THERP Dependency	Basic Mean HEP	Nominal Mean HEP	Error Factor
A	CRS fails to close one SDC loop Suc. Iso. valve SI-401 A(B) (Omission)	0.003	3.0	T20-7 #3	SBS	3	T20-16 #2	ZD	0.003749	0.011248	3.0
B	RO fails to remind CRS to close SI-401 A(B) for appropriate train	0.1	5.0	T20-22 #1	SBS	3	T20-16 #2	HD	0.161383	0.742075	5.0
										# 0.353909	2.2
C	RO fails to close SI-401 A(B)in appropriate SDC train (Commission)	0.001	3.0	T20-12 #3	SBS	3	T20-16 #2	ZD	0.001249	0.003749	3.0
D	CRS fails to remind RO to close SI-401 A(B) in appropriate train	0.1	5.0	T20-22 #1	SBS	3	T20-16 #2	MD	0.161383	0.557844	5.0
										# 0.298605	2.4
E	CRS fails to determine if RCS level not stabilizing (Omission)	0.003	3.5	T20-7 #3	SBS	3	T20-16 #2	ZD	0.003749	0.011248	3.0
F	RO fails to remind CRS to determine if RCS level not stabilizing	0.1	5.0	T20-22 #1	SBS	3	T20-16 #2	HD	0.161383	0.742075	5.0
										# 0.353909	2.2
G	RO fails to correctly determine if RCS level not stabilizing (Commission)	0.003	3.0	T20-10 #1	SBS	3	T20-16 #3	ZD	0.003749	0.011248	3.0
H	CRS fails to tell RO to determine if RCS level not stabilizing	0.1	5.0	T20-22 #1	SBS	3	T20-16 #2	MD	0.161383	0.557844	5.0
										# 0.298605	2.4

Table C19 (cont.):

Table C19: HEPS for Sequence 5, FTI-B; Fail to Isolate (2 SDC Trains)

	Human Action / Error	Basic Median HEP	Error Factor	Source/ THERP Table #	Step-by-Step or Dynamic	Modifier for PSFs	Modifier Source	THERP Dependency	Basic Mean HEP	Nominal Mean HEP	Error Factor
I	CRS fails to place isolated train in service (step 12.1 of OP901-046)	0.003	3.0	T20-7 #3	SBS	3	T20-16 #2	ZD	0.003749	0.011248	3.0
J	RO fails to remind CRS to place isolated SDC train in service	0.1	5.0	T20-22 #1	SBS	3	T20-16 #2	HD	0.161383	0.742075	5.0
										# 0.353909	2.2
K	RO fails to place isolated SDC train in service (Commission)	0.001	3.0	T20-12 #3	SBS	3	T20-16 #2	ZD	0.001249	0.003749	3.0
L	CRS fails to verify RO placed correct SDC train in service	0.1	5.0	T20-22 #1	SBS	3	T20-16 #2	MD	0.161383	0.557844	5.0
										# 0.298605	2.4
M	CRS fails to close SI-401 A(B) on opposite SDC train	0.003	3.0	T20-7 #3	SBS	3	T20-16 #2	ZD	0.003749	0.011248	3.0
N	RO fails to remind CRS to close SI-401 A(B) on opposite SDC train	0.1	5.0	T20-22 #1	SBS	3	T20-16 #2	HD	0.161383	0.742075	5.0
										# 0.353909	2.2
O	RO fails to close correct SI-401 A(B) valve on appropriate train (Commission)	0.001	3.0	T20-12 #3	SBS	3	T20-16 #2	ZD	0.001249	0.003749	3.0
P	CRS fails to verify RO closed correct SI-401 A(B) valve	0.1	5.0	T20-22 #1	SBS	3	T20-16 #2	MD	0.161383	0.557844	5.0
										# 0.298605	2.4

Table C20: Failure Paths & Total Failure Probability (Seq. 5, FTI-B)

Table C20 : Failure Paths and Total Failure Probabilities

Sequence 5: FTI-B; Fail to Isolate (2 SDC Trains)

	Failure Path	Calculations	Results
1	AB	0.011248 x 0.353909	0.00398
2	AbCD	0.011248 x 0.003749 x 0.298605	0.000012
3	AbCdEF	0.011248 x 0.003749 x 0.011248 x 0.353909	*
4	AbCdEfGH	0.011248 x 0.003749 x 0.011248 x 0.011248 x 0.298605	*
5	AbCdEfGhIJ	0.011248 x 0.003749 x 0.011248 x 0.011248 x 0.011248 x 0.353909	*
6	AbCdEfGhIjKL	0.011248 x 0.003749 x 0.011248 x 0.011248 x 0.011248 x 0.003749 x 0.298605	*
7	AbCdEfGhIjKlMN	0.011248 x 0.003749 x 0.011248 x 0.011248 x 0.011248 x 0.003749 x 0.011248 x 0.353909	*
8	AbCdEfGhIjKlMnOP	0.011248 x 0.003749 x 0.011248 x 0.011248 x 0.011248 x 0.003749 x 0.011248 x 0.003749 x 0.298605	*
9	AbCdEfGhIjKlmOP	0.011248 x 0.003749 x 0.011248 x 0.011248 x 0.011248 x 0.003749 x 0.003749 x 0.298605	*
10	AbCdEfGhIjkMN	0.011248 x 0.003749 x 0.011248 x 0.011248 x 0.011248 x 0.011248 x 0.353909	*
11	AbCdEfGhIjkMnOP	0.011248 x 0.003749 x 0.011248 x 0.011248 x 0.011248 x 0.011248 x 0.003749 x 0.298605	*
12	AbCdEfGhIjkmOP	0.011248 x 0.003749 x 0.011248 x 0.011248 x 0.011248 x 0.003749 x 0.298605	*
13	AbCdEfGhIKL	0.011248 x 0.003749 x 0.011248 x 0.011248 x 0.003749 x 0.298605	*
14	AbCdEfGhIKlMN	0.011248 x 0.003749 x 0.011248 x 0.011248 x 0.003749 x 0.011248 x 0.353909	*
15	AbCdEfGhIKlMnOP	0.011248 x 0.003749 x 0.011248 x 0.011248 x 0.003749 x 0.011248 x 0.003749 x 0.298605	*
16	AbCdEfGhIKlmOP	0.011248 x 0.003749 x 0.011248 x 0.011248 x 0.003749 x 0.003749 x 0.298605	*
17	AbCdEfGhIkMN	0.011248 x 0.003749 x 0.011248 x 0.011248 x 0.011248 x 0.353909	*
18	AbCdEfGhIkMnOP	0.011248 x 0.003749 x 0.011248 x 0.011248 x 0.011248 x 0.003749 x 0.298605	*
19	AbCdEfGhIkmOP	0.011248 x 0.003749 x 0.011248 x 0.011248 x 0.003749 x 0.298605	*
20	AbCdEfgIJ	0.011248 x 0.003749 x 0.011248 x 0.011248 x 0.353909	*

Table C20 (cont.):

Table C20 : Failure Paths and Total Failure Probabilities

Sequence 2: FTI-B; Fail to Isolate (2 SDC Trains)

	Failure Path	Calculations	Results
21	AbCdEJgIjKL	0.011248 x 0.003749 x 0.011248 x 0.011248 x 0.003749 x 0.298605	*
22	AbCdEJgIjKlMN	0.011248 x 0.003749 x 0.011248 x 0.011248 x 0.003749 x 0.011248 x 0.353909	*
23	AbCdEJgIjKlMnOP	0.011248 x 0.003749 x 0.011248 x 0.011248 x 0.003749 x 0.011248 x 0.003749 x 0.298605	*
24	AbCdEJgIjKlmOP	0.011248 x 0.003749 x 0.011248 x 0.011248 x 0.003749 x 0.003749 x 0.298605	*
25	AbCdEJgIjkMN	0.011248 x 0.003749 x 0.011248 x 0.011248 x 0.011248 x 0.353909	*
26	AbCdEJgIjkMnOP	0.011248 x 0.003749 x 0.011248 x 0.011248 x 0.011248 x 0.003749 x 0.298605	*
27	AbCdEJgIjkmOP	0.011248 x 0.003749 x 0.011248 x 0.011248 x 0.003749 x 0.298605	*
28	AbCdEJgIKL	0.011248 x 0.003749 x 0.011248 x 0.003749 x 0.298605	*
29	AbCdEJgIKlMN	0.011248 x 0.003749 x 0.011248 x 0.003749 x 0.011248 x 0.353909	*
30	AbCdEJgIKlMnOP	0.011248 x 0.003749 x 0.011248 x 0.003749 x 0.011248 x 0.003749 x 0.298605	*
31	AbCdEJgIKlmOP	0.011248 x 0.003749 x 0.011248 x 0.003749 x 0.003749 x 0.298605	*
32	AbCdEJgIkMN	0.011248 x 0.003749 x 0.011248 x 0.011248 x 0.353909	*
33	AbCdEJgIkMnOP	0.011248 x 0.003749 x 0.011248 x 0.011248 x 0.003749 x 0.298605	*
34	AbCdEJgIkmOP	0.011248 x 0.003749 x 0.011248 x 0.003749 x 0.298605	*
35	AbCdEJGH	0.011248 x 0.003749 x 0.011248 x 0.298605	*
36	AbCdeGhIJ	0.011248 x 0.003749 x 0.011248 x 0.011248 x 0.353909	*
37	AbCdeGhIJKL	0.011248 x 0.003749 x 0.011248 x 0.011248 x 0.003749 x 0.298605	*
38	AbCdeGhIJKlMN	0.011248 x 0.003749 x 0.011248 x 0.011248 x 0.003749 x 0.011248 x 0.353909	*
39	AbCdeGhIJKlMnOP	0.011248 x 0.003749 x 0.011248 x 0.011248 x 0.003749 x 0.011248 x 0.003749 x 0.298605	*
40	AbCdeGhIJKlmOP	0.011248 x 0.003749 x 0.011248 x 0.011248 x 0.003749 x 0.003749 x 0.298605	*
41	AbCdeGhIJkMN	0.011248 x 0.003749 x 0.011248 x 0.011248 x 0.011248 x 0.353909	*
42	AbCdeGhIJkMnOP	0.011248 x 0.003749 x 0.011248 x 0.011248 x 0.011248 x 0.003749 x 0.298605	*

Table C20 (cont.):

Tabie C20 : Failure Paths and Total Failure Probabilities

Sequence 5: FTI-B; Fail to Isolate (2 SDC Trains)

	Failure Fa	Calculations	Results
43	AbCdeGhIjkmOP	0.011248 x 0.003749 x 0.011248 x 0.011248 x 0.003749 x 0.298605	*
44	AbCdeGhIKL	0.011248 x 0.003749 x 0.011248 x 0.003749 x 0.298605	*
45	AbCdeGhIKlMN	0.011248 x 0.003749 x 0.011248 x 0.003749 x 0.011248 x 0.353909	*
46	AbCdeGhIKlMnOP	0.011248 x 0.003749 x 0.011248 x 0.003749 x 0.011248 x 0.003749 x 0.298605	*
47	AbCdeGhIKlmOP	0.011248 x 0.003749 x 0.011248 x 0.003749 x 0.003749 x 0.298605	*
48	AbCdeGhIkMN	0.011248 x 0.003749 x 0.011248 x 0.011248 x 0.353909	*
49	AbCdeGhIkMnOP	0.011248 x 0.003749 x 0.011248 x 0.011248 x 0.003749 x 0.298605	*
50	AbCdeGhIkmOP	0.011248 x 0.003749 x 0.011248 x 0.003749 x 0.298605	*
51	AbCdegIJ	0.011248 x 0.003749 x 0.011248 x 0.353909	*
52	AbCdegIJKL	0.011248 x 0.003749 x 0.011248 x 0.003749 x 0.298605	*
53	AbCdegIJKlMN	0.011248 x 0.003749 x 0.011248 x 0.003749 x 0.011248 x 0.353909	*
54	AbCdegIJKlMnOP	0.011248 x 0.003749 x 0.011248 x 0.003749 x 0.011248 x 0.003749 x 0.298605	*
55	AbCdegIJKlmOP	0.011248 x 0.003749 x 0.011248 x 0.003749 x 0.003749 x 0.298605	*
56	AbCdegIJkMN	0.011248 x 0.003749 x 0.011248 x 0.011248 x 0.353909	*
57	AbCdegIJkMnOP	0.011248 x 0.003749 x 0.011248 x 0.011248 x 0.003749 x 0.298605	*
58	AbCdegIJkmOP	0.011248 x 0.003749 x 0.011248 x 0.003749 x 0.298605	*
59	AbCdegIKL	0.011248 x 0.003749 x 0.003749 x 0.298605	*
60	AbCdegIKlMN	0.011248 x 0.003749 x 0.003749 x 0.011248 x 0.353909	*
61	AbCdegIKlMnOP	0.011248 x 0.003749 x 0.003749 x 0.011248 x 0.003749 x 0.298605	*
62	AbCdegIKlmOP	0.011248 x 0.003749 x 0.003749 x 0.003749 x 0.298605	*
63	AbCdegIkMN	0.011248 x 0.003749 x 0.011248 x 0.353909	*
64	AbCdegIkMnOP	0.011248 x 0.003749 x 0.011248 x 0.003749 x 0.298605	*

Table C20 (cont.):

Table C20 : Failure Paths and Total Failure Probabilities

Sequence 5: FTI-B; Fail to Isolate (2 SDC Trains)

	Failure Path	Calculations	Results
65	AbCdeglkmOP	0.011248 x 0.003749 x 0.003749 x 0.298605	*
66	AbcEF	0.011248 x 0.011248 x 3.353909	0.000044
67	AbcEfGH	0.011248 x 0.011248 x 0.011248 x 0.298605	*
68	AbcEfGhIJ	0.011248 x 0.011248 x 0.011248 x 0.011248 x 0.353909	*
69	AbcEfGhIjKL	0.011248 x 0.011248 x 0.011248 x 0.011248 x 0.003749 x 0.298605	*
70	AbcEfGhIjKIMN	0.011248 x 0.011248 x 0.011248 x 0.011248 x 0.003749 x 0.011248 0.353909	*
71	AbcEfGhIjKIMnOP	0.011248 x 0.011248 x 0.011248 x 0.011248 x 0.003749 x 0.011248 x 0.003749 x 0.298605	*
72	AbcEfGhIjKlmOP	0.011248 x 0.011248 x 0.011248 x 0.011248 x 0.003749 x 0.003749 x 0.298605	*
73	AbcEfGhIjkMN	0.011248 x 0.011248 x 0.011248 x 0.011248 x 0.011248 x 0.353909	*
74	AbcEfGhIjkMnOP	0.011248 x 0.011248 x 0.011248 x 0.011248 x 0.011248 x 0.003749 x 0.298605	*
75	AbcEfGhIjkmOP	0.011248 x 0.011248 x 0.011248 x 0.011248 x 0.003749 x 0.298605	*
76	AbcEfGhIKL	0.011248 x 0.011248 x 0.011248 x 0.003749 x 0.298605	*
77	AbcEfGhIKIMN	0.011248 x 0.011248 x 0.011248 x 0.003749 x 0.011248 x 0.353909	*
78	AbcEfGhIKIMnOP	0.011248 x 0.011248 x 0.011248 x 0.003749 x 0.011248 x 0.003749 x 0.298605	*
79	AbcEfGhIKlmOP	0.011248 x 0.011248 x 0.011248 x 0.003749 x 0.003749 x 0.298605	*
80	AbcEfGhIkMN	0.011248 x 0.011248 x 0.011248 x 0.011248 x 0.353909	*
81	AbcEfGhIkMnOP	0.011248 x 0.011248 x 0.011248 x 0.011248 x 0.003749 x 0.298605	*
82	AbcEfGhIkmOP	0.011248 x 0.011248 x 0.011248 x 0.003749 x 0.298605	*
83	AbcEfgIJ	0.011248 x 0.011248 x 0.011248 x 0.353909	*
84	AbcEfgIJKL	0.011248 x 0.011248 x 0.011248 x 0.003749 x 0.298605	*
85	AbcEfgIJKIMN	0.011248 x 0.011248 x 0.011248 x 0.003749 x 0.011248 x 0.353909	*
86	AbcEfgIJKIMnOP	0.011248 x 0.011248 x 0.011248 x 0.003749 x 0.011248 x 0.003749 x 0.298605	*

Table C20 (cont.):

Table C20 : Failure Paths and Total Failure Probabilities

Sequence 5: FTI-B; Fail to Isolate (2 SDC Trains)

	Failure Path	Calculations	Results
87	AbcEIgIJKlmOP	0.011248 x 0.011248 x 0.011248 x 0.003749 x 0.003749 x 0.298605	*
88	AbcEIgIJkMN	0.011248 x 0.011248 x 0.011248 x 0.011248 x 0.353909	*
89	AbcEIgIJkMnOP	0.011248 x 0.011248 x 0.011248 x 0.011248 x 0.003749 x 0.298605	*
90	AbcEIgIJkmOP	0.011248 x 0.011248 x 0.011248 x 0.003749 x 0.298605	*
91	AbcEIgIKL	0.011248 x 0.011248 x 0.003749 x 0.298605	*
92	AbcEIgIKlMN	0.011248 x 0.011248 x 0.003749 x 0.011248 x 0.353909	*
93	AbcEIgIKlMnOP	0.011248 x 0.011248 x 0.003749 x 0.011248 x 0.003749 x 0.298605	*
94	AbcEIgIKlmOP	0.011248 x 0.011248 x 0.003749 x 0.003749 x 0.298605	*
95	AbcEIgIkMN	0.011248 x 0.011248 x 0.011248 x 0.353909	*
96	AbcEIgIkMnOP	0.011248 x 0.011248 x 0.011248 x 0.003749 x 0.298605	*
97	AbcEIgIkmOP	0.011248 x 0.011248 x 0.003749 x 0.298605	*
98	AbceGH	0.011248 x 0.011248 x 0.298605	0.000037
99	AbceGhIJ	0.011248 x 0.011248 x 0.011248 x 0.353909	*
100	AbceGhIJKL	0.011248 x 0.011248 x 0.011248 x 0.003749 x 0.298605	*
101	AbceGhIJKlMN	0.011248 x 0.011248 x 0.011248 x 0.003749 x 0.011248 x 0.353909	*
102	AbceGhIJKlMnOP	0.011248 x 0.011248 x 0.011248 x 0.003749 x 0.011248 x 0.003749 x 0.298605	*
103	AbceGhIJKlmOP	0.011248 x 0.011248 x 0.011248 x 0.003749 x 0.003749 x 0.298605	*
104	AbceGhIJkMN	0.011248 x 0.011248 x 0.011248 x 0.011248 x 0.353909	*
105	AbceGhIJkMnOP	0.011248 x 0.011248 x 0.011248 x 0.011248 x 0.003749 x 0.298605	*
106	AbceGhIJkmOP	0.011248 x 0.011248 x 0.011248 x 0.003749 x 0.298605	*
107	AbceGhIKL	0.011248 x 0.011248 x 0.003749 x 0.298605	*
108	AbceGhIKlMN	0.011248 x 0.011248 x 0.003749 x 0.011248 x 0.353909	*

Table C20 (cont.):

Table C20 : Failure Paths and Total Failure Probabilities

Sequence 5: FTI-B; Fail to Isolate (2 SDC Trains)

Failure Path		Calculations	Results
109	AbceGhIKlMnOP	0.011248 x 0.011248 x 0.003749 x 0.011248 x 0.003749 x 0.298605	*
110	AbceGhiKlmOP	0.011248 x 0.011248 x 0.003749 x 0.003749 x 0.298605	*
111	AbceGhIkMN	0.011248 x 0.011248 x 0.011248 x 0.353909	*
112	AbceGhIkMnOP	0.011248 x 0.011248 x 0.011248 x 0.003749 x 0.298605	*
113	AbceGhIkmOP	0.011248 x 0.011248 x 0.003749 x 0.298605	*
114	AbcegIJ	0.011248 x 0.011248 x 0.353909	0.000044
115	AbcegIJKL	0.011248 x 0.011248 x 0.003749 x 0.298605	*
116	AbcegIJKlMN	0.011248 x 0.011248 x 0.003749 x 0.011248 x 0.353909	*
117	AbcegIJKlMnOP	0.011248 x 0.011248 x 0.003749 x 0.011248 x 0.003749 x 0.298605	*
118	AbcegIJKlmOP	0.011248 x 0.011248 x 0.003749 x 0.003749 x 0.298605	*
119	AbcegIJkMN	0.011248 x 0.011248 x 0.011248 x 0.353909	*
120	AbcegIJkMnOP	0.011248 x 0.011248 x 0.011248 x 0.003749 x 0.298605	*
121	AbcegIJkmOP	0.011248 x 0.011248 x 0.003749 x 0.298605	*
122	AbcegIKL	0.011248 x 0.003749 x 0.298605	0.000012
123	AbcegIKlMN	0.011248 x 0.003749 x 0.011248 x 0.353909	*
124	AbcegIKlMnOP	0.011248 x 0.003749 x 0.011248 x 0.003749 x 0.298605	*
125	AbcegIKlmOP	0.011248 x 0.003749 x 0.003749 x 0.298605	*
126	AbcegIkMN	0.011248 x 0.011248 x 0.353909	0.000044
127	AbcegIkMnOP	0.011248 x 0.011248 x 0.003749 x 0.298605	*
128	AbcegIkmOP	0.011248 x 0.003749 x 0.298605	0.000012
129	aCD	0.003749 x 0.298605	0.001119
130	aCdEF	0.003749 x 0.011248 x 0.353909	0.000014

Table C20 (cont.):

Table C20 : Failure Paths and Total Failure Probabilities

Sequence 5: FTI-B; Fail to Isolate (2 CCDC Trains)

Failure Path	Calculations	Results
131 aCdEfGlk	0.003749 x 0.011248 x 0.011248 x 0.298605	*
132 aCdEfGhIJ	0.003749 x 0.011248 x 0.011248 x 0.011248 x 0.353909	*
133 aCdEfGhIJKL	0.003749 x 0.011248 x 0.011248 x 0.011248 x 0.003749 x 0.298605	*
134 aCdEfGhIJKlMN	0.003749 x 0.011248 x 0.011248 x 0.011248 x 0.003749 x 0.011248 x 0.353909	*
135 aCdEfGhIJKlMnOP	0.003749 x 0.011248 x 0.011248 x 0.011248 x 0.003749 x 0.011248 x 0.003749 x 0.298605	*
136 aCdEfGhIJKlmOP	0.003749 x 0.011248 x 0.011248 x 0.011248 x 0.003749 x 0.003749 x 0.298605	*
137 aCdEfGhIJkMN	0.003749 x 0.011248 x 0.011248 x 0.011248 x 0.011248 x 0.353909	*
138 aCdEfGhIJkMnOP	0.003749 x 0.011248 x 0.011248 x 0.011248 x 0.011248 x 0.003749 x 0.298605	*
139 aCdEfGhIJkmOP	0.003749 x 0.011248 x 0.011248 x 0.011248 x 0.003749 x 0.298605	*
140 aCdEfGhIKL	0.003749 x 0.011248 x 0.011248 x 0.003749 x 0.298605	*
141 aCdEfGhIKlMN	0.003749 x 0.011248 x 0.011248 x 0.003749 x 0.011248 x 0.353909	*
142 aCdEfGhIKlMnOP	0.003749 x 0.011248 x 0.011248 x 0.003749 x 0.011248 x 0.003749 x 0.298605	*
143 aCdEfGhIKlmOP	0.003749 x 0.011248 x 0.011248 x 0.003749 x 0.003 [illegible] 8605	*
144 aCdEfGhIkMN	0.003749 x 0.011248 x 0.011248 x 0.011248 x 0.353909	*
145 aCdEfGhIkMnOP	0.003749 x 0.011248 x 0.011248 x 0.011248 x 0.003749 x 0.298605	*
146 aCdEfGhIkmOP	0.003749 x 0.011248 x 0.011248 x 0.003749 x 0.298605	*
147 aCdEfgIJ	0.003749 x 0.011248 x 0.011248 x 0.353909	*
148 aCdEfgIJKL	0.003749 x 0.011248 x 0.011248 x 0.003749 x 0.298605	*
149 aCdEfgIJKlMN	0.003749 x 0.011248 x 0.011248 x 0.003749 x 0.011248 x 0.353909	*
150 aCdEfgIJKlMnOP	0.003749 x 0.011248 x 0.011248 x 0.003749 x 0.011248 x 0.003749 x 0.298605	*
151 aCdEfgIJKlmOP	0.003749 x 0.011248 x 0.011248 x 0.003749 x 0.003749 x 0.298605	*
152 aCdEfgIJkMN	0.003749 x 0.011248 x 0.011248 x 0.011248 x 0.353909	*

Table C20 (cont.):

Table C20 : Failure Paths and Total Failure Probabilities

Sequence 5: FTI-B; Fail to Isolate (2 SDC Trains)

	Failure Path	Calculations	Results
153	aCdEfg-jkMnOP	0.003749 x 0.011248 x 0.011248 x 0.011248 x 0.003749 x 0.298605	*
154	aCdEfgIjkmOP	0.003749 x 0.011248 x 0.011248 x 0.003749 x 0.298605	*
155	aCdEfgIKL	0.003749 x 0.011248 x 0.003749 x 0.298605	*
156	aCdEfgIKMN	0.003749 x 0.011248 x 0.003749 x 0.011248 x 0.353909	*
157	aCdEfgIKlMnOP	0.003749 x 0.011248 x 0.003749 x 0.011248 x 0.003749 x 0.298605	*
158	aCdEfgIKlmOP	0.003749 x 0.011248 x 0.003749 x 0.003749 x 0.298605	*
159	aCdEfgIkMN	0.003749 x 0.011248 x 0.011248 x 0.353909	*
160	aCdEfgIkMnOP	0.003749 x 0.011248 x 0.011248 x 0.003749 x 0.298605	*
161	aCdEfgIkmOP	0.003749 x 0.011248 x 0.003749 x 0.298605	*
162	aCdeGH	0.003749 x 0.011248 x 0.298605	0.000012
163	aCdeGhIJ	0.003749 x 0.011248 x 0.011248 x 0.353909	*
164	aCdeGhIjKL	0.003749 x 0.011248 x 0.011248 x 0.003749 x 0.298605	*
165	aCdeGhIjKlMN	0.003749 x 0.011248 x 0.011248 x 0.003749 x 0.011248 x 0.353909	*
166	aCdeGhIjKlMnOP	0.003749 x 0.011248 x 0.011248 x 0.003749 x 0.011248 x 0.003749 x 0.298605	*
167	aCdeGhIjKlmOP	0.003749 x 0.011248 x 0.011248 x 0.003749 x 0.003749 x 0.298605	*
168	aCdeGhIjkMN	0.003749 x 0.011248 x 0.011248 x 0.011248 x 0.353909	*
169	aC[illegible]IjkMnOP	0.003749 x 0.011248 x 0.011248 x 0.011248 x 0.003749 x 0.298605	*
170	aCdeGhIjkmOP	0.003749 x 0.011248 x 0.011248 x 0.003749 x 0.298605	*
171	aCdeGhlKL	0.003749 x 0.011248 x 0.003749 x 0.298605	*
172	aCdeGhlKlMN	0.003749 x 0.011248 x 0.003749 x 0.011248 x 0.353909	*
173	aCdeGhlKlMnOP	0.003749 x 0.011248 x 0.003749 x 0.011248 x 0.003749 x 0.298605	*
174	aCdeGhlKlmOP	0.003749 x 0.011248 x 0.003749 x 0.003749 x 0.298605	*

Table C20 (cont.):

Table C20 : Failure Paths and Total Failure Probabilities

Sequence 5: FTI-B; Fail to Isolate (2 SDC Trains)

Failure Path		Calculations	Results
175	aCdeGhIkMN	0.003749 x 0.011248 x 0.011248 x 0.353909	*
176	aCdeGhIkMnOP	0.003749 x 0.01[illegible]48 x 0.011248 x 0.003749 x 0.298605	*
177	aCdeGhIkmOP	0.003749 x 0.011248 x 0.003749 x 0.298605	*
178	aCdegIJ	0.003749 x 0.011248 x 0.353909	0.000014
179	aCdegIJKL	0.003749 x 0.011248 x 0.003749 x 0.298605	*
180	aCdegIJKIMN	0.003749 x 0.011248 x 0.003749 x 0.011248 x 0.353909	*
181	aCdegIJKIMnOP	0.003749 x 0.011248 x 0.003749 x 0.011248 x 0.003749 x 0.298605	*
182	aCdegIJKImOP	0.003749 x 0.011248 x 0.003749 x 0.003749 x 0.298605	*
183	aCdegIJkMN	0.003749 x 0.011248 x 0.011248 x 0.353909	*
184	aCdegIJkMnOP	0.003749 x 0.011248 x 0.011248 x 0.003749 x 0.298605	*
185	aCdegIJkmOP	0.003749 x 0.011248 x 0.003749 x 0.298605	*
186	aCdegiKL	0.003749 x 0.003749 x 0.298605	0.000004
187	aCdegIKIMN	0.003749 x 0.003749 x 0.011248 x 0.353909	*
188	aCdegIKIMnOP	0.003749 x 0.003749 x 0.011248 x 0.003749 x 0.298605	*
189	aCdegIKImOP	0.003749 x 0.003749 x 0.003749 x 0.298605	*
190	aCdegIkMN	0.003749 x 0.011248 x 0.353909	0.000014
191	aCdegIkMnOP	0.003749 x 0.011248 x 0.003749 x 0.298605	*
192	aCdegIkmOP	0.003749 x 0.003749 x 0.298605	0.000004
193	acEF	0.011248 x 0.353909	0.00398
194	acEFGH	0.011248 x 0.011248 x 0.298605	0.000037
195	acEFGhIJ	0.011248 x 0.011248 x 0.011248 x 0.353909	*
196	acEFGhIJKL	0.011248 x 0.011248 x 0.011248 x 0.003749 x 0.298605	*

Table C20 (cont.):

Table C20 : Failure Paths and Total Failure Probabilities

Sequence 5: FTI-B; Fail to Isolate (2 SDC Trains)

Failure Path	Calculations	Results
197 acEfGhIjKlMN	0.011248 x 0.011248 x 0.011248 x 0.003749 x 0.011248 x 0.353909	*
198 acEfGhIjKlMnOP	0.011248 x 0.011248 x 0.011248 x 0.003749 x 0.011248 x 0.003749 x 0.298605	*
199 acEfGhIjK1mOP	0.011248 x 0.011248 x 0.011248 x 0.003749 x 0.003749 x 0.298605	*
200 acEfGhIjkMN	0.011248 x 0.011248 x 0.011248 x 0.011248 x 0.353909	*
201 acEfGhIjkMnOP	0.011248 x 0.011248 x 0.011248 x 0.011248 x 0.003749 x 0.298605	*
202 acEfGhIjkmOP	0.011248 x 0.011248 x 0.011248 x 0.003749 x 0.298605	*
203 acEfGhiKL	0.011248 x 0.011248 x 0.003749 x 0.298605	*
204 acEfGhiKlMN	0.011248 x 0.011248 x 0.003749 x 0.011248 x 0.353909	*
205 acEfGhiKlMnOP	0.011248 x 0.011248 x 0.003749 x 0.011248 x 0.003749 x 0.298605	*
206 acEfGhiKlmOP	0.011248 x 0.011248 x 0.003749 x 0.003749 x 0.298605	*
207 acEfGhikMN	0.011248 x 0.011248 x 0.011248 x 0.353909	*
208 acEfGf \MnOP	0.011248 x 0.011248 x 0.011248 x 0.003749 x 0.298605	*
209 acEfGhikmOP	0.011248 x 0.011248 x 0.003749 x 0.298605	*
210 acEfgIJ	0.011248 x 0.011248 x 0.353909	0.000044
211 acEfgIJKL	0.011248 x 0.011248 x 0.003749 x 0.298605	*
212 acEfgIjKlMN	0.011248 x 0.011248 x 0.003749 x 0.011248 x 0.353909	*
213 acEfgIjKlMnOP	0.011248 x 0.011248 x 0.003749 x 0.011248 x 0.003749 x 0.298605	*
214 acEfgIjKlmOP	0.011248 x 0.011248 x 0.003749 x 0.003749 x 0.298605	*
215 acEfgIjkMN	0.011248 x 0.011248 x 0.011248 x 0.353909	*
216 acEfgIjkMnOP	0.011248 x 0.011248 x 0.011248 x 0.003749 x 0.298605	*
217 acEfgIjkmOP	0.011248 x 0.011248 x 0.003749 x 0.298605	*
218 acEfgIKL	0.011248 x 0.003749 x 0.298605	0.000012

Table C20 (cont.):

Table C20 : Failure Paths and Total Failure Probabilities

Sequence 5: FTI-B; Fail to Isolate (2 SDC Trains)

Failure Path	Calculations	Results
219 acEfgIKlMN	0.011248 x 0.003749 x 0.011248 x 0.353909	*
220 acEfgIKlMnOP	0.011248 x 0.003749 x 0.011248 x 0.003749 x 0.298605	*
221 acEfgIKlmOP	0.011248 x 0.003749 x 0.003749 x 0.298605	*
222 acEfgIkMN	0.011248 x 0.011248 x 0.353909	0.000044
223 acEfgIkMnOP	0.011248 x 0.011248 x 0.003749 x 0.298605	*
224 acEfgIkmOP	0.011248 x 0.003749 x 0.298605	0.000012
225 aceGH	0.011248 x 0.298605	0.003358
226 aceGhIJ	0.011248 x 0.011248 x 0.353909	0.000044
227 aceGhIJKL	0.011248 x 0.011248 x 0.003749 x 0.298605	*
228 aceGhIJKlMN	0.011248 x 0.011248 x 0.003749 x 0.011248 x 0.353909	*
229 aceGhIJKlMnOP	0.011248 x 0.011248 x 0.003749 x 0.011248 x 0.003749 x 0.298605	*
230 aceGhIJKlmOP	0.011248 x 0.011248 x 0.003749 x 0.003749 x 0.298605	*
231 aceGhIJkMN	0.011248 x 0.011248 x 0.011248 x 0.353909	*
232 aceGhIJkMnOP	0.011248 x 0.011248 x 0.011248 x 0.003749 x 0.298605	*
233 aceGhIJkmOP	0.011248 x 0.011248 x 0.003749 x 0.298605	*
234 aceGhIKL	0.011248 x 0.003749 x 0.298605	0.000011
235 aceGhIKlMN	0.011248 x 0.003749 x 0.011248 x 0.353909	*
236 aceGhIKlMnOP	0.011248 x 0.003749 x 0.011248 x 0.003749 x 0.298605	*
237 aceGhIKlmOP	0.011248 x 0.003749 x 0.003749 x 0.298605	*
238 aceGhIkMN	0.011248 x 0.011248 x 0.353909	0.000044
239 aceGhIkMnOP	0.011248 x 0.011248 x 0.003749 x 0.298605	*
240 aceGhIkmOP	0.011248 x 0.003749 x 0.298605	0.000012

Table C20 (cont.):

Table C20 : Failure Paths and Total Failure Probabilities

Sequence 3: FTI-B; Fail to Isolate (2 SDC Trains)

	Failure Path	Calculations	Results
241	acegIJ	0.011248 x 0.353909	0.00398
242	acegIjKL	0.011248 x 0.003749 x 0.298605	0.000012
243	acegIjKlMN	0.011248 x 0.003749 x 0.011248 x 0.353909	*
244	acegIjKlMnOP	0.011248 x 0.003749 x 0.011248 x 0.003749 x 0.298605	*
245	acegIjKlmOP	0.011248 x 0.003749 x 0.003749 x 0.298605	*
246	acegIjkMN	0.011248 x 0.011248 x 0.353909	0.000044
247	acegIjkMnOP	0.011248 x 0.011248 x 0.003749 x 0.298605	*
248	acegIjkmOP	0.0 [illegible] 8 x 0.003749 x 0.298605	0.000012
249	acegIKL	0.003749 x 0.298605	0.001119
250	acegIKlMN	0.003749 x 0.011248 x 0.353909	0.000014
251	acegIKlMnOP	0.003749 x 0.011248 x 0.003749 x 0.298605	*
252	acegIklmOP	0.003749 x 0.003749 x 0.298605	0.000004
253	acegIkMN	0.011248 x 0.353909	0.00398
254	acegIkMnOP	0.011248 x 0.003749 x 0.298605	0.000012
255	acegIkmOP	0.003749 x 0.298605	0.001119
		Total Failure Probability	**0.023**
		Error Factor	**2.77**

Summary of CE ISLOCA HRA

Detailed HRA analyses were conducted for each of the significant scenarios identified in this ISLOCA PRA. Extensive documentation for each analysis has been provided above (e.g., descriptions of the scenarios, human errors, and both median and mean HEPs).

Data from each human action in each sequence was then used in an uncertainty analysis. HEPs for individual tasks/subtasks, in individual event trees, were entered into IRRAS, the Integrated Reliability and Risk Analysis System. Using the Latin Hypercube Sampling Methodology in IRRAS, with a sample size of 5,000, the HRA analysts were able to propagate uncertainty throughout each analysis and were then able to calculate a final EF (error factor) for each total failure probability. Results from the traditional HRA and uncertainty analysis are summarized in Table C21. Individual human actions are listed in the first column (with sequence number) followed by:

1- the HRA point estimate (total mean failure probability) using THERP,
2- the suggested EF for that probability (from THERP Table 20-20),
3- the calculated mean value from the uncertainty analysis (IRRAS),
4- the calculated EF from the uncertainty analysis,
5- the median value (from IRRAS), and finally,
6- both the 5th and 95th percentile value from the uncertainty analysis.

Table C21: Summary of Results for CE ISLOCA HRA

Seq. #/ Action	Point Est. (THERP)	EF-THERP T20-20	Mean (IRRAS)	EF Calc.	Median (IRRAS)	5th %ile (IRRAS)	95th %ile (IRRAS)
2 - FTD	0.018	5	0.0167	4.26	0.0111	0.0029	0.0472
2 - FTDGN (Proc.)	0.02	5	0.0192	3.96	0.0136	0.0036	0.0540
2 - FTI (Proc.)	1.00						
2 - FTDGN (Know.)	0.39	5	0.3617	2.02	0.3306	0.1656	0.6685
2 - FTI (Know.)	0.019	5	0.0188	2.97	0.0151	0.0051	0.0449
2 - FTDGN (Small Break)	0.016	5	0.016	3.73	0.011	0.0036	0.041
2 - FTI (Small Break)	0.019	5	0.0188	2.97	0.0151	0.0051	0.0449
5 - FTD	0.008	5	0.0074	11.86	0.0025	0.0002	0.0293
5 - FTDGN	0.008	5	0.0074	12.11	0.0024	0.0002	0.0294
5 - FTI (1 Train)	0.02	5	0.0219	2.77	0.0179	0.0072	0.0497
5 -FTI (2 Trains)	0.02	5	0.0219	2.77	0.0179	0.0072	0.0497

Table C21: Summary of Results for CE ISLOCA HRA

Conclusions

The HRA found that operator error could contribute to ISLOCA scenarios. Risk-significant human error initiators were found to be unlikely during normal operations involving interfacing systems. This is due, in part, to the existence of vital administrative procedures and related operator training, as well as the presence of controlled interlocks and procedural guidance which prevent the inadvertent operation of pressure isolation MOVs. The CE HRA analysis also found a significantly higher probability for operator error during detection, diagnosis, and isolation of a LOCA following a break outside containment, as compared to human error initiating actions. This general finding results from an interaction of the following variables:

1 - For Sequence 2, the applicable procedure (OP-902-002) does not provide any guidance for requisite operator action to isolate the break.

2 - For Sequence 2, operator training was focused on scenarios in which operators were directed not to override safety injection actuations. Because of this, the operators' situation awareness may be directed away from required actions to isolate the affected LPSI train (i.e., by closing the appropriate SI flow control valve).

3 - There is a limited amount of time after the sequence initiator, before a break, for the detection, diagnosis, and isolation of ISLOCA before core damage.

4 - Operators are exposed to a higher workload and elevated levels of stress at the time when actions to detect, diagnose, and isolate an ISLOCA are needed.

References

C-1 T. G. Ryan, "A Task Analysis Linked Approach for Integrating the Human Factor in Reliability Assessment of NPP", Reliability Engineering and System Safety, vol. 22, 1988.

C-2 A. Swain and H. Gutman, Handbook of Human Reliability Analysis with Emphasis on Nuclear Power Plant Applications, NUREG/CR-1278, August, 1983.

C-3 G. Hannaman and A. Spurgin, Systematic Human Action Reliability Procedure (SHARP), EPRI NP-3583, 1984.

C-4 R. Hall (ed.), A Guide for General Principles of Human Action Reliability Analysis for Nuclear Power Generation Stations, IEEE Draft Standard P1082/D7, August, 1989.

C-5 U.S. Nuclear Regulatory Commission, Technical Specifications, Docket number 50-382 W3, SES FSAR, January, 1979.

C-6 U.S. Nuclear Regulatory Commission Inspection Report 50-412/90-10 and 50-414/90-10.

C-7 J. Ball, Interfacing System LOCA Inspection Report, Docket number 50-382/90-200, September 14, 1990. U. S. Nuclear Regulatory Commission, Washington, D. C.

C-8 G. Hannaman, A. Spurgin, and Y. Lukic, Human Cognitive Reliability Model for PRA Analysis, NUS-4531, Electric Power Research Institute, 1984.

C-9 K. Russell, M. McKay, M. Sattison, N. Skinner, S. Wood, and D. Rasmuson, Integrated Reliability and Risk Analysis System (ver. 2.5), February, 1991. EG&G Idaho, Inc. Idaho Falls, ID.

C-10 Technical Specification Change Request NPF-38- (Draft), Docket number 50-382.

Appendix D

Use of Constrained Lognormal Distribution in Human Reliability Analysis

Appendix D
Use of Constrained Lognormal Distribution
In Human Reliability Analysis

1. Motivation

As discussed in [D-1], use of a lognormal distribution can sometimes lead to erroneous results when it is used to represent a probability. These problems arise because a probability, which must lie between 0 and 1, is being modeled by a lognormal random variable, whose only constraint is that it take on values ≥ 0; there is no upper limit. One area where this problem sometimes arises is human reliability analysis, or HRA. One of the frequently used tools in HRA is [D-2], also known as THERP. Human reliability analysts use tables of human error probabilities (HEPs) in THERP to obtain median estimates and error factors (HEPs are assumed in THERP to be lognormally distributed), which can be used in an uncertainty analysis. However, THERP will, under some circumstances, provide combinations of medians and error factors which are not meaningful. For example, THERP may recommend the use of a median HEP of 0.5 with an associated error factor of 5, producing a 95th percentile probability greater than unity. The method documented below is one approach to solving this problem.

2. The Constrained Lognormal Distribution

An intuitive approach to solving this problem is suggested in [D-1]. There the authors recommend the use of a constrained lognormal distribution, whose random variate assumes values between 0 and 1. The cumulative distribution function (cdf) of such a random variable is obtained as follows. First, the probability that a lognormal random variable (unconstrained) is less than some value x is given by

$$P(X \leq x) = \Phi\left(\frac{\ln x - \mu}{\sigma}\right) \qquad (1)$$

where μ and σ are the parameters of the distribution and Φ is the cumulative

normal function. Constraining the random variable X to be less than 1 is heuristically equivalent to asking for the conditional probability that X is less than or equal to some value x, given that it is less than or equal to 1. Thus, one has

$$P(X \le x | X \le 1) = \frac{\Phi(\frac{\ln x - \mu}{\sigma})}{\Phi(\frac{-\mu}{\sigma})}, \quad 0 \le x \le 1 \tag{2}$$

$$= 1, \quad x > 1.$$

This expression allows one to calculate percentiles and moments of the distribution. For example, the expected value of X will be given by

$$E(X) = \int_0^1 \frac{\frac{1}{\sqrt{2\pi}\sigma} \exp[-\frac{(\ln x - \mu)^2}{2\sigma^2}]}{\Phi(-\frac{\mu}{\sigma})} dx. \tag{3}$$

This integral, and the integrals for the higher moments, can be evaluated numerically for specific values of μ and σ. This problem of truncating the probability values can also be approached through a transformation of variables process as described in the next section.

3. A Transformation of Variables Approach

Section 2 presented a somewhat heuristic approach to constraining the THERP HEPs. This section presents an alternative approach. One starts by defining a transformation of variables that will restrict the unconstrained lognormal random variable to lie between 0 and 1. If Y is a random variable that is lognormally distributed with parameters μ and σ^2, denoted $Y \sim \Lambda(\mu,\sigma^2)$, then the random variable X, defined by the transformation

$$Y = \frac{X - \tau}{\theta - X} \tag{4}$$

will be a truncated lognormal random variable constrained to values between τ and θ [D-4]. In the present case one wants X to take on values between 0 and 1, so the transformation becomes

$$Y = \frac{X}{1-X}. \tag{5}$$

This is a one-to-one transformation from X onto Y with a Jacobian given by

$$J = \frac{1}{(1-X)^2}. \tag{6}$$

The pdf of Y is

$$g(y) = \frac{1}{\sqrt{2\pi}\sigma y}\exp\left[-\frac{(\ln y-\mu)^2}{2\sigma^2}\right]. \tag{7}$$

Therefore, the pdf of X is given by

$$\begin{aligned} f(x) &= \frac{1}{\sqrt{2\pi}\sigma\left(\frac{x}{1-x}\right)}\exp\left[-\frac{\left[\ln\left(\frac{x}{1-x}\right)-\mu\right]^2}{2\sigma^2}\right]\frac{1}{(1-x)^2} \\ &= \frac{1}{\sqrt{2\pi}\sigma x(1-x)}\exp\left[-\frac{\left[\ln\left(\frac{x}{1-x}\right)-\mu\right]^2}{2\sigma^2}\right]. \end{aligned} \tag{8}$$

The graph of f(x) is shown in the figure below.

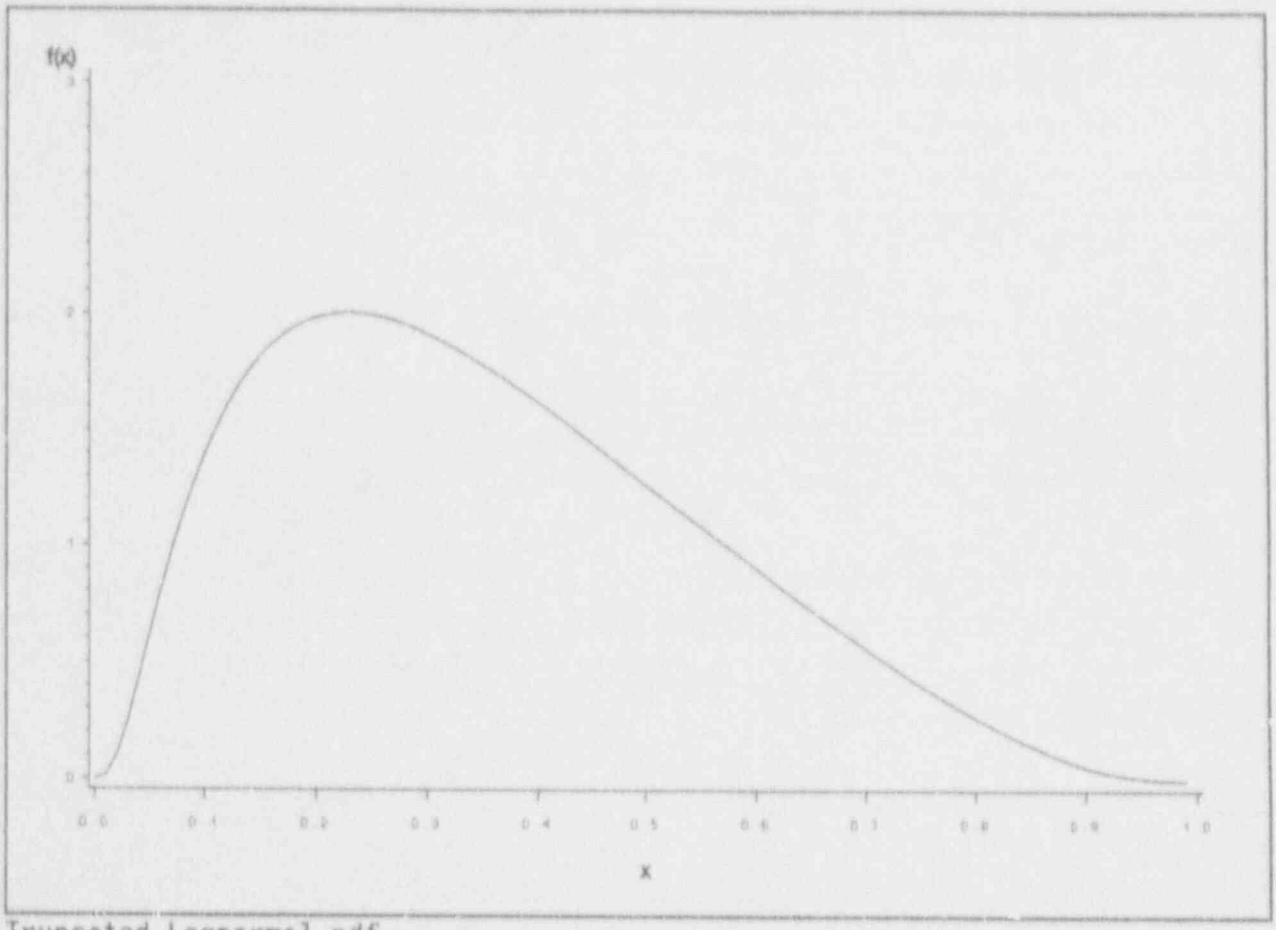

Truncated Lognormal pdf

No simple analytic expression for the mean value of this distribution exists (see [D-3] for the exact result). However, the expression for the expected value of X can be integrated numerically without difficulty, or tables in [D-3] can be used to approximate the mean, skewness, and kurtosis. The resulting mean value for this example (median = 0.5, error factor = 5) is $E(X) = 0.36$.

The percentiles of this distribution can be found by integrating the pdf as follows. Let x_p be the value of X such that $P(X \leq x_p) = p$. One has

$$P(X \le x_p) = \int_0^{x_p} \frac{1}{\sqrt{2\pi}\sigma x(1-x)} \exp\left[-\frac{\left[\ln\left(\frac{x}{1-x}\right)-\mu\right]^2}{2\sigma^2}\right] dx \qquad (9)$$

$$= \Phi\left[\frac{\ln\left(\frac{x_p}{1-x_p}\right)-\mu}{\sigma}\right].$$

The integral was evaluated by making the substitution

$$z = \ln\left(\frac{x}{1-x}\right). \qquad (10)$$

One can compare percentiles obtained from (9) to those from (2). Using (9), one finds that the median value of X is 0.33, compared with 0.37 calculated with (2). Thus, the percentiles obtained with (2) are somewhat conservative relative to the percentiles obtained with (9).[1]

Some might question the use of a (truncated) lognormal distribution; a beta distribution, in which the random variable is constrained, a priori, to lie between 0 and 1 might seem more appropriate. In answer to this potential objection the authors show in the following paragraphs that the truncated lognormal distribution <u>is</u> a beta distribution, so any possible objection on this basis is simply a question of terminology.

The "proof" utilizes a Pearson plot [D-5] of β_2 vs. β_1 where β_1 and β_2 are measures of skewness and kurtosis, respectively. They are defined by

$$\sqrt{\beta_1} = \frac{E[X-E(X)]^3}{[Var(X)]^{\frac{3}{2}}} \qquad (11)$$

---

[1]The reason the distribution functions, and hence the percentiles, are different is because the random variable defined in this section is different from the random variable defined in Section 2. The cdf of a random variable is unique; therefore, the conditional cdf in Section 2 will differ from the cdf of the constrained random variable defined in Section 3.

and

$$\beta_2 = \frac{E[X-E(X)]^4}{[Var(X)]^2}. \tag{12}$$

The third and fourth moments of X about its mean that are required for these calculations were obtained by numerical integration (they could also be found from tables given in [D-3]). One finds that

$$\sqrt{\beta_1} = 0.50 \tag{13}$$

and

$$\beta_2 = 2.50. \tag{14}$$

Plotting β_1 and β_2 shows that the truncated lognormal distribution is indeed a beta distribution.

Since uncertainty analysis software typically does not allow the use of a truncated lognormal distribution, but does allow use of a beta distribution, the following paragraphs will show how to estimate the beta distribution parameters using the mean and variance of the truncated lognormal distribution.

First, recall that the pdf of a beta-distributed random variable X is given by

$$f(x) = \frac{x^{\alpha-1}(1-x)^{\beta-1}}{B(\alpha,\beta)} \tag{15}$$

$$for \quad 0 \le x \le 1$$

where $B(\alpha,\beta)$ is the beta function, defined as

$$B(\alpha,\beta) = \int_0^1 x^{\alpha-1}(1-x)^{\beta-1}dx$$

$$= \frac{\Gamma(\alpha)\Gamma'\beta)}{\Gamma(\alpha+\beta)}. \qquad (16)$$

$$\Gamma(\alpha) = \int_0^\infty x^{\alpha-1}e^{-x}dx.$$

It can be shown that the mean and variance of X are related to the parameters of the beta distribution by

$$E(X) = \frac{\alpha}{\alpha+\beta} \qquad (17)$$

and

$$Var(X) = \frac{\alpha\beta}{(\alpha+\beta+1)(\alpha+\beta)^2}. \qquad (18)$$

By integrating numerically, or using the tables in [D-3], one finds that E(X) = 0.36 and Var(X) = 0.04. This gives two equations in two unknowns, which can be solved to find α = 1.88 and β = 3.36. These parameters are then used to specify the beta distribution in the uncertainty analysis software. The graph on the next page compares the beta and truncated lognormal pdfs. Note that the method of moments does not produce an exact fit. However, the fit is judged to be sufficient for the purposes of this analysis.

One can generalize these results, as Johnson has done [D-3]. The truncated lognormal distribution is really a special case of the bounded Johnson distribution defined in [D-3]. Johnson shows that the random variable defined by

$$Z = \gamma + \delta \ln\left(\frac{X-\epsilon}{\lambda+\epsilon-X}\right) \qquad (19)$$

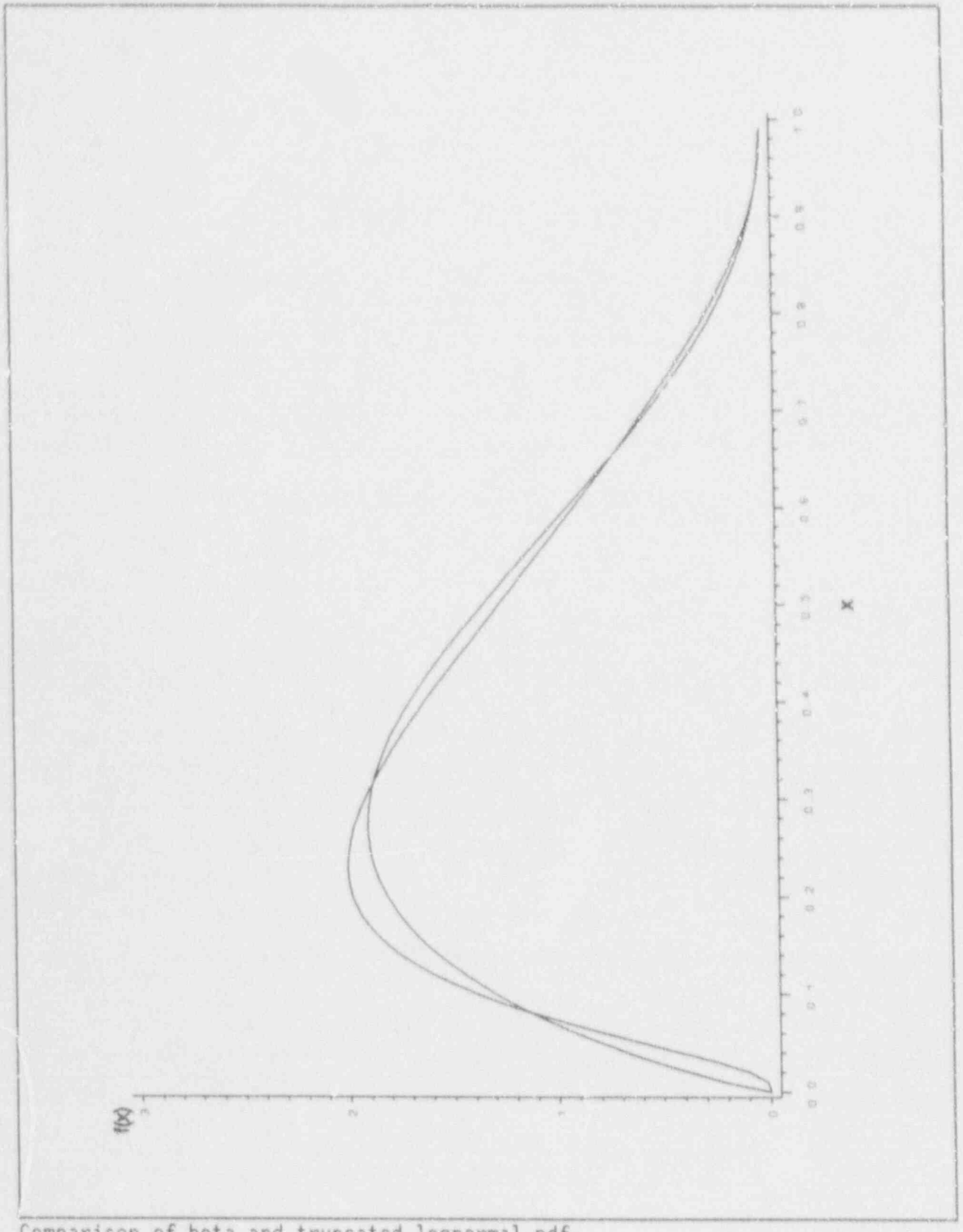

Comparison of beta and truncated lognormal pdfs

where

$$Y = \frac{X-\epsilon}{\lambda+\epsilon-X} \sim \Lambda\left(\frac{-\gamma}{\delta}, \frac{1}{\delta^2}\right) \tag{20}$$

has a standard normal distribution. The pdf of X is given by

$$f(x) = \frac{\delta\lambda}{\sqrt{2\pi}(\lambda+\epsilon-x)(x-\epsilon)} \exp\left\{-\frac{1}{2}\left[\gamma+\delta\ln\frac{x-\epsilon}{\lambda+\epsilon-x}\right]^2\right\} \tag{21}$$

for $\epsilon \leq x \leq \epsilon+\lambda$. In this particular case, one has $\epsilon=0$, $\lambda=1$, $\delta=\sigma^{-1}$, and $\gamma=-\mu/\sigma$. Johnson also shows in [D-3] that β_1 and β_2 lie between the lognormal line and the line $\beta_2 - \beta_1 - 1 = 0$ on a Pearson plot. This is precisely the region that encompasses the beta distribution (note that the beta distribution is a Type I Pearson distribution), so one has an alternative demonstration that the so-called truncated lognormal distribution is really a beta distribution. In addition, the distribution is skewed to the right because, as is shown in [D-3], positive values of γ correspond to positive skewness. Positive skewness is desirable as it reflects the lognormality of the data in THERP.

Another potential approach to constraining the range of the random variable would be to retain the unconstrained median value from THERP but reduce the error factor so that the 95th percentile probability is unity. However, this is an *ad hoc* approach which does not give consistent, justifiable results in all cases. In addition, for median values greater than about 0.5, retaining the unconstrained median gives a very drastic reduction in the coefficient of variation (ratio of the standard deviation to the mean), implying far more knowledge of the range of values about the mean than is justified (i.e., a reduction in the uncertainty, perhaps leading to an underestimation of the contribution of this variable to overall sequence uncertainty). This is shown graphically in the attached figures, which illustrate probability density functions for three cases

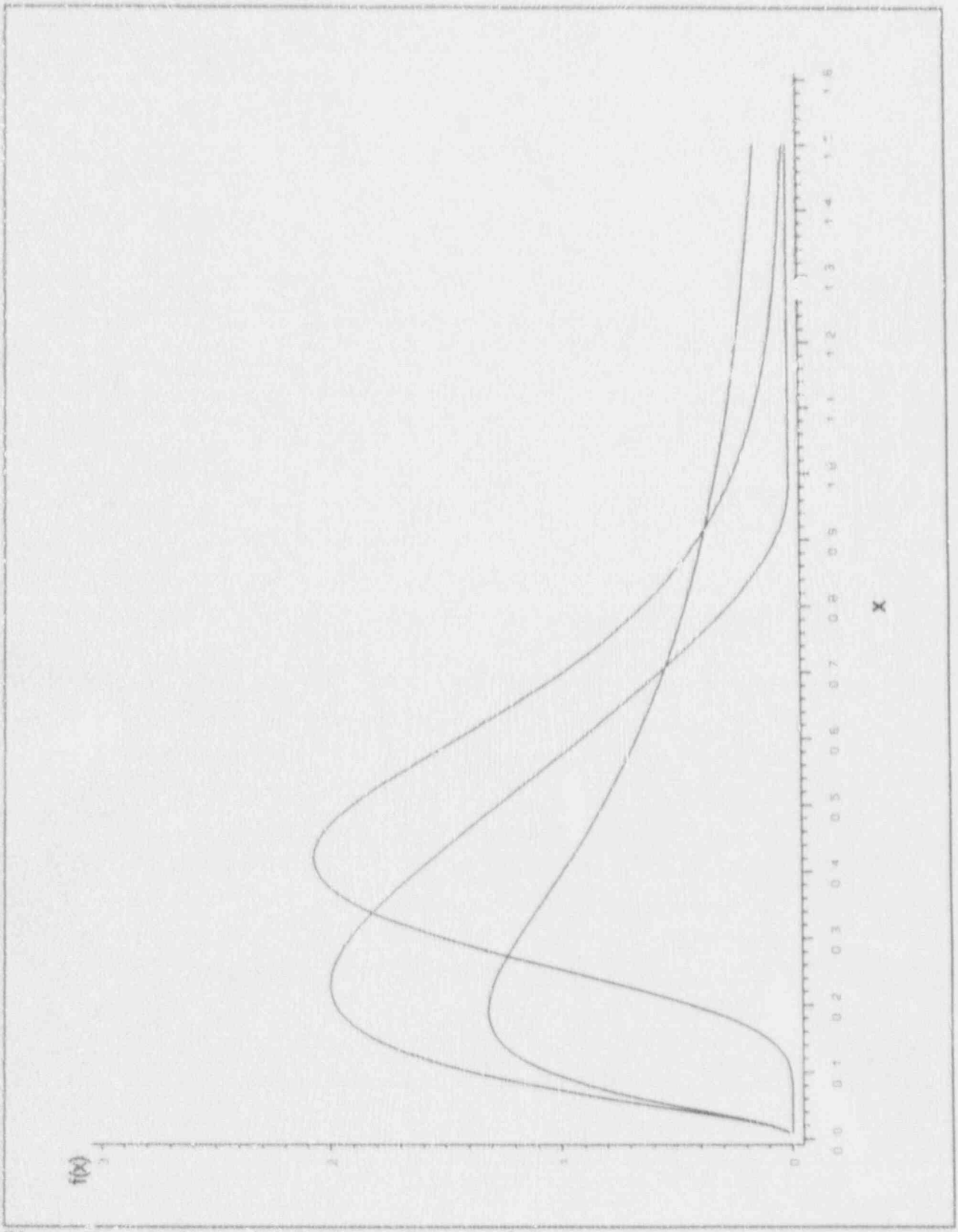

Figure 3 Median of 0.5, Error Factor of 5

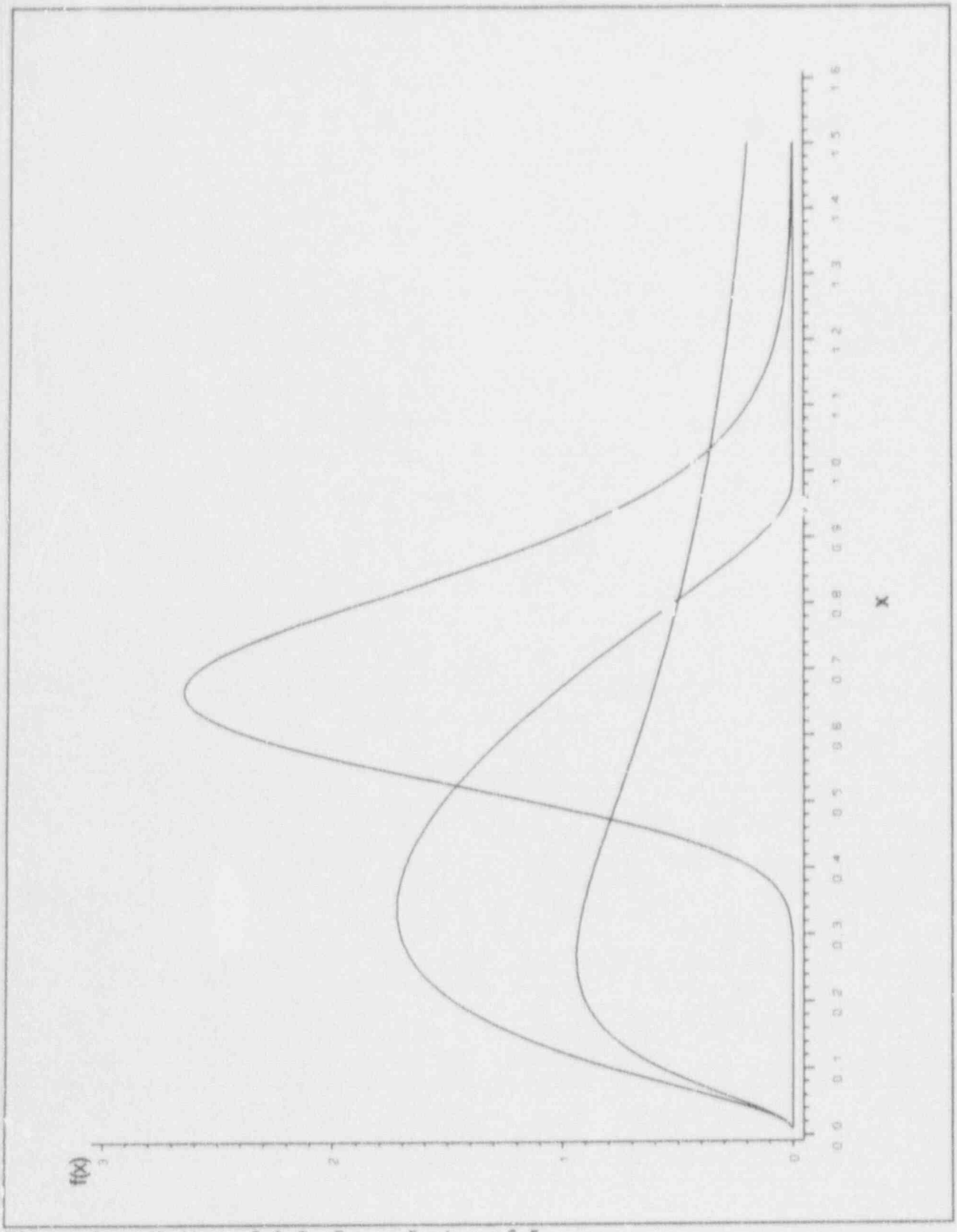

Figure 4 Median of 0.7, Error Factor of 5

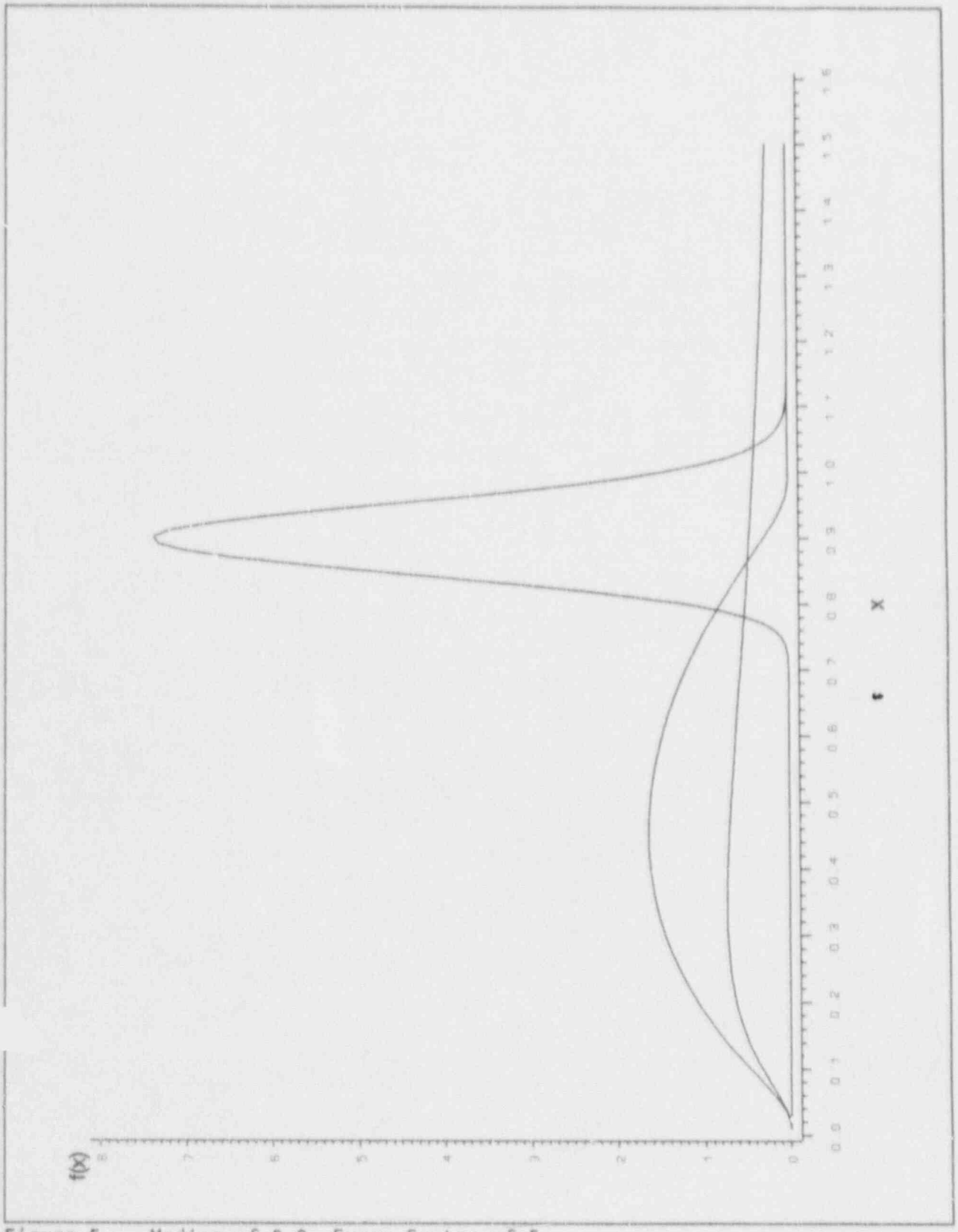

Figure 5 Median of 0.9, Error Factor of 5

4. Approximating the Constrained Distribution

Because of limitations in the software used for the uncertainty analysis, the basic approach will be to obtain percentiles of the constrained distribution using (8), then use an unconstrained distribution passing through these points to estimate the constrained mean. An example of this is shown below.

Assume that THERP has provided a median HEP of 0.5 with an associated error factor of 5. This value is constrained to be less than 1 as follows. First, one needs to find the parameters, μ and σ, of the unconstrained distribution. These are obtained from

$$\mu = \ln X_{0.5} \tag{22}$$

and

$$\sigma = \frac{\ln EF}{1.645}. \tag{23}$$

Using the values of 0.5 and 5, one finds that $\mu = -0.693$ and $\sigma = 0.978$.

Next use (8) to find the 50th and 95th percentiles of the constrained distribution. Solving for x in (8), and denoting constrained values of X by X^*, one finds that $X^*_{0.5} = 0.334$ and $X^*_{0.95} = 0.714$. The constrained error factor is then 2.14.

Now find the unconstrained lognormal distribution that passes through these percentiles. Using (21) and (22), one obtains $\mu' = -1.097$ and $\sigma' = 0.462$. The mean of this distribution is given by

$$E(X') = \exp(\mu' + \frac{\sigma'^2}{2}) \tag{24}$$

$$= 0.37.$$

To repeat, this is the mean of an unconstrained lognormal distribution passing

through the median and 95th percentile of the constrained distribution. Because the new unconstrained distribution includes values of the random variable that are greater than 1, the mean of this distribution is somewhat greater than the mean of the constrained distribution (0.36), so the estimate is somewhat conservative.

As a check, one can calculate the probability that the new unconstrained random variable is greater than 1. This is given by

$$P(X'>1) = 1 - P(X'\leq 1) = 1 - \Phi\left(\frac{1-\mu'}{\sigma'}\right)$$
$$\approx 0.99 \qquad (25)$$
$$= 0.01.$$

This provides some confidence that the unconstrained estimate of the mean is reasonably close to the true constrained mean.

The three distributions utilized in the analysis are shown in the following figure.

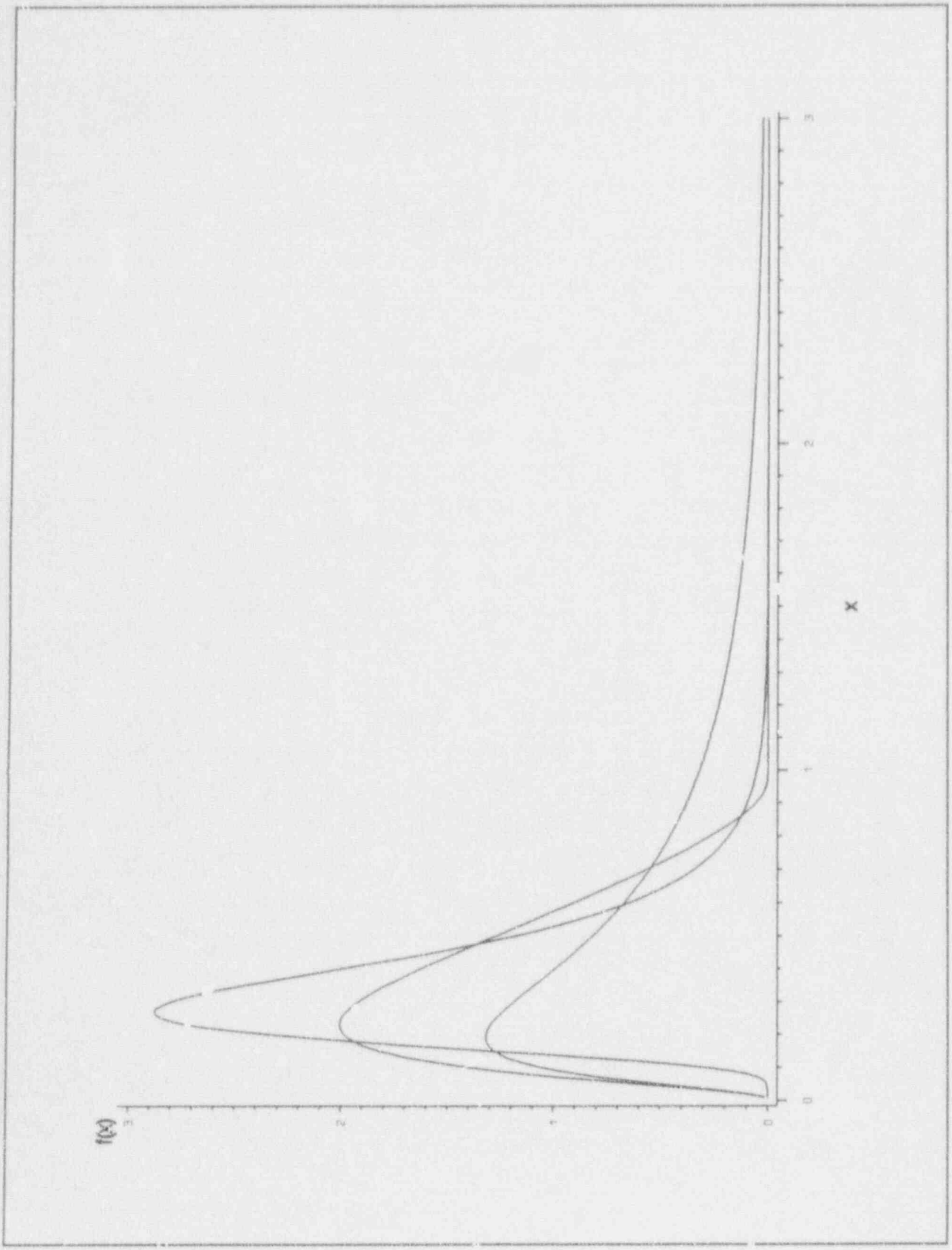
M(x)
x
0
1
2
3
0
1
2
3

5. Conclusions

The use of a truncated lognormal (beta or bounded Johnson) distribution would appear to be a reasonable way to deal with situations in which THERP produces a credible best estimate HEP but provides an uncertainty range that is not meaningful. For calculational ease, one can utilize the unconstrained lognormal approximation to this distribution or, if more rigor is desired and resources are available to do the necessary calculations, one can use the truncated lognormal distribution directly to propagate uncertainties.

The method is based on the assumption that the HEPs in THERP are lognormally distributed (i.e., positively skewed) over the range where data is available for estimation. Using a truncated lognormal distribution (i.e, a beta distribution in which both parameters are greater than 1) preserves the general lognormal shape (i.e., positive skewness) and is therefore compatible with the assumptions in THERP regarding lognormality.

An alternative approach would be to retain the unconstrained median value from THERP but adjust the error factor so that the majority of the distribution lies to the left of 1. This approach has the advantage of being simple to implement. It also leaves the original median value unchanged. This approach does reduce the mean value, but not by quite as much as using the bounded Johnson distribution. The principal objection to this approach is that it leaves the range of the random variable unbounded. Of course, one can make the probability that the random variable assumes values greater than one as small as desired by suitable choice of an error factor; however, there is an accompanying decrease in the coefficient of variation, which is undesirable. The authors' preference is for a more rigorous method.

The method of transforming variables is felt to be desirable because it retains the order-of-magnitude point estimate implied by the original median value. In the case of human error probabilities from THERP, more than order-of-magnitude accuracy is not implied (e.g., 0.01 - 0.1, 0.1 - 1). The method also maintains the positive skewness of the original lognormal distribution, but employs a random variable whose range is restricted, *a priori*, to values

between 0 and 1.

Finally, the authors feel that the constrained lognormal distribution is a natural model for cases where the random variable being modeled represents a probability, and the values of the variable are skewed to the right (mean > median). For actual empirically derived data, the maximum likelihood method for estimating the distribution parameters is tractable and provides minimum variance unbiased estimators. Therefore, fitting a constrained lognormal distribution to probability data (e.g., observed human error rates) is no more difficult than fitting an unconstrained lognormal distribution. However, the constrained lognormal distribution will produce a reasonable uncertainty range, even for median probabilities well above 0.1, for which an unconstrained lognormal distribution is really not an appropriate model.

References

D-1. G. Apostolakis and S. Kaplan, "Pitfalls In Risk Calculations," Reliability Engineering 2 1981, pp. 135- 45.

D-2. A. Swain and H. Gutman, *Handbook of Human Reliability Analysis with Emphasis on Nuclear Power Plant Applications*, NUREG/CR-1278, August 1983.

D-3. N. L. Johnson, "Systems of Frequency Curves Generated by Methods of Translation," Biometrika 36, 1949, p. 149.

D-4. J. Aitchison and J. A. C. Brown, *The Lognormal Distribution With Special Reference To Its Uses In Economics*, Cambridge University Press, 1957.

D-5. G. J. Hahn and S. S. Shapiro, *Statistical Models In Engineering*, John Wiley & Sons, Inc., 1968.

Appendix E

Core Uncovery Timing Calculations

Appendix E

Large Break ISLOCA Core Uncovery calculation for a CE PWR

E.1 INTRODUCTION

This appendix documents the bounding calculation used to estimate the time for the onset of core uncovery for a large break interfacing system LOCA (ISLOCA) sequence. This accident sequence was applied to a CE PWR rated at a core power of 3390 Mw. In particular, the core uncovery time estimate was made after ECCS pump suction was lost from the refueling water storage pool (RWSP). It is possible that core uncovery may occur prior to losing suction to the RWSP, but this issue was not addressed in this document. The uncovery time is defined as the time at which the collapsed vessel liquid level will drop below the top of the core fuel rods. The break was assumed to be outside of containment on one of the LPI injection lines; was approximated as an equivalent (30 % of an 8 inch break) primary system break. Large break LOCA assumptions were made; including the assumption that the remaining ECCS trains would immediately reach their rated runout values, and that RCS pressure feed back from decay and piping stored energy would not significantly perturb the ECCS injection rates. The *Mathematica* computer code was used to do the numerical calculations presented in the following analysis.

E.2 Estimate of time to lose ECCS

This section presents a time estimate to lose suction from the RWSP. A time correction was added to this estimate to account for the presence of SIT injection. This time correction is believed to be very conservative. A number of assumptions were incorporated into the suction loss time estimate and included:

• The ECCS water supply was limited to 443,000 gal with a nominal density of 62 lbm/ft^3.

• The SIT's were available and the corresponding delay time contribution to core uncovery was estimated by dividing the total ECCS pump runout flow rate by the total volume of the SIT liquid inventory.

• It was assumed that the transient is initiated at 100 % power conditions and that the reactor was immediately scramed.

• Three HPI, three charging pumps, and one LPI were available to recover the primary system. The run-out rate for each HPI equals 910 gpm and for the LPI 5500 gpm. The charging pumps were rated at 42 gpm.

• The RCS depressurization was large enough to cause all ECCS pumps to immediately transition to their run-out injection rates.

The following variables were defined:

Tank = is the mass of the RWSP tank in lbm

RUNOUTFLOW = is the total ECCS run out flow rate

TIME1 =is the time in hours for the RWSP to empty

Equating the ECCS runout rate to the break flow rate, the estimated time to empty the RWSP is calculated as follows:

Tank= 443000. GAL * .1337 ft^3/GAL * 62.0 lbm/ft^3

RUNOUTFLOW= (3*910.+ 3*42. +5500.)*62.0*.002228 lbm/sec

TIME = Tank/RUNOUTFLOW

TIME1=TIME/(3600. SEC/hr) (*time to empty RWSP in hr*)

time to empty RWSP = 0.883729 hr

Sources of uncertainty in this estimate are as follows:

• The ECCS injection rates will not immediately relate to their rated run out discharge rates.

•There is some uncertainty in the known ECCS pump run out mass flow rates.

•The simultaneous use of 3 HPI pumps is an off normal configuration. Generally only two pumps are in operation. It was judged that the assumption of 3 pumps in operation is conservative.

•SIT injection may temporarily alter the RCS pressurization response and reduce LPI flow.

• Primary to secondary heat transfer may also induce RCS pressure feed back that could reduce ECCS injection flows.

•Flooding the auxiliary building may disrupt or destroy the ECCS pumping equipment before the RWSP tank is empty.

An additional time correction to core uncovery was made for the loop safety injection tanks (SIT's). The minimum liquid volume of each SIT equals 1679 ft^3 which is representative of some CE plants. We will assume that one SIT empties directly out the break and will not contribute to delaying core uncovery. Once the accumulators are activated we will assume that they empty at an average rate equal to the total run-out rate of all the ECCS pumps. As the accumulators empty, it is assumed an equal amount of liquid is forced out the break. Hence, the actual dwell time for the accumulator liquid in the RCS is equated with the accumulator injection time. This assumption is conservative since this time scale is shown to be small. In order to make the dwell time estimate, which is equated with the time correction, we define the following variables:

SITVOL = the total liquid volume of the SIT 's

TIME = the estimated time for the SIT's to drain in hours

SITVOL= 3*1679. ft^3 (*total SIT liquid volume *)

TIME2 = (SITVOL/RUNOUTFLOW)*(62.0 lbm/ft^3)/(3600. SEC/hr)

additional delay time = 0.075 hr

TIME3 = TIME1+TIME2

effective time to lose ECCS = 0.959 hr

Therefore the time to lose ECCS is approximately one hour.

E.3 Estimate of core uncovery time

The remainder of this narrative will detail how the time to core uncovery was calculated. This time is referenced to the beginning of the transient. In order to estimate the uncovery time the following assumptions were made:

• No credit for cooling is given to any possible liquid remaining in the reactor coolant loops. This assumption is conservative since after the RWSP has drained some liquid in the primary loops will drain back into the vessel region. Unless a full scale systems calculation is done, there is no way of making a reliable estimate of how much liquid would actually drain into the vessel and help extend the time to core uncovery.

• It was assumed that the vessel upper head and upper plenum region above the loops are completely voided by the time the RWSP has emptied. This assumption is reasonable since most PWR large break LOCA scenarios lead to voiding in these regions.

• At the instant ECCS is lost it was assumed that the partially filled vessel is at bulk subcooled conditions of 100 F and 20 psia. The assumed vessel liquid temperature is not based on rigorous quantitative arguments. Unless a full scale simulation is performed to model the ECCS/vessel liquid mixing dynamics it is not clear that an exact pressure and bulk temperature can be easily defined.

• Assumed vessel volume distributions are based on a Westinghouse 3411 MW 4-loop plant. Volume data for a 3390 MW CE plant were not available. However, since the power levels of these two system are close, it is expected that the volume scaling will also be very similar.

Using steam table data the following variables are defined:

hl20 = the enthalpy of the subcooled vessel liquid at 20 psia, 100F.

hls20 = the saturation enthalpy of the vessel liquid at 20 psia, 100 F.

rho = the bulk density of the liquid at 100 F.

VOLREMAIN = the volume of the reactor vessel minus the regions above the hot and cold legs. This volume was estimated to be 3300 ft^3.

TOTALEN1 = the total sensible heat needed to heat the reactor vessel coolant from subcooled to liquid saturated conditions.

The above variable definitions were used to estimate the time to reach bulk saturation conditions. Some uncertainty exists here, since temperature gradients may result in non-uniform heating, leading to significant heat up of the core liquid, with the liquid in the lower plenum remaining relatively cool.

hl20 = 68.04 btu/lbm

hls20 = 196.3 btu/lbm

rho=62. (lbm/ft^3)

VOLREMAIN= 3300. ft^3

TOTALEN1= rho*(hls20-hl20)*VOLREMAIN*1055. J/btu

sensible heat need to reach saturation = 2.769 10^{10} J

Additional energy added to the vessel liquid is assumed to result in liquid vaporization. In order to initiate core voiding, all the liquid above the core is assumed to be vaporized. From an actual physics standpoint, bulk boiling in the vessel will cause core voiding before

the liquid in the upper plenum is boiled off. This will not be of concern because the core mixture level will still be above the fuel rod region. The total energy needed to vaporize the liquid region above the fuel rods is equated to the energy needed to vaporize the saturated liquid in the upper plenum. To complete this energy balance calculation the following variables are defined.

volvap = the remaining upper plenum volume of saturated liquid to be vaporized.

deltah =the latent heat change

rhosat = the liquid saturation density

TOTALEN2 = the total energy needed for upper plenum vaporization.

With the appropriate substitutions and units changes we have:

volvap= 857. ft^3

deltah = (1156.3-196.3) btu/lbm

rhosat = 59.4 lbm/ft^3

TOTALEN2= volvap*deltah*rhosat*1055. J/btu

energy to boiloff liquid in upper plenum = 5.156 10^{19} J

Therefore, the total energy needed to initiate core uncovery becomes:

TOTE = (TOTALEN1 + TOTALEN2) = 7.92 10^{10} J

This analysis used a core decay response which approximates an ANS decay power response for a reactor with an infinite operation period. The normalized decay rates are given as follows:

Time(s)	Normalized Power
100.	.0331
400.	.0235
800.	.0196
1000.	.0185
2000.	.0157

4000.	.0128
8000.	.0105
10000.	.00965
20000.	.00795
60000.	.00566
100000.	.00475

Using the above data, we shall define **decay(t)** as the normalized core decay power. The expression **decay(t)** was calculated as a polynomial function of time using supplied Mathematica curve fit routines. The expression for the normalized power was approximated as:

$$\textbf{decay(t)} = 0.01590 - 8.75\ 10^{-7}\ t + 2.5*10^{-11}\ t^2$$

Note that **decay(t)** is a good approximation in the range 4000-10000 sec, and becomes progressively less accurate outside of this time interval.

To do the energy balance formulation the total integrated core decay power between the time **TIME3** and some unknown time **t** was equated to the total energy **TOTE** needed for core uncovery. Recall that the core scram was coincident with beginning of the transient and that **TIME3** is the time at which ECCS cooling has ended. To calculate the core decay power the normalized power function **decay(t)** is multiplied by the initial core power. The nominal 100 % power for the CE plant in this analysis is 3390 Mw. The energy balance formulation was written as follows:

$$TOTE = P \int_{TIME3}^{t} decay(t)dt$$

Where **P** is the initial core power. Using the appropriate numerical and symbolic algorithms supplied with Mathematica and making the correct units changes, the uncovery time solution is **t= 1.476 hr.**

Appendix F

Calculation of System Rupture Probability

Appendix F
Calculation of System Rupture Probability

Interfacing system rupture probability is calculated from system pressure and component fragility data. The component fragility data are obtained from structural analyses performed by the ABB Impell Corporation (see Appendix H). The following sections describe the component fragility data, and the methods used to calculate rupture probabilities. The first section describes the system pressure data. This is followed by a description of the component pressure fragility data and limiting assumptions. Then the individual component failure probability calculations are described, followed by the method used to obtain the system rupture probability from the individual failure probabilities.

SYSTEM PRESSURE

Interfacing system rupture probabilities are required for the event trees in Appendix B. Two significant sequences survived the screening process. These are Sequences 2 and 5. Sequence 2 involves pressurization of the low pressure safety injection (LPSI) system to normal operating reactor coolant system (RCS) pressure as a result of failure of the isolation check valves and opening of the isolation MOV during quarterly stroke-testing. Pressure relief valves in the LPSI pump discharge lines have very small capacities (5 gpm each). Therefore, the discharge piping will rapidly pressurize to the cold leg pressure of 2306 psig. Table F.1 provides a list of the low-pressure rated components that will be subjected to RCS pressures.

In Sequence 5 the operators enter shutdown cooling as per procedure, and valves SI-401, SI-405, and SI-407 are opened while the plant is at ~400 psig and 350° F. Note that this is a conservative assumption; the entry into shutdown cooling may be made at lower pressures and temperatures, but these are the maximum allowable by procedure. If check valves SI-108 and SI-1071 fail to seat, 150 psig-rated piping and components will be subjected to higher-than-design pressure. The components that may fail as a result are listed in Table F.1.

COMPONENT PRESSURE FRAGILITY DATA

The pressure capacities for each type of component in the interfacing systems have been evaluated by the ABB Impell Corporation (see Appendix H). The pressure capacities for these component types have been developed under the assumption of quasi-steady state pressure conditions. While a variety of analytical techniques have been used to obtain pressure fragility data for the above components, they all are expressed as follows:

$$P = \hat{P} * M * S \qquad (1)$$

where

$\hat{P}$ = the component median pressure capacity

M = a lognormally distributed random variable having unit median and a logarithmic standard deviation, β_m, representing modeling uncertainties

S = a lognormally distributed random variable having unit median and a logarithmic standard deviation, β_s, representing material property uncertainties

The random variable P is lognormally distributed with logarithmic standard deviation β_c. In the tabulations provided in Appendix H, the separate uncertainty parameters, β_m and β_s, are not routinely provided. Instead one composite value, β_c, is used to represent both kinds of uncertainty, where β_c is given by

$$\beta_c = \sqrt{\beta_m^2 + \beta_c^2}.$$

The component pressure capacities and uncertainty parameters from Appendix H are summarized in Table F.1. Application of the above data for determining system failure probabilities requires some understanding of the failure modes represented. The following discussions provide a summary of the important failure modes and data limitations.

Piping

Piping failure is assumed to result when pressure-induced hoop stress in the unflawed pipe causes failure strain to be reached. Variability in the

Table F-1. LPSI system component pressure capacity data

Component	Med. Fail. Pressure	Mean Fail Pressure	Ln Mean	Ln Std. Dev.	Error Factor	A P(A)=.001
Sequence 2	at 600° F.					
Flange - 10 inch, 300 psi	1888	2150	7.543	0.41	1.96	529.7
Piping - 6 inch sched. 40s	3790	4044	8.240	0.36	1.81	1241.6
Piping - 8 inch sched. 40s	3345	3569	8.115	0.36	1.81	1095.8
Piping - 10 inch sched. 40s	3044	3248	8.021	0.36	1.81	997.2
Sequence 5	at 400° F.					
Flange - 10 inch 150 psi flange	941	949	6.855	0.13	1.24	628.9
Flange - 24 inch 150 psi flange	640	646	6.471	0.13	1.24	427.7
Piping - 10 inch sched. 40s piping	3271	3490	8.093	0.36	1.81	1071.5
Piping - 14 inch sched. 30 piping	2545	2715	7.842	0.36	1.81	833.7
Piping - 20 inch sched. 20 piping	1752	1869	7.469	0.36	1.81	573.9
Piping - 24 inch sched. 20 piping	1450	1547	7.279	0.36	1.81	475.0

pressure stress results from many factors, such as variability in material strength and wall thickness. Most important among these factors is the existence, size, and orientation of preexisting flaws or cracks in the piping system. Data on these factors are not currently available, so Impell has developed variability data for the lognormal pressure capacity distribution by assuming that there is a failure probability of 0.001 at the yield stress of the piping. This implies that the probability of existence of a large flaw is 0.001. The authors of the Impell report believe this may be an overly conservative assumption and recommend that this assumption should be reevaluated if it is found that a significant contribution to risk occurs from pipe rupture at pressures well below the median burst pressure.

The data provided in Table F.1 include no allowance for the number of feet of piping in the system. The data are also dependent on both the degree to which piping has been corroded and on the temperature to which the piping is exposed. In this analysis, a corrosion allowance of 0.020 in. is used. System temperature is, however, time-dependent, with the lowest temperatures occurring before peak pressure is reached. Since failure pressures generally decrease with increasing temperature, it is conservative to assume a higher temperature than is expected at peak pressure. In this analysis, a system temperature of 600° F. is used in Sequence 2, 400° F. in Sequence 5.

Flanges

The flanges subject to overpressurization in Sequences 2 and 5 are 300 psi-rated 10-inch, and 150 psi-rated 24-inch flanges. The data provided in Appendix H are tabulated according to the initial bolt stress, percent joint relaxation, and bolt yield stress. The initial bolt stress is calculated from data in Table 3-1 of Appendix H, and from the plant's general torquing procedure. Appendix H uses a median initial bolt stress of 25,000 psi, and 25% median joint relaxation. From Table 3-7 in Appendix H, the gross leak pressure (GLP) is found to be 1888 psi. This GLP is a median value for a lognormal distribution with a composite logarithmic standard deviation of 0.12, representing both uncertainty in modeling and data variability.

Similarly, for 24-inch, 150-psi flanges, Appendix H gives a median GLP of 640 psi. For 10-inch, 150-psi flanges, the median GLP is 941 psi.

Leakage from flanged connections can occur at pressures below the GLP. Leak rates for 10-inch, 300-psi flanges are on the order of 1 mg/sec at GLP. For 24-inch flanges, the leak rate at the GLP is approximately 37 mg/sec. Above GLP the flange gasket can separate from the flange surface and significant leak areas can develop. For 10-inch, 300-psi flanges, these leak rates range from 0.03 $in.^2$ at 1.25*GLP to 7.39 $in.^2$ at 2.0*GLP. The corresponding leak rates for 24-inch flanges are 0.05 and 2.79 $in.^2$.

In Sequence 5, flange failures made a negligible contribution to the system rupture probability; therefore, no distinction was made between small and large leaks. In Sequence 2, however, failure of the 10-inch, 300-psi flange at the LPSI discharge flow indicator was a significant contributor to the rupture probability of the interfacing system. In this case, flange failures were grouped into two classes, based on the expected leak area. From Appendix H, at twice the GLP, the leak area is 7.39 in. This is equivalent to a break diameter of slightly more than three inches. Therefore, two times the GLP was used as the criterion for defining a large flange failure. Failures at less than twice the GLP were classified as small leaks, which were judged to be recoverable by the operators in time to prevent core damage (see Appendix C).

In developing the above pressure capacity and leak area data Impell had to make assumptions about the maximum value of the ratio of incremental gasket load to total pressure load. The authors of the Impell report caution that because high strength flange bolts are used at the study plant, some flange inelastic behavior can be expected at higher pressures. This may affect the calculated leak rates. Therefore, they caution that additional study of flange behavior may be required if leakage through flanged connections is found to be a significant contributor to risk.

Valves

Impell postulated three failure modes for valves within the LPSI system. They include failure of the valve body, failure of the stem packing, and failure of the bolted bonnet seal. Impell judged that failure of the valve body would not be likely because the wall thickness of the valve body is greater than the surrounding piping. Packing failure was dismissed because overpressurization would tend to improve the packing seal, and failure, if it were to occur, would result in a negligible leak rate. Failure of the bolted bonnet was considered to be the only credible failure mode for valves but could not be evaluated because the detailed information needed on the bonnet seals was not available. However, it is expected that the fragility of the bonnet seals at the CE plant will be similar to those at the Westinghouse and B&W plants, where all valves affected by overpressurization have large enough leak capacities to justify not including them in the component failure calculations.

One check valve was of particular interest at the CE plant. This was SI-107 (A and B) which prevents reverse flow in the LPSI suction line to the RWSP. This valve is rated to 150 psig, so it could fail in Sequence 5. The failure mode of interest was internal failure that would allow reverse flow into the RWSP. Because detailed information on the dimensions of the internal hinged plates was unavailable, the pressure capacity for this failure mode could not be calculated. However, based on the limited available information, Impell judged that the pressure capacity for this failure mode would be high; therefore, our analysis of Sequence 5 assumed that SI-107 closed on demand, preventing reverse flow to the RWSP.

Calculational Methods

Determination of system rupture probability requires "summing" the probability of component failure over the number of components in the system. The following discussion presents the method used to calculate single component failure probabilities and the resulting system rupture probability.

Convolution

The pressure capacity of a system component is characterized in terms of a random variable P_f, which is assumed to be distributed lognormally with a median and logarithmic standard deviation. The probability density function of P_f is

$$f(p_f) = \frac{1}{\sqrt{2\pi}\beta_c p_f} \exp-\left[\frac{(\ln p_f - \mu_f)^2}{2\beta_c^2}\right]$$

where $P_f \geq 0$ and μ_f is the natural logarithm of the median failure pressure.[1]

The system pressure is characterized in terms of a normally distributed random variable P_s, with a probability density function given by

$$g(p_s) = \frac{1}{\sqrt{2\pi}\sigma_s} \exp-\left[\frac{(p_s-\mu_s)^2}{2\sigma_s^2}\right]$$

where μ_s is the mean (median) system pressure and σ_s is the standard deviation.[2]

A random variable representing the component failure margin is then

---

[1] In the following discussion random variables will be denoted with capital letters and values assumed by random variables will be denoted with lowercase letters, e.g., P_f is the random variable representing failure pressure and p_f represents actual values of the failure pressure.

[2] In Sequence 5, system pressure was characterized by a single value of 400 psig (the distribution is a delta function). This represents a bounding pressure for the calculation of system rupture probability. Because of the extremely low probability of system rupture at this bounding pressure, this simplification is justified.

defined as

$$Z = P_f - P_s.$$

The probability density function of Z is obtained from P_f and P_s, by convolution, as follows

$$h(z) = \int_0^\infty f_{P_s}(p_f - z)\, f_{P_f}(p_f)\, dp_f$$

$$= \int_0^\infty \frac{1}{2\pi\sigma_s\beta_c p_f} e^{-\frac{(p_f - z - \mu_s)^2}{2\sigma_s^2}} e^{-\frac{(\ln p_f - \beta_c)^2}{2\beta_c^2}}\, dp_f.$$

The probability of system failure is obtained by finding the probability that $Z \leq 0$:

$$P(failure) = P(Z \leq 0) = \int_{-\infty}^{0} h(z)\, dz.$$

To simplify the above calculations, the system probability was characterized by a single pressure, rather than a distribution, thus allowing the rupture probability to be calculated by hand.[3] Based on comparison calculations with the full Monte Carlo simulations performed for the previous two ISLOCA analyses, this is a valid approximation. The reason it is valid is that system pressure is defined fairly accurately in the cases of interest here; assigning a standard deviation of 50 psi, as has been done in the previous analyses, does not affect the results significantly.

The probability of system rupture is calculated from the Boolean union of the individual component failure probabilities as expressed in the following equation

---

[3]The system pressure distribution in this case can be described by a delta function.

$$P(\text{component failure}) = \bigcup_{i=1}^{n} P_{f_i}$$

where P_{fi} is the failure probability of the i^{th} component in the system. Assuming the failures to be independent allows us to simplify this equation to

$$P(\text{component failure}) = \bigcup_{i=1}^{n} P_{f_i}$$

$$= 1 - \prod_{i=1}^{n} (1 - P_{f_i}) .$$

Results

The results from the component failure analysis are provided in Tables F.2 and F.3, along with the calculated system rupture probability.

Table F.2 Rupture Probabilities for Sequence 2

Component	Median Failure Pressure (psig)	Rupture Probability**
10-in., sch 40 pipe	3044	0.22
6-in., sch. 40 pipe	3790	0.08
8-in., sch. 40 pipe	3345	0.16
10-in., 300-psi flange	1888	0.12*
System rupture probability		0.47

*This is the probability of a large flange failure. The probability of a small flange failure is 0.57.

**Based on a system pressure of 2306 psig.

Table F.3 Rupture Probabilities for Sequence 5

Component	Median Failure Pressure (psig)	Rupture Probability*
10-in., sch. 40 pipe	3271	negligible
14-in., sch. 30 pipe	2545	negligible
20-in., sch. 20 pipe	1752	negligible
24-in., sch. 20 pipe	1450	negligible
10-in., 150-psi flange	941	negligible
24-in., 150-psi flange	640	negligible
System rupture probability		negligible

*Based on a system pressure of 400 psig.

Appendix G

ISLOCA Consequence Analysis

ISLOCA Consequence Analysis

1.0 INTRODUCTION

This appendix analyzes the effect of decontamination factors (DFs) on the offsite consequences of an ISLOCA accident sequence. The fission product source terms in this analysis are those generated for the Event V accident sequences at the Sequoyah plant for the June 1989 draft of NUREG-1150. In using these ISLOCA accident sequences, source term release information was obtained from the SEQSOR program and partitioned into a small number of source term groups using PARTITION. The consequences of these releases were calculated with the MELCOR Accident Consequence Code System (MACCS), using the Surry plant site input decks developed for the June 1989 draft of NUREG-1150. For this report consequences were calculated for the base case sequences and eight sensitivity studies in which the effect of varying the [illegible]ver a range of values was examined. Two additional sensitivities examined the effect of increasing the release elevation from the base case value of 0.0 m to 10.0 m.

2.0 ISLOCA ACCIDENT SEQUENCE DEFINITION AND SELECTION

In the NUREG-1150 terminology, the ISLOCA sequences at Sequoyah are defined by plant damage state (PDS) Group 4 - V. The accident sequences in this PDS group are initiated by failure of the check valves between the reactor coolant system (RCS) and the low pressure injection system (LPIS). The LPIS is then overpressurized and ruptures, resulting in a release path from the RCS to the auxiliary building, bypassing the containment. For Sequoyah, there are two types of V sequences: wet and dry. For the wet V sequences the fire sprays in the auxiliary building scrub the release. The dry V sequences are not scrubbed by the fire sprays.

The starting point of the analysis in this report was the results obtained from analyzing the Sequoyah V sequence, PDSG 4, accident progression event tree (APET). This APET was analyzed as part of the Containment Performance Improvement (CPI) project studying improvements for the ice condenser containment. Therefore, reanalyzing this APET was not necessary as

the results were readily available. Using the NUREG-1150 methodology, this APET was evaluated 200 times, once for each latin hypercube sample (LHS). Each evaluation or observation resulted in hundreds of different accident sequences. For each observation, the accident sequences were sorted and grouped into a smaller number of similar accident progression bins (APBs). Because the APET analyzed the wet and dry V sequences together, each observation contained both scrubbed (wet) and unscrubbed (dry) APBs. However, for this analysis, the consequences of the wet and dry sequences were calculated separately. Therefore, the APET analysis results were manually edited to separate the dry APBs from the wet APBs. The total number of APBs for all observations was 2,642 and 2,941 for the dry and wet V sequences, respectively. The number of unique APBs over all observations was 42 and 46, respectively. Listings of the unique APBs for the dry and wet V sequences are given in Tables G.1 and G.2. For the sake of brevity, listings of the APBs over all 200 observations are not provided here, but have been stored on magnetic tape and can be made available upon request.

Table G.1 Listing of the unique APBs over all 200 LHS observations for the dry V sequences at Sequoyah.

AHADBCAADAAAAA
AHADBCAADAAAAB
AHADBCAADAABBB
AHADBCAADBAAAA
AHADBCAADBAAAB
AHADBCAADBABBB
AHADBCAADCAAAA
AHADBCAADCAAAB
AHADBCAADCAAAD
AHADBCAADCABBA
AHADBCAADCABBB
AHADBCAADDAAAA
AHADBCAADDAAAB
AHADBCAADDAAAD
AHADBCAADDABBA
AHADBCAADDABBB
AHADBCABDAAAAA
AHADBCABDAAAAB
AHADBCABDAABBB
AHADBCABDBAAAA
AHADBCABDBAAAB
AHADBCABDBABBB
AHADBCABDCAAAA
AHADBCABDCAAAB
AHADBCABDCAAAD
AHADBCABDCABBA
AHADBCABDCABBB
AHADBCABDDAAAA
AHADBCABDDAAAB
AHADBCABDDAAAD
AHADBCABDDABBA
AHADBCABDDABBB
AHADDCAADBBACA
AHADDCAADBBACB
AHADDCAADBBACD
AHADDCAADBBBCA
AHADDCAADBBBCB
AHADDCABDBBACA
AHADDCABDBBACB
AHADDCABDBBACD
AHADDCABDBBBCA
AHADDCABDBBBCB

Table G.2 Listing of the unique APBs over all 200 LHS observations for the wet V sequences at Sequoyah.

BHADBCAADAAAAA
BHADBCAADAAAAB
BHADBCAADAABBA
BHADBCAADAABBB
BHADBCAADBAAAA
BHADBCAADBAAAB
BHADBCAADBABBA
BHADBCAADBABBB
BHADBCAADCAAAA
BHADBCAADCAAAB
BHADBCAADCAAAD
BHADBCAADCABBA
BHADBCAADCABBB
BHADBCAADDAAAA
BHADBCAADDAAAB
BHADBCAADDAAAD
BHADBCAADDABBA
BHADBCAADDABBB
BHADBCABDAAAAA
BHADBCABDAAAAB
BHADBCABDAABBA
BHADBCABDAABBB
BHADBCABDBAAAA
BHADBCABDBAAAB
BHADBCABDBABBA
BHADBCABDBABBB
BHADBCABDCAAAA
BHADBCABDCAAAB
BHADBCABDCAAAD
BHADBCABDCABBA
BHADBCABDCABBB
BHADBCABDDAAAA
BHADBCABDDAAAB
BHADBCABDDAAAD
BHADBCABDDABBA
BHADBCABDDABBB
BHADDCAADBBACA
BHADDCAADBBACB
BHADDCAADBBACD
BHADDCAADBBBCA
BHADDCAADBBBCB
BHADDCABDBBACA
BHADDCABDBBACB
BHADDCABDBBACD
BHADDCABDBBBCA
BHADDCABDBBBCB

3.0 SOURCE TERM ANALYSIS

3.1 Source Term Description

The next step in the consequence analysis was to determine the source term release information for each APB in each observation. The source term for a given bin contains the release fractions for nine radionuclide classes released during the early and late phases of the accident, and additional information about the release timings, the energy of the releases, and the height of the releases. The nine radionuclide classes are: noble gases, iodine, cesium, tellurium, strontium, ruthenium, lanthanum, cerium, and barium.

The source term analysis was performed with the SEQSOR code. SEQSOR is a parametric computer code used to calculate the source terms for each APB in each observation for Sequoyah. In order to study the effect of varying the V sequence DF, minor modifications were made to the SEQSOR source code and its input files. These modifications are described below.

3.2 Decontamination Factors

For the dry V sequences, the base case DF for all release classes had a uniform value of 1.0 and the release elevation was 0.0 m. The sensitivity analysis involved calculating the source terms with uniform-valued DFs of 5, 10, 50, and 100 for all release classes except the noble gases, for which the DF remained at the base case value of 1.0. For the first two calculations, with DFs of 5 and 10, the release elevation remained at the base case value of 0.0 m. For the last two calculations, with DFs of 50 and 100, the release elevation was specified as 10.0 m. For the dry V sequences, the DFs are specified within the SEQSOR code. Therefore, minor code modifications were required to model the DFs used in the sensitivity analyses. A sample of these code modifications is listed in Table G.3 for the dry V sequence with a DF of 5.0. The release elevation parameter is also specified within the SEQSOR code. The SEQSOR code modification required to specify different elevations is listed in Table G.4.

Table G.3 Listing of SEQSOR code modifications for the dry V sequence with DF = 5.0.

Modification 1:

```
C DJP
C     VDF=1.0
      VDF=5.0
C DJP
```

Modification 2:

```
C DJP
C       DFE=1.0
        DFE=5.0
C DJP
```

Modification 3:

```
C DJP
C     FOR V-SEQUENCE WITH WATER:
C     IF(CHH.EQ.'B')THEN
C        DFE=VDF
C        DO 22621 ISP=2,NSP
C              DFL(ISP)=AMAX1(VDF,VPS(ISP))
C2621   CONTINUE
C DJP
C     FOR DRY V-SEQUENCE:
      IF(CHH.EQ.'A')THEN
         DFE=VDF
         DO 22621 ISP=2,NSP
               DFL(ISP)=AMAX1(VDF,VPS(ISP))
22621   CONTINUE
C DJP
```

Table G.4 Listing of SEQSOR code modifications required to specify a release elevation of 10.0 m.

Modification 1:

```
C DJP
C     ELEV = 0.
      ELEV = 10.0
C DJP
```

Table G.5 Distribution VDF for the base case analysis of the wet V sequences as specified in the SEQSOR input file ISTDAT.DAT.

0%	1%	5%	25%	50%	75%	95%	99%	100%
5.1E+03	4.5E+03	4.1E+03	1.3E+02	6.2E+00	3.0E+00	1.8E+00	1.7E+00	1.6E+00

For the wet V sequences, the base case DF was specified as a distribution to be sampled upon. This distribution is input into SEQSOR as the parameter VDF in the SEQSOR input file, ISTDAT.DAT. The distribution VDF is given in Table G.5 for the base case analysis of the wet V sequences. As for the dry V sequences, sensitivity analyses were performed with uniform-valued DFs of 5, 10, 50, and 100 for all release classes except the noble gases, for which the DF remained at the base case value of 1.0. For the first two sensitivity calculations, with DFs of 5 and 10, the release elevation remained at the base case value of 0.0 m. The calculations with DFs of 50 and 100 were performed with the release elevation specified both at the base case value of 0.0 m and at 10.0 m. No SEQSOR code modifications were necessary for these wet V sequences. Instead, the distribution of parameter VDF in the SEQSOR input file ISTDAT.DAT was replaced with a uniform-valued DF.

3.3 Partitioning Into Source Term Groups

Because source terms are calculated for each APB for each observation in the sample (a total of 2,642 and 2,941 source terms for the dry and wet V sequences, respectively), the output from the SEQSOR calculations is quite voluminous and will not be reproduced here. However, this output has been stored on magnetic tape and can be made available upon request. Also, because of the very large number of APBs, performing consequence calculations for each APB is not practicable. Instead, APBs with similar source terms were grouped together using the PARTITION computer program. PARTITION takes the source term information output from SEQSOR and estimates the early and chronic health effects of each source term for each APB. Source terms with similar effects are then grouped together into source term groups. PARTITION is an interactive program and the number of source term groups is specified by the user. The number of source term groups can be further reduced by repooling small source term groups. For the analyses in this report, the final number of source term groups for each sensitivity was 2 except for the base case wet V sequence for which 3 source term groups were used. Table G.6 lists the record of the interactive computer session for the dry V sequence with DF = 5.0 sensitivity.

When the partitioning and repooling is completed, PARTITION creates a single frequency-weighted source term for each source term group. This source term information is then output by PARTITION under the file name MACCS.INP.

4.0 CONSEQUENCE ANALYSIS

A PC version of the MELCOR Accident Consequence Code System Version 1.5.11 (MACCS 1.5.11) was utilized for the consequence analysis. The computer code comprises a single FORTRAN77 program consisting of three basic modules, ATMOS, EARLY, and CHRONC, which are exercised in sequence. This program has been developed for the purpose of evaluating the severe accident consequences at commercial LWR power plants.

Table G.6 Listing of PARTITION interactive computer record for the dry V sequence with DF = 5.0.

```
 DO YOU WANT SUMMARY CONSEQUENCE RESULTS FOR EACH SAMPLE ELEMENT
 (NO PARTITIONING PERFORMED)? (Y OR N)
N

 LIST OF FILES READ FROM PARTITION.INP:
      MASTER BIN LIST FILE =../dry_nbr_mas.kep
      SOURCE TERM WEIGHT FILE =../seqwgt.inp
      SOURCE TERM FILE =../../dry5/release.out
      APB COND PROB FILE =../dry_seq.frq
      PDS FREQ FILE =../temac.lst

 SOURCE TERM FILE CONTAINS SOURCE TERMS WITH  9 RELEASE FRACTIONS

                                    PERCENT OF
                        NUMBER OF   TOTAL WEIGHTED
                       SOURCE TERMS  FREQUENCIES
      EF>0 AND CF>0        2642         100.00
      EF=0 AND CF>0           0           0.00
      EF=0 AND CF=0           0           0.00
      TOTAL                2642         100.00

 FOR EF>0 AND CF>0, RANGE OF X=LOG10(CF)=  3.0140 TO   4.5220
                    RANGE OF Y=LOG10(EF)=  0.8222 TO   1.7031

 <PRESS RETURN TO CONTINUE>

 THE GRID SIZE FOR THE DATA IS DETERMINED BY THE RATIO:
     (MAX VALUE IN A GRID CELL)/(MIN VALUE IN A GRID CELL)
 GRID SIZES CORRESPONDING TO POSSIBLE RATIOS USED WITH THESE
 DATA ARE AS FOLLOWS:

          RATIO          GRID SIZE
       1.34 TO  1.37       7 X 12
       1.38 TO  1.40       7 X 11
       1.41 TO  1.41       6 X 11
       1.42 TO  1.47       6 X 10
       1.48 TO  1.50       6 X  9
       1.51 TO  1.54       5 X  9
       1.55 TO  1.64       5 X  8
       1.65 TO  1.66       5 X  7
       1.67 TO  1.78       4 X  7
       1.79 TO  1.96       4 X  6
       1.97 TO  2.00       3 X  6
       2.01 TO  2.38       3 X  5
       2.39 TO  2.75       3 X  4
       2.76 TO  3.18       2 X  4
       3.19 TO  5.67       2 X  3
       5.68 TO  7.60       2 X  2
       7.61 TO 10.00       1 X  2
```

Table G.6 Continued

```
 SELECT GRID SIZE BY ENTERING DESIRED RATIO
    9.000000
 THE SPECIFIED RATIO PRODUCES A GRID SIZE OF  1 X  2
 IS THIS GRID SIZE ACCEPTABLE?  (Y OR N)
Y

 CELL COUNTS WITHIN THE GRID FOR A TOTAL COUNT OF  2642:

         1      2
     +------+------+
  1  |  681 | 1961 |
     +------+------+

 <PRESS RETURN TO CONTINUE>

 PERCENTAGE OF WEIGHTED FREQUENCIES CONTAINED IN EACH CELL:

         1      2
     +------+------+
  1  |16.12 |83.88 |
     +------+------+

 DO YOU WISH TO POOL THE VALUES IN ANY CELLS WITH
 ADJACENT CELLS?  (Y OR N)
N

 MEAN CF AND EF COORDINATES FOR EACH CELL:

            1              2
         CF    EF       CF    EF
   1    3.39  0.95     4.04  1.35

 FOR EF=0 AND CF>0, RANGE OF X=LOG10(CF)=******** TO ********
 ENTER THE NUMBER OF GROUPS TO BE USED TO PARTITION
 BASED ONLY ON CF    (0 < NUMBER OF GROUPS < 13)
            1

 CELL COUNTS WITHIN THE GRID FOR A TOTAL COUNT OF     0:

         1
     +-------+
  1  |       |
     +-------+

 PERCENTAGE OF WEIGHTED FREQUENCIES CONTAINED IN EACH CELL:

         1
     +-------+
  1  |       |
     +-------+
```

Table G.6 Continued

```
 DO YOU WISH TO POOL THE VALUES IN ANY CELLS WITH
 ADJACENT CELLS?  (Y OR N)
N

 DO YOU WISH TO REDO POOLING? (Y OR N)
N

 ENTER THE EVACUATION ESCAPE TIME (SEC)
    1800.000

 ENTER THE EVACUATION DELAY TIME (SEC)
    7200.000

 DO YOU WISH TO ENTER A SUBGROUP 2 CUTOFF TIME FOLLOWING
 START OF RELEASE 1? (Y OR N)
Y
 ENTER CUTOFF TIME (S)
    3600.000

 DO YOU WISH TO POOL THE SUBGROUP 3 SOURCE TERMS WITH SUBGROUP 4
 SOURCE TERMS? (Y OR N)
Y

 ENTER THE CONDITIONAL PROBABILITY BELOW WHICH
 SUBCELLS WILL BE COMBINED
   0.0000000E+00

 DO YOU WISH TO GENERATE LINE PRINTER PLOTS FOR
 INDIVIDUAL SOURCE TERM PARAMETERS FOR SOURCE TERM
 CELLS AND SUBCELLS?  (Y OR N)
N

 DO YOU WISH TO GENERATE FILE FOR USE IN CALCULATION
 OF PARTIAL CORRELATION COEFFICIENTS?  (Y OR N)
Y
```

Table G.7 Listing of the PARTITION output file MACCS.INP containing the source term information of the source term groups for the dry V sequence with DF = 5.0.

```
SEQSOR SOURCE TERMS FOR MACCS
          9           3
          1           4  2.1082160E-08  0.1612279
  -4799.998       8449.999       1250.000       3649.999       1800.000
   10250.00       21599.99      0.0000000E+00   3699999.      0.9902838
 2.1361155E-02  2.1777147E-02  2.3204859E-03  6.5133086E-04  1.5444255E-04
 3.5504778E-05  1.4072780E-04  7.4236863E-04   169999.9      9.7354446E-03
 2.2498136E-02  9.7113749E-04  1.0220926E-02  4.1008261E-03  4.6844118E-05
 4.1119891E-04  4.2428359E-04  3.1941610E-03
          1  0.0000000E+00  0.0000000E+00  0.0000000E+00
          2  0.0000000E+00  0.0000000E+00  0.0000000E+00
          3  0.0000000E+00  0.0000000E+00  0.0000000E+00
          4  2.1082160E-08   1.000000      0.1612279
  -4799.998       8449.999       1250.000       3649.999       1800.000
   10250.00       21599.99      0.0000000E+00   3699999.      0.9902838
 2.1361155E-02  2.1777147E-02  2.3204859E-03  6.5133086E-04  1.5444255E-04
 3.5504778E-05  1.4072780E-04  7.4236863E-04   169999.9      9.7354446E-03
 2.2498136E-02  9.7113749E-04  1.0220926E-02  4.1008261E-03  4.6844118E-05
 4.1119891E-04  4.2428359E-04  3.1941610E-03
          2           4  1.0967797E-07  0.8387731
  -4800.000       8449.995       1250.000       3650.001       1800.001
   10250.01       21600.01      0.0000000E+00   3700003.      0.9866727
 7.8708678E-02  7.9747535E-02  1.9105045E-02  1.9408649E-02  3.5171590E-03
 1.9877709E-03  1.2582630E-02  1.9511884E-02   170000.1      1.3340072E-02
 7.0597276E-02  1.1536309E-02  3.9632775E-02  1.2491394E-02  1.3667987E-04
 1.0439638E-03  8.7401050E-04  1.0390015E-02
          1  0.0000000E+00  0.0000000E+00  0.0000000E+00
          2  0.0000000E+00  0.0000000E+00  0.0000000E+00
          3  0.0000000E+00  0.0000000E+00  0.0000000E+00
          4  1.0967797E-07   1.000000      0.8387731
  -4800.000       8449.995       1250.000       3650.001       1800.001
   10250.01       21600.01      0.0000000E+00   3700003.      0.9866727
 7.8708678E-02  7.9747535E-02  1.9105045E-02  1.9408649E-02  3.5171590E-03
 1.9877709E-03  1.2582630E-02  1.9511884E-02   170000.1      1.3340072E-02
 7.0597276E-02  1.1536309E-02  3.9632775E-02  1.2491394E-02  1.3667987E-04
 1.0439638E-03  8.7401050E-04  1.0390015E-02
          3           4  0.0000000E+00  0.0000000E+00
```

MACCS requires six input files. The EARLY and CHRONC modules each require their own input files, as well as two auxiliary data files: a site data file and a dose conversion file. The June 1989 draft NUREG-1150 EARLY and CHRONC input files for Surry were obtained from Sandia National Laboratories (SNL). They are not reproduced here but are available upon request. These two input files did not require modification for this analysis.

The dose conversion file used was "MACCS DOSE CONVERSION FILE: MOD SER #32, 6-JUL-89, 15:59:19 SANDIA NATIONAL LABORATORIES, J. JOHNSON." This is the most recent dosimetry file provided by SNL for MACCS 1.5. The site data file used was also from the NUREG-1150 MACCS 1.5.11 Surry model. These files are not reproduced here but are available upon request.

The ATMOS module requires a meteorological file for the site and an ATMOS input deck. The meteorological data file used was the NUREG-1150 MACCS 1.5.11 METSUR data file for the Surry site and was obtained from SNL. The ATMOS input deck contains the source term release information and a number of other input parameters which are site and plant-specific. Because this analysis combines the Sequoyah plant with the Surry site, the ATMOS input deck obtained from SNL had to be modified. Also, the source term information output from PARTITION was reformatted and then appended to the MACCS ATMOS input deck. A detailed listing of the ATMOS input file used for this analysis follows:

ATMOS Input Description

Variable Name - **FILE25**
Purpose - Specify EARLY User Input File.

```
FILE25='C:\MACCS\ISLOCA\V1_EAR.INP',  STATUS='OLD', ACTION='READ'
```

Variable Name - **FILE26**
Purpose - Specify CHRONC User Input File.

```
FILE26='C:\MACCS\ISLOCA\V1_CHR.INP',  STATUS='OLD', ACTION='READ'
```

Variable Name - **FILE27**
Purpose - Specify DOSE Factors Input Data File.

```
FILE27='C:\MACCS\ISLOCA\dosdat8',      STATUS='OLD', ACTION='READ'
```

Variable Name - **FILE28**
Purpose - Specify Meteorological Input Data File.

```
FILE28='C:\MACCS\ISLOCA\metsur',       STATUS='OLD', ACTION='READ'
```

Variable Name - **FILE29**
Purpose - Specify Site Input Data File.

```
FILE29='C:\MACCS\ISLOCA\sursi10',      STATUS='OLD', ACTION='READ'
```

Variable Name - **FILE06**
Purpose - Specify MACCS Output File (Case Specific).

```
CASE 1, STG 1: FILE06='C:\MACCS\ISLOCA\DRY\V1_MACCS.01', STATUS='UNKNOWN',
                    CARRIAGE CONTROL='FORTRAN'

CASE 1, STG 2: FILE06='C:\MACCS\ISLOCA\DRY\V1_MACCS.02', STATUS='UNKNOWN',
                    CARRIAGE CONTROL='FORTRAN'
```

ATMOS Input (cont.)

```
CASE 2, STG 1: FILE06='C:\MACCS\ISLOCA\DRY5\V5_MACCS.01', STATUS='UNKNOWN',
               CARRIAGE CONTROL='FORTRAN'

CASE 2, STG 2: FILE06='C:\MACCS\ISLOCA\DRY5\V5_MACCS.02', STATUS='UNKNOWN',
               CARRIAGE CONTROL='FORTRAN'

CASE 3, STG 1: FILE06='C:\MACCS\ISLOCA\DRY10\V10MACCS.01', STATUS='UNKNOWN',
               CARRIAGE CONTROL='FORTRAN'

CASE 3, STG 2: FILE06='C:\MACCS\ISLOCA\DRY10\V10MACCS.02', STATUS='UNKNOWN',
               CARRIAGE CONTROL='FORTRAN'

CASE 4, STG 1: FILE06='C:\MACCS\ISLOCA\DRY50\V50MACCS.01', STATUS='UNKNOWN',
               CARRIAGE CONTROL='FORTRAN'

CASE 4, STG 2: FILE06='C:\MACCS\ISLOCA\DRY50\V50MACCS.02', STATUS='UNKNOWN',
               CARRIAGE CONTROL='FORTRAN'

CASE 5, STG 1: FILE06='C:\MACCS\ISLOCA\DRY100\V100MACC.01', STATUS='UNKNOWN',
               CARRIAGE CONTROL='FORTRAN'

CASE 5, STG 2: FILE06='C:\MACCS\ISLOCA\DRY100\V100MACC.02', STATUS='UNKNOWN',
               CARRIAGE CONTROL='FORTRAN'

CASE 6, STG 1: FILE06='C:\MACCS\ISLOCA\WET\W1_MACCS.01', STATUS='UNKNOWN',
               CARRIAGE CONTROL='FORTRAN'

CASE 6, STG 2: FILE06='C:\MACCS\ISLOCA\WET\W1_MACCS.02', STATUS='UNKNOWN',
               CARRIAGE CONTROL='FORTRAN'

CASE 6, STG 3: FILE06='C:\MACCS\ISLOCA\WET\W1_MACCS.03', STATUS='UNKNOWN',
               CARRIAGE CONTROL='FORTRAN'
```

ATMOS Input (cont.)

```
CASE 7, STG 1: FILE06='C:\MACCS\ISLOCA\WET5\W5_MACCS.01', STATUS='UNKNOWN',
               CARRIAGE CONTROL='FORTRAN'

CASE 7, STG 2: FILE06='C:\MACCS\ISLOCA\WET5\W5_MACCS.02', STATUS='UNKNOWN',
               CARRIAGE CONTROL='FORTRAN'

CASE 8, STG 1: FILE06='C:\MACCS\ISLOCA\WET10\W10MACCS.01', STATUS='UNKNOWN',
               CARRIAGE CONTROL='FORTRAN'

CASE 8, STG 2: FILE06='C:\MACCS\ISLOCA\WET10\W10MACCS.02', STATUS='UNKNOWN',
               CARRIAGE CONTROL='FORTRAN'

CASE 9, STG 1: FILE06='C:\MACCS\ISLOCA\WET50\W50MACCS.01', STATUS='UNKNOWN',
               CARRIAGE CONTROL='FORTRAN'

CASE 9, STG 2: FILE06='C:\MACCS\ISLOCA\WET50\W50MACCS.02', STATUS='UNKNOWN',
               CARRIAGE CONTROL='FORTRAN'

CASE 10, STG 1: FILE06='C:\MACCS\ISLOCA\WET50\W51MACCS.01', STATUS='UNKNOWN',
                CARRIAGE CONTROL='FORTRAN'

CASE 10, STG 2: FILE06='C:\MACCS\ISLOCA\WET50\W51MACCS.02', STATUS='UNKNOWN',
                CARRIAGE CONTROL='FORTRAN'

CASE 11, STG 1: FILE06='C:\MACCS\ISLOCA\WET100\W100MACC.01', STATUS='UNKNOWN',
                CARRIAGE CONTROL='FORTRAN'

CASE 11, STG 2: FILE06='C:\MACCS\ISLOCA\WET100\W100MACC.02', STATUS='UNKNOWN',
                CARRIAGE CONTROL='FORTRAN'

CASE 12, STG 1: FILE06='C:\MACCS\ISLOCA\WET100\W110MACC.01', STATUS='UNKNOWN',
                CARRIAGE CONTROL='FORTRAN'
```

```
CASE 12, STG 2: FILE06='C:\MACCS\ISLOCA\WET100\W110MACC.02', STATUS='UNKNOWN',
                CARRIAGE CONTROL='FORTRAN'

Variable Name   - ATNAM1
Purpose         - Identifier for specific ATMOS case.

RIATNAM1001  'SURRY SITE, SEQUOYAH SOURCE TERMS FOR ISLOCA'

Variable Name   - ENDAT1
Purpose         - Flag to indicate that this is the last program in the series
                  to be run.
Source          - NUREG-1150 MACCS 1.5.11 Surry Model.

OCENDAT1001  .FALSE. (SET THIS VALUE TO .TRUE. TO SKIP EARLY AND CHRONC)

Variable Name   - NUMRAD
Purpose         - Number of radial spatial elements defined in the model.
Source          - NUREG-1150 MACCS 1.5.11 Surry Model.

GENUMRAD001  26

Variable Name   - SPAEND
Purpose         - Distance in meters to the end of the spacial intervals.
Source          - NUREG-1150 MACCS 1.5.11 Surry Model.

*  SURRY
*
GESPAEND001      .16       .52      1.21      1.61      2.13
GESPAEND002     3.22      4.02      4.83      5.63      8.05
GESPAEND003    11.27     16.09     20.92     25.75     32.19
GESPAEND004    40.23     48.28     64.37     80.47    112.65
GESPAEND005   160.93    241.14    321.87    563.27    804.67
GESPAEND006  1609.34
```

Variable Name - **NUMISO**
Purpose - Number of nuclides defined in the model.
Source - NUREG-1150 MACCS 1.5.11 Sequoyah Model.

ISN 41SO001 60

Variable Name - **MAXGRP**
Purpose - Number of nuclide groups defined in the model.
Source - NUREG-1150 MACCS 1.5.11 Sequoyah Model.

ISMAXGRP001 9

Variable Name - **WETDEP**
Purpose - Logical flag for each of the nuclide groups that indicate whether they are subject to wet deposition.
Source - NUREG-1150 MACCS 1.5.11 Surry Model.

Variable Name - **DRYDEP**
Purpose - Logical flag for each of the nuclide groups that indicate whether they are subject to dry deposition.
Source - NUREG-1150 MACCS 1.5.11 Surry Model.

*	WETDEP	DRYDEP
*		
ISDEPFLA001	.FALSE.	.FALSE.
ISDEPFLA002	.TRUE.	.TRUE.
ISDEPFLA003	.TRUE.	.TRUE.
ISDEPFLA004	.TRUE.	.TRUE.
ISDEPFLA005	.TRUE.	.TRUE.
ISDEPFLA006	.TRUE.	.TRUE.
ISDEPFLA007	.TRUE.	.TRUE.
ISDEPFLA008	.TRUE.	.TRUE.
ISDEPFLA009	.TRUE.	.TRUE.

Variable Name - **NUCNAM**
Purpose - Identifying name associated with each on the nuclides.
Source - NUREG-1150 MACCS 1.5.11 Surry Model.

Variable Name - **PARENT**
Purpose - Name of parent nuclide if any.
Source - NUREG-1150 MACCS 1.5.11 Surry Model.

Variable Name - **IGROUP**
Purpose - Chemical group to which nuclide is assigned.
Source - NUREG-1150 MACCS 1.5.11 Surry Model.

Variable Name - **HAFLIF**
Purpose - Half-life of the isotope in seconds.
Source - NUREG-1150 MACCS 1.5.11 Surry Model.

*	NUCNAM	PARENT	IGROUP	HAFLIF(S)	
*					
ISOTPGRP001	CO-58	NONE	6	6.160E+06	
ISOTPGRP002	CO-60	NONE	6	660E+08	
ISOTPGRP003	KR-85	NONE	1	3.386E+08	
ISOTPGRP004	KR-85M	NONE	1	1.613E+04	
ISOTPGRP005	KR-87	NONE	1	4.560E+03	
ISOTPGRP006	KR-88	NONE	1	1.008E+04	
ISOTPGRP007	RB-86	NONE	3	1.611E+06	
ISOTPGRP008	SR-89	NONE	5	4.493E+06	
ISOTPGRP009	SR-90	NONE	5	8.865E+08	
ISOTPGRP010	SR-91	NONE	5	3.413E+04	
ISOTPGRP011	SR-92	NONE	5	9.756E+03	NEW
ISOTPGRP012	Y-90	SR-90	7	2.307E+05	
ISOTPGRP013	Y-91	SR-91	7	5.080E+06	
ISOTPGRP014	Y-92	SR-92	7	1.274E+04	NEW
ISOTPGRP015	Y-93	NONE	7	3.636E+04	NEW

ATMOS Input (cont.)

ISOTPGRP016	ZR-95	NONE	7	5.659E+06	
ISOTPGRP017	ZR-97	NONE	7	6.048E+04	
ISOTPGRP018	NB-95	ZR-95	7	3.033E+06	
ISOTPGRP019	MO-99	NONE	6	2.377E+05	
ISOTPGRP020	TC-99M	MO-99	6	2.167E+04	
ISOTPGRP021	RU-103	NONE	6	3.421E+06	
ISOTPGRP022	RU-105	NONE	6	1.598E+04	
ISOTPGRP023	RU-106	NONE	6	3.188E+07	
ISOTPGRP024	RH-105	RU-105	6	1.278E+05	
ISOTPGRP025	SB-127	NONE	4	3.283E+05	
ISOTPGRP026	SB-129	NONE	4	1.562E+04	
ISOTPGRP027	TE-127	SB-127	4	3.366E+04	
ISOTPGRP028	TE-127M	NONE	4	9.418E+06	
ISOTPGRP029	TE-129	SB-129	4	4.200E+03	
ISOTPGRP030	TE-129M	NONE	4	2.886E+06	
ISOTPGRP031	TE-131M	NONE	4	1.080E+05	
ISOTPGRP032	TE-132	NONE	4	2.808E+05	
ISOTPGRP033	I-131	TE-131M	2	6.947E+05	
ISOTPGRP034	I-132	TE-132	2	8.226E+03	
ISOTPGRP035	I-133	NONE	2	7.488E+04	
ISOTPGRP036	I-134	NONE	2	3.156E+03	
ISOTPGRP037	I-135	NONE	2	2.371E+04	
ISOTPGRP038	XE-133	I-133	1	4.571E+05	
ISOTPGRP039	XE-135	I-135	1	3.301E+04	
ISOTPGRP040	CS-134	NONE	3	6.501E+07	
ISOTPGRP041	CS-136	NONE	3	1.123E+06	
ISOTPGRP042	CS-137	NONE	3	9.495E+08	
ISOTPGRP043	BA-139	NONE	9	4.986E+03	NEW
ISOTPGRP044	BA-140	NONE	9	1.105E+06	
ISOTPGRP045	LA-140	BA-140	7	1.448E+05	
ISOTPGRP046	LA-141	NONE	7	1.418E+04	NEW
ISOTPGRP047	LA-142	NONE	7	5.724E+03	NEW
ISOTPGRP048	CE-141	LA-141	8	2.811E+06	PARENT ADDED

ISOTPGRP049	CE-143	NONE	8	1.188E+05
ISOTPGRP050	CE-144	NONE	8	2.457E+07
ISOTPGRP051	PR-143	CE-143	7	1.173E+06
ISOTPGRP052	ND-147	NONE	7	9.495E+05
ISOTPGRP053	NP-239	NONE	8	2.030E+05
ISOTPGRP054	PU-238	CM-242	8	2.809E+09
ISOTPGRP055	PU-239	NP-239	8	7.700E+11
ISOTPGRP056	PU-240	CM-244	8	2.133E+11
ISOTPGRP057	PU-241	NONE	8	4.608E+08
ISOTPGRP058	AM-241	PU-241	7	1.366E+10
ISOTPGRP059	CM-242	NONE	7	1.408E+07
ISOTPGRP060	CM-244	NONE	7	5.712E+08

Variable Name - **CWASH1**
Purpose - Linear term of the washout factor.
Source - NUREG-1150 MACCS 1.5.11 Surry Model.

WDCWASH1001 9.5E-5 (JON HELTON AFTER JONES, 1986)

Variable Name - **CWASH2**
Purpose - The exponential term for the washout factor.
Source - NUREG-1150 MACCS 1.5.11 Surry Model.

WDCWASH2001 0.8 (JON HELTON AFTER JONES, 1986)

Variable Name - **NPSGRP**
Purpose - The number of particle size groups that are used for dry deposition.
Source - NUREG-1150 MACCS 1.5.11 Surry Model.

DDNPSGRP001 1

Variable Name - **VDEPOS**
Purpose - The representative dry deposition velocities associated with each of the particle size groups.
Source - NUREG-1150 MACCS 1.5.11 Surry Model.

DDI'DEPOS001 0.01

Variable Name - **CYSIGA**
Purpose - The linear term in the expression for sigma-y for 6 stability classes.
Source - NUREG-1150 MACCS 1.5.11 Surry Model.

* STABILITY CLASS:	A	B	C	D	E	F
*						
DPCYSIGA001	0.3658	0.2751	0.2089	0.1474	0.1046	0.0722

Variable Name - **CYSIGB**
Purpose - The exponential term of the expression for sigma-y, 6 stability classes.
Source - NUREG-1150 MACCS 1.5.11 Surry Model.

* STABILITY CLASS:	A	B	C	D	E	F
*						
DPCYSIGB001	.9031	.9031	.9031	.9031	.9031	.9031

Variable Name - **CZSIGA**
Purpose - The linear term of the expression for sigma-z, 6 stability classes.
Source - NUREG-1150 MACCS 1.5.11 Surry Model.

* STABILITY CLASS:	A	B	C	D	E	F
*						
DPCZSIGA001	2.5E-4	1.9E-3	.2	.3	.4	.2

Variable Name - **CZSIGB**
Purpose - The exponential term of the expression for sigma-z, 6 stability classes.
Source - NUREG-1150 MACCS 1.5.11 Surry Model.

* STABILITY CLASS;	A	B	C	D	E	F
*						
DPCZSIGB001	2.125	1.6021	.8543	.6532	.6021	.6020

Variable Name - **YSCALE**
Purpose - The linear scaling factor for the sigma-y function.
Source - NUREG-1150 MACCS 1.5.11 Surry Model.

DPYSCALE001 1.

Variable Name - **ZSCALE**
Purpose - The linear scaling factor for the sigma-z function.
Source - NUREG-1150 MACCS 1.5.11 Surry Model.

DPZSCALE001 1.27

Variable Name - **TIMBAS**
Purpose - The time base for the expansion factor (seconds).
Source - NUREG-1150 MACCS 1.5.11 Surry Model.

PMTIMBAS001 600. (10 MINUTES)

Variable Name - **BRKPNT**
Purpose - The break point in the formula used for calculating the plume meander expansion factor.
Source - NUREG-1150 MACCS 1.5.11 Surry Model.

PMBRKPNT001 3600. (1 HOUR)

Variable Name - **XPFAC1**
Purpose - Exponential expansion factor number 1.
Source - NUREG-1150 MACCS 1.5.11 Surry Model.

PMXPFAC1001 0.2

Variable Name - **XPFAC2**
Purpose - Exponential expansion factor number 2.
Source - NUREG-1150 MACCS 1.5.11 Surry Model.

PMXPFAC2001 0.25

Variable Name - **SCLCRW**
Purpose - Scaling factor for the critical wind speed for entrainment of a buoyant plume.
Source - NUREG-1150 MACCS 1.5.11 Surry Model.

PRSCLCRW001 1.

Variable Name - **SCLADP**
Purpose - Scaling factor for the a-d stability plume rise formula.
Source - NUREG-1150 MACCS 1.5.11 Surry Model.

PRSCLADP001 1.

Variable Name - **SCLEFP**
Purpose - Scaling factor for the e-f stability plume rise formula.
Source - NUREG-1150 MACCS 1.5.11 Surry Model.

PRSCLEFP001 1.

Variable Name - **BUILDW**
Purpose - Width of the reactor building in meters.
Source - NUREG-1150 MACCS 1.5.11 Sequoyah Modal.

WEBUILDW001 40. * SEQUOYAH

Variable Name - **BUILDH**
Purpose - Height of the reactor building in meters.
Source - NUREG-1150 MACCS 1.5.11 Sequoyah Model.

WEBUILDH001 40. * SEQUOYAH

Variable Name - **IDEBUG**
Purpose - Debug output flag (0 - no debug).
Source - NUREG-1150 MACCS 1.5.11 Surry Model.

OCIDEBUG001 0

Variable Name - **NUCOUT**
Purpose - Specifies which nuclide will appear on the dispersion listing if one is produced. The dispersion listing is only produced if IDEBUG is greater than zero.
Source - NUREG-1150 MACCS 1.5.11 Surry Model.

OCNUCOUT001 CS-137

Variable Name - **METCOD**
Purpose - Meteorological sampling option code.
metcod = 1, user specified day and hour in the year,
2, weather category bin sampling,
3, 120 hours of weather specified on the atmos user input file,
4, constant met,

5, stratified random samples for each day of the year.

Source - NUREG-1150 MACCS 1.5.11 Surry Model.

M1METCOD001 2

Variable Name - **ISTRDY**
Purpose - Day in the year on which the weather sequence is to begin (Not used if METCOD is specified as 2.)
Source - NUREG-1150 MACCS 1.5.11 Surry Model.

M3ISTRDY001 1

Variable Name - **ISTRDY**
Purpose - Hour of day on which the weather sequence is to begin (Not used if METCOD is specified as 2.)
Source - NUREG-1150 MACCS 1.5.11 Surry Model.

M3ISTRHR001 1

Variable Name - **LIMSPA**
Purpose - Last Spacial Interval for Measured Weather
Source - NUREG-1150 MACCS 1.5.11 Surry Model.

M2LIMSPA001 25

Variable Name - **BNDMXH**
Purpose - Boundary weather mixing layer height.
Source - NUREG-1150 MACCS 1.5.11 Surry Model.

M2BNDMXH001 1000. (METERS)

Variable Name - **IBDSTB**
Purpose - Boundary weather stability class index.
Source - NUREG-1150 MACCS 1.5.11 Surry Model.

M2IBDSTB001 4 (D-STABILITY)

Variable Name - **BNDRAN**
Purpose - Boundary weather rain rate.
Source - NUREG-1150 MACCS 1.5.11 Surry Model.

M2BNDRAN001 5.0 (MM/HR)

Variable Name - **BNDWND**
Purpose - Boundary weather wind speed.
Source - NUREG-1150 MACCS 1.5.11 Surry Model specifies 4.0 M/S. However, 5.0 was used in these calculations. Sensitivity calculations indicate this difference in wind speed has no effect on the consequence results.

M2BNDWND001 5.0 (M/S)

Variable Name - **NSMPLS**
Purpose - Number of samples per bin.
Source - NUREG-1150 MACCS 1.5.11 Surry Model.

M4NSMPLS001 4 (THIS NUMBER SHOULD BE SET TO 4 FOR RISK ASSESSMENT)

Variable Name - **NRNINT**
Purpose - Number of rain distance intervals for binning.
Source - NUREG-1150 MACCS 1.5.11 Surry Model.

M4NRNINT001 6

Variable Name - **RNDSTS**
Purpose - Endpoints of the rain distance intervals (kilometers).
Source - NUREG-1150 MACCS 1.5.11 Surry Model.

M4RNDSTS001 3.22 5.63 11.27 20.92 4 80.47

Variable Name - **NRINTN**
Purpose - Number of rain intensity breakpoints.
Source - NUREG-1150 MACCS 1.5.11 Surry Model.

M4NRINTN001 3

Variable Name - **RNRATE**
Purpose - Rain intensity breakpoints for weather binning (millimeters per hour).
Source - NUREG-1150 MACCS 1.5.11 Surry Model.

M4RNRATE001 2. 4. 6.

Variable Name - **IRSEED**
Purpose - Initial seed for random number generator.
Source - NUREG-1150 MACCS 1.5.11 Surry Model.

M4IRSEED001 79

Variable Name - **CORINV**
Purpose - Defines the total core inventory for each nuclide, NUCNAM.
Source - 3412 MWTH PWR core inventory, end-of-cycle, supplied by D. E. Bennett, 5/14/36, NUREG-1150 MACCS 1.5.11 Model.

```
*            NUCNAM     CORINV(CI)
*
RDCORINV001   CO-58        3.223E+16
```

ATMOS Input (cont.)

RDCORINV002	CO-60	2.465E+16
RDCORINV003	KR-85	2.475E+16
RDCORINV004	KR-85M	1.159E+18
RDCORINV005	KR-87	2.118E+18
RDCORINV006	KR-88	2.864E+18
RDCORINV007	RB-86	1.888E+15
RDCORINV008	SR-89	3.590E+18
RDCORINV009	SR-90	1.938E+17
RDCORINV010	SR-91	4.616E+18
RDCORINV011	SR-92	4.803E+18
RDCORINV012	Y-90	2.079E+17
RDCORINV013	Y-91	4.374E+18
RDCORINV014	Y-92	4.821E+18
RDCORINV015	Y-93	5.454E+18
RDCORINV016	ZR-95	5.526E+18
RDCORINV017	ZR-97	5.759E+18
RDCORINV018	NB-95	5.224E+18
RDCORINV019	MO-99	6.098E+18
RDCORINV020	TC-99M	5.263E+18
RDCORINV021	RU-103	4.542E+18
RDCORINV022	RU-105	2.954E+18
RDCORINV023	RU-106	1.032E+18
RDCORINV024	RH-105	2.046E+18
RDCORINV025	SB-127	2.787E+17
RDCORINV026	SB-129	9.872E+17
RDCORINV027	TE-127	2.692E+17
RDCORINV028	TE-127M	3.564E+16
RDCORINV029	TE-129	9.267E+17
RDCORINV030	TE-129M	2.443E+17
RDCORINV031	TE-131M	4.680E+17
RDCORINV032	TE-132	4.658E+18
RDCORINV033	I-131	3.206E+18
RDCORINV034	I-132	4.725E+18

RDCORINV035	I-133	6.779E+18
RDCORINV036	I-134	7.440E+18
RDCORINV037	I-135	6.392E+18
RDCORINV038	XE-133	6.782E+18
RDCORINV039	XE-135	1.273E+18
RDCORINV040	CS-134	4.324E+17
RDCORINV041	CS-136	1.316E+17
RDCORINV042	CS-137	2.417E+17
RDCORINV043	BA-139	6.282E+18
RDCORINV044	BA-140	6.216E+18
RDCORINV045	A-140	6.352E+18
RDCORINV046	LA-141	5.826E+18
RDCORINV047	LA-142	5.616E+18
RDCORINV048	CE-141	5.651E+18
RDCORINV049	CE-143	5.494E+18
RDCORINV050	CE-144	3.405E+18
RDCORINV051	PR-143	5.395E+18
RDCORINV052	ND-147	2.412E+18
RDCORINV053	NP-239	6.464E+19
RDCORINV054	PU-238	3.664E+15
RDCORINV055	PU-239	8.263E+14
RDCORINV056	PU-240	1.042E+15
RDCORINV057	PU-241	1.755E+17
RDCORINV058	AM-241	1.159E+14
RDCORINV059	CM-242	4.436E+16
RDCORINV060	CM-244	2.596E+15

Variable Name - **SCLCRW**
Purpose - Scaling factor to adjust the core inventory.
Source - NUREG-1150 MACCS 1.5.11 Sequoyah Model.

RDCORSCA001 1.003

Variable Name - **PSDIST**
Purpose - Particle size distribution for each nuclide group.
Source - NUREG-1150 MACCS 1.5.11 Surry Model.

RDPSDIST001 1.0
RDPSDIST002 1.0
RDPSDIST003 1.0
RDPSDIST004 1.0
RDPSDIST005 1.0
RDPSDIST006 1.0
RDPSDIST007 1.0
RDPSDIST008 1.0
RDPSDIST009 1.0

Variable Name - **ATNAM2**
Purpose - Descriptive text identifying the source term. This text is used to identify specific source terms in the output (case specific.)

Case 1, STG 1:
RDATNAM2001 'SEQUOYAH SOURCE TERM AS OBTAINED FROM'
RDATNAM2002 'SEQSOR, FULL APET DRY BASE CASE, DFV=1.0'
RDATNAM2003 'SOURCE TERM-001, GROUP-003'

Case 1, STG 2:
RDATNAM2001 'SEQUOYAH SOURCE TERM AS OBTAINED FROM'
RDATNAM2002 'SEQSOR, FULL APET DRY BASE CASE, DFV=1.0'
RDATNAM2003 'SOURCE TERM-002, GROUP-004'

Case 2, STG 1:
RDATNAM2001 'SEQUOYAH SOURCE TERM AS OBTAINED FROM'
RDATNAM2002 'SEQSOR, FULL APET DRY CASE, DFV=5.0'
RDATNAM2003 'SOURCE TERM-001, GROUP-001'

ATMOS Input (cont.)

```
Case 2, STG 2:
RDATNAM2001 'SEQUOYAH SOURCE TERM AS OBTAINED FROM'
RDATNAM2002 'SEQSOR, FULL APET DRY CASE, DFV=5.0'
RDATNAM2003 'SOURCE TERM-002, GROUP-002'

Case 3, STG 1:
RDATNAM2001 'SEQUOYAH SOURCE TERM AS OBTAINED FROM'
RDATNAM2002 'SEQSOR, FULL APET DRY CASE, DFV=10.0'
RDATNAM2003 'SOURCE TERM-001, GROUP-001'

Case 3, STG 2:
RDATNAM2001 'SEQUOYAH SOURCE TERM AS OBTAINED FROM'
RDATNAM2002 'SEQSOR, FULL APET DRY CASE, DFV=10.0'
RDATNAM2003 'SOURCE TERM-002, GROUP-002'

Case 4, STG 1:
RDATNAM2001 'SEQUOYAH SOURCE TERM AS OBTAINED FROM'
RDATNAM2002 'SEQSOR, FULL APET DRY CASE, DFV=50.0'
RDATNAM2003 'RELEASE ELEVATION = 10.0 m.'
RDATNAM2004 'SOURCE TERM-001, GROUP-002'

Case 4, STG 2:
RDATNAM2001 'SEQUOYAH SOURCE TERM AS OBTAINED FROM'
RDATNAM2002 'SEQSOR, FULL APET DRY CASE, DFV=50.0'
RDATNAM2003 'RELEASE ELEVATION = 10.0 m.'
RDATNAM2004 'SOURCE TERM-002, GROUP-003'

Case 5, STG 1:
RDATNAM2001 'SEQUOYAH SOURCE TERM AS OBTAINED FROM'
RDATNAM2002 'SEQSOR, FULL APET DRY CASE, DFV=100.0'
RDATNAM2003 'RELEASE ELEVATION = 10.0 m.'
RDATNAM2004 'SOURCE TERM-001, GROUP-002'
```

Case 5, STG 2:
RDATNAM2001 'SEQUOYAH SOURCE TERM AS OBTAINED FROM'
RDATNAM2002 'SEQSOR, FULL APET DRY CASE, DFV=100.0'
RDATNAM2003 'RELEASE ELEVATION = 10.0 m.'
RDATNAM2004 'SOURCE TERM-002, GROUP-003'

Case 6, STG 1:
RDATNAM2001 'SEQUOYAH SOURCE TERM AS OBTAINED FROM'
RDATNAM2002 'SEQSOR, FULL APET WET BASE, DFV SAMPLED'
RDATNAM2003 'SOURCE TERM-001, GROUP-006'

Case 6, STG 2:
RDATNAM2001 'SEQUOYAH SOURCE TERM AS OBTAINED FROM'
RDATNAM2002 'SEQSOR, FULL APET WET BASE, DFV SAMPLED'
RDATNAM2003 'SOURCE TERM-002, GROUP-007'

Case 6, STG 3:
RDATNAM2001 'SEQUOYAH SOURCE TERM AS OBTAINED FROM'
RDATNAM2002 'SEQSOR, FULL APET WET BASE, DFV SAMPLED'
RDATNAM2003 'SOURCE TERM-003, GROUP-008'

Case 7, STG 1:
RDATNAM2001 'SEQUOYAH SOURCE TERM AS OBTAINED FROM'
RDATNAM2002 'SEQSOR, FULL APET WET CASE, DFV=5.0'
RDATNAM2003 'SOURCE TERM-001, GROUP-001'

Case 7, STG 2:
RDATNAM2001 'SEQUOYAH SOURCE TERM AS OBTAINED FROM'
RDATNAM2002 'SEQSOR, FULL APET WET CASE, DFV=10.0'
RDATNAM2003 'SOURCE TERM-002, GROUP-002'

```
Case 8, STG 1:
RDATNAM2001 'SEQUOYAH SOURCE TERM AS OBTAINED FROM'
RDATNAM2002 'SEQSOR, FULL APET WET CASE, DFV=10.0'
RDATNAM2003 'SOURCE TERM-001, GROUP-001'

Case 8, STG 2:
RDATNAM2001 'SEQUOYAH SOURCE TERM AS OBTAINED FROM'
RDATNAM2002 'SEQSOR, FULL APET WET CASE, DFV=10.0'
RDATNAM2003 'SOURCE TERM-002, GROUP-002'

Case 9, STG 1:
RDATNAM2001 'SEQUOYAH SOURCE TERM AS OBTAINED FROM'
RDATNAM2002 'SEQSOR, FULL APET WET CASE, DFV=50.0'
RDATNAM2003 'RELEASE ELEVATION IS 0.0 m.'
RDATNAM2004 'SOURCE TERM-001, GROUP-002'

Case 9, STG 2:
RDATNAM2001 'SEQUOYAH SOURCE TERM AS OBTAINED FROM'
RDATNAM2002 'SEQSOR, FULL APET WET CASE, DFV=50.0'
RDATNAM2003 'RELEASE ELEVATION IS 0.0 m.'
RDATNAM2004 'SOURCE TERM-002, GROUP-003'

Case 10, STG 1:
RDATNAM2001 'SEQUOYAH SOURCE TERM AS OBTAINED FROM'
RDATNAM2002 'SEQSOR, FULL APET WET CASE, DFV=50.0'
RDATNAM2003 'RELEASE ELEVATION IS 10.0 m.'
RDATNAM2004 'SOURCE TERM-001, GROUP-002'

Case 10, STG 2:
RDATNAM2001 'SEQUOYAH SOURCE TERM AS OBTAINED FROM'
RDATNAM2002 'SEQSOR, FULL APET WET CASE, DFV=50.0'
RDATNAM2003 'RELEASE ELEVATION IS 10.0 m.'
RDATNAM2004 'SOURCE TERM-002, GROUP-003'
```

Case 11, STG 1:
RDATNAM2001 'SEQUOYAH SOURCE TERM AS OBTAINED FROM'
RDATNAM2002 'SEQSOR, FULL APET WET CASE, DFV=100.0'
RDATNAM2003 'RELEASE ELEVATION IS BASE VALUE, 0.0 m.'
RDATNAM2004 'SOURCE TERM-001, GROUP-002'

Case 11, STG 2:
RDATNAM2001 'SEQUOYAH SOURCE TERM AS OBTAINED FROM'
RDATNAM2002 'SEQSOR, FULL APET WET CASE, DFV=100.0'
RDATNAM2003 'RELEASE ELEVATION IS BASE VALUE, 0.0 m.'
RDATNAM2004 'SOURCE TERM-002, GROUP-003'

Case 12, STG 1:
RDATNAM2001 'SEQUOYAH SOURCE TERM AS OBTAINED FROM'
RDATNAM2002 'SEQSOR, FULL APET WET CASE, DFV=100.0'
RDATNAM2003 'RELEASE ELEVATION IS 10.0 m.'
RDATNAM2004 'SOURCE TERM-001, GROUP-002'

Case 12, STG 2:
RDATNAM2001 'SEQUOYAH SOURCE TERM AS OBTAINED FROM'
RDATNAM2002 'SEQSOR, FULL APET WET CASE, DFV=100.0'
RDATNAM2003 'RELEASE ELEVATION IS 10.0 m.'
RDATNAM2004 'SOURCE TERM-002, GROUP-003'

Variable Name - CALARM
Purpose - Time after accident initiation when the accident reaches general emergency conditions (as defined in NUREG-0654), or when plant personnel can reliably predict that general emergency conditions will be attained
Source - NUREG-1150 SEQSOR source term information for Sequoyah Model.

RDOALARM001 1250.0

Variable Name - **MAXRIS**

Purpose - Selection of risk dominant plume.

Source - NUREG-1150 MACCS 1.5.11 Sequoyah Model (for small release fractions, on the order of 1.0E-02 or less, plume selection has little effect on consequence results.)

RDMAXRIS001 1

Variable Name - **REFTIM**

Purpose - Specifies the representative time point of each plume segment (0.0 = leading edge, 0.5 = midpoint, 1.0 = trailing edge). The radioactive decay, dry deposition, and dispersion calculations are all performed as if the entire contents of the plume segment are located at this point.

Source - A value of 0.0 is assumed for the first plume in this analysis. This results in a conservative calculation. For the second plume, a value of 0.5 is used in accordance with the NUREG-1150 MACCS 1.5.11 Surry Model.

RDREFTIM001 0.00 0.50

Variable Name - **NUMREL**

Purpose - Number of plume segments that are released.

Source - NUREG-1150 SEQSOR source term information for Sequoyah Model.

RDNUMREL001 2

Variable Name - **PLHEAT**

Purpose - Heat content of plume release (w).

Source - NUREG-1150 SEQSOR source term information for Sequoyah Model.

Dry V sequences:
RDPLHEAT001 3.70E+06 1.70E+05

Wet V sequences:
RDPLHEAT001 1.85E+06 1.70E+05

Variable Name - **PLHITE**
Purpose - Height of plume segments at release (m).
Source - NUREG-1150 SEQSOR source term information for Sequoyah Model for cases 1, 2, 3, 6, 7, 8, 9, and 11. MELCOR calculations for cases 4, 5, 10, and 12.

Cases 1, 2, 3, 6, 7, 8, 9, and 11:
RDPLHITE001 0. 0.

Cases 4, 5, 10, and 12:
RDPLHITE001 10.0 10.0

Variable Name - **PLUDUR**
Purpose - Duration of plume segments (s).
Source - NUREG-1150 SEQSOR source term information for Sequoyah Model.

RDPLUDUR001 1800. 21600.

Variable Name - **PDELAY**
Purpose - Specifies the start time of each plume segment in seconds from the time of accident initiation, e.g., reactor scram.
Source - NUREG-1150 SEQSOR source term information for Sequoyah Model.

RDPDELAY001 3650. 10250.

Variable Name - **RELFAC**

Purpose - Release fractions for isotope groups in release (Case Dependant).

Sources - Cases 1 and 6 represent the base case analyses for the dry and wet V sequences, respectively, as obtained from the NUREG-1150 SEQSOR source term information for Sequoyah. The remaining cases are obtained by modifying the V sequence DFs of the NUREG-1150 SEQSOR source term code for Sequoyah. For all cases except one, the accident progression bins have been partitioned into two source term groups. The one exception is case 6 for which three source term groups were used.

* . . . 2 GROUPS: XE, R I CS TE SR RU LA CE BA

Case 1, Source Term Group 1:
* Dry V sequence, DF=1.0, Release Elevation=0.0

RDRELFRC001 9.84E-01 4.56E-01 4.63E-01 1.16E-01 1.21E-01 2.19E-02 1.24E-02
7.88E-02 1.22E-01
RDRELFRC002 1.62E-02 3.32E-02 4.31E-03 1.84E-01 6.56E-02 7.73E-04 4.71E-03
3.46E-03 5.52E-02

Case 1, Source Term Group 2:
* Dry V sequence, DF=1.0, Release Elevation=0.0

RDRELFRC001 9.94E-01 1.29E-01 1.27E-01 1.25E-02 2.48E-03 6.69E-04 1.25E-04
4.72E-04 2.92E-03
RDRELFRC002 5.73E-03 6.17E-02 2.10E-02 8.03E-02 3.56E-02 2.73E-04 4.72E-03
5.12E-03 2.78E-02

Case 2, Source Term Group 1:
* Dry V sequence, DF=5.0, Release Elevation=0.0

RDRELFRC001 9.90E-01 2.14E-02 2.18E-02 2.32E-03 6.51E-04 1.54E-04 3.55E-05
1.41E-04 7.42E-04
RDRELFRC002 9.74E-03 2.25E-02 9.71E-04 1.02E-02 4.10E-03 4.68E-05 4.11E-04
4.24E-04 3.19E-03

Case 2, Source Term Group 2:
* Dry V sequence, DF=5.0, Release Elevation=0.0

RDRELFRC001 9.87E-01 7.87E-02 7.97E-02 1.91E-02 1.94E-02 3.52E-03 1.99E-03
1.26E-02 1.95E-02
RDRELFRC002 1.33E-02 7.06E-02 1.15E-02 3.96E-02 1.25E-02 1.37E-04 1.04E-03
8.74E-04 1.04E-0[illegible]

Case 3, Source Term Group 1:
* Dry V sequence, DF=10.0, Release Elevation=0.0

RDRELFRC001 9.91E-01 1.39E-02 1.43E-02 1.42E-03 2.65E-04 6.55E-05 1.39E-05
5.40E-05 3.11E-04
RDRELFRC002 8.73E-03 2.14E-02 1.14E-03 1.12E-02 6.01E-03 1.23E-04 8.06E-04
7.03E-04 5.21E-03

Case 3, Source Term Group 2:
* Dry V sequence, DF=10.0, Release Elevation=0.0

RDRELFRC001 9.86E-01 4.09E-02 4.14E-02 1.02E-02 1.06E-02 1.91E-03 1.08E-03
6.85E-03 1.06E-02
RDRELFRC002 1.40E-02 7.84E-02 1.24E-02 2.33E-02 5.44E-03 4.27E-05 3.71E-04
3.11E-04 4.44E-03

Case 4, Source Term Group 1:
* Dry V sequence, DF=50.0, Release Elevation=10.0

RDRELFRC001 9.85E-01 7.75E-03 7.89E-03 1.92E-03 1.97E-03 3.56E-04 2.02E-04
1.28E-03 1.98E-03
RDRELFRC002 1.50E-02 5.72E-02 3.46E-03 4.72E-03 1.14E-03 1.35E-05 8.39E-05
6.40E-05 9.52E-04

Case 4, Source Term Group 2:
* Dry V sequence, DF=50.0, Release Elevation=10.0

RDRELFRC001 9.98E-01 3.04E-03 2.96E-03 2.86E-04 3.65E-05 1.28E-05 1.60E-06
5.35E-06 4.62E-05
RDRELFRC002 1.79E-03 1.16E-01 4.06E-02 3.01E-02 1.00E-03 6.15E-06 1.44E-04
1.58E-04 7.82E-04

Case 5, Source Term Group 1:
* Dry V sequence, DF=100.0, Release Elevation=10.0

RDRELFRC001 9.85E-01 3.88E-03 3.94E-03 9.61E-04 9.86E-04 1.78E-04 1.01E-04
6.38E-04 9.91E-04
RDRELFRC002 1.50E-02 5.74E-02 3.43E-03 3.14E-03 5.68E-04 6.71E-06 4.20E-05
3.20E-05 4.76E-04

Case 5, Source Term Group 2:
* Dry V sequence, DF=100.0, Release Elevation=10.0

RDRELFRC001 9.98E-01 1.52E-03 1.48E-03 1.43E-04 1.82E-05 6.38E-06 7.96E-07
2.66E-06 2.30E-05
RDRELFRC002 1.79E-03 1.16E-01 4.06E-02 2.92E-02 5.02E-04 3.07E-06 7.18E-05
7.87E-05 3.92E-04

Case 6, Source Term Group 1:
* Wet V sequence, Base case sampled DF, Release Elevation=0.0

RDRELFRC001 9.86E-01 1.81E-02 1. 4E-02 1.87E-03 2.06E-04 6.24E-05 9.88E-06
3.38E-05 2.73E-04
RDRELFRC002 1.40E-02 4.18E-02 3.26E-03 1.66E-02 9.26E-03 2.09E-04 1.34E-03
1.22E-03 8.13E-03

Case 6, Source Term Group 2:
* Wet V sequence, Base case sampled DF, Release Elevation=0.0

RDRELFRC001 9.94E-01 1.82E-01 1.81E-01 5.77E-02 5.17E-02 9.37E-03 5.32E-03
3.38E-02 5.20E-02
RDRELFRC002 5.91E-03 4.64E-02 1.66E-03 4.12E-02 1.34E-02 7.55E-04 5.70E-04
2.29E-03 1.21E-02

Case 6, Source Term Group 3:
* Wet V sequence, Base case sampled DF, Release Elevation=0.0

RDRELFRC001 9.98E-01 5.06E-02 4.98E-02 4.39E-03 4.39E-04 1.65E-04 1.83E-05
5.98E-05 5.66E-04
RDRELFRC002 1.95E-03 1.03E-01 3.80E-02 5.18E-02 1.13E-02 6.89E-05 1.62E-03
1.77E-03 8.87E-03

Case 7, Source Term Group 1:
* Wet V sequence, DF=5.0, Release Elevation=0.0

RDRELFRC001 9.90E-01 2.12E-02 2.14E-02 1.87E-03 3.64E-04 9.49E-05 2.09E-05
8.32E-05 4.31E-04
RDRELFRC002 9.56E-03 2.38E-02 1.05E-03 1.13E-02 6.23E-03 1.06E-04 7.64E-04
8.10E-04 5.00E-03

Case 7, Source Term Group 2:
* Wet V sequence, DF=5.0, Release Elevation=0.0

RDRELFRC001 9.91E-01 7.19E-02 7.25E-02 1.53E-02 1.17E-02 2.15E-03 1.18E-03
7.44E-03 1.19E-02
RDRELFRC002 8.95E-03 6.48E-02 1.19E-02 3.73E-02 1.24E-02 2.56E-04 1.28E-03
1.42E-03 1.06E-02

Case 8, Source Term Group 1:
* Wet V sequence, DF=10.0, Release Elevation=0.0

RDRELFRC001 9.91E-01 1.41E-02 1.43E-02 1.27E-03 1.52E-04 4.12E-05 8.11E-06
3.13E-05 1.88E-04
RDRELFRC002 8.61E-03 2.16E-02 1.08E-03 1.20E-02 7.20E-03 1.61E-04 1.02E-03
9.26E-04 6.27E-03

Case 8, Source Term Group 2:
* Wet V sequence, DF=10.0, Release Elevation=0.0

RDRELFRC001 9.91E-01 3.81E-02 3.84E-02 8.48E-03 6.71E-03 1.23E-03 6.78E-04
4.27E-03 6.80E-03
RDRELFRC002 9.30E-03 7.48E-02 1.35E-02 2.21E-02 4.79E-03 8.90E-05 3.82E-04
5.17E-04 3.97E-03

Case 9, Source Term Group 1:
* Wet V sequence, DF=50.0, Release Elevation=0.0

RDRELFRC001 9.89E-01 6.81E-03 6.90E-03 1.46E-03 1.13E-03 2.06E-04 1.14E-04
7.16E-04 1.14E-03
RDRELFRC002 1.07E-02 4.75E-02 2.56E-03 3.81E-03 1.09E-03 2.57E-05 1.04E-04
1.16E-04 9.41E-04

Case 9, Source Term Group 2:
* Wet V sequence, DF=50.0, Release Elevation=0.0

RDRELFRC001 9.98E-01 2.92E-03 2.85E-03 2.77E-04 4.07E-05 1.28E-05 1.79E-06
6.12E-06 5.08E-05
RDRELFRC002 1.70E-03 1.14E-01 4.09E-02 3.01E-02 1.20E-03 7.39E-06 1.73E-04
1.89E-04 9.37E-04

Case 10, Source Term Group 1:
* Wet V sequence, DF=50.0, Release Elevation=10.0

RDRELFRC001 9.89E-01 6.81E-03 6.90E-03 1.46E-03 1.13E-03 2.06E-04 1.14E-04
7.16E-04 1.14E-03
RDRELFRC002 1.07E-02 4.75E-02 2.56E-03 3.81E-03 1.09E-03 2.57E-05 1.04E-04
1.16E-04 9.41E-04

Case 10, Source Term Group 2:
* Wet V sequence, DF=50.0, Release Elevation=10.0

RDRELFRC001 9.98E-01 2.92E-03 2.85E-03 2.77E-04 4.07E-05 1.28E-05 1.79E-06
6.12E-06 5.08E-05
RDRELFRC002 1.70E-03 1.14E-01 4.09E-02 3.01E-02 1.20E-03 7.39E-06 1.73E-04
1.89E-04 9.37E-04

Case 11, Source Term Group 1:
* Wet V sequence, DF=100.0, Release Elevation=0.0

RDRELFRC001 9.89E-01 3.41E-03 3.45E-03 7.28E-04 5.63E-04 1.03E-04 5.69E-05
3.58E-04 5.71E-04
RDRELFRC002 1.07E-02 4.77E-02 2.54E-03 2.43E-03 5.45E-04 1.29E-05 5.22E-05
5.79E-05 4.70E-04

Case 11, Source Term Group 2:
* Wet V sequence, DF=100.0, Release Elevation=0.0

RDRELFRC001 9.98E-01 1.46E-03 1.43E-03 1.38E-04 2.03E-05 6.40E-06 8.93E-07
3.05E-06 2.54E-05
RDRELFRC002 1.70E-03 1.14E-01 4.08E-02 2.92E-02 6.01E-04 3.69E-06 8.61E-05
9.44E-05 4.69E-04

Case 12, Source Term Group 1:
* Wet V sequence, DF=100.0, Release Elevation=10.0

RDRELFRC001 9.89E-01 3.41E-03 3.45E-03 7.28E-04 5.63E-04 1.03E-04 5.69E-05
3.58E-04 5.71E-04
RDRELFRC002 1.07E-02 4.77E-02 2.54E-03 2.43E-03 5.45E-04 1.29E-05 5.22E-05
5.79E-05 4.70E-04

Case 12, Source Term Group 2:
* Wet V sequence, DF=100.0, Release Elevation=10.0

RDRELFRC001 9.98E-01 1.46E-03 1.43E-03 1.38E-04 2.03E-05 6.40E-06 8.93E-07
3.05E-06 2.54E-05
RDRELFRC002 1.70E-03 1.14E-01 4.08E-02 2.92E-02 6.01E-04 3.69E-06 8.61E-05
9.44E-05 4.69E-04

5.0 RESULTS

The consequence results for the dry and wet V sequences are summarized in this section. The complete output files from the 25 MACCS calculations are stored on magnetic tape and are available upon request. For the dry V sequence, five cases were analyzed, one base case and four sensitivity cases. For each case, the APBs were partitioned into two source term groups. For each source term group, a MACCS calculation was performed - a total of ten for the dry V sequence cases. Table G.8 reports three consequence measures for each source term group for each dry V sequence case. Table G.8 also includes the conditional frequency weighting for each source term group for each case as obtained from PARTITION. The three consequence measures reported here are the mean number of early fatalities and latent cancer fatalities within a 1000-mile radius, and the mean population dose, in person-rem, within a 50-mile radius. The uncertainty distributions calculated by MACCS for each measure are not reported here but can be obtained from the stored MACCS output.

Table G.9 reports similar results for the wet V sequence cases. For the wet V sequence, seven cases were analyzed, one base case and six sensitivity cases. Again, the reported consequence measures are mean values.

The mean consequences for each sensitivity case, conditional upon the occurrence of that particular V sequence, are obtained by multiplying the mean consequence measure for each source term group by the conditional probability of the source term group and summing over all source term groups:

$$CONS_k = \sum_{i=1}^{n} CSTGP_i * CONS_{ik}(FP_i)$$

where,

$CONS_k$ = mean magnitude of consequence measure k

$CSTGP_i$ = the conditional probability of source term group i

FP_i = fission product source term for source term group i

$CONS_{ik}$ = mean magnitude of consequence measure k for source term group i, given fission product source term (FP_i)

Table G.8 Conditional probabilities and MACCS consequence results for each source term group for each dry V sequence sensitivity.

Sensitivity Case DF	Release Elevation	Source Term Group	Conditional Probability	Mean Early Fatalities	Mean Latent Fatalities	Mean 50-Mile Dose (person-rem)
1.0	0.0	1	6.69E-01	1.49E+02	6.79E+03	8.05E+06
		2	3.31E-01	8.08E-01	2.47E+03	2.22E+06
5.0	0.0	1	1.61E-01	1.33E-01	6.06E+02	9.33E+05
		2	8.39E-01	1.92E+00	2.05E+03	2.38E+06
10.0	0.0	1	2.29E-01	1.11E-01	5.04E+02	8.59E+05
		2	7.71E-01	4.90E-01	1.37E+03	1.76E+06
50.0	10.0	1	8.29E-01	7.38E-02	4.34E+02	8.20E+05
		2	1.71E-01	5.86E-02	9.14E+02	1.19E+06
100.0	10.0	1	8.28E-01	6.20E-02	2.99E+02	6.41E+05
		2	1.72E-01	5.63E-02	8.70E+02	1.12E+06

Table G.9 Conditional probabilities and MACCS consequence results for each source term group for each wet V sequence sensitivity.

Sensitivity Case DF	Release Elevation	Source Term Group	Conditional Probability	Mean Early Fatalities	Mean Latent Fatalities	Mean 50-Mile Dose (person-rem)
Base Case[a]	0.0	1	4.87E-01	2.09E-01	6.33E+02	1.04E+06
		2	3.17E-01	1.11E+01	3.42E+03	3.88E+06
		3	1.96E-01	3.94E-01	1.6 E+03	1.77E+06
5.0	0.0	1	2.14E-01	2.28E-01	5.94E+02	9.48E+05
		2	7.86E-01	1.20E+00	1.73E+03	2.02E+06
10.0	0.0	1	3.16E-01	1.96E-01	4.98E+02	8.63E+05
		2	6.84E-01	4.96E-01	1.21E+03	1.61E+06
50.0	0.0	1	8.17E-01	1.80E-01	3.40E+02	6.90E+05
		2	1.83E-01	1.59E-01	9.01E+02	1.17E+06
50.0	10.0	1	8.17E-01	1.21E-01	3.48E+02	6.98E+05
		2	1.83E-01	1.06E-01	9.13E+02	1.18E+06
100.0	0.0	1	8.17E-01	1.60E-01	2.37E+02	5.37E+05
		2	1.83E-01	1.54E-01	8.60E+02	1.10E+06
100.0	10.0	1	8.17E-01	1.07E-01	2.41E+02	5.42E+05
		2	1.83E-01	1.03E-01	8.70E+02	1.11E+06

a. Wet V sequence base case DF is a sampled distribution as given in Table G.5

Tables G.10 and G.11 present the mean consequence results for the dry and wet V sequence sensitivity cases, respectively. These results are also presented graphically on Figures G.1 through G.6. Comparisons of the dry and wet V sequence consequence results are also presented graphically in Figures G.7, G.8, and G.9.

Table G.10 Mean MACCS consequence results for each dry V sequence sensitivity.

Sensitivity Case DF	Release Elevation	Mean Early Fatalities	Mean Latent Fatalities	Mean 50-Mile Dose (person-rem)
1.0	0.0	9.99E+01	5.36E+03	6.12E+06
5.0	0.0	1.63E+00	1.82E+03	2.15E+06
10.0	0.0	4.03E-01	1.17E+03	1.55E+06
50.0	10.0	7.12E-02	5.16E+02	8.83E+05
100.0	10.0	6.10E-02	3.97E+02	7.24E+05

Table G.11 Mean MACCS consequence results for each wet V sequence sensitivity.

Sensitivity Case DF	Release Elevation	Mean Early Fatalities	Mean Latent Fatalities	Mean 50-Mile Dose (person-rem)
Base[a]	0.0	3.69E+00	1.71E+03	2.08E+06
5.0	0.0	9.92E-01	1.49E+03	1.79E+06
10.0	0.0	4.01E-01	9.85E+02	1.37E+06
50.0	0.0	1.76E-01	4.43E+02	7.78E+05
50.0	10.0	1.18E-01	4.51E+02	7.86E+05
100.0	0.0	1.59E-01	3.51E+02	6.40E+05
100.0	10.0	1.06E-01	3.56E+02	6.46E+05

a. Wet V sequence base case DF is a sampled distribution as given in Table G.5.

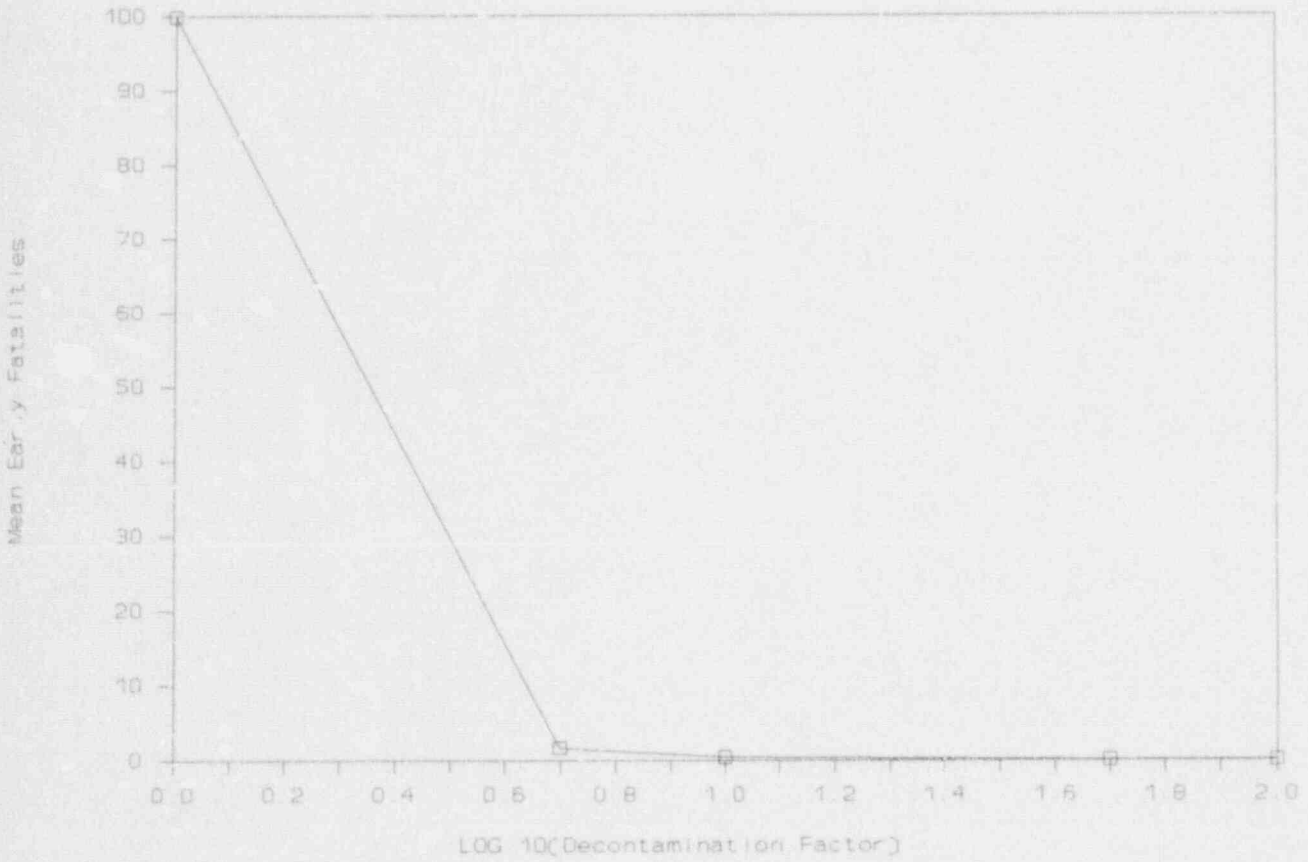

Figure G.1 Mean early fatality consequence results as a function of decontamination factor for the dry V sequences.

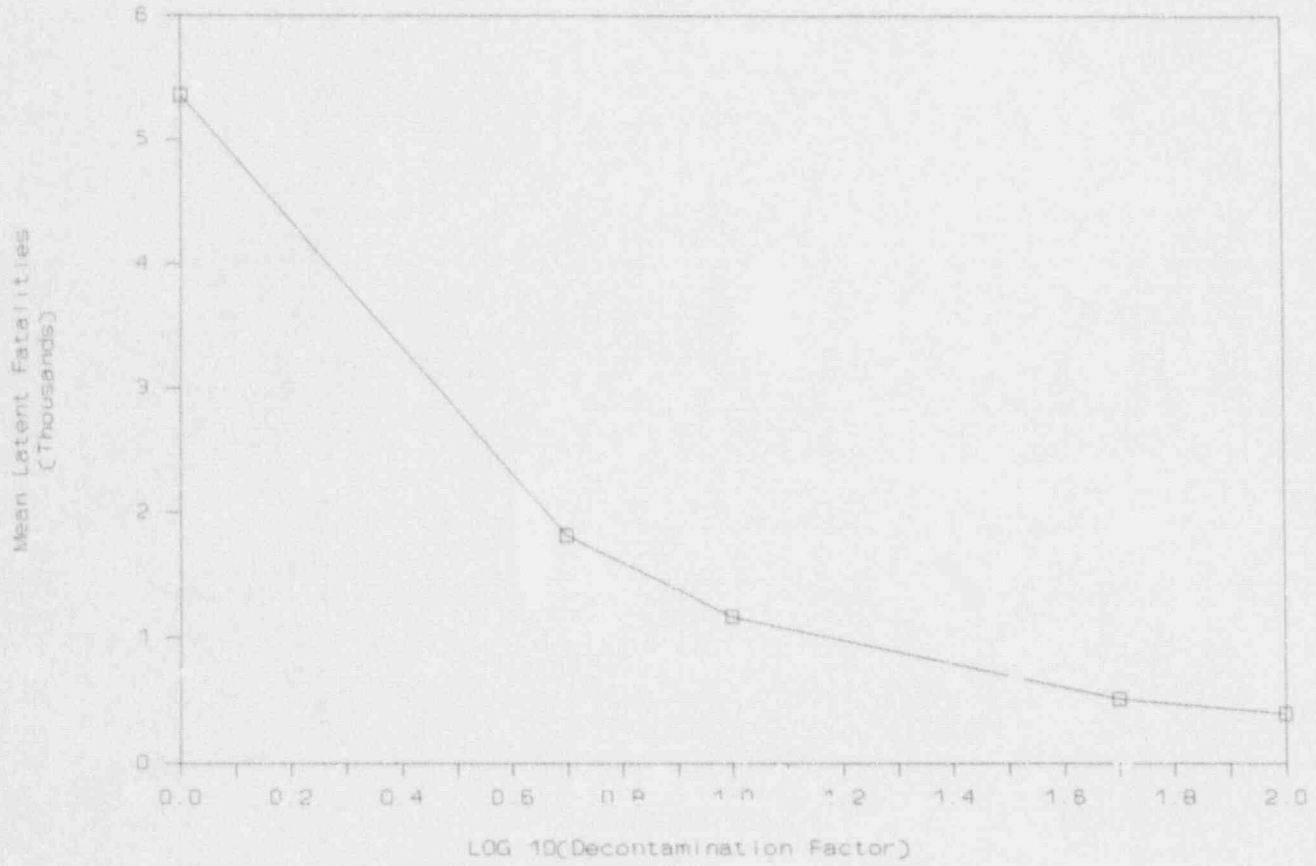

Figure G.2 Mean latent fatality consequence results as a function of decontamination factor for the dry V sequences.

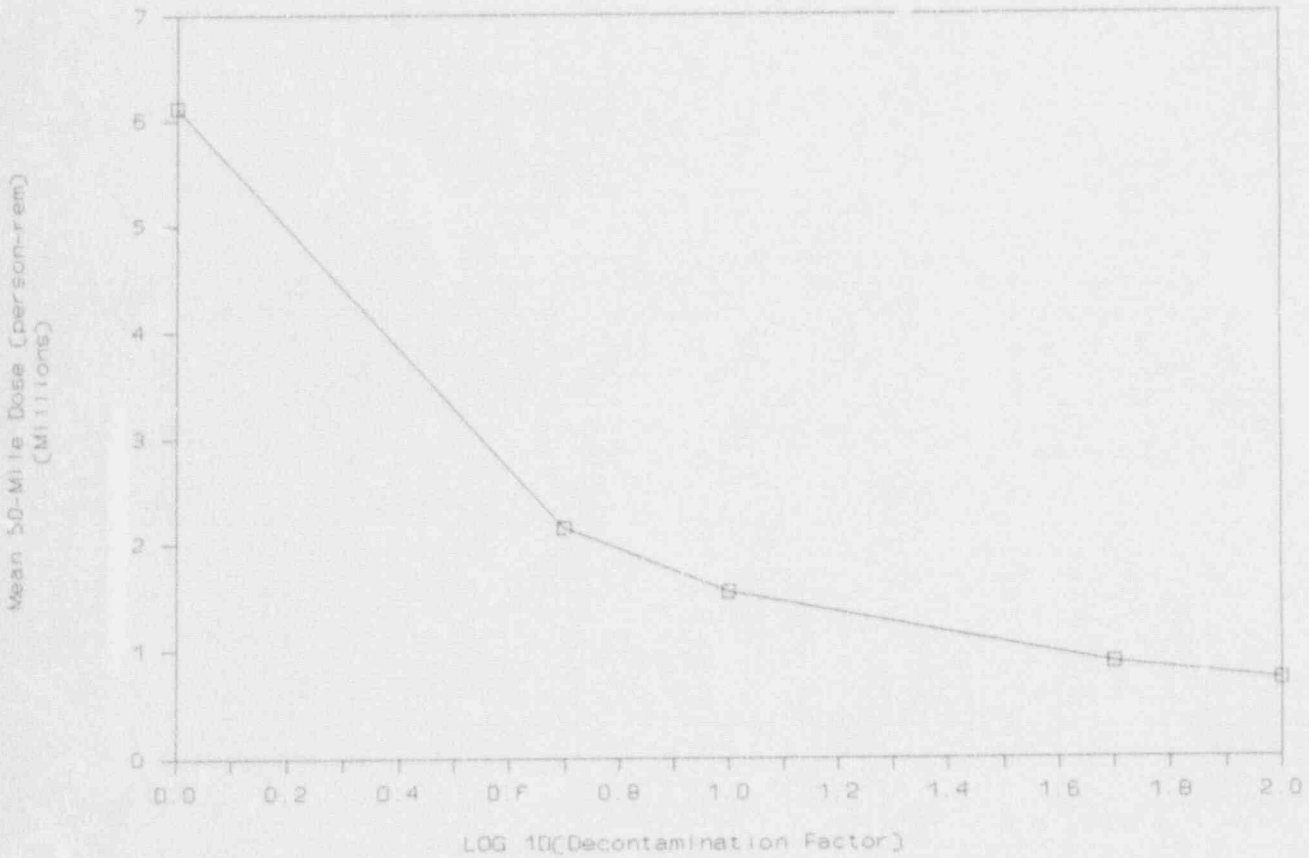

Figure G.3 Mean 50-mile population dose consequence results as a function of decontamination factor for the dry V sequences.

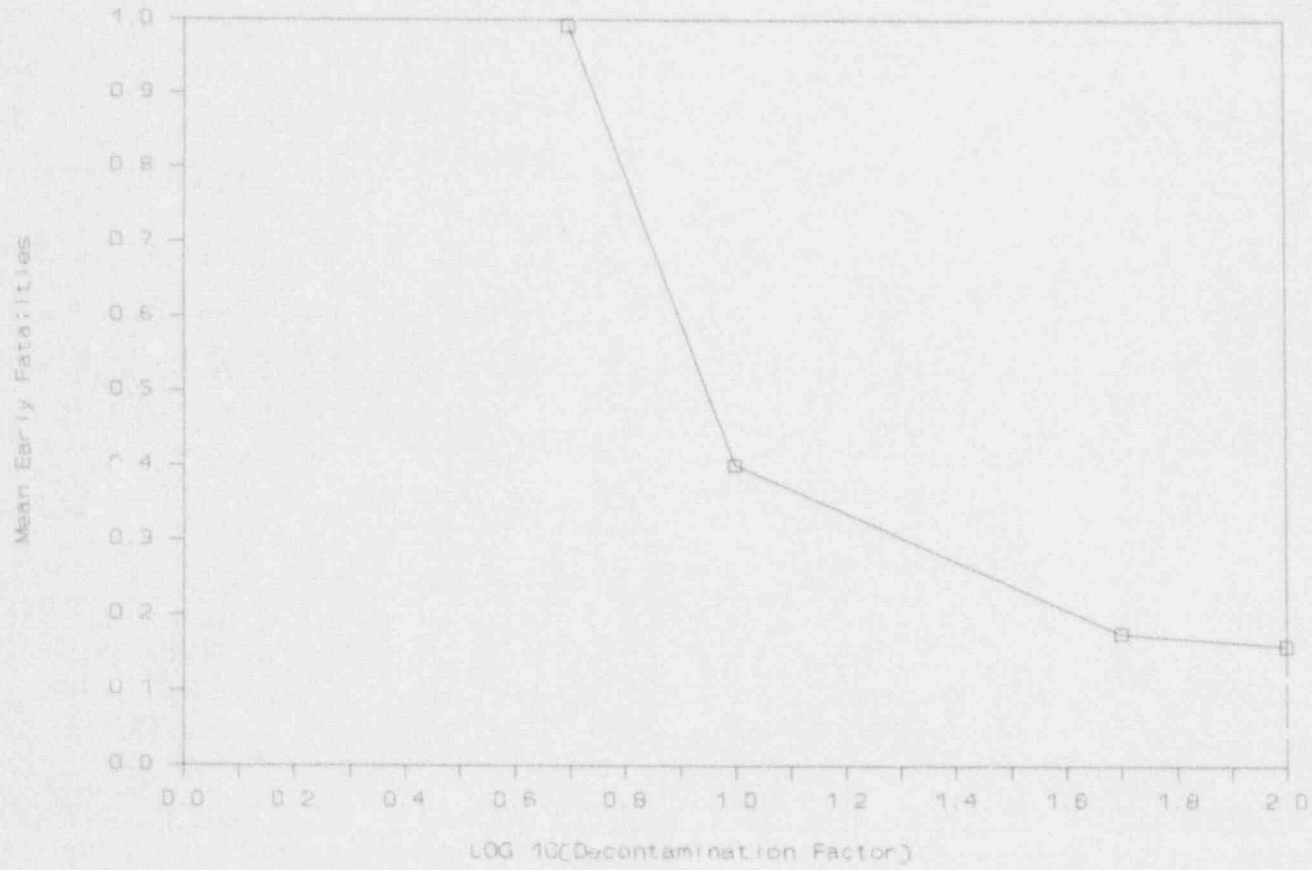

Figure G.4 Mean early fatality consequence results as a function of decontamination factor for the wet V sequences (all release elevations are 0.0 m).

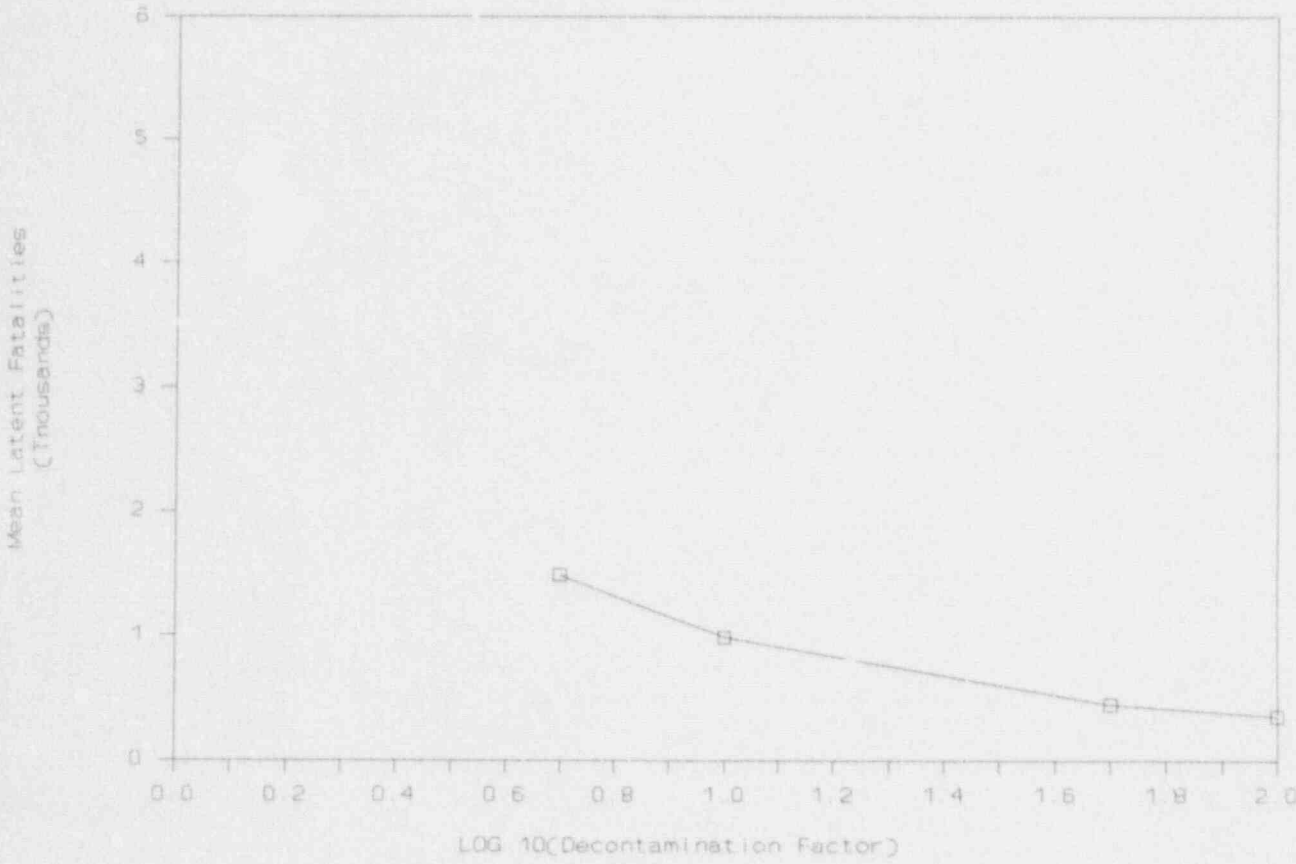

Figure G.5 Mean latent fatality consequence results as a function of decontamination factor for the wet V sequences (all release elevations are 0.0 m).

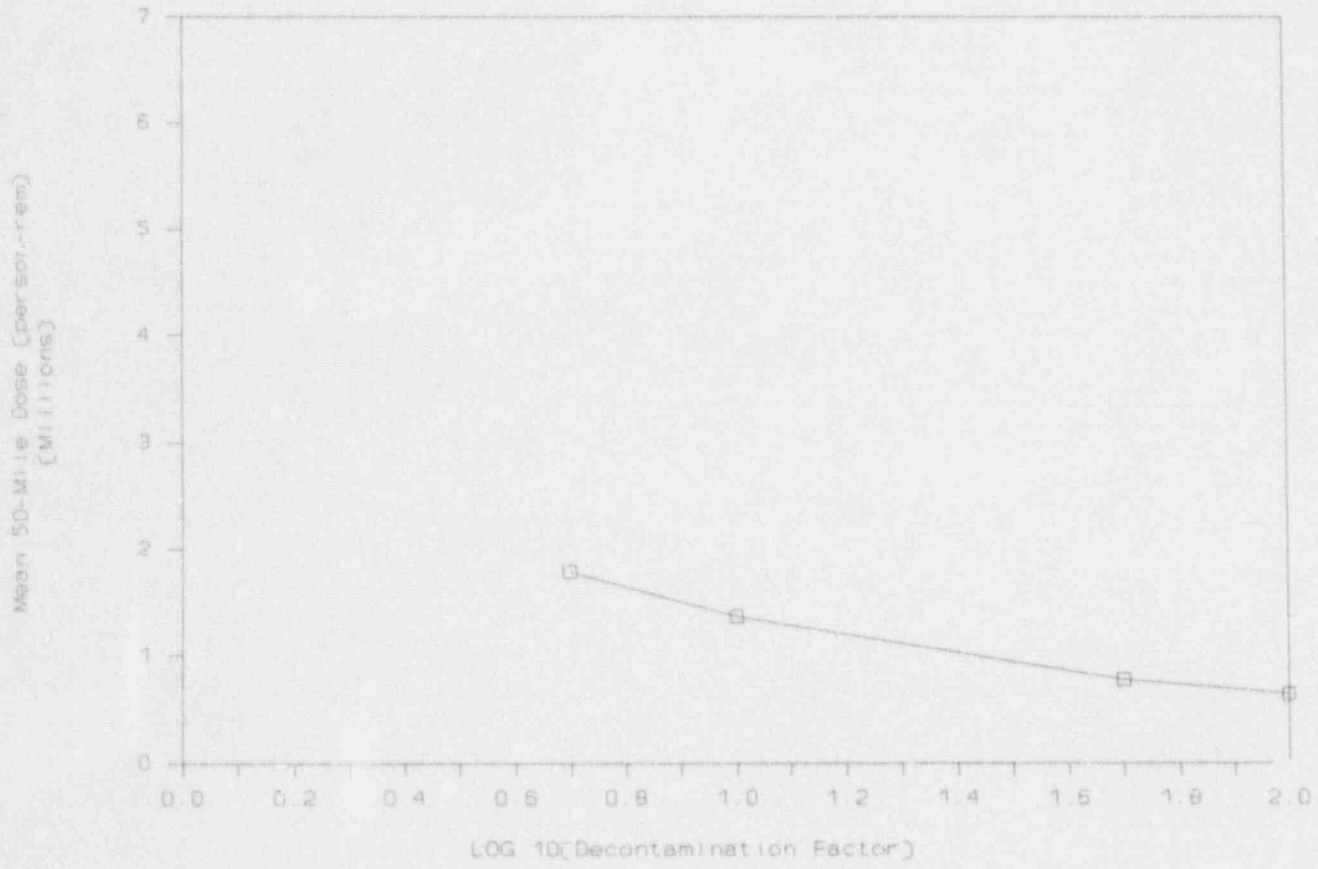

Figure G.6 Mean 50-mile population dose consequence results as a function of decontamination factor for the wet V sequences (all release elevations = 0.0 m).

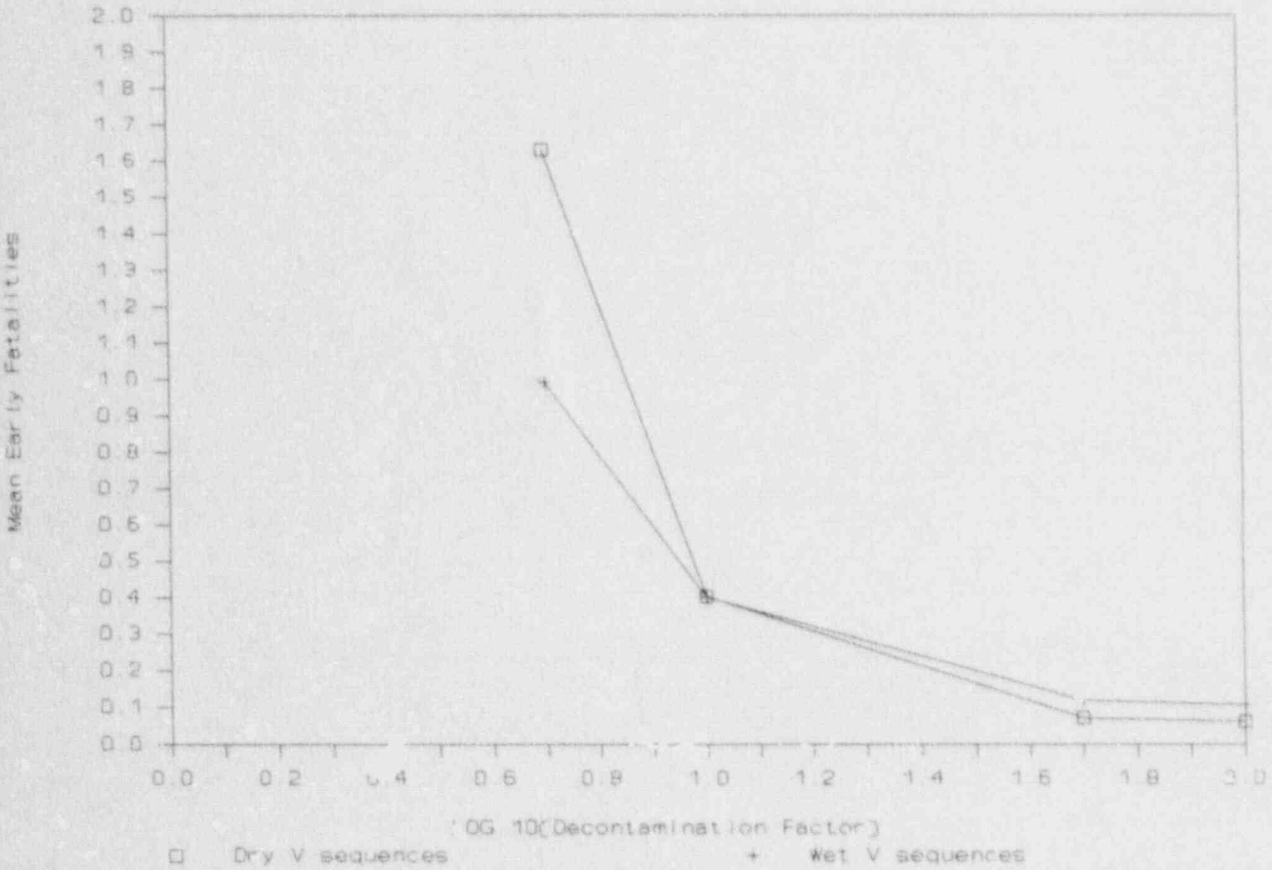

Figure G.7 Comparison of the dry and wet V sequences mean early fatality consequence results as a function of decontamination factor (release elevation = 10.0 m for DFs of 50.0 and 100.0, otherwise the elevation = 0.0 m).

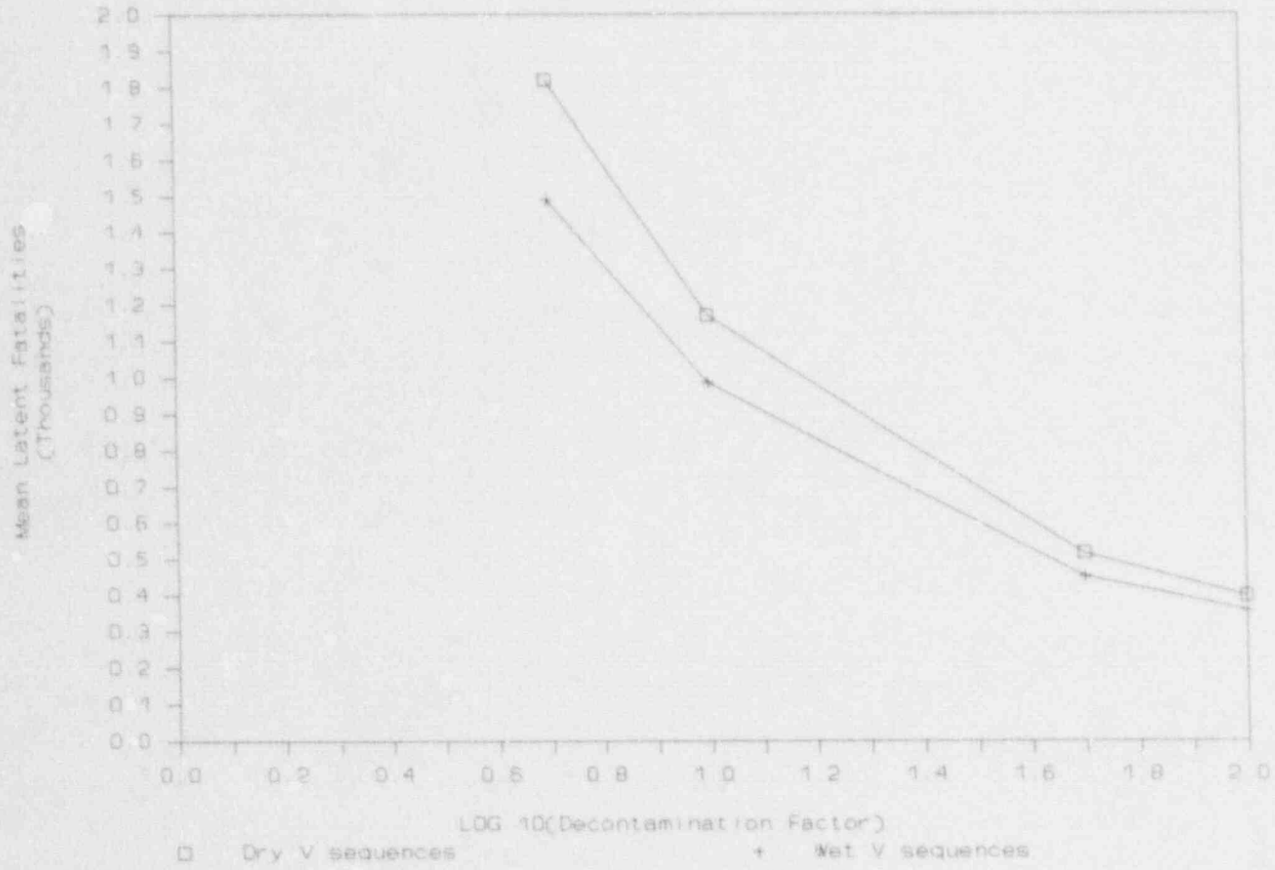

Figure G.8 Comparison of the dry and wet V sequences mean latent fatality consequence results as a function of decontamination factor (release elevation = 10.0 m for DFs of 50.0 and 100.0, otherwise elevation = 0.0 m).

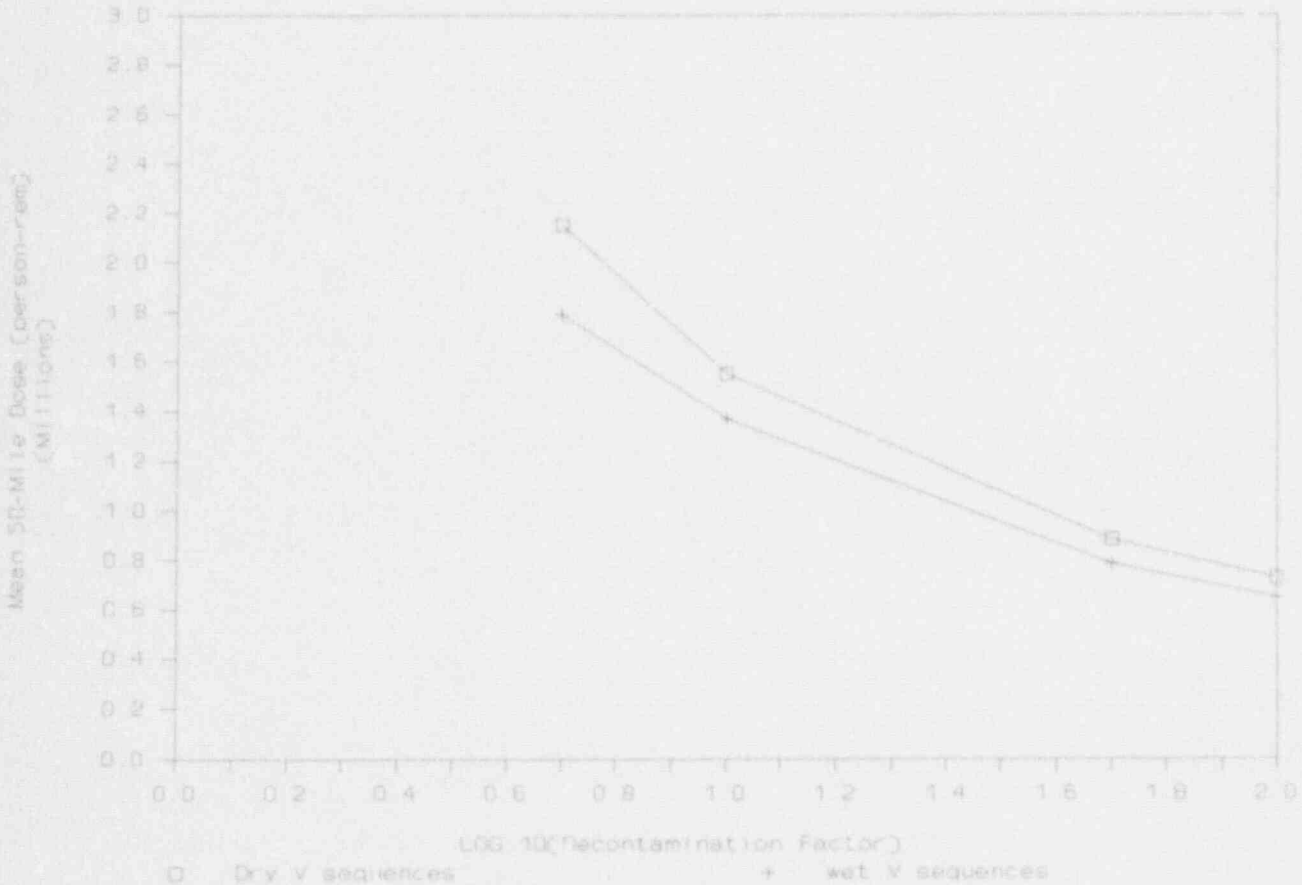

Figure G.9 Comparison of the dry and wet V sequences mean 50-mile population dose consequence results as a function of decontamination factor (release elevation = 10.0 m for DFs of 50.0 and 100.0, otherwise elevation = 0.0 m).

Appendix H

Component Failure Analysis

Pressure-Dependent Fragilities for Piping Components - Reference Combustion Engineering Plant

Prepared by
D. A. Wesley*, D. K. Nakaki, H. Hadidi-Tamjed*

ABB Impell Corporation
27401 Los Altos, Suite 480
Mission Viejo, CA 92691

Under Subcontract to:
Idaho National Engineering Laboratory
EG&G Idaho, Inc.
Idaho Falls, ID 83415

June, 1991

*EQE Inc.
Costa Mesa, CA

TABLE OF CONTENTS

TABLE OF CONTENTS (Continued)

LIST OF TABLES

LIST OF TABLES (Continued)

LIST OF TABLES (Continued)

LIST OF FIGURES

RECORD OF REVISIONS

Revision No.	Description
0	Issue of final report

1. INTRODUCTION

The work presented in this report is described in Revision 4 of the Task Action Plan for Generic Issue 105, ***Interfacing System LOCA in LWRs***, dated February 13, 1990. It is anticipated that the results documented here will facilitate the resolution of this high priority generic issue in a timely manner as well as the effort being undertaken by EPRI/NUMARC.

A probabilistic risk assessment of a reference Combustion Engineering plant is being conducted by EG&G Idaho, Inc., to evaluate the probability of plant damage from interfacing System Loss of Coolant Accidents (ISLOCA). ABB Impell Corporation is under subcontract to EG&G Idaho, Inc., to establish the pressure capacities of several low pressure systems to withstand pressures and temperatures above the design levels. The probability of failure as a function of internal pressure has been developed for the critical modes of failure of two fluid systems subject to potential overpressurization. The two segments identified by EG&G for the reference Combustion Engineering plant are the low pressure safety injection line (LPSI) on the suction side of the safety injection pump back to the refueling water storage pool, and the LPSI discharge lines to the reactor coolant system cold legs. Included in this evaluation are the pumps, valves, and flanged connections for this system. No vessels or heat exchangers were identified for evaluation. The variability in the probability of failure is included, and the estimated leak rates or leak areas are given for the controlling modes of failure. For this evaluation, all failures are based on quasi-static pressures since the probability of dynamic effects resulting from such causes as water hammer have been initially judged to be negligible for the reference Combustion Engineering plant.

The pressure capacities of the pipes and vessels are evaluated using limit state analyses for the various failure modes considered. The capacities are dependent on several factors, including the material properties, modeling assumptions, and the postulated failure criteria. A major source of uncertainty in the failure criteria is the expected strain resulting in failure. All welds are full penetration and the probability of failure at membrane strains below yield is considered to be quite low. On the other hand, biaxial strains and gage length effects as well as strain concentrations and bending significantly reduces the expected hoop strain at failure when compared to elongation data developed from standard specimen ultimate tests. Since test data from vessel tests are extremely limited, considerable variability is introduced,

not only in the failure criteria but in analytical modeling and other assumptions. In particular the limited data that do exist are related to finite length cylinders with internal pressure loading only, and no test results are available for such effects as thermal or bending strains in pipe, strain concentrations at branch connections, or nozzle loads on tanks. Since many of the base parameters are random and the methods used to evaluate the capacities are subject to some uncertainty, the pressure capacity for any failure mode is also considered to be a random variable.

A different approach must be used to evaluate the pressure capacities for gasketed flange connections, valves, and pumps. Unlike the failure modes for piping, vessels, and heat exchangers, which lend themselves to evaluation by general structural mechanics techniques, the failure modes for gasketed flange connections, valves, and pumps are very complex and the evaluation must rely primarily on the results from ongoing gasket research test programs and available vendor information and test data.

It is assumed that the pressure capacities have a lognormal distribution. This assumption is made because a lognormal distribution has been shown to be a valid description of the variability in material strengths. In addition, for a random variable that can be expressed as the product and quotient of several random variables, the distribution of the dependent variable tends to be lognormal regardless of the distributions of the independent base variables.

With the pressure capacity assumed to be a lognormal random variable and denoting it as P, the probability of failure occurring at a pressure less than or equal to a specific value p is expressed as:

$$P_f = \text{Prob}(P \leq p) = \Phi\left[\frac{\ln(p/\hat{P})}{\beta_c}\right] \qquad (1\text{-}1)$$

where: P_f = probability that failure occurs at a pressure $P \leq p$

P = random pressure capacity

β_c = logarithmic standard deviation of P

$\hat{P}$ = median pressure capacity

$\Phi(\cdot)$ = cumulative distribution function for a standard normal random variable

In Equation 1-1, the pressure capacity for a given failure mode is probabilistically described by the following expression,

$$P = \hat{P} \cdot M \cdot S \qquad (1-2)$$

in which $\hat{P}$ is the median pressure capacity, M is a lognormally distributed random variable having a unit median and a logarithmic standard deviation β_M representing the uncertainty in modeling, and S is also a lognormally distributed random variable with a unit median value and a logarithmic standard deviation β_S representing the uncertainty in the material properties. The overall uncertainty in the median capacity is obtained by taking the square root of the sum of the squares of β_M and β_S.

The median pressure capacity represents the internal pressure level for which there is a 50% probability of failure (leakage or burst) for a given failure mode. The median values are evaluated from limit state analyses for the different failure modes. The uncertainties, β_M and β_S, are associated with variability due to a lack of knowledge related to differences between the analytical model and the real structure. Modeling uncertainties are associated with the assumptions used to develop analytical models and their ability to properly represent the failure condition. The strength uncertainties are associated with variabilities related to the material resistance. Examples of the sources of strength uncertainties include: variability in steel yield and ultimate strengths, stress-strain relationships, and the influence of elevated temperatures on material strength.

Uncertainties will exist in the estimated pressure capacities due to differences between the analytical idealization of the structure and the real conditions. There are numerous possible sources of modeling uncertainties. Examples of the sources of modeling uncertainties include: assumptions used to develop the internal force distributions, failure criteria, and the use of empirical formulae. Moreover, since the uncertainties are dependent on the particular

failure mode under consideration, they must be evaluated on a case-by-case basis. However, in many instances, the evaluation of these uncertainties would require very detailed analysis and/or extensive data which may not be available. As a result, it was necessary to use subjective evaluation and engineering judgment to estimate these uncertainties.

The evaluation of the median capacities and the associated variabilities for the postulated failure modes for piping is discussed in Section 2 while the evaluation of median capacities and variabilities for flanged connections and valves are discussed in Sections 3 and 4, respectively.

2. PIPE

The piping of pertinence for ISLOCA consideration at the reference Combustion Engineering plant is fabricated from 304 Stainless Steel (i.e., SA 312, TP 304). The material properties for 304 Stainless Steel from Reference 1 were used for the pipe material. Ultimate strength values at room temperature up to 800°F (References 2 and 3) available in the literature were used to establish expected median strengths for the 304 SS. Table 2-1 shows the expected median ultimate strengths for room temperature, 400°F, 600°F, and 800°F, as well as the corresponding values for yield strength and elongation. Also shown for comparison are the corresponding ASME Code values. Table 2-2 shows similar expected median and code values for 316 SS (SA 312, TP 316, and TP 316 H for pipe).

As is apparent from these tables, a significant margin of safety often exists when the median material properties are compared with the corresponding code (lower bound) values. In a few instances, however, the median values available in the literature are close to, or even slightly lower than, the Code value; particularly for the 800°F temperature range. In all cases, however, since the systems and components being evaluated here were designed, for the most part, for relatively low pressures and temperature, ultimate pressure capacities for these components, governed by stresses near median ultimate values rather than the code design stress intensity, S_m, or allowable stress, S, values, are expected to be well in excess of the system design pressures.

2.1 Median Cylinder and Pipe Failure Pressure Criteria

Design stresses in piping system pressure vessels include provision for stresses resulting from deadweight, thermal expansion, nozzle loads, earthquake and other loads as well as internal pressure. Stresses from other than internal pressure may constitute a major or even the controlling portion of the design allowable stress. At overpressure conditions, however, the percentage of available strength required to resist the nonpressure loads may be expected to decrease (i.e., the deadweight stress in a piping system does not increase with an increase in pressure, and while thermal stresses may increase above the design case, they are not expected to be the controlling load). Thus, the failure criteria developed for pipe and pressure vessel burst is concentrated on the internal pressure effects, as reflected in the

hoop stress in a cylinder, while still retaining some consideration for other loads such as bending or branch connections in pipe, or nozzle loads in tanks. The goal was to develop criteria which could reasonably include these additional effects without requiring a detailed evaluation in order to obtain the actual magnitudes of the bending stresses, etc., at every location and temperature.

Failure due to hoop stress in a basically unflawed cylinder can be expected when the failure strain is reached. Several factors influence the failure strain when compared to the elongation predicted from a simple uniaxial 2-inch gage specimen, however. First, an unrestrained cylinder is in a state of biaxial stress and it is known that failure strains are reduced for multiaxial stress states. Manjoine (Reference 4) suggests a triaxial reduction factor of the form:

$$T.F. = \frac{\sqrt{2}(\sigma_1 + \sigma_2 + \sigma_3)}{[(\sigma_1 - \sigma_2)^2 + (\sigma_1 - \sigma_3)^2 + (\sigma_2 - \sigma_3)^2]^{1/2}} \qquad (2\text{-}1)$$

where $\sigma_i (i = 1,2,3)$ are the principal stresses.

For an unrestrained cylinder with no bending subjected to internal pressure, the hoop stress is twice the axial stress and the maximum radial stress equal to the internal pressure is small, compared to the hoop and axial stresses. For this condition,

$$\sigma_1 = 2\sigma_2 \qquad \text{and} \qquad \sigma_3 = 0$$

and T. F. = 1.73

Including provision for bending such th[illegible]

$$\sigma_1 = \sigma_2 \qquad \text{and} \qquad \sigma_3 = 0$$

results in T.F. = 2.

Thus, failure strain in a cylinder fabricated from a material with uniaxial elongation, ϵ, due to hoop stress could be expected in the range of:

$$\epsilon_{f.r.} = \frac{\epsilon}{1.73} \quad to \quad \frac{\epsilon}{2}$$

Another factor which can influence the failure strain in a pipe or vessel is the effective gage length. Part of the elongation reported for a 2-inch uniaxial test specimen results from necking. For longer specimens, the necking portion of the elongation remains essentially constant so that the total elongation for longer length specimen is less (i.e., the elongation for a uniaxial 8-inch test specimen is less than for a 2-inch specimen). For a segment of pipe, the effective gage length may be expected to be of the order of the pipe circumference, and a further reduction on failure strain of the order of 1.5 to 2 is estimated. For pressure vessels with strain concentrations due to under- or over-reinforced nozzles and other discontinuities, failure is expected at somewhat lower average strains. Based on failure strain values which have been reduced to account for the triaxial and gage length effects and based on the typical stress-strain relationships for strain hardening carbon and austenitic steels, failure stresses can therefore be expected at about 0.9 and 0.85 of the ultimate uniaxial stress, respectively. Based on the limited available data, these ratios are assumed independent of temperature. Therefore, including the increased radius at failure and using the corrected stress, the median pressure for failure in a thin-walled circular cylinder can be found from the simple relationship:

$$P_f = \frac{\bar{\sigma}_f \, t}{r(1+\epsilon_f)} \qquad (2\text{-}2)$$

where: P_f is the median failure pressure

$\bar{\sigma}_f$ is the median failure stress

t is the wall thickness (nominal)

r is the initial inside radius

and ϵ_f is the median hoop strain at failure

This approach defines the failure pressure in terms of hoop stress which is an easy parameter to quantify but includes some provision for the biaxial stress-state and strain concentration effects.

2.2 Cylinder and Pipe Failure Pressure Variability

The variability associated with the calculated cylinder failure pressure results from a number of sources including material strength, wall thickness, variability in the stress-strain relationship, uncertainty related to the biaxial stress condition, necking and strain concentration effects on the failure strain and bending or discontinuity stresses. Most important, however, may be the existence, size, and orientation of partial through-wall flaws in the cylinder wall. To conduct a rigorous, probabilistic fracture mechanics evaluation of all the piping and vessels important for ISLOCA requires a knowledge of the crack depth, crack length, crack orientation, and fracture toughness including biaxial load and corrosion effects, both now and at end of plant life. In addition to a mean or median value of the above parameters, the statistical distribution and coefficient of variation would be required. Current evaluations are being conducted to accumulate and evaluate this type of data, but a rigorous evaluation based on this type of data requires consideration of the stress-state at every pipe weld and component over the entire range of temperatures which is beyond the scope of the current program.

Therefore, for the current investigation, the variability was developed for a log-normal distribution by assuming a probability of failure of 0.001 corresponding to yield in the cylinder. This approach, in essence, assumes the possibility that a large flaw may exist which would be required to fail the cylinder at yield but eliminates the need to determine how the flaw was developed. Since the controlling failure condition is based on hoop stress, the above assumption of failure at yield implies the controlling flaw is an axial crack although a larger circumferential crack could also lead to the same failure at yield. Whether the crack was present at fabrication or whether it was initiated and grew due to causes such as thermal fatigue, water hammer, or corrosion, is unknown and is not required with this assumption.

In essence then, the assumption of 0.001 probability of failure at yield implies a 0.001 probability of the existence of a very large flaw or combination of a large flaw with high thermal stress, etc. This is believed to be a very conservative (probably overconservative) assumption. If it is found that a significant contribution to the total risk occurs due to pipe or

vessel burst at pressures well below the median burst pressures, then this assumption should be reevaluated. This would require that burst, as opposed to flange leakage, is determined to be the dominant failure mode but could easily be evaluated by sensitivity studies where the variability is based on probability of failure at yield is assumed to be 10^{-4} or 10^{-5}, for instance, or by truncating the tails of the distribution in the range of .02 to .04. If the overall risk is found to be sensitive to these assumptions, further research into the probability of expected flaw size may be necessary.

2.3 Cylinder and Pipe Failure Stress and Variability

Using the methods described in Sections 2.1 and 2.2 above, median hoop failure stresses and variabilities were developed for the materials and temperature range for both pipes and vessels. Due to the possibility of strain concentrations due to nozzles and other discontinuity stresses in tanks, somewhat lower median failure stresses, along with decreased variabilities, were used for tanks and vessels compared to pipe. Table 2-3 shows the failure stresses and corresponding lognormal standard deviations for the material used in this investigation.

In general, the failure stresses decrease with temperature, but due primarily to change in the ratio of yield-to-ultimate with temperature, the lognormal standard deviation tends to increase with temperature. Note, however, the tendency of the failure stress for the low carbon steels to increase in the 400° to 600°F range. This characteristic results from the corresponding increase in ultimate strength in same temperature range, although the yield strength of the same material shows essentially a monotonic decrease with temperature (c.f., Reference 5). The lognormal standard deviations, shown in Table 2-3, are considered to be representative (although probably conservative) for cylinders with median pressure determined essentially for unflawed vessels but admitting the possibility of the presence of very large flaws. As such, a lognormal distribution is considered reasonable for failure pressure of the order of plus one standard deviation and below. However, at failure pressures in the high end of the distribution, the use of the lognormal distribution is inappropriate and some upper bound cutoff is required. This occurs physically since the presence of flaws can significantly reduce the failure pressure below the median unflawed cylinder, but the absence of flaws cannot further strengthen the cylinder above the assumed median unflawed cylinder capacity. This upper bound cutoff is controlled essentially by the ultimate strength of the

material without including the biaxial load and strain concentration reduction effects. In essence, the upper bound cutoff is expected to correspond more closely to the failure of a cylinder with no bending, nozzles, branch connections, or flaws, and is representative of the results obtained from finite length unflawed cylinder test results. The cutoff is also not a discrete value but has a median with associated uncertainty governed by the material strength properties.

2.4 Pipe Capacities

All pipe of concern for the reference Combustion Engineering plant ISLOCA investigation is fabricated from TP 304 stainless steel. Median burst pressures for the temperature range of interest are presented for various assumed levels of corrosion in Tables 2-4 through 2-6. The associated variabilities at these temperatures are given in Table 2-3. Note that the variabilities given in Table 2-3 are for failure stress but can also be used for failure pressure since the contribution of other elements to the total variability is expected to be negligible.

Table 2-1. 304 Stainless Steel Material Properties

Temperature (°F)	Ultimate Strength (ksi)		Yield Strength (ksi)		Elongation (%) (2-inch gage)	
	Median	Code*	Median	Code	Median	Code
R.T.	86	75	37	30	60	35 (long.) 25 (trans.)
400	74	64.4	23	20.7	53	
600	70	63.5	19.5	18.2	49	
800	65.5	62.7	16.5	16.8	46	

* SA 312, TP 304, and TP 304 H

Table 2-2. 316 Stainless Steel Material Properties

Temperature (°F)	Ultimate Strength (ksi)		Yield Strength (ksi)		Elongation (%) (2-inch gage)	
	Median	Code*	Median	Code	Median	Code
R.T.	86.5	75	42	30	46	35 (long.) 25 (trans.)
400	81.5	71.8	35	21.4	43	
600	77.5	71.8	31	18.8	41.5	
800	73	70.9	28	17.6	40	

* SA 312, TP 316, and TP 316 H

Table 2-3. Failure Stresses and Variability for 304 SS

Temperature (°F)	Pipe		Vessel	
	$\hat{\sigma}$, (ksi)	β	$\hat{\sigma}$, (ksi)	β
R.T.	74	0.22	67	0.19
400	62.9	0.33	57.9	0.30
600	59.5	0.36	54.6	0.33
800	55.7	0.39	51.2	0.37

where $\hat{\sigma}$, denotes the median hoop failure stress

Table 2-4. 304 Stainless Steel Pipe Failure Pressures

CORROSION ALLOWANCE = 0.000

Pipe Size (in)	Schedule	OD (in)	ID (in)	MEDIAN FAILURE PRESSURES 70°F	400°F	600°F	800°F
1-1/2	40S	1.900	1.610	9968	8556	7963	7525
	80	1.900	1.500	14757	12666	11788	11140
	160	1.900	1.337	23303	20001	18615	17591
2	40S	2.375	2.067	8246	7078	6587	6225
	80	2.375	1.939	12443	10680	9940	9393
	160	2.375	1.689	22476	19292	17955	16967
3	10S	3.500	3.260	4074	3497	3254	3075
	40S	3.500	3.068	7792	6688	6225	5882
	80	3.500	2.900	11449	9827	9146	8643
	160	3.500	2.624	18474	15857	14758	13946
4	10S	4.500	4.260	3118	2676	2490	2353
	40S	4.500	4.026	6515	5592	5205	4918
	80	4.500	3.826	9749	8367	7787	7359
	160	4.500	3.438	17094	14672	13655	12904
6	10S	6.625	6.357	2333	2002	1864	1761
	40S	6.625	6.065	5110	4386	4082	3857
	80	6.625	5.761	8299	7123	6630	6265
	120	6.625	5.501	11307	9705	9032	8536
	160	6.625	5.189	15314	13145	12234	11561
8	10S	8.625	8.329	1967	1688	1571	1485
	20	8.625	8.125	3405	2923	2720	2571
	40S	8.625	7.981	4465	3833	3567	3371
	80	8.625	7.625	7258	6229	5798	5479
	120	8.625	7.189	11054	9488	8830	8344
	140	8.625	7.001	12837	11018	10254	9690
	160	8.625	6.813	14718	12633	11757	11110
10	10S	10.750	10.420	1753	1504	1400	1323
	20	10.750	10.250	2699	2317	2156	2038
	40S	10.750	10.020	4032	3460	3221	3043
	80	10.750	9.564	6862	5890	5482	5180
	120	10.750	9.064	10294	8835	8223	7770
	140	10.750	8.750	12649	10857	10104	9548
	160	10.750	8.500	14649	12573	11702	11058
12	10S	12.750	12.390	1608	1380	1284	1214
	20	12.750	12.250	2259	1939	1804	1705
	Std	12.750	12.000	3459	2969	2763	2611
	40	12.750	11.938	3764	3231	3007	2841
	80	12.750	11.376	6684	5737	5339	5046
	120	12.750	10.750	10296	8837	8224	7772
	140	12.750	10.500	11858	10178	9473	8952
	160	12.750	10.126	14340	12308	11455	10825
14	10S	14.000	13.624	1527	1311	1220	1153
	20	14.000	13.375	2586	2220	2066	1952
	Std	14.000	13.250	3132	2689	2502	2365
	40	14.000	13.125	3689	3167	2947	2785
	80	14.000	12.500	6641	5700	5305	5013
	120	14.000	11.814	10240	8789	8180	7730
	140	14.000	11.500	12026	10326	9610	9081
	160	14.000	11.188	13909	11938	11111	10500

Calculation 304P000

Table 2-4. 304 Stainless Steel Pipe Failure Pressures (Continued)

CORROSION ALLOWANCE = 0.000

Pipe Size (in)	Schedule	OD (in)	ID (in)	MEDIAN FAILURE PRESSURES 70°F	400°F	600°F	800°F
16	10S	16.000	15.624	1332	1143	1064	1005
	20	16.000	15.375	2250	1931	1797	1698
	Std	16.000	15.250	2722	2336	2174	2054
	40	16.000	15.000	3689	3167	2947	2785
	80	16.000	14.314	6518	5595	5207	4920
	120	16.000	13.564	9939	8530	7939	7502
	140	16.000	13.124	12127	10409	9687	9154
	160	16.000	12.814	13759	11810	10991	10387
18	10S	18.000	17.624	1181	1013	943	891
	20	18.000	17.375	1991	1709	1590	1503
	Std	18.000	17.250	2406	2065	1922	1816
	40	18.000	16.876	3686	3164	2944	2782
	80	18.000	16.126	6431	5520	5137	4855
	120	18.000	15.250	9979	8565	7972	7533
	140	18.000	14.876	11621	9975	9283	8773
	160	18.000	14.433	13677	11739	10925	10324
20	10S	20.000	19.564	1293	1059	985	931
	20S	20.000	19.250	2156	1851	1722	1628
	40	20.000	18.814	3488	2994	2787	2633
	80	20.000	17.938	6361	5460	5082	4802
	120	20.000	17.000	9766	8382	7801	7372
	140	20.000	16.500	11739	10075	9377	8861
	160	20.000	16.064	13559	11638	10831	10236
24	10S	24.000	23.500	1177	1011	941	889
	20S	24.000	23.250	1785	1532	1426	1348
	40	24.000	22.626	3361	2884	2684	2537
	80	24.000	21.564	6251	5366	4994	4719
	120	24.000	20.376	9842	8448	7862	7430
	140	24.000	19.876	11482	9855	9172	8668
	160	24.000	19.314	13426	11524	10725	10135

Calculation 304P000

Table 2-5. 304 Stainless Steel Pipe Failure Pressures

CORROSION ALLOWANCE = 0.020

Pipe Size (in)	Schedule	OD (in)	ID (in)	MEDIAN FAILURE PRESSURES 70°F	400°F	600°F	800°F
1-1/2	40S	1.900	1.610	8593	7375	6864	6487
	80	1.900	1.500	13281	11399	10609	10026
	160	1.900	1.337	21647	18580	17292	16341
2	40S	2.375	2.067	7175	6158	5732	5418
	80	2.375	1.939	11302	9700	9028	8532
	160	2.375	1.689	21166	18167	16908	15978
3	10S	3.500	3.260	3395	2914	2712	2563
	40S	3.500	3.068	7071	6069	5648	5338
	80	3.500	2.900	10686	9172	8536	8067
	160	3.500	2.624	17631	15133	14084	13309
4	10S	4.500	4.260	2598	2230	2075	1961
	40S	4.500	4.026	5966	5120	4765	4503
	80	4.500	3.826	9170	7871	7325	6922
	160	4.500	3.438	16450	14119	13141	12418
6	10S	6.625	6.357	1985	1704	1585	1498
	40S	6.625	6.065	4745	4072	3790	3582
	80	6.f	5.761	7915	6794	6323	5975
	120	6.	5.501	10905	9360	8711	8232
	160	6.'	5.189	14888	12778	11893	11239
8	10S	8.625	8.329	1701	1460	1359	1284
	20	8.625	8.125	3133	2689	2503	2365
	40S	8.625	7.981	4188	3595	3345	3161
	80	8.625	7.625	6967	5980	5566	5259
	120	8.625	7.189	10746	9223	8584	8112
	140	8.625	7.001	12521	10747	10002	9452
	160	8.625	6.813	14393	12354	11498	10865
10	10S	10.750	10.420	1540	1322	1230	1163
	20	10.750	10.250	2484	2132	1984	1875
	40S	10.750	10.020	3811	3271	3044	2877
	80	10.750	9.564	6631	5691	5297	5006
	120	10.750	9.064	10049	8625	8028	7586
	140	10.750	8.750	12396	10640	9902	9357
	160	10.750	8.500	14388	12349	11494	10861
12	10S	12.750	12.390	1429	1227	1142	1079
	20	12.750	12.250	2078	1784	1660	1569
	Std	12.750	12.000	3274	2810	2616	2472
	40	12.750	11.938	3579	3072	2859	2701
	80	12.750	11.376	6489	5570	5184	4899
	120	12.750	10.750	10090	8660	8060	7617
	140	12.750	10.500	11648	9997	9304	8793
	160	12.750	10.126	14122	12121	11281	10660
14	10S	14.000	13.624	1365	1171	1090	1030
	20	14.000	13.375	2420	2077	1933	1827
	Std	14.000	13.250	2965	2545	2369	2238
	40	14.000	13.125	3521	3022	2812	2658
	80	14.000	12.500	6464	5548	5163	4879
	120	14.000	11.814	10052	8628	8030	7588
	140	14.000	11.500	11838	10160	9456	8936
	160	14.000	11.188	13711	11768	10953	10350

Calculation 304P020

Table 2-5. 304 Stainless Steel Pipe Failure Pressures (Continued)

CORROSION ALLOWANCE = 0.020

Pipe Size (in)	Schedule	OD (in)	ID (in)	MEDIAN FAILURE PRESSURES 70°F	400°F	600°F	800°F
16	10S	16.000	15.624	1190	1021	951	898
	20	16.000	15.375	2106	1807	1682	1589
	Std	16.000	15.250	2576	2211	2058	1945
	40	16.000	15.000	3542	3040	2829	2674
	80	16.000	14.314	6364	5462	5083	4804
	120	16.000	13.564	9775	8390	7809	7379
	140	16.000	13.124	11958	10264	9553	9027
	160	16.000	12.814	13586	11661	10853	10256
18	10S	18.000	17.624	1055	906	843	796
	20	18.000	17.375	1863	1599	1488	1407
	Std	18.000	17.250	2278	1955	1819	1719
	40	18.000	16.876	3555	3051	2839	2683
	80	18.000	16.126	6294	5402	5028	4751
	120	18.000	15.250	9834	8441	7856	7424
	140	18.000	14.876	11473	9847	9165	8660
	160	18.000	14.433	13523	11607	10803	10208
20	10S	20.000	19.564	1120	961	895	846
	20S	20.000	19.250	2041	1752	1630	1541
	40	20.000	18.814	3371	2893	2693	2545
	80	20.000	17.938	6238	5354	4983	4709
	120	20.000	17.000	9636	8270	7697	7274
	140	20.000	16.500	11604	9960	9270	8760
	160	20.000	16.064	13421	11520	10721	10132
24	10S	24.000	23.500	1083	930	865	818
	20S	24.000	23.250	1690	1450	1350	1276
	40	24.000	22.626	3263	2800	2606	2463
	80	24.000	21.564	6149	5278	4912	4642
	120	24.000	20.376	9734	8355	7776	7348
	140	24.000	19.876	11371	9760	9083	8584
	160	24.000	19.314	13312	11426	10634	10049

Calculation 304P020

Table 2-6. 304 Stainless Steel Pipe Failure Pressures

CORROSION ALLOWANCE = 0.040

Pipe Size (in)	Schedule	OD (in)	ID (in)	MEDIAN FAILURE PRESSURES 70°F	400°F	600°F	800°F
1-1/2	40S	1.900	1.610	7218	6195	5766	5449
	80	1.900	1.500	11506	10133	9431	8912
	160	1.900	1.337	19992	17159	15970	15091
2	40S	2.375	2.067	6104	5239	4876	4608
	80	2.375	1.939	10160	8721	8116	7670
	160	2.375	1.689	19855	17042	15861	14988
3	10S	3.500	3.260	2716	2331	2170	2050
	40S	3.500	3.068	6349	5450	5072	4793
	80	3.500	2.900	9923	8517	7927	7491
	160	3.500	2.624	16787	14409	13410	12672
4	10S	4.500	4.260	2078	1784	1660	1569
	40S	4.500	4.026	5416	4648	4326	4088
	80	4.500	3.826	8592	7374	6863	6486
	160	4.500	3.438	15807	13567	12627	11932
6	10S	6.625	6.357	1637	1405	1307	1235
	40S	6.625	6.065	4380	3759	3499	3306
	80	6.625	5.761	7531	6464	6016	5685
	120	6.625	5.501	10502	9014	8390	7928
	160	6.625	5.189	14461	12412	11552	10917
8	10S	8.625	8.329	1435	1232	1146	1083
	20	8.625	8.125	2861	2455	2285	2159
	40S	8.625	7.981	3911	3357	3124	2952
	80	8.625	7.625	6677	5731	5334	5040
	120	8.625	7.189	10438	8959	8338	7880
	140	8.625	7.001	12204	10475	9749	9213
	160	8.625	6.813	14068	12075	11238	10620
10	10S	10.750	10.420	1328	1140	1061	1002
	20	10.750	10.250	2268	1946	1811	1712
	40S	10.750	10.020	3590	3081	2868	2710
	80	10.750	9.564	6400	5493	5112	4831
	120	10.750	9.064	9805	8416	7833	7402
	140	10.750	8.750	12143	10422	9700	9166
	160	10.750	8.500	14128	12126	11286	10665
12	10S	12.750	12.390	1251	1073	999	944
	20	12.750	12.250	1897	1628	1516	1432
	Std	12.750	12.000	3090	2652	2468	2332
	40	12.750	11.938	3393	2912	2711	2561
	80	12.750	11.376	6295	5403	5028	4752
	120	12.750	10.750	9884	8483	7895	7461
	140	12.750	10.500	11437	9816	9136	8633
	160	12.750	10.126	13903	11933	11106	10495
14	10S	14.000	13.624	1202	1032	960	908
	20	14.000	13.375	2255	1935	1801	1702
	Std	14.000	13.250	2798	2402	2235	2112
	40	14.000	13.125	3352	2877	2678	2530
	80	14.000	12.500	6287	5396	5022	4746
	120	14.000	11.814	9865	8467	7880	7447
	140	14.000	11.500	11645	9995	9302	8791
	160	14.000	11.188	13513	11599	10795	10201

Calculation 304P040

Table 2-6. 304 Stainless Steel Pipe Failure Pressures (Continued)

CORROSION ALLOWANCE = 0.040

Pipe Size (in)	Schedule	OD (in)	ID (in)	MEDIAN FAILURE PRESSURES 70°F	400°F	600°F	800°F
16	10S	16.000	15.624	1048	900	837	791
	20	16.000	15.375	1962	1684	1567	1481
	Std	16.000	15.250	2431	2087	1942	835
	40	16.000	15.000	3394	2913	2711	2562
	80	16.000	14.314	6209	5329	4960	4687
	120	16.000	13.564	9612	8250	7678	7256
	140	16.000	13.124	11790	10119	9418	8900
	160	16.000	12.814	13414	11513	10715	10126
18	10S	18.000	17.624	929	798	742	702
	20	18.000	17.375	1736	1490	1387	1310
	Std	18.000	17.250	2149	1845	1717	1623
	40	18.000	16.876	3423	2938	2735	2584
	80	18.000	16.126	6156	5284	4918	4647
	120	18.000	15.250	9689	8316	7740	7314
	140	18.000	14.876	11324	9719	9046	8548
	160	18.000	14.433	13370	11475	10680	10093
20	10S	20.000	19.564	1007	864	804	760
	20S	20.000	19.250	1926	1653	1539	1454
	40	20.000	18.814	3253	2792	2599	2456
	80	20.000	17.938	6115	5248	4884	4616
	120	20.000	17.000	9505	8158	7593	7175
	140	20.000	16.500	11470	9845	9163	8659
	160	20.000	16.064	13284	11401	10611	10028
24	10S	24.000	23.500	989	849	790	747
	20S	24.000	23.250	1595	1369	1274	1204
	40	24.000	22.626	3165	2716	2528	2389
	80	24.000	21.564	6046	5189	4830	4564
	120	24.000	20.376	9625	8261	7689	7266
	140	24.000	19.876	11259	9664	8994	8499
	160	24.000	19.314	13197	11327	10542	9962

Calculation 304P040

3. GASKETED-FLANGE CONNECTIONS

3.1 Introduction

Although most of the piping joints in the safety injection system are full penetration butt welds, a number of gasketed-flange connections are required for the installation and maintenance of flow-restricting orifices, flow elements, and major equipment components. The elements of the flanged joints include standard ANSI B16.5 flanges with asbestos-filled, spiral-wound gaskets.

The lines designed for 150, 300, and 400lb rated service employ raised-face flanges fabricated from Type 304 stainless steel and are secured by means of SA-193 B8 bolts or studs and SA-564 Grade 630-HT 1100 studs. The minimum room temperature yield and ultimate strengths for the SA-193 B8 material are 30,000 and 75,000 psi, respectively. Similarly, for the SA-564 Grade 630 material, the minimum room temperature yield and ultimate strengths are 115,000 and 140,000 psi, respectively.

3.2 Variables Affecting Flanged Joint Leakage

The behavior of gasketed-flanges under pressure and temperature conditions is quite complex. The propensity for leakage, under a given pressure loading, is as much or more dependent upon the previous history of the joint than it is on its state at the time the pressure is applied. As a result, numerous variables are introduced. These include:

- Bolt/Stud Preload
- Bolt/Stud Temperature
- Bolt/Stud Yield Strength
- Bolt/Stud Stress-Strain Relationship
- Bolt Relaxation
- Flange Flexibility
- Initial Gasket Stress
- Gasket Loading Stiffness

- Gasket Unloading/Reloading Stiffness
- Gasket Creep and Relaxation
- Pipe Bending Moments

3.2.1 Bolt/Stud Preload

Reference 6 provides bolt torquing procedures for flanged connections. The procedure indicates that the bolt torque values are to be obtained from vendor information or other approved site documents. However, for cases when the torque value cannot be obtained from vendor information or approved site documents, Reference 6 does provide recommended torque values for various bolt sizes and bolt materials. Using these data and noting that there is variability in the expected bolt torque values since vendors typically provide a recommended range of bolt torques, the SA-193 B8 bolts were considered to have a median initial prestress of 25,000 psi. In the parameter studies, a range of bolt preload stresses from 20,000 to 30,000 psi was considered and the range from 25,000 to 30,000 psi was taken to represent a 2.33β variation. For the SA-564 Grade 630 bolts, the median bolt preload stress was taken as 60,000 psi and the range from 50,000 to 60,000 was taken as a 2.33β variation. On the pipelines and components of interest, SA-193 B8 bolts are used with the 150lb flanges, both SA-193 B8 and SA-564 Grade 630 bolts are used with 300lb flanges, while the 400lb flanges are installed with the SA-193 B8 bolts.

It should be remembered that the uncertainty variability is related to the parameter of interest such as leak rate or leak area. Thus, the variability is calculated from the variation in say, leak rate resulting from the variations in initial bolt stress noted above.

3.2.2 Bolt/Stud Temperature

The maximum operating temperatures for the low pressure portions of the safety systems under consideration range from 120 to 350°F. As a result, the bolt temperature is likely to be less than 200°F during normal operation. However, during the ISLOCA event, the reactor coolant system pressure and temperature conditions of 2250 psi and 650°F can propagate back through the initially cold, non-operating systems. Based on preliminary analyses of the system, it is our understanding that the pressure propagates much more rapidly than the fluid temperature. Specifically, a relatively large leak at the flange connection or

downstream (reverse flow condition) of the flange connection must occur in order for the flange or flange bolting temperatures to rise substantially. In addition, for higher temperature conditions in the pipe, flow must continue for a relatively long period of time before the bolting temperature will rise substantially. Thus, it was judged that potential flange leakage will most likely occur under high-pressure, low-temperature conditions and that leak rates and leak areas will increase somewhat as the flange and bolt temperatures increase. Based on these considerations, a bolt temperature of approximately 140°F was taken to represent the median case and the effect of higher bolt temperatures was not considered. Evaluation of higher bolt temperatures, should they occur, can be modeled employing lower elastic modulus, yield strength, and ultimate strength values.

3.2.3 Bolt/Stud Yield Strength

The SA-193 Grade B8 bolt material is a Type 304 stainless steel. The material properties of Type 304 stainless steel are given in Table 2-1 of this report. Consistent with the selected 140°F median value for the flange bolt/stud temperature, a value of 33,000 psi was taken as the median bolt yield strength. The ASME code minimum value of 27,500 psi was taken to represent a -2.33β variation.

The SA-564 Grade 630 bolt/stud material is a precipitation-hardened, high alloy steel. At the 140°F median temperature, the median bolt/stud yield strength was taken to be 122,000 psi. The ASME code minimum yield strength of 111,000 psi was taken as a -2.33β variation.

3.2.4 Bolt/Stud Stress-Strain Relationship

References 2 and 3 provide limited data on the stress-strain curve to failure for Type 304 stainless steel at room and elevated temperatures. These data were interpolated to estimate the strain at failure for a bolt temperature of 140°F and were scaled to median material properties. The resulting curve was approximated in a piecewise linear fashion. A similar approach was used for the SA-564 Grade 630bolt/stud material to arrive at a piecewise linear stress-strain relation.

3.2.5 Bolt Relaxation

For stainless steel bolts which are initially torqued to prestress levels exceeding the material yield strength, some relaxation will occur. This relaxation requires substantial time, particularly at the relatively low bolt temperatures experienced during normal plant operation. Relaxation during the course of the ISLOCA event is judged to be negligible. Since the bolts used at the reference Combustion Engineering plant are not initially torqued to prestress levels exceeding the material yield strength, bolt relaxation was not included in this study.

3.2.6 Flange Flexibility

The flanged joint consists of the flange, the flange bolting, and the gasket. To study specific variables most test programs isolate one or more of the joint elements, such as the flexibility of the flange. However, to properly characterize the overall joint behavior, all three elements must function as part of an integral unit. In order to evaluate the joint behavior, three axisymmetric elastic finite element joint models (Reference 8) were developed. The models were for a 4"-300lb flange, a 12"-300lb flange, and a 4"-150lb flange and included the flange and pipe structure, bolt stiffness, and gasket unloading stiffness. Material properties were taken at 200°F. As expected, it was found that flange flexibility affects the way that the pressure load is carried by the gasket and bolting. As the relative flange stiffness increases, a greater portion of the pressure load goes to loading the bolting and a lesser portion goes to unloading the gasket. Thus, for larger flanges or more flexible flanges (lower pressure rating), the portion of the pressure load going to the unloading of the gasket increases. This can be seen in Figure 3-1 which plots the results of the three analyses. In this figure, the ratio of the load removed from the gasket to the total pressure load is plotted versus nominal flange size. For the elastic case of the 4"-300lb flange, about 43% of the total pressure load goes to unloading the gasket while the remaining 57% is carried by increased bolt load. The ratio for the larger 12"-300lb flange is approximately 86% and the ratio for the lighter weight 4"-150lb flange is about 59%. It is likely that the variation of the ratio with flange size is more complex than the linear variation shown, but project time constraints limited the scope of this supporting study. Due to the lack of specific data, the maximum value of the incremental gasket load to total pressure load ratio was set at 1.0. However, for flanges which are flexible relative to the gasket, experience has shown that the ratio can be greater than 1.0 such that an increase in pressure results in a decrease in flange bolt tension.

Both SA-193 B8 and SA-564 Grade 630 flange bolts are used for the gasketed-flange connections at the reference Combustion Engineering plant. Since the SA-193 B8 material is a relatively low strength Type 304 stainless steel, leak areas at higher pressure are primarily governed by the inelastic deformation of the bolts with the flange remaining essentially elastic. On the other hand, the SA-564 Grade 630 material has a high yield strength and the flanges are stressed to higher levels. At high pressures, some inelastic behavior in the flange could be expected, in which case the inelastic deformation of the flange at the gasket could be a significant contributor to the leak areas. However, further detailed studies of flange flexibility with high strength bolts was not pursued because the flanges joined by the high strength bolts were found to have high gross leak pressure capacities.

3.2.7 Initial Gasket Stress

Over the past several years, the Pressure Vessel Research Committee (PVRC) of the Welding Research Council has sponsored a major ongoing gasket test program as part of its Long Range Flanged Joint Improvement Program. Most of the tests have been conducted with nitrogen or helium as the test fluid; however, a limited data set exists for tests using water. Some of the results of the test program are reported in References 9 through 12. These results clearly indicate that the leak resistance of a gasketed-flange joint is a function of the initial level to which the gasket is stressed during the preloading of the flange bolting. The higher the initial gasket stress, the greater the leak resistance. The gasket stress versus deflection curve (Figure 3-2) and the mass leak rate versus gasket stress curve (Figure 3-3) for a typical spiral-wound gasket are both characterized by the presence of a "knee" at a gasket stress of approximately 5,000 psi. Above 5,000 psi, the leak rate drops more rapidly with increasing stress indicating improved sealing performance. Thus, although the controlled variable in assembling a flanged connection is bolt preload, it is the resulting gasket stress which determines the leak resistance of the joint for the pressure loading.

3.2.8 Gasket Loading Stiffness

The loading stiffness parameter is of importance since it determines whether or not the flange raised face bottoms out on the 0.125" thick compression gauge ring due to the bolt preload. Spiral-wound gaskets used for virtually all applications are fabricated to the requirements of Military Specification MIL-G-21032E, including Amendment 2 (Reference 13).

This standard specifies the test load and corresponding deflection for each gasket size and service rating. Gaskets with an initial nominal thickness of 0.175" are to be compressed to a thickness of 0.130 ± 0.005" under the specified test load while gaskets with an initial nominal thickness of 0.125" are to be compressed to a thickness of 0.100 ± 0.005". Figure 3-2 shows the gasket stress versus deflection for the loading sequence of a typical spiral-wound gasket and Table 3-1 presents the range of gasket stiffness (expressed as gasket stress per inch of deflection) which meet the specification. The Reference 13 specified test load is shown together with the resulting bolt stress (based on bolt stress area). Test loads greater than 557000 lbs are not specified since this load is judged to be the practical limit of testing facilities. However, since the specified test load corresponds to the load resulting from prestressing the flange bolts to approximately 30,000 psi (based on bolt thread root area), the stiffness for larger size gaskets can also be computed. 300 and 600lb rated gaskets are interchangeable for sizes 3" and smaller and therefore, the stiffnesses are identical. The stiffnesses associated with the nominal compressed thickness (T_g=0.130) were taken to be median centered and the range from a compressed thickness of 0.125 to 0.135" was considered to represent a $\pm 2.33\beta$ variation. In this study, for the sake of economy in the computing effort, the gasket stiffnesses for 300lb rated flanges were conservatively used for the 400lb rated gaskets, as well.

Based upon the definition of the gasket test load noted above, prestressing the flange bolts to less than 30,000 psi will not result in a lock-up between the flange and the compression gauge ring. However, prestressing the bolts to 30,000 psi or greater may or may not result in lock-up depending on the gasket loading stiffness.

3.2.9 Gasket Unloading/Reloading Stiffness

The unloading stiffness characterizes the recovery of the gasket as the gasket stress is reduced due to increase in pressure, bolt relaxation, or other means. Figure 3-2 depicts the loading and unloading/reloading behavior of a typical spiral-wound gasket. Review of the available test data indicates that the recovery behavior for all spiral wound gaskets is quite similar and can reasonably be expressed as an unloading/reloading stiffness of about 1,000,000 psi/inch. This appears to be a reasonable value for new gaskets such as those used in the test program. However, hardening due to gasket aging may substantially increase

the gasket unloading/reloading stiffness, resulting in a decrease of the Gross Leak Pressure and an increase in the joint leak rate. It is important to note that reloading of the gasket due to removal of the pressure load, for example, follows the unloading stiffness curve.

3.2.10 Gasket Creep and Relaxation

It is understood from experience that gaskets behave nonlinearly and that they creep, even at room temperature. Until recently, information available on the creep and relaxation of commonly-used fabricated gaskets was scarce. Such information is vital for the proper understanding of the behavior of bolted flange joints. The previously mentioned PVRC-sponsored test program provided a vehicle for gathering creep and relaxation data for spiral-wound gaskets which is reported in Reference 12. The results indicate that maximum creep occurs at the lower stress levels and is particularly extensive at about 5,000 psi which coincides with the yield plateau in the stress-deflection diagram. For constant stress, most of the creep occurs in the first 10 to 15 minutes, while for cyclic stress, 20 to 25 stress cycles are requ Cyclic creep exhibits nearly the same overall behavior as constant stress creep, but is more extensive. In contrast, gasket relaxation is greatest at a higher initial stress level but is reasonably constant in terms of percent relaxation. Most of the gasket relaxation also occurs in the first 10 to 15 minutes after initial prestressing of the bolts. It is also of interest to note that lock-up of the flange and compression gauge ring significantly limits the gasket relaxation.

In a real life gasketed-bolted-flange connection, the gasket is subjected to neither pure creep or pure relaxation, even under steady-state operating conditions, since gasket creep causes the bolt load and deflection to change when there is no lock-up between the flange and the compression gauge ring. It is expected that, in many cases, the flange bolting was initially tightened and then retightened some minutes or hours later or possibly during or after the preservice hyd tic pressure test. Retightening eliminates much of the effect of initial short term creep and relaxation. Thus to account for relaxation and cyclic creep for those cases where lock-up between the flange and compression gauge ring does not occur (150lb flanges with low initial bolt stress and 300 and 400lb flanges with low bolt stress and high gasket loading stiffness), a joint relaxation of 25% was taken to be median-centered while the range from 0 to 25% was taken to represent a $\pm 3.0\beta$ variation.

3.2.11 Pipe Bending Moments

Bending moments in the piping at the flange connection due to deadweight or thermal loads are carried by tension in the bolting. Based on normal practice, the piping supports are placed such that deadweight pipe stresses are relatively low and thus, the additional bolt stress is small. If the flange bolting is elastic, it was felt that the reduced gasket stress on the one side is balanced by an increased gasket stress on the other such that the joint mass leak rate will be about the same whether or not the bending moment is considered. On the other hand, if the flange bolting is inelastic, the bending moment could result in some increase in the calculated leak area but the increase would be limited by redistribution of the bending moment. Thus, pipe bending stress was not considered specifically in the evaluation of the flange joint. It is judged that the variabilities from other sources and conservatisms introduced into the approach cover the potential effect of pipe bending moments.

3.3 Flange Joint Behavior

The behavior of gasketed-flange connections, due to increasing pressure of the ISLOCA event, is characterized in the manner described in the following steps.

1. The flange bolts are torqued to prestress levels satisfying the requirements of Reference 6 resulting in an initial gasket stress.

2. Over the course of normal operation, gaskets sustain cyclic creep and relaxation. If Step 1 produced lock-up between the flange and compression gauge ring, the relaxation reduces the gasket stress with a corresponding increase in the lock-up stress and negligible change in the bolt stress. If Step 1 did not produce lock-up, the creep and relaxation reduces the gasket stress with a corresponding reduction in the bolt stress.

3. At the initiation of the ISLOCA event, the increasing pressure must first overcome the lock-up load, if any, with no reduction of the gasket stress or increase in bolt stress.

4. Further increase in pressure to the Gross Leak Pressure is shared by the gasket and bolts in accordance with Figure 3-1 resulting in a decrease in the gasket stress and an increase in the bolt stress. Gross Leak Pressure is defined as the point at which the gasket stress and the pressure are equal. However, for cases in which joint lock-up does not occur, Gross Leak Pressure was defined as either the point at which the gasket stress and the pressure are equal or the point at which the flange bolts yield, whichever occurs first.

5. Further increase in pressure above the Gross Leak Pressure results in a corresponding increase in the bolt stress accompanied by increases in bolt length up to the bolt failure strain in accordance with the bolt stress-strain diagram.

These steps were used consistently in the evaluation of the myriad of cases covering the sizes, pressure ratings, and ranges of the variables affecting leakage.

3.4 Calculation of Leak Rate and Leak Area

The definition of the onset of gross leakage, or the Gross Leak Pressure, as the point at which the gasket stress is equal to the pressure being retained, is used quite generally throughout the gasket industry. This definition has come about, it appears, from gasket tests where some "O"-ring and flat face gaskets have suffered blowout. Although it is doubtful that spiral-wound gaskets are on the verge of catastrophic failure when the gasket stress is reduced to the point that it equals the pressure, the potential certainly exists. For pressures less than the Gross Leak Pressure, the mass leak rate is calculated from the results of the gasket leakage test with water reported in Reference 11. Leakage of this form is related to the presence of seams and crevasses in the flange/seal joint rather than any apparent leak area. In this test, 4"-600lb rated gaskets were subjected to both standard and cyclic load pressure sequences. The results are presented in Figure 3-4 which is a plot of Gasket Stress versus the Tightness Parameter (T_p). T_p is defined as:

$$T_p = \frac{p}{p^*}\left[\frac{L^*_{RM}}{L_{RM}}\right]^a \qquad (3\text{-}1)$$

where p = Internal Fluid Gauge Pressure (psig)

p^* = Reference Atmospheric Pressure (14.7 psia)

L^*_{RM} = Reference Mass Leak Rate (1 mg/sec)

L_{RM} = Total Mass Leak Rate through the Gasket (mg/sec)

and a = Tightness Parameter Exponent (1.0 for water)

Thus, the total mass leak rate for the water case is computed as:

$$L_{RM} = \frac{p}{(14.7 \cdot T_p)} \tag{3-2}$$

Since the leak rate data correspond to the total mass leakage from the 4"-600lb rated gasket and not, for example, the leakage per unit mean circumference, a correction must be made to the calculated mass leak rate to account for the various gasket sizes. Since the probability of leakage increases with gasket perimeter, it is reasonable to assume that leakage through a larger diameter gasket will increase in proportion to the gasket diameter. In addition, a correction factor must be introduced to account for variations in the gasket width. It should be noted that the calculation of gasket width and gasket area should not include the outer 1/8" which is ineffective in the sealing process. The leak rate at the Gross Leak Pressure is then determined as:

$$LR_{GLP} = \frac{(D_o + D_i)(p)}{348.6 W_G}\left[\frac{1}{e^{(6.1872 - 6.2361(9.2103 - \ln SG_a) - .79131(\ln SG_a - \ln SG))}}\right] \tag{3-3}$$

where D_o = Gasket Outside Diameter (in)

D_i = Gasket Inside Diameter (in)

W_c = Gasket Width (in)

SG_o = Initial Gasket Stress (psi) = Actual Gasket Stress/(1 - JR/100)

SG = Current Gasket Stress (psi)

and JR = Joint Relaxation expressed in percent of SG_o

Note that in Equation 3-3 the quantity, 348.6, is the product of 14.7 from Equation 3-2 and 23.714 which is the value of $(D_o + D_i)/W_c$ for a 4"-600lb rated gasket. The quantity in the denominator of the term within the brackets in Equation 3-3 represents the Tightness Parameter (T_p) which is obtained by curve-fitting using the curves shown in Figure 3-4.

It is difficult to determine the significance of a leak rate in milligrams per second. However, if a drop of water is idealized as a 1/8 inch diameter solid sphere, a leak rate of 1 mg/sec would correspond to 3.5 drops per minute or about one drop every 17 seconds. By the time the leak rate increased to 17 mg/sec, the joint leakage would be about 1 drop per second which could be of concern for nuclear operation depending on the location of nearby electrical equipment. Leak rates of 200 to 500 mg/sec would constitute a spray of water which could possibly inhibit some operator actions in the vicinity.

For pressures above the Gross Leak Pressure, it was judged that the leakage is no longer due to seams and crevasses in the flange/seal joint but due to actual separation of the flange and gasket. Thus, a leak area is calculated which is intended to be in addition to the leak rate calculated at Gross Leak Pressure. The leak area is calculated as the mean gasket perimeter times the separation distance at the gasket. The separation distance is affected by bolt extension, gasket recovery, and flange flexibility. Of these, the contribution of bolt extension is by far the most dominant one. Therefore, the separation distance calculated in this study includes the effect of bolt extension only. Note that excluding the effect of gasket recovery from the leak area calculation is conservative and leads to slightly higher leak area values. The leak area at pressures above the Gross Leak Pressure is equated as shown in Equations 3-4 and 3-5, respectively, for the case where the bolt stress is less than or equal to the bolt material yield stress and for the case where the bolt stress exceeds the material yield.

The term, $f(p_{GL}, JR, SG_s, SG_{pGL}, K_G)$, represents the remaining recoverable gasket deflection beyond GLP. It should be noted that some gasket recovery occurs prior to GLP. Due to the difficulties involved in arriving at a reasonably accurate estimate of the term, $f(p_{GL}, JR, SG_s, SG_{pGL}, K_G)$, and recognizing the fact that the effect of bolt extension on the leak area far exceeds that of the gasket recovery, this term was conservatively neglected.

For bolt stress ≤ yield

$$A_L = \frac{\pi(D_o + D_i)}{2}\left[L_B\left\{\frac{(p - p_{GL})(A_p)}{N_B(A_B)(E_B)}\right\} - f(p_{GL}, JR, SG_s, SG_{pGL}, K_G)\right] \quad (3\text{-}4)$$

For bolt stress > yield

$$A_L = \frac{\pi(D_o + D_i)}{2}\left[L_B\left\{\frac{(S_{BY} + S_{BU})}{E_B}\cdot\left[S_{BU} + \frac{(p - p_{GL})(A_p)}{N_B(A_B)} - S_{BY}\right]/E_B\right\} + f(p_{GL}, JR, SG_s, SG_{pGL}, K_G)\right] \quad (3\text{-}5)$$

where L_B = Bolt/Stud Length (in)

p_{GL} = Gross Leak Pressure (psi)

A_p = Pressure Area (in^2) - based on gasket inside diameter

N_B = Number of Flange Bolts

A_B = Bolt Tensile Stress Area (in^2) - per bolt

E_B = Bolt Material Elastic Modulus (psi)

SG_{pGL} = Gasket Stress at Gross Leak Pressure (psi)

$f(p_{GL}, JR, SG_s, SG_{pGL}, K_G)$ = Recoverable Gasket Deflection (in)

K_G = Gasket Unloading/Reloading Stiffness (psi/in)

S_{By} = Bolt Material Yield Stress (psi)

S_{Ba} = Actual Bolt Stress (psi) = $(1 - JR/100)S_{Bo}$ for no lockup case
= S_{Bo} for lockup case

S_{Bo} = Initial Bolt Stress (psi)

and E'_B = Bolt Modulus for appropriate inelastic portion of the stress-strain diagram (psi)

3.5 Gasketed-Flange Connection Capacities and Variabilities

Based on the gasket loading stiffness of Table 3-1 (for median case, Tg=0.130) and gasket load to total load ratios of Figure 3-1, the gasketed- flange connection capacities and variabilities of 150, 300, and 400lb rated flanges were evaluated and are discussed in the following sections. As mentioned in section 3.2.8, for the sake of savings in the computation effort, the gasket stiffnesses for the 300lb flanges were conservatively used for the 400lb rated flanges as well.

3.5.1 150lb Flanges

Tables 3-2 through 3-10 present the results of the analyses for the 150lb rated flanges. Table 3-2 shows the dimensional data for the gaskets and flange bolting which are standard for 150lb ANSI flanges. The numerical results for the Gross Leak Pressures, leak rates (pressure $\leq$ Gross Leak Pressure), and leak areas (pressure $\geq$ Gross Leak Pressure) are shown in Tables 3-3 through 3-10 for the various cases studied. For the particular components of interest with 150lb rated flanges, the flanges are joined by SA-193 Grade B8 bolts. In the tables of results, the parameter variation cases studied include variation in the initial bolt stress (Tables 3-3 through 3-5), variation in the amount of joint relaxation (Tables 3-6 through 3-9), and variation in the bolt yield strength (Table 3-10). In reviewing these tables, recall that the median case corresponds to an initial bolt stress of 25,000 psi and joint relaxation of 25%, with a median bolt yield strength of 33,000 psi.

In each table, the effective gasket stress, the actual gasket stress, and the gasket deflection are shown. The effective gasket stress is defined here as the gasket stress due to the bolt prestress as unaffected by the gasket compression gauge ring, while the actual gasket stress represents the stress limited by the compression gauge ring. That is, in cases where the bolt preload is great enough to cause the flange to bear upon the compression gauge ring (i.e, the condition of gasket bottom-out or joint lock-up), the gasket stress is limited by the maximum deflection of the gasket. The gasket deflections are computed using the gasket stiffnesses shown in Table 3-1.

In Tables 3-3 through 3-10, the effective and actual gasket stresses are equal for most of the flanges, which indicates that the bolt initial stress is not large enough to bottom-out the flange on the compression gauge ring and the resulting gasket deflection is less than the maximum deflection of the nominal 0.175" gasket. Only for the cases with an initial bolt stress of 30,000 psi (Table 3-5) do some of the flanges bottom-out on the gasket. As previously described, the Gross Leak Pressure was calculated as the point at which the gasket stress equals the internal pressure. The exception is for cases in which the bolt preload is not sufficient to bottom-out the gasket, where Gross Leak Pressure was taken as the lower between the pressure required to yield the flange bolts and the previously mentioned definition of Gross Leak Pressure. This criterion was based on the evaluation methods developed for Reference 1. In general, the calculated Gross Leak Pressure is greater for the smaller flanges and trends lower as the flange size increases. The mass leak rates and leak areas are calculated as described in Section 3.4.

From Tables 3-3 through 3-9, the Gross Leak Pressures for the smaller flanges in which joint lock-up does not occur (initial bolt stress equal to 20,000 and 25,000 psi) is governed by the yielding of the flange bolts. However, for the larger flanges, the bolt yield stress occurs after the gasket stress has decreased to match the retained pressure. As a result, by decreasing the initial bolt stress from 25,000 to 20,000 psi (Tables 3-3 and 3-4), the Gross Leak Pressures for the smaller flanges show an increase since a greater internal pressure is required to reach the bolt yield stress, while the Gross Leak Pressures for the larger flanges show a decrease since the gasket seating stress is smaller. From Table 3-5, increasing the bolt preload to 30,000 psi increases the Gross Leak Pressure for all flange sizes, since it produces joint lock-up for some flanges while also increasing the gasket seating stress. In Tables 3-6 through 3-9, increases in the amount of joint relaxation shows an increase in the Gross Leak Pressure for

the smaller flanges, but a decrease in the Gross Leak Pressure for the larger flanges. The mass leak rates decrease with increasing initial bolt stress and, at a given pressure, increasing the joint relaxation tends to increase the leak rate. The leak areas increase with increasing initial bolt stress since the increased bolt stress approaches the bolt yield stress. However, the leak areas reported in Tables 3-3 through 3-10 are given in terms of multiples of the Gross Leak Pressure and not at constant pressures. In Table 3-10, it can be seen that the leak areas are substantially increased with a reduced bolt yield stress, since the leak areas increase rapidly with increasing pressure once the flange bolts have yielded.

The estimation of the leak rate variabilities were based on the results of the 8"-150# flange cases. It was judged that the uncertainties would not vary substantially with flange size and, as a result, a constant uncertainty was used for all flanges. In Figure 3-5, the mass leak rates are plotted as a function of pressure for the various 8"-150# flange cases. As shown in Figure 3-5, the variations in the leak rate due to the initial bolt stress are greater than that due to the variations in the amount of joint relaxation. The uncertainty in the leak rate due to the joint relaxation was estimated based on the judgment that the range from 25% to 0% joint relaxation reasonably represented a -3β variation. An uncertainty variability of $\beta_{JR} = 0.20$ was selected to represent the variability over the entire pressure range. In a similar manner, the uncertainty variability due to the initial bolt preload was evaluated based on the judgment that the range from 25000 psi to 30000 psi reasonably represented a 2.33β variation. An uncertainty variability of $\beta_{BP} = 0.59$ was selected to represent the variability over the entire pressure range. Therefore, the overall uncertainty variability for the leak rate of the 150# rated was taken as:

$$\beta_{LR} = (0.20^2 + 0.59^2)^{1/2} = 0.62$$

3.5.2 300lb Flanges

The results of the analyses for the 300lb rated flanges are presented in Tables 3-11 through 3-23. Table 3-11 shows the dimensional data for the gaskets and flange bolting which are standard for 300lb ANSI flanges while Tables 3-12 through 3-23 present the calculated Gross Leak Pressures, leak rates (pressure $\leq$ Gross Leak Pressure), and leak areas (pressure $>$ Gross Leak Pressure) for the various cases studied. For the 300lb flanges, both SA-193 B8 and SA-564 Grade 630 bolts/studs are used on the pipelines of interest. Tables 3-12 through

3-19 provide results for the flanges joined by the SA-193 B8 bolts while Tables 3-20 through 3-23 provide results for the flanges joined by the SA-564 Grade 630 bolts. Among the tables, the cases studied include variation in the initial bolt/stud stress (Tables 3-12 through 3-14 and 3-20), variation in joint relaxation (Tables 3-15 through 3-18 and 3-21 through 3-22), and variation in bolt yield strength (Tables 3-19 and 3-23). Recall that for the 300lb flanges with the SA-193 B8 bolts, the median case corresponds to an initial bolt stress of 25,000 psi and a joint relaxation of 25%. For the flanges with the SA-564 Grade 630 bolts, the median case corresponds to an initial bolt stress of 60,000 psi and a joint relaxation of 25%.

Each table includes the effective gasket stress, defined here as the gasket stress due to bolt preload unaffected by the presence of the compression gauge ring, the actual gasket stress, limited by the presence of the compression gauge ring, and the resulting gasket loading deflection. For the flanges with the SA-193 B8 bolts (Tables 3-12 through 3-19), the effective and actual gasket stresses for most of the flanges are equal indicating that the bolt preload is insufficient to bottom-out the flange on the compression gauge ring. Only for the cases with an initial bolt stress of 30,000 psi (Table 3-14) do some of the flanges bottom-out on the compression gauge ring.

Reviewing Tables 3-12 through 3-18, the results for the 300lb flanges are similar to those for the 150lb flanges. The Gross Leak Pressures for the smaller flanges in which joint lock-up does not occur (initial bolt stress equal to 20,000 and 25,000 psi) are governed by yield of the flange bolts. However, for the larger flanges, bolt yield occurs after the gasket stress has decreased to match the pressure retained. As a result, by decreasing the initial bolt stress from 25,000 to 20,000 psi (Tables 3-12 and 3-13), the Gross Leak Pressures for the smaller flanges show an increase since a greater internal pressure is required to reach the bolt yield stress while the Gross Leak Pressures for the larger flanges show a decrease since the gasket seating stress is smaller. Increasing the joint relaxation shows a similar trend. The Gross Leak Pressure for the smaller flanges increases while it decreases for the larger flanges with increasing joint relaxation. In all cases for the SA-193 B8 bolts, the computed leak rates are quite low. The leak areas are dependent on the pressure required to develop yield in the flange bolts. Once yielding occurs in the flange bolts, the leak area increases substantially. The influence of reducing the bolt yield stress can be seen by comparing Tables 3-13 and 3-19. Decreasing the bolt yield stress resulted in lower Gross Leak Pressures for the smaller flanges. With the decreased bolt yield stress, the leak areas are increased.

Tables 3-20 through 3-23 show the results for the 300lb flanges with the SA-564 Grade 630 bolts. For these cases, the initial bolt stress is much higher than for the SA-193 B8 bolts. As a result, the prestress is sufficiently high to properly seat the gasket and bottom-out the flange on the gasket compression gauge ring. As expected, the Gross Leak Pressures are much higher than for the cases with the softer bolts. The computed leak rates are very low. In addition, the leak areas beyond Gross Leak Pressure are low since bolt yielding does not occur until very high pressures.

The mass leak rates are typically low for pressures less than Gross Leak Pressure and the Gross Leak Pressures are relatively high for the median case shown in Table 3-16. Therefore, the specific value of the uncertainty variability for the leak rate is relatively unimportant. Based on results from Reference 1 for 300lb rated flanges, a combined uncertainty variability of 0.51 was used to represent the variability due to the initial bolt stress and the bolt relaxation.

3.5.3 400lb Flanges

The results of the analyses for the 400lb rated flanges are presented in Tables 3-24 through 3-32. Table 3-24 shows the dimensional data for the gaskets and flange bolting which are standard for 400lb ANSI flanges while Tables 3-25 through 3-32 present the calculated leak rates (pressure $\leq$ Gross Leak Pressure) and leak areas (pressure > Gross Leak Pressure) for the various cases studied. The cases include variation in initial bolt/stud stress (Tables 3-25 through 3-27), variation in joint relaxation (Tables 3-26 and 3-28 through 3-31), and variation in bolt yield strength (Tables 3-26 and 3-32). For the 400lb rated flanges on the lines of interest, only the SA-193 B8 bolts are used. The median case corresponds to an initial bolt stress of 25,000 psi and a joint relaxation of 25%.

For most of the cases in Tables 3-25 through 3-31, the effective gasket stress exceeds the actual gasket stress indicating that the bolt preload is sufficient to bottom-out the flange on the compression gauge ring. For those cases, the gasket deflection is equal to the maximum deflection of the nominal 0.175" gasket. The cases for which joint lock-up does not occur correspond to the smallest flanges with the median initial bolt stress and all flanges with the lower bound initial bolt stress. For these cases, similar trends as for the 150lb and 300lb flanges with respect to the initial bolt stress and joint relaxation can be seen.

For the flanges with joint lock-up, it can be seen that the Gross Leak Pressure increases with increasing initial bolt stress. Joint relaxation has little influence on the flange leak resistance. This is due to the lock-up between the flange and the compression gauge ring. The effect of variation in the bolt material yield stress can be seen in Tables 3-26 and 3-32. For the cases with joint lock-up, decreasing the bolt yield stress has no effect on the Gross Leak Pressure or the mass leak rate, but does increase the leak area.

The computed leak rates for the 400lb flanges are very low and the Gross Leak Pressures are high for the median case (Table 3-29). As noted for the 300lb flanges, the specific value of the uncertainty variability for the leak rate is of little importance. Therefore, the uncertainty variability of 0.51 used for the 300lb flanges was also used for the 400lb flanges.

TABLE 3-1

STIFFNESSES FOR ASBESTOS-FILLED SPIRAL WOUND GASKETS

Flange Diameter (in)	Pressure Rating (#)	GASKET				BOLTS				Gasket Test Load (lbs)	Bolt Stress at GTL (psi)	GASKET STIFFNESS		
		OD (in)	ID (in)	Width (in)	Area (sq in)	Number	Diameter (in)	Area (sq in)	Length (in)			T_g=0.125 (psi/in)	T_g=0.130 (psi/in)	T_g=0.135 (psi/in)
1-1/2	150	2.750	2.125	0.2500	1.865	4	1/2	0.1416	1.625	15100	26660	161902	179892	202278
	300	2.750	2.125	0.2500	1.865	4	3/4	0.3340	1.875	36200	27096	388137	431263	485171
	600	2.750	2.125	0.2500	1.865	4	3/4	0.3340	2.375	36200	27096	388137	431263	485171
2	150	3.375	2.750	0.2500	2.356	4	5/8	0.2256	1.750	24200	26817	205416	228240	256770
	300	3.375	2.750	0.2500	2.356	8	5/8	0.2256	2.000	48400	26817	410832	456480	513540
	600	3.375	2.750	0.2500	2.356	8	5/8	0.2256	2.625	48400	26817	410832	456480	513540
2-1/2	150	3.875	3.250	0.2500	2.749	4	5/8	0.2256	2.000	24200	26817	176071	195634	220089
	300	3.875	3.250	0.2500	2.749	8	3/4	0.3340	2.250	72500	27133	527485	586094	659356
	600	3.875	3.250	0.2500	2.749	8	3/4	0.3340	2.875	72500	27133	527485	586094	659356
3	150	4.750	4.000	0.3125	4.234	4	5/8	0.2256	2.125	24200	26817	114318	127021	142898
	300	4.750	4.000	0.3125	4.234	8	3/4	0.3340	2.500	72500	27133	342483	380537	428104
	600	4.750	4.000	0.3125	4.234	8	3/4	0.3340	3.125	72500	27133	342483	380537	428104
4	150	5.875	5.000	0.3750	6.332	8	5/8	0.2256	2.125	48500	26870	153184	170204	191479
	300	5.875	5.000	0.3750	6.332	8	3/4	0.3340	2.750	72500	27133	228966	254429	286232
	600	5.875	4.750	0.5000	8.247	8	7/8	0.4612	3.625	101000	27374	244947	272163	306184
6	150	8.250	7.188	0.4688	11.275	8	3/4	0.3340	2.250	72500	27133	128606	142895	160757
	300	8.250	7.188	0.4688	11.275	12	3/4	0.3340	3.125	100700	25125	178629	198477	223286
	600	8.250	6.875	0.6250	14.726	12	1	0.6051	4.375	190000	26166	258043	286715	322554
8	150	10.375	9.188	0.5313	16.220	8	3/4	0.3340	2.500	72500	27133	89394	99327	111743
	300	10.375	9.188	0.5313	16.220	12	7/8	0.4612	3.500	150800	27248	185940	206600	232425
	600	10.375	8.875	0.6875	20.654	12	1-1/8	0.7627	5.000	262000	28626	253710	281900	317137
10	150	12.500	11.313	0.5313	19.767	12	7/8	0.4612	2.625	151000	27284	152781	169756	190.376
	300	12.500	11.313	0.5313	19.767	16	1	0.6051	4.000	264400	27310	267518	297242	334398
	600	12.500	10.813	0.7813	28.455	16	1-1/4	0.9684	5.625	446000	28785	313474	348304	391842
12	150	14.750	13.375	0.6250	27.489	12	7/8	0.4612	2.750	151000	27284	109862	122069	137328
	300	14.750	13.375	0.6250	27.489	16	1-1/8	0.7627	4.250	349400	28632	254211	282457	317764
	600	14.750	12.875	0.8750	37.797	20	1-1/4	0.9684	5.875	557000	28759	294730	327478	368413
14	150	16.000	14.625	0.6250	29.943	12	1	0.6051	3.000	198000	27268	132250	146944	165312
	300	16.000	14.625	0.6250	29.943	20	1-1/8	0.7627	4.500	436000	28583	291217	323574	364021
	600	16.000	14.250	0.8125	38.448	20	1-3/8	1.1538	6.125	---	27408	328998	365553	411247
16	150	18.250	16.625	0.7500	40.939	16	1	0.6051	3.125	264000	27268	128973	143303	161216
	300	18.250	16.625	0.7500	40.939	20	1-1/4	0.9684	4.750	557000	28759	272113	302348	340141
	600	18.250	16.250	0.9375	50.621	20	1-1/2	1.4041	6.625	---	27643	306701	340778	383376
18	150	20.750	18.688	0.9688	59.822	16	1-1/8	0.7627	3.375	---	27252	111226	123584	139032
	300	20.750	18.688	0.9688	59.822	24	1-1/4	0.9684	5.000	---	27565	214187	237985	267733
	600	20.750	18.500	1.0625	65.298	20	1-5/8	1.7723	7.125	---	28439	308754	343060	385943
20	150	22.750	20.688	0.9688	65.909	20	1-1/8	0.7627	3.625	---	27262	126192	140213	157740
	300	22.750	20.688	0.9688	65.909	24	1-1/4	0.9684	5.250	---	27565	194406	2160.	243008
	600	22.750	20.500	1.0625	71.974	24	1-5/8	1.7723	7.625	---	28439	336140	373488	420175
24	150	27.000	24.750	1.0625	86.161	20	1-1/4	0.9684	4.000	---	27565	123927	137696	154838
	300	27.000	24.750	1.0625	86.161	24	1-1/2	1.4041	5.750	---	27643	216232	240258	270290
	600	27.000	24.750	1.0625	86.161	24	1-7/8	2.4107	8.625	---	29657	385000	427778	481250
44	300	47.625	45.625	0.9375	137.138	40	1-3/8	1.1538	10.215	---	27408	307457	368948	461185

Reference: MIL-G-21032E, Amendment 2

Calculation GASSTIF

GTL = Gasket Test Load

T_g = Compressed Gasket Thickness

TABLE 3-2
150# ANSI FLANGE AND GASKET DATA

Flange Diameter (in)	GASKET OD (in)	GASKET ID (in)	GASKET Width (in)	GASKET Area (sq in)	Pressure Area (sq in)	BOLTS Number	BOLTS Diameter (in)	BOLTS Area (sq in)	BOLTS Length (in)
Flanges									
1-1/2	2.750	2.125	0.2500	1.865	3.547	4	1/2	0.1416	1.625
2	3.375	2.750	0.2500	2.356	5.940	4	5/8	0.2236	1.750
2-1/2	3.875	3.250	0.2500	2.749	8.296	4	5/8	0.2256	2.000
3	4.750	4.000	0.3125	4.234	12.566	4	5/8	0.2256	2.125
4	5.875	5.000	0.3750	6.332	19.635	8	5/8	0.2256	2.125
6	8.250	7.188	0.4688	11.275	40.574	8	3/4	0.3340	2.250
8	10.375	9.188	0.5313	16.220	66.298	8	3/4	0.3340	2.500
10	12.500	11.313	0.5313	19.767	100.509	12	7/8	0.4612	2.625
12	14.750	13.375	0.6250	27.489	140.500	12	7/8	0.4612	2.750
14	16.000	14.625	0.6250	29.943	167.989	12	1	0.6051	3.000
16	18.250	16.625	0.7500	40.939	217.077	16	1	0.6051	3.125
18	20.750	18.688	0.9688	59.822	274.279	16	1-1/8	0.7627	3.375
20	22.750	20.688	0.9688	65.909	336.129	20	1-1/8	0.7627	3.625
24	27.000	24.750	1.0625	86.161	481.105	20	1-1/4	0.9684	4.000

Bolt areas correspond to tensile stress area

TABLE 3-3

150# FLANGE GASKET STRESS, GROSS LEAK PRESSURE, AND LEAK RATE

INITIAL BOLT STRESS = 20000 psi

JOINT RELAXATION = 0%

Flange Diameter (in)	Eff Gasket Stress (psi)	Act Gasket Stress (psi)	Gasket Deflect (in)	Gross Leak Pressure (psi)	Leak Rate at GLP (mg/sec)	Leak Rate at .25GLP (mg/sec)	Leak Rate at .50GLP (mg/sec)	Leak Rate at .75GLP (mg/sec)	Leak Area at 1.25GLP (sq in)	Leak Area at 1.5GLP (sq in)	Leak Area at 1.75GLP (sq in)	Leak Area at 2.0GLP (sq in)	Bolt Stress at 2.0GLP (psi)
Flanges													
1-1/2	6073	6073	0.034	3273	14	2	5	9	0.21	0.52	0.83	1.14	51764
2	7660	7660	0.034	3427	5	1	2	3	0.34	0.80	1.27	1.96	54059
2-1/2	6566	6566	0.033	2617	13	2	4	7	0.55	1.21	1.85	3.11	56085
3	4263	4263	0.034	1657	118	16	37	68	0.52	1.34	2.16	3.36	53913
4	5700	5700	0.034	2015	26	3	8	15	0.26	1.24	2.21	3.18	50904
6	4740	4740	0.033	1347	74	8	20	38	0.01	0.91	2.27	3.63	46588
8	3295	3295	0.033	757	535	43	123	248	0.01	0.03	1.70	3.46	42167
10	5600	5600	0.033	1004	38	3	7	16	0.02	0.03	1.24	3.42	40061
12	4027	4027	0.033	659	213	15	39	83	0.02	0.04	0.06	2.27	36727
14	4850	4850	0.033	734	86	6	15	32	0.02	0.04	0.07	2.87	36974
16	4730	4730	0.033	750	94	7	17	36	0.03	0.05	0.08	3.28	36827
18	4080	4080	0.033	731	183	14	36	75	0.03	0.06	0.09	3.59	36419
20	4629	4629	0.033	759	102	7	19	40	0.04	0.07	0.11	4.61	36721
24	4496	4496	0.033	683	127	9	22	48	0.05	0.10	0.15	6.44	36962

Bolt Yield Stress = 33,000 psi (SA193 B8)

DGmax = 0.050 in

Calculation 1502000

TABLE 3-4

150# FLANGE GASKET STRESS, GROSS LEAK PRESSURE, AND LEAK RATE

INITIAL BOLT STRESS = 25000 psi

JOINT RELAXATION = 0%

Flange Diameter (in)	Eff Gasket Stress (psi)	Act Gasket Stress (psi)	Gasket Deflect (in)	Gross Leak Pressure (psi)	Leak Rate at GLP (mg/sec)	Leak Rate at .25GLP (mg/sec)	Leak Rate at .50GLP (mg/sec)	Leak Rate at .75GLP (mg/sec)	Leak Area at 1.25GLP (sq in)	Leak Area at 1.5GLP (sq in)	Leak Area at 1.75GLP (sq in)	Leak Area at 2.0GLP (sq in)	Bolt Stress at 2.0GLP (psi)
Flanges													
1-1/2	7591	7591	0.042	2323	4	0	1	1	0.22	0.44	0.66	0.88	47545
2	9575	9575	0.042	2383	1	0	0	0	0.32	0.64	0.97	1.29	48686
2-1/2	8207	8207	0.042	1740	3	0	1	1	0.44	0.87	1.31	1.75	49000
3	5329	5329	0.042	1222	33	3	6	10	0.61	1.21	1.82	2.43	50021
4	7125	7125	0.042	1794	8	1	2	3	0.86	1.73	2.59	3.61	52512
6	5925	5925	0.041	1684	23	2	6	12	1.61	3.31	5.03	8.87	58235
8	4118	4118	0.041	948	166	15	38	77	0.80	3.00	5.20	7.82	52708
10	7000	7000	0.041	1255	12	1	2	5	0.02	2.74	5.47	8.20	50076
12	5033	5033	0.041	824	66	5	12	26	0.02	1.49	4.59	7.69	45909
14	6062	6062	0.041	917	27	2	5	10	0.03	1.88	5.61	9.35	46218
16	5912	5912	0.041	938	29	2	5	11	0.03	2.15	6.54	10.93	46033
18	5100	5100	0.041	913	57	4	11	23	0.04	2.37	7.60	12.83	45524
20	5786	5786	0.041	949	32	2	6	12	0.05	3.03	9.33	15.64	45902
24	5620	5620	0.041	854	40	3	7	15	0.06	4.22	12.63	21.04	46203

Bolt Yield Stress = 33,000 psi (SA193-B8)

DGmax = 0.050 in

Calculation 1502500

TABLE 3-5
150# FLANGE GASKET STRESS, GROSS LEAK PRESSURE, AND LEAK RATE

INITIAL BOLT STRESS = 30000 psi

JOINT RELAXATION = 0%

Flange Diameter (in)	Eff Gasket Stress (psi)	Act Gasket Stress (psi)	Gasket Deflect (in)	Gross Leak Pressure (psi)	Leak Rate at GLP (mg/sec)	Leak Rate at .25GLP (mg/sec)	Leak Rate at .50GLP (mg/sec)	Leak Rate at .75GLP (mg/sec)	Leak Area at 1.25GLP (sq in)	Leak Area at 1.5GLP (sq in)	Leak Area at 1.75GLP (sq in)	Leak Area at 2.0GLP (sq in)	Bolt Stress at 2.0GLP (psi)
Flanges													
1-1/2	9109	9000	0.050	4877	2	0	1	1	0.65	1.77	3.89	6.81	77133
2	11490	11400	0.050	5120	1	0	0	0	1.07	2.94	6.69	11.06	80766
2-1/2	9848	9800	0.050	3916	2	0	0	1	1.69	4.58	10.58	*	83922
3	6394	6350	0.050	2477	15	2	5	8	1.76	4.93	11.42	19.17	80607
4	8550	8500	0.050	3015	3	0	1	2	1.45	4.68	10.20	19.36	76171
6	7110	7110	0.050	2020	9	1	2	5	2.04	5.00	10.05	19.65	69882
8	4942	4942	0.050	1136	64	6	15	30	2.64	5.28	10.00	17.05	63250
10	8400	8400	0.049	1506	5	0	1	2	3.15	6.43	10.58	17.98	60091
12	6040	6040	0.050	988	25	2	5	10	1.95	5.67	9.39	15.46	55091
14	7275	7275	0.049	1101	10	1	2	4	2.38	6.67	11.35	19.07	55462
16	7095	7095	0.050	1126	11	1	2	4	2.78	8.05	13.32	22.21	55240
18	6120	6120	0.049	1096	22	2	4	9	3.24	9.52	15.80	25.71	54628
20	6943	6943	0.050	1138	12	1	2	5	3.97	11.54	19.10	31.65	55082
24	6744	6744	0.049	1024	15	1	3	6	5.37	15.46	25.54	42.91	55443

* Bolt Ultimate Strength Exceeded

Bolt Ultimate Strength = 82,500 psi (SA193 B8)

Bolt Yield Stress = 33,000 psi (SA193 B8)

DGmax = 0.050 in

Calculation 150000

TABLE 3-6

150# FLANGE GASKET STRESS, GROSS LEAK PRESSURE, AND LEAK RATE

INITIAL BOLT STRESS = 25000 psi

JOINT RELAXATION = 15%

Flange Diameter (in)	Eff Gasket Stress (psi)	Act Gasket Stress (psi)	Gasket Deflect (in)	Gross Leak Pressure (psi)	Leak Rate at GLP (mg/sec)	Leak Rate at .25GLP (mg/sec)	Leak Rate at .50GLP (mg/sec)	Leak Rate at .75GLP (mg/sec)	Leak Area at 1.25GLP (sq in)	Leak Area at 1.5GLP (sq in)	Leak Area at 1.75GLP (sq in)	Leak Area at 2.0GLP (sq in)	Bolt Stress at 2.0GLP (psi)
Flanges													
1-1/2	6453	6453	0.041	3412	4	1	2	3	0.32	0.65	0.97	1.49	54364
2	8139	8139	0.041	3500	1	0	0	1	0.47	0.95	1.42	2.33	56039
2-1/2	6976	6976	0.041	2556	4	0	1	2	0.64	1.28	1.92	3.21	56500
3	4529	4529	0.041	1760	35	5	11	20	0.64	1.71	2.62	4.44	57283
4	6057	6057	0.041	2141	8	1	2	4	0.64	1.57	3.09	4.25	54086
6	5036	5036	0.041	1431	22	2	6	11	0.06	1.51	0.36	4.40	43500
8	3501	3501	0.041	804	161	15	37	74	0.01	0.71	2.58	4.45	44802
10	5950	5950	0.040	1067	12	1	2	5	0.02	0.03	2.30	4.62	42565
12	4278	4278	0.041	700	64	5	12	25	0.02	0.04	0.99	3.62	39023
14	5153	5153	0.040	780	26	2	4	10	0.02	0.05	1.31	4.49	39285
16	5025	5025	0.040	797	28	2	5	11	0.03	0.06	1.46	5.19	39128
18	4335	4335	0.040	776	55	4	11	23	0.03	0.07	1.45	5.90	38695
20	4918	4918	0.040	806	31	2	6	12	0.04	0.08	2.01	7.36	39016
24	4777	4777	0.040	726	38	3	7	14	0.05	0.11	2.94	10.09	39272

Bolt Yield Stress = 30,000 psi (SA193-B7)

DGmax = 0.050 in

Calculation 1502515

TABLE 3-7
150# FLANGE GASKET STRESS, GROSS LEAK PRESSURE, AND LEAK RATE

INITIAL BOLT STRESS = 25000 psi

JOINT RELAXATION = 25%

Flange Diameter (in)	Eff Gasket Stress (psi)	Act Gasket Stress (psi)	Gasket Deflect (in)	Gross Leak Pressure (psi)	Leak Rate at GLP (mg/sec)	Leak Rate at .25GLP (mg/sec)	Leak Rate at .50GLP (mg/sec)	Leak Rate at .75GLP (mg/sec)	Leak Area at 1.25GLP (sq in)	Leak Area at 1.5GLP (sq in)	Leak Area at 1.75GLP (sq in)	Leak Area at 2.0GLP (sq in)	Bolt Stress at 2.0GLP (psi)
Flanges													
1-1/2	5693	5693	0.040	3068	4	1	2	3	0.07	0.36	0.65	0.94	48529
2	7181	7181	0.040	3213	1	0	0	1	0.15	0.59	1.02	1.45	50680
2-1/2	6155	6155	0.040	2453	4	1	1	2	0.29	0.91	1.52	2.25	52580
3	3996	3996	0.041	1553	34	5	11	20	0.19	0.96	1.73	2.50	50544
4	5344	5344	0.040	1889	8	1	2	4	0.01	0.80	1.71	2.61	47723
6	4444	4444	0.040	1263	22	2	6	11	0.01	0.31	1.58	2.86	43676
8	3089	3089	0.040	710	157	14	36	73	0.01	0.02	0.83	2.48	39531
10	5250	5250	0.039	941	11	1	2	5	0.02	0.03	0.18	2.23	37557
12	3775	3775	0.040	618	62	4	11	24	0.02	0.03	0.05	0.91	34432
14	4547	4547	0.040	688	25	2	4	9	0.02	0.04	0.06	1.25	34663
16	4434	4434	0.040	704	28	2	5	11	0.02	0.05	0.07	1.36	34525
18	3825	3825	0.040	685	54	4	10	22	0.03	0.06	0.09	1.27	34143
20	4340	4340	0.040	711	30	2	5	12	0.04	0.07	0.11	1.85	34426
24	4215	4215	0.039	640	37	3	6	14	0.05	0.08	0.14	2.79	34652

Bolt Yield Stress = 33,000 psi (SA193-B8)

DGmax = 0.050 in

Calculation 1502S25

TABLE 3-8

150# FLANGE GASKET STRESS, GROSS LEAK PRESSURE, AND LEAK RATE

INITIAL BOLT STRESS = 25000 psi

JOINT RELAXATION = 33%

Flange Diameter (in)	Ld Gasket Stress (psi)	Act Gasket Stress (psi)	Gasket Deflect (in)	Gross Leak Pressure (psi)	Leak Rate at GLP (mg/sec)	Leak Rate at .25GLP (mg/sec)	Leak Rate at .50GLP (mg/sec)	Leak Rate at .75GLP (mg/sec)	Leak Area at 1.25GLP (sq in)	Leak Area at 1.5GLP (sq in)	Leak Area at 1.75GLP (sq in)	Leak Area at 2.0GLP (sq in)	Bolt Stress at 2.0GLP (psi)
Flanges													
1-1/2	5086	5086	0.046	2741	4	1	1	3	0.39	0.11	0.37	0.63	43352
2	6415	6415	0.039	2870	1	0	0	1	0.00	0.24	0.62	1.01	45274
2-1/2	5499	5499	0.039	2192	4	0	1	2	0.00	0.43	0.98	1.53	46972
3	3570	3570	0.040	1387	34	5	11	19	0.01	0.36	1.05	1.74	45152
4	4774	4774	0.040	1687	7	1	2	4	0.01	0.09	0.90	1.72	42632
6	3970	3970	0.039	1128	21	4	6	11	0.01	0.02	0.48	1.62	39017
8	2759	2759	0.040	631	153	14	35	71	0.01	0.02	0.03	0.90	35314
10	4690	4690	0.039	841	11	1	2	5	0.01	0.03	0.04	0.32	33551
12	3372	3372	0.040	552	61	4	11	24	0.02	0.03	0.05	0.06	30759
14	4062	4062	0.039	514	25	2	4	9	0.02	0.04	0.06	0.07	30966
16	3961	3961	0.039	629	27	2	5	10	0.02	0.04	0.07	0.09	30842
18	3417	3417	0.039	512	52	4	10	21	0.03	0.05	0.08	0.10	30501
20	3877	3877	0.039	636	29	2	5	11	0.03	0.06	0.09	0.13	30754
24	3765	3765	0.039	572	36	2	6	14	0.04	0.08	0.13	0.17	30956

Bolt Yield Stress = 33,000 psi (SA193 B8)

DGmax = 0.050 in

Calculation 1502533

TABLE 3-9

150# FLANGE GASKET STRESS, GROSS LEAK PRESSURE, AND LEAK RATE

INITIAL BOLT STRESS = 25000 psi

JOINT RELAXATION = 50%

Flange Diameter (in)	Eff Gasket Stress (psi)	Act Gasket Stress (psi)	Gasket Deflect (in)	Gross Leak Pressure (psi)	Leak Rate at GLP (mg/sec)	Leak Rate at .25GLP (mg/sec)	Leak Rate at .50GLP (mg/sec)	Leak Rate at .75GLP (mg/sec)	Leak Area at .25GLP (sq in)	Leak Area at 1.5GLP (sq in)	Leak Area at 1.75GLP (sq in)	Leak Area at 2.0GLP (sq in)	Bolt Stress at 2.0GLP (psi)
Flanges													
1-1/2	3796	3796	0.038	2045	4	1	1	2	0.00	0.00	0.00	0.01	32352
2	4787	4787	0.037	2142	1	0	0	1	0.00	0.00	0.01	0.07	33787
2-1/2	4103	4103	0.039	1636	3	0	1	2	0.00	0.01	0.01	0.23	35053
3	2664	2664	0.039	1035	32	4	10	18	0.00	0.01	0.01	0.11	33696
4	3563	3563	0.038	1259	7	1	2	4	0.00	0.01	0.01	0.02	31815
6	2962	2962	0.038	842	20	2	5	10	0.01	0.01	0.02	0.03	29118
8	2059	2059	0.039	473	144	13	33	67	0.01	0.02	0.02	0.03	26354
10	3500	3500	0.038	828	10	1	2	4	0.01	0.02	0.03	0.04	25038
12	2517	2517	0.039	412	57	4	10	22	0.01	0.02	0.03	0.05	22955
14	3031	3031	0.038	459	23	2	4	9	0.01	0.03	0.04	0.06	23109
16	2956	2956	0.038	469	25	2	5	10	0.02	0.03	0.05	0.07	23017
18	2550	2550	0.039	457	49	4	10	20	0.02	0.04	0.06	0.08	22762
20	2893	2893	0.038	474	28	2	5	11	0.02	0.05	0.07	0.09	22951
24	2810	2810	0.038	427	34	2	6	13	0.03	0.06	0.09	0.12	23101

Bolt Yield Stress = 33,000 psi (SA193-B8)

DGmax = 0.050 in

Calculation 1502550

TABLE 3-10

150# FLANGE GASKET STRESS, GROSS LEAK PRESSURE, AND LEAK RATE

INITIAL BOLT STRESS = 25000 psi

JOINT RELAXATION = 0%

Flange Diameter (in)	Eff Gasket Stress (psi)	Act Gasket Stress (psi)	Gasket Deflect (in)	Gross Leak Pressure (psi)	Leak Rate at GLP (mg/sec)	Leak Rate at .25GLP (mg/sec)	Leak Rate at .50GLP (mg/sec)	Leak Rate at .75GLP (mg/sec)	Leak Area at 1.25GLP (sq in)	Leak Area at 1.5GLP (sq in)	Leak Area at 1.75GLP (sq in)	Leak Area at 2.0GLP (sq in)	Bolt Stress at 2.0GLP (psi)
Flanges													
1-1/2	7591	7591	0.042	726	3	0	0	0	0.07	0.14	0.21	0.28	32045
2	9575	9575	0.042	745	1	0	0	0	0.10	0.20	0.30	0.40	32402
2-1/2	8207	8207	0.042	544	3	0	0	0	0.14	0.27	0.41	0.55	32500
3	5329	5329	0.042	382	26	1	2	3	0.19	0.38	0.57	0.76	32819
4	7125	7125	0.042	560	6	0	0	1	0.27	0.54	0.81	1.08	32598
6	5925	5925	0.041	549	18	1	2	2	0.55	1.11	1.66	2.22	35833
8	4118	4118	0.041	560	149	8	19	32	1.30	2.60	3.90	5.20	41389
10	7000	7000	0.041	1255	12	1	2	5	2.62	5.35	8.79	14.96	50076
12	5033	5033	0.041	824	66	5	12	26	1.63	4.73	7.82	12.94	45909
14	6062	6062	0.041	917	27	2	5	10	1.99	5.72	9.46	15.87	46218
16	5912	5912	0.041	938	29	2	5	11	2.32	6.71	11.10	18.47	46033
18	5100	5100	0.041	913	57	4	11	23	2.70	7.94	13.17	21.38	45524
20	5786	5786	0.041	949	32	2	6	12	3.31	9.62	15.92	26.33	45902
24	5620	5620	0.041	854	40	3	7	15	4.47	12.88	21.29	35.69	46203

Bolt Yield Stress = 27,500 psi (SA193-B8)

DGmax = 0.059 in

Calculation 1502500Y

TABLE 3-11
300# ANSI FLANGE AND GASKET DATA

Flange Diameter (in)	GASKET OD (in)	GASKET ID (in)	GASKET Width (in)	GASKET Area (sq in)	Pressure Area (sq in)	BOLTS Number	BOLTS Diameter (in)	BOLTS Area (sq in)	BOLTS Length (in)
Flanges									
1-1/2	2.750	2.125	0.2500	1.865	3.547	4	3/4	0.3340	1.875
2	3.375	2.750	0.2500	2.356	5.940	8	5/8	0.2256	2.000
2-1/2	3.875	3.250	0.2500	2.749	8.296	8	3/4	0.3340	2.250
3	4.750	4.000	0.3125	4.234	12.566	8	3/4	0.3340	2.500
4	5.875	5.000	0.3750	6.332	19.635	8	3/4	0.3340	2.750
6	8.250	7.188	0.4688	11.275	40.574	12	3/4	0.3340	3.125
8	10.375	9.188	0.5313	16.220	66.296	12	7/8	0.4612	3.500
10	12.500	11.313	0.5313	19.767	100.509	16	1	0.6051	4.000
12	14.750	13.375	0.6250	27.489	140.500	16	1-1/8	0.7896	4.250
14	16.000	14.625	0.6250	29.943	167.989	20	1-1/8	0.7896	4.500
16	18.250	16.625	0.7500	40.939	217.077	20	1-1/4	0.9985	4.750
18	20.750	18.688	0.9688	59.822	274.279	24	1-1/4	0.9985	5.000
20	22.750	20.688	0.9688	65.909	336.129	24	1-1/4	0.9985	5.250
24	27.000	24.750	1.0625	86.161	431.105	24	1-1/2	1.4899	5.750

Bolt areas correspond to tensile stress area

TABLE 3-12

300# FLANGE GASKET STRESS, GROSS LEAK PRESSURE, AND LEAK RATE

INITIAL BOLT STRESS = 20000 psi

JOINT RELAXATION = 0%

Flange Diameter (in)	Eff Gasket Stress (psi)	Act Gasket Stress (psi)	Gasket Deflect. (in)	Gross Leak Pressure (psi)	Leak Rate at GLP (mg/sec)	Leak Rate at .25GLP (mg/sec)	Leak Rate at .50GLP (mg/sec)	Leak Rate at .75GLP (mg/sec)	Leak Area at 1.25GLP (sq in)	Leak Area at 1.5GLP (sq in)	Leak Area at 1.75GLP (sq in)	Leak Area at 2.0GLP (sq in)	Bolt Stress at 2.0GLP (psi)
Flanges													
1-1/2	14325	14325	0.033	6897	0	0	0	0	0.32	0.64	0.96	3.59	51310
2	15320	15320	0.034	5809	0	0	0	0	0.45	0.90	1.35	1.83	52118
2-1/2	19441	19441	0.033	6344	0	0	0	0	0.60	1.21	1.81	2.58	52697
3	12622	12622	0.033	4388	0	0	0	0	0.86	1.73	2.59	3.85	53635
4	8439	8439	0.033	3104	3	0	1	2	1.31	2.61	3.92	6.38	55807
6	7110	7110	0.036	2386	9	1	3	5	1.45	3.68	5.92	9.65	55029
8	6824	6824	0.033	1825	12	1	3	6	0.02	2.72	5.59	8.46	49082
10	9796	9796	0.033	2014	2	0	0	1	0.03	1.85	5.66	9.48	45923
12	9192	9192	0.033	1688	3	0	1	1	0.03	0.06	3.29	7.59	41208
14	10548	10543	0.033	1596	1	0	0	1	0.03	0.07	0.10	4.30	36974
16	9756	9756	0.032	1548	2	0	0	1	0.04	0.08	0.12	4.96	36827
18	8012	8012	0.034	1435	5	0	1	2	0.05	0.09	0.14	5.31	36419
20	7272	7272	0.034	1192	10	1	2	4	0.05	0.11	0.16	6.67	36721
24	8300	8300	0.035	1261	5	0	1	2	0.07	0.14	0.22	9.25	36962

Bolt Yield Stress = 33,000 psi (SA193-B8)

DGmax = 0.050 in

Calculation 3002000

TABLE 3-13
300# FLANGE GASKET STRESS, GROSS LEAK PRESSURE, AND LEAK RATE

INITIAL BOLT STRESS = 25000 psi

JOINT RELAXATION = 0%

Flange Diameter (in)	Eff Gasket Stress (psi)	Act Gasket Stress (psi)	Gasket Deflect (in)	Gross Leak Pressure (psi)	Leak Rate at GLP (mg/sec)	Leak Rate at .25GLP (mg/sec)	Leak Rate at .50GLP (mg/sec)	Leak Rate at .75GLP (mg/sec)	Leak Area at 1.25GLP (sq in)	Leek Area at 1.5GLP (sq in)	Leak Area at 1.75GLP (sq in)	Leak Area at 2.0GLP (sq in)	Bolt Stress at 2.0GLP (psi)
Flanges													
1-1/2	17906	17906	0.042	4245	0	0	0	0	0.20	0.39	0.59	0.79	44268
2	19150	19150	0.042	3575	0	0	0	0	0.28	0.55	0.83	1.10	44765
2-1/2	24301	24301	0.041	3904	0	0	0	0	0.37	0.74	1.12	1.49	45121
3	15778	15778	0.041	2700	0	0	0	0	0.53	1.06	1.60	2.13	45698
4	10549	10549	0.042	1910	1	0	0	0	0.80	1.61	2.41	3.22	47035
6	8887	8887	0.045	1756	3	0	0	1	1.64	3.29	4.93	6.57	50778
8	8530	8530	0.041	2024	4	0	1	2	3.18	6.36	9.54	16.31	57242
10	12245	12245	0.041	2517	1	0	0	0	3.51	8.28	13.05	22.87	57404
12	11490	11490	0.041	2109	1	0	0	0	0.85	6.24	11.61	16.99	51510
14	13185	13185	0.041	1995	0	0	0	0	0.04	2.84	8.42	14.02	46218
16	12195	12195	0.040	1935	1	0	0	0	0.05	3.27	9.94	16.62	46033
18	10015	10015	0.042	1793	2	0	0	1	0.06	3.51	11.26	19.01	45524
20	9090	9090	0.042	1490	3	0	1	1	0.07	4.39	13.52	22.65	45902
24	10375	10375	0.043	1576	2	0	0	1	0.09	6.07	18.15	30.24	46203

Bolt Yield Stress = 33,000 psi (SA193-B8)

DGmax = 0.050 in

Calculation 3002500

TABLE 3-14

300# FLANGE GASKET STRESS, GROSS LEAK PRESSURE, AND LEAK RATE

INITIAL BOLT STRESS = 30000 psi

JOINT RELAXATION = 0%

Flange Diameter (in)	Eff Gasket Stress (psi)	Act Gasket Stress (psi)	Gasket Deflect. (in)	Gross Leak Pressure (psi)	Leak Rate at GLP (mg/sec)	Leak Rate at .25GLP (mg/sec)	Leak Rate at .50GLP (mg/sec)	Leak Rate at .75GLP (mg/sec)	Leak Area at 1.25GLP (sq in)	Leak Area at 1.5GLP (sq in)	Leak Area at 1.75GLP (sq in)	Leak Area at 2.0GLP (sq in)	Bolt Stress at 2.0GLP (psi)
Flanges													
1-1/2	21487	21487	0.050	13850	0	0	0	0	1.83	5.64	*	*	92871
2	22979	22800	0.050	12652	0	0	0	0	3.62	9.78	*	*	99790
2-1/2	29161	29161	0.050	14393	0	0	0	0	5.99	14.65	*	*	104178
3	18933	18933	0.050	9024	0	0	0	0	5.71	16.93	*	*	99174
4	12659	12659	0.050	5425	0	0	0	0	5.67	17.56	*	*	92591
6	10665	9990	0.050	3464	2	0	0	1	4.07	12.06	28.09	48.53	79881
8	10236	10236	0.049	2738	1	0	0	1	4.30	12.19	24.80	50.26	73622
10	14694	14694	0.049	3021	0	0	0	0	5.72	12.74	25.83	50.51	68885
12	13788	13788	0.049	2531	0	0	0	0	6.45	12.89	22.77	38.39	61812
14	15822	15822	0.040	2394	0	0	0	0	3.58	10.30	17.02	28.61	55462
16	14634	14634	0.048	2322	0	0	0	0	4.23	12.24	20.25	33.76	55240
18	12018	11900	0.050	2152	1	0	0	0	4.80	14.11	23.41	38.09	54828
20	10908	10800	0.050	1788	1	0	0	0	5.75	16.71	27.67	45.84	55082
24	12450	12000	0.050	1891	1	0	0	0	7.71	22.22	36.72	61.68	55443

* Bolt Ultimate Strength Exceeded

Bolt Ultimate Strength = 82,500 psi (SA193-B8)

Bolt Yield Stress = 33,000 psi (SA193-B8)

DGmax = 0.050 in

Calculation 3003000

TABLE 3-15

300# FLANGE GASKET STRESS, GROSS LEAK PRESSURE, AND LEAK RATE

INITIAL BOLT STRESS = 25000 psi

JOINT RELAXATION = 15%

Flange Diameter (in)	Eff Gasket Stress (psi)	Act Gasket Stress (psi)	Gasket Deflect. (in)	Gross Leak Pressure (psi)	Leak Rate at GLP (mg/sec)	Leak Rate at .25GLP (mg/sec)	Leak Rate at .50GLP (mg/sec)	Leak Rate at .75GLP (mg/sec)	Leak Area at 1.25GLP (sq in)	Leak Area at 1.5GLP (sq in)	Leak Area at 1.75GLP (sq in)	Leak Area at 2.0GLP (sq in)	Bolt Stress at 2.0GLP (psi)
Flanges													
1-1/2	15220	15220	0.042	6234	0	0	0	0	0.29	0.58	0.87	1.16	49549
2	16277	16277	0.042	5231	0	0	0	0	0.41	0.81	1.22	1.62	50279
2-1/2	20656	20656	0.041	5734	0	0	0	0	0.55	1.09	1.64	2.19	50803
3	13411	13411	0.041	3966	0	0	0	0	0.78	1.56	2.34	3.13	51651
4	8967	8967	0.042	2805	1	0	0	0	1.18	2.36	3.54	5.25	53614
6	7554	7554	0.045	2536	3	0	1	2	2.30	4.67	7.16	12.52	58468
8	7251	7251	0.041	1939	4	0	1	2	0.92	3.97	7.02	10.29	52149
10	10408	10408	0.041	2140	1	0	0	0	0.03	3.46	7.51	11.56	48794
12	9766	9766	0.041	1793	1	0	0	0	0.03	0.81	5.37	9.94	43783
14	11207	11207	0.041	1695	0	0	0	0	0.04	0.07	1.97	6.73	39285
16	10366	10366	0.040	1645	1	0	0	0	0.04	0.08	2.22	7.89	39128
18	8512	8512	0.042	1524	2	0	0	1	0.05	0.10	2.15	8.74	38695
20	7726	7726	0.042	1267	3	0	1	1	0.06	0.12	2.90	10.67	39016
24	8819	8819	0.043	1339	2	0	0	1	0.08	0.15	4.23	14.50	39272

Bolt Yield Stress = 33,000 psi (SA193-B8)

DGmax = 0.050 in

Calculation 3002515

TABLE 3-16

300# FLANGE GASKET STRESS, GROSS LEAK PRESSURE, AND LEAK RATE

INITIAL BOLT STRESS = 25000 psi

JOINT RELAXATION = 25%

Flange Diameter (in)	Eff Gasket Stress (psi)	Act Gasket Stress (psi)	Gasket Deflect. (in)	Gross Leak Pressure (psi)	Leak Rate at GLP (mg/sec)	Leak Rate at .25GLP (mg/sec)	Leak Rate at .50GLP (mg/sec)	Leak Rate at .75GLP (mg/sec)	Leak Area at 1.25GLP (sq in)	Leak Area at 1.5GLP (sq in)	Leak Area at 1.75GLP (sq in)	Leak Area at 2.0GLP (sq in)	Bolt Stress at 2.0GLP (psi)
Flanges													
1-1/2	13429	13429	0.042	7561	0	0	0	0	0.35	0.70	1.05	1.52	53070
2	14362	14362	0.042	6368	0	0	0	0	0.49	0.98	1.48	2.22	53956
2-1/2	18226	18226	0.041	6954	0	0	0	0	0.66	1.30	1.99	3.08	54591
3	11833	11833	0.041	4810	0	0	0	0	0.95	1.90	2.84	4.60	55619
4	7912	7912	0.042	3391	1	0	0	1	1.42	2.84	4.27	7.45	57870
6	6665	6665	0.045	2237	3	0	1	1	0.60	2.70	4.79	6.88	51590
8	6398	6398	0.041	1711	4	0	1	2	0.02	1.48	4.17	6.86	46014
10	9184	9184	0.041	1888	1	0	0	0	0.03	0.24	3.81	7.39	43053
12	8617	8617	0.041	1582	1	0	0	0	0.03	0.06	1.21	5.24	38632
14	9889	9889	0.041	1496	0	0	0	0	0.03	0.05	0.09	1.87	34663
16	9146	9146	0.040	1451	1	0	0	0	0.04	0.07	0.11	2.07	34525
18	7511	7511	0.042	1345	2	0	0	1	0.04	0.09	0.13	1.89	34143
20	6817	6817	0.042	1118	3	0	1	1	0.05	0.10	0.15	2.68	34426
24	7781	7781	0.043	1182	2	0	0	1	0.07	0.13	0.20	4.01	34652

Bolt Yield Stress = 33,000 psi (SA193-B8)

DGmax = 0.050 in

Calculation 3002525

TABLE 3-17
300# FLANGE GASKET STRESS, GROSS LEAK PRESSURE, AND LEAK RATE

INITIAL BOLT STRESS = 25000 psi

JOINT RELAXATION = 33%

Flange Diameter (in)	Eff Gasket Stress (psi)	Act Gasket Stress (psi)	Gasket Deflect. (in)	Gross Leak Pressure (psi)	Leak Rate at GLP (mg/sec)	Leak Rate at .25GLP (mg/sec)	Leak Rate at .50GLP (mg/sec)	Leak Rate at .75GLP (mg/sec)	Leak Area at 1.25GLP (sq in)	Leak Area at 1.5GLP (sq in)	Leak Area at 1.75GLP (sq in)	Leak Area at 2.0GLP (sq in)	Bolt Stress at 2.0GLP (psi)
Flanges													
1-1/2	11997	11997	0.042	7733	0	0	0	0	0.24	0.60	0.96	1.33	51653
2	12830	12830	0.042	7102	0	0	0	0	0.52	1.06	1.61	2.66	56014
2-1/2	16281	16281	0.041	7930	0	0	0	0	0.75	1.51	2.27	3.92	57621
3	10571	10571	0.041	5038	0	0	0	0	0.77	1.77	2.76	4.51	55372
4	7068	7068	0.042	3029	1	0	0	1	0.46	1.74	3.02	4.29	51697
6	5954	5954	0.045	1999	3	0	1	1	0.01	1.12	2.99	4.86	46087
8	5715	5715	0.041	1529	3	0	1	2	0.02	0.04	1.89	4.29	41106
10	8204	8204	0.041	1687	1	0	0	0	0.02	0.05	0.85	4.05	38461
12	7698	7698	0.041	1413	1	0	0	0	0.03	0.05	0.06	1.48	34511
14	8834	8834	0.041	1338	0	0	0	0	0.03	0.06	0.08	0.11	30966
16	8171	8171	0.040	1296	1	0	0	0	0.03	0.07	0.10	0.13	30842
18	6710	6710	0.042	1201	2	0	0	1	0.04	0.08	0.12	0.15	30503
20	6090	6090	0.042	998	3	0	1	1	0.05	0.09	0.14	0.18	30754
24	6951	6951	0.043	1056	1	0	0	1	0.06	0.12	0.18	0.24	30956

Bolt Yield Stress = 33,000 psi (SA193-B8)

DGmax = 0.050 in

Calculation 3002533

TABLE 3-18

300# FLANGE GASKET STRESS, GROSS LEAK PRESSURE, AND LEAK RATE

INITIAL BOLT STRESS = 25000 psi

JOINT RELAXATION = 50%

Flange Diameter (in)	Eff Gasket Stress (psi)	Act Gasket Stress (psi)	Gasket Deflect (in)	Gross Leak Pressure (psi)	Leak Rate at GLP (mg/sec)	Leak Rate at .25GLP (mg/sec)	Leak Rate at .50GLP (mg/sec)	Leak Rate at .75GLP (mg/sec)	Leak Area at 1.25GLP (sq in)	Leak Area at 1.5GLP (sq in)	Leak Area at 1.75GLP (sq in)	Leak Area at 2.0GLP (sq in)	Bolt Stress at 2.0GLP (psi)
Flanges													
1-1/2	8953	8953	0.042	5771	0	0	0	0	0.00	0.00	0.14	0.40	38696
2	9575	9575	0.042	5300	0	0	0	0	0.00	0.01	0.42	0.83	41801
2-1/2	12150	12150	0.041	5997	0	0	0	0	0.00	0.14	0.71	1.29	43407
3	7889	7889	0.041	3760	0	0	0	0	0.01	0.01	0.67	1.41	41322
4	5275	5275	0.042	2261	1	0	0	1	0.01	0.01	0.35	1.30	38580
6	4444	4444	0.045	1492	2	0	1	1	0.01	0.02	0.03	0.55	34393
8	4265	4265	0.041	1141	3	0	1	2	0.01	0.03	0.04	0.05	30676
10	6122	6122	0.041	1259	1	0	0	0	0.02	0.04	0.05	0.07	28702
12	5745	5745	0.041	1055	1	0	0	0	0.02	0.04	0.06	0.08	25755
14	6592	6592	0.041	997	0	0	0	0	0.02	0.04	0.06	0.08	23109
16	6098	6098	0.040	967	1	0	0	0	0.02	0.05	0.07	0.10	23017
18	5007	5007	0.042	897	1	0	0	1	0.03	0.06	0.09	0.12	22762
20	4545	4545	0.042	745	3	0	0	1	0.03	0.07	0.10	0.14	22951
24	5188	5188	0.043	788	1	0	0	1	0.04	0.09	0.13	0.18	23101

Bolt Yield Stress = 33,000 psi (SA193-B8)

DGmax = 0.050 in

Calculation 3002550

TABLE 3-19

300# FLANGE GASKET STRESS, GROSS LEAK PRESSURE, AND LEAK RATE

INITIAL BOLT STRESS = 25000 psi

JOINT RELAXATION = 0%

Flange Diameter (in)	Eff Gasket Stress (psi)	Act Gasket Stress (psi)	Gasket Deflect (in)	Gross Leak Pressure (psi)	Leak Rate at GLP (mg/sec)	Leak Rate at .25GLP (mg/sec)	Leak Rate at .50GLP (mg/sec)	Leak Rate at .75GLP (mg/sec)	Leak Area at 1.25GLP (sq in)	Leak Area at 1.5GLP (sq in)	Leak Area at 1.75GLP (sq in)	Leak Area at 2.0GLP (sq in)	Bolt Stress at 2.0GLP (psi)
Flanges													
1-1/2	17906	17906	0.042	1326	0	0	0	0	0.06	0.12	0.18	0.25	31021
2	19150	19150	0.042	1117	0	0	0	0	0.09	0.17	0.26	0.35	31176
2-1/2	24301	24301	0.041	1220	0	0	0	0	0.12	0.23	0.35	0.47	31288
3	15778	15778	0.041	844	0	0	0	0	0.17	0.33	0.50	0.67	31468
4	10549	10549	0.042	597	1	0	0	0	0.25	0.50	0.75	1.01	31886
6	8887	8887	0.045	549	2	0	0	0	0.51	1.03	1.54	2.05	33056
8	8530	8530	0.041	632	3	0	0	0	0.99	1.99	2.98	3.97	35076
10	12245	12245	0.041	1003	1	0	0	0	1.90	3.80	5.70	7.60	37917
12	11490	11490	0.041	1729	1	0	0	0	4.40	8.81	13.21	21.74	46731
14	13185	13185	0.041	1995	0	0	0	0	2.98	8.58	14.18	23.86	46218
16	12195	12195	0.040	1935	1	0	0	0	3.52	10.20	16.87	28.16	46033
18	10015	10015	0.042	1793	2	0	0	1	4.00	11.76	19.51	31.78	45524
20	9090	9090	0.042	1490	3	0	1	1	4.79	13.93	23.06	38.24	45902
24	10375	10375	0.043	1576	2	0	0	1	6.43	18.51	30.60	51.45	46203

Bolt Yield Stress = 27,500 psi (SA193-B8)

DGmax = 0.050 in

Calculation: 3002500Y

TABLE 3-20
300# FLANGE GASKET STRESS, GROSS LEAK PRESSURE, AND LEAK RATE

INITIAL BOLT STRESS = 50000 psi

JOINT RELAXATION = 0%

Flange Diameter (in)	Eff Gasket Stress (psi)	Act Gasket Stress (psi)	Gasket Deflect. (in)	Gross Leak Pressure (psig)	Leak Rate at GLP (mg/sec)	Leak Rate at .25GLP (mg/sec)	Leak Rate at .50GLP (mg/sec)	Leak Rate at .75GLP (mg/sec)	Leak Area at 1.25GLP (sq in)	Leak Area at 1.5GLP (sq in)	Leak Area at 1.75GLP (sq in)	Leak Area at 2.0GLP (sq in)	Bolt Stress at 2.0GLP (psi)
Flanges													
1-1/2	35812	21550	0.050	15557	0	0	0	0	0.01	0.01	0.02	0.02	111020
2	38299	22800	0.050	15365	0	0	0	0	0.01	0.02	0.03	0.03	121192
2-1/2	48601	29300	0.050	17700	0	0	0	0	0.01	0.02	0.04	0.76	128119
3	31556	19050	0.050	11284	0	0	0	0	0.02	0.03	0.05	0.38	124022
4	21098	12700	0.050	6991	0	0	0	0	0.02	0.04	0.06	0.08	119305
6	17774	9900	0.050	4777	2	0	0	[illegible]	0.03	0.06	0.09	0.13	110147
8	17060	10350	0.050	3971	1	0	0	1	0.04	0.09	0.13	0.18	106778
10	24489	14850	0.050	4559	0	0	0	0	0.06	0.12	0.18	0.24	103963
12	22979	14100	0.050	4007	0	0	0	0	0.07	0.14	0.22	0.29	97844
14	26370	16200	0.050	3989	0	0	0	0	0.08	0.16	0.24	0.32	92436
16	24390	15100	0.050	3870	0	0	0	0	0.09	0.19	0.28	0.38	92067
18	20029	11900	0.050	3586	1	0	0	0	0.11	0.22	0.33	0.44	91047
20	18180	10800	0.050	2980	1	0	0	0	0.13	0.26	0.39	0.52	91803
24	20751	12000	0.050	3152	1	0	0	0	0.17	0.34	0.51	0.68	92406

Bolt Yield Stress = 122,000 psi (SA564-630)

DGmax = 0.050 in

Calculation 3005000.WR1

TABLE 3-21
300# FLANGE GASKET STRESS, GROSS LEAK PRESSURE, AND LEAK RATE

INITIAL BOLT STRESS = 60000 psi

JOINT RELAXATION = 75%

Flange Diameter (in)	Eff Gasket Stress (psi)	Act Gasket Stress (psi)	Gasket Deflect. (in)	Gross Leak Pressure (psi)	Leak Rate at GLP (mg/sec)	Leak Rate at .25GLP (mg/sec)	Leak Rate at .50GLP (mg/sec)	Leak Rate at .75GLP (mg/sec)	Leak Area at 1.25GLP (sq in)	Leak Area at 1.5GLP (sq in)	Leak Area at 1.75GLP (sq in)	Leak Area at 2.0GLP (sq in)	Bolt Stress at 2.0GLP (psi)
Flanges													
1-1/2	42974	21550	0.050	17896	0	0	0	0	0.01	0.01	0.02	0.02	119998
2	45959	22800	0.050	16722	0	0	0	0	0.01	0.02	0.03	0.92	131894
2-1/2	58322	29300	0.050	19332	0	0	0	0	0.01	0.03	0.38	2.14	139926
3	37867	19050	0.050	12397	0	0	0	0	0.02	0.03	0.05	2.33	136253
4	25318	12700	0.050	7768	0	0	0	0	0.02	0.05	0.07	2.39	132577
6	21329	9900	0.050	5433	2	0	1	1	0.04	0.07	0.11	1.29	125280
8	20472	10350	0.050	4583	2	0	0	1	0.05	0.10	0.15	0.81	123220
10	29387	14850	0.050	5324	0	0	0	0	0.07	0.14	0.21	0.29	121414
12	27575	14100	0.050	4741	0	0	0	0	0.09	0.17	0.26	0.34	115770
14	31674	16200	0.050	4787	0	0	0	0	0.10	0.19	0.29	0.38	110923
16	29268	15100	0.050	4644	0	0	0	0	0.11	0.23	0.34	0.45	110480
18	24035	11900	0.050	4304	1	0	0	0	0.13	0.26	0.39	0.53	109257
20	21816	10800	0.050	3576	1	0	0	0	0.15	0.31	0.46	0.62	110164
24	24901	12000	0.050	3782	1	0	0	0	0.21	0.41	0.62	0.82	110887

Bolt Yield Stress = 122,000 psi (SA564-630)

DGmax = 0.050 in

Calculation 3006000.WR1

TABLE 3-22

300# FLANGE GASKET STRESS, GROSS LEAK PRESSURE, AND LEAK RATE

INITIAL BOLT STRESS = 60000 psi

JOINT RELAXATION = 25%

Flange Diameter (in)	Eff Gasket Stress (psi)	Act Gasket Stress (psi)	Gasket Deflect. (in)	Gross Leak Pressure (psi)	Leak Rate at GLP (mg/sec)	Leak Rate at .25GLP (mg/sec)	Leak Rate at .50GLP (mg/sec)	Leak Rate at .75GLP (mg/sec)	Leak Area at 1.25GLP (sq in)	Leak Area at 1.5GLP (sq in)	Leak Area at 1.75GLP (sq in)	Leak Area at 2.0GLP (sq in)	Bolt Stress at 2.0GLP (psi)
Flanges													
1-1/2	42974	16163	0.050	15430	0	0	0	0	0.01	0.01	0.02	0.02	103465
2	45959	17100	0.050	14576	0	0	0	0	0.01	0.02	0.02	0.03	114972
2-1/2	58322	21975	0.050	16946	0	0	0	0	0.01	0.02	0.03	0.12	122655
3	37867	14288	0.050	10967	0	0	0	0	0.02	0.03	0.05	0.06	120537
4	25318	9525	0.050	6993	0	0	0	0	0.02	0.04	0.06	0.08	119340
6	21329	7425	0.050	5059	2	0	1	1	0.03	0.07	0.10	0.13	116659
8	20472	7763	0.050	4354	2	0	0	1	0.05	0.10	0.15	0.19	117078
10	29387	11138	0.050	5141	0	0	0	0	0.07	0.14	0.21	0.28	117236
12	27575	10575	0.050	4657	0	0	0	0	0.08	0.17	0.25	0.34	113715
14	31644	12150	0.050	4787	0	0	0	0	0.10	0.19	0.29	0.38	110923
16	29268	11325	0.050	4644	0	0	0	0	0.11	0.23	0.34	0.45	110480
18	24035	8925	0.050	4304	1	0	0	0	0.13	0.26	0.39	0.53	109257
20	21816	8100	0.050	3576	1	0	0	0	0.15	0.31	0.46	0.62	110164
24	24901	9000	0.050	3782	1	0	0	0	0.21	0.41	0.62	0.82	110987

Bolt Yield Stress = 122,000 psi (SA564-630)

DGmax = 0.050 in

Calculation 3006025.WR1

TABLE 3-23

300# FLANGE GASKET STRESS, GROSS LEAK PRESSURE, AND LEAK RATE

INITIAL BOLT STRESS = 60000 psi

JOINT RELAXATION = 0%

Flange Diameter (in)	Eff Gasket Stress (psi)	Act Gasket Stress (psi)	Gasket Deflect. (in)	Gross Leak Pressure (psi)	Leak Rate at GLP (mg/sec)	Leak Rate at .25GLP (mg/sec)	Leak Rate at .50GLP (mg/sec)	Leak Rate at .75GLP (mg/sec)	Leak Area at 1.25GLP (sq in)	Leak Area at 1.5GLP (sq in)	Leak Area at 1.75GLP (sq in)	Leak Area at 2.0GLP (sq in)	Bolt Stress at 2.0GLP (psi)
Flanges													
1-1/2	42974	21550	0.050	17896	0	0	0	0	0.01	0.01	0.02	0.62	119998
2	45955	22800	0.050	16722	0	0	0	0	0.01	0.02	0.66	1.89	131894
2-1/2	58322	29300	0.050	19332	0	0	0	0	0.01	0.03	1.66	3.41	139926
3	37867	19050	0.050	12397	0	0	0	0	0.02	0.03	1.75	4.08	136253
4	25318	12700	0.050	7768	0	0	0	0	0.02	0.05	1.65	4.77	132577
6	21329	9900	0.050	5433	2	0	1	1	0.04	0.07	0.29	5.14	125280
8	20472	10350	0.050	4583	2	0	0	1	0.05	0.10	0.15	6.27	123220
10	29387	14850	0.050	5324	0	0	0	0	0.07	0.14	0.21	7.48	121414
12	27575	14100	0.050	4741	0	0	0	0	0.09	0.17	0.26	4.48	115770
14	31644	16200	0.050	4787	0	0	0	0	0.10	0.19	0.29	0.38	110923
16	29268	15100	0.050	4644	0	0	0	0	0.11	0.23	0.34	0.45	110480
18	24035	11900	0.050	4304	1	0	0	0	0.13	0.26	0.39	0.53	109257
20	21816	10800	0.050	3576	1	0	0	0	0.15	0.31	0.46	0.62	110164
24	24901	12000	0.050	3782	1	0	0	0	0.21	0.41	0.62	0.82	110887

Bolt Yield Stress = 111,000 psi (SA564 630)

DGmax = 0.050 in

Calculation 3006000Y.WR1

TABLE 3-24
400# ANSI FLANGE AND GASKET DATA

Flange Diameter (in)	GASKET OD (in)	GASKET ID (in)	GASKET Width (in)	GASKET Area (sq in)	Pressure Area (sq in)	BOLTS Number	BOLTS Diameter (in)	BOLTS Area (sq in)	BOLTS Length (in)
Flanges									
1-1/2	2.750	2.125	0.2500	1.865	3.547	4	3/4	0.3340	2.125
2	3.375	2.750	0.2500	2.356	5.940	8	5/8	0.2256	2.375
2-1/2	3.875	3.250	0.2500	2.749	8.296	8	3/4	0.3340	2.625
3	4.750	4.000	0.3125	4.234	12.566	8	3/4	0.3340	2.875
4	5.875	5.000	0.3750	6.332	19.635	8	7/8	0.4612	3.125
6	8.250	7.188	0.4688	11.275	40.574	12	7/8	0.4612	3.625
8	10.375	9.188	0.5313	16.220	66.296	12	1	0.6051	4.125
10	12.500	11.313	0.5313	19.767	100.509	16	1-1/8	0.7896	4.625
12	14.750	13.375	0.6250	27.489	140.500	16	1-1/4	0.9985	4.875
14	16.000	14.625	0.6250	29.943	167.989	20	1-1/4	0.9985	5.125
16	18.250	16.625	0.7500	40.939	217.077	20	1-3/8	1.2319	5.375
18	20.750	18.688	0.9688	59.822	274.279	24	1-3/8	1.2319	5.625
20	22.750	20.688	0.9688	65.909	336.129	24	1-1/2	1.4899	5.875
24	27.000	24.750	1.0625	86.161	481.105	24	1-3/4	1.8983	6.375

Bolt areas correspond to tensile stress area

TABLE 3-25
400# FLANGE GASKET STRESS, GROSS LEAK PRESSURE, AND LEAK RATE

INITIAL BOLT STRESS = 20000 psi

JOINT RELAXATION = 0%

Flange Diameter (in)	Eff Gasket Stress (psi)	Act Gasket Stress (psi)	Gasket Deflect. (in)	Gross Leak Pressure (psi)	Leak Rate at GLP (mg/sec)	Leak Rate at .25GLP (mg/sec)	Leak Rate at .50GLP (mg/sec)	Leak Rate at .75GLP (mg/sec)	Leak Area at 1.25GLP (sq in)	Leak Area at 1.5GLP (sq in)	Leak Area at 1.75GLP (sq in)	Leak Area at 2.0GLP (sq in)	Bolt Stress at 2.0GLP (psi)
Flanges													
1-1/2	14325	14325	0.033	6897	0	0	0	0	0.36	0.73	1.09	4.07	51310
2	15320	15320	0.034	5209	0	0	0	0	0.53	1.07	1.60	2.18	52118
2-1/2	19441	19441	0.033	6344	0	0	0	0	0.71	1.41	2.12	2.98	52697
3	12622	12622	0.033	4388	0	0	0	0	0.99	1.99	2.98	4.42	53635
4	11653	11653	0.046	4286	1	0	0	0	1.48	2.97	4.45	7.25	55807
6	9817	9817	0.050	3295	2	0	0	1	1.68	4.27	6.86	11.20	55029
8	8953	8953	0.045	2395	3	0	1	1	0.03	3.21	6.59	9.97	49082
10	12783	12783	0.043	2628	1	0	0	0	0.03	2.13	6.55	10.96	45923
12	11624	11624	0.041	2134	1	0	0	0	0.04	0.07	3.78	8.71	41208
14	13339	13339	0.041	2018	0	0	0	0	0.04	0.08	0.11	4.90	36974
16	12036	12036	0.040	1910	1	0	0	0	0.04	0.09	0.13	5.64	36827
18	9884	9884	0.042	1770	2	0	0	1	0.05	0.10	0.16	5.98	36419
20	10851	10800	0.050	1779	1	0	0	0	0.06	0.12	0.18	7.47	36721
24	10575	10575	0.044	1506	1	0	0	1	0.08	0.16	0.24	10.26	36962

Bolt Yield Stress = 33,000 psi (SA193-B8)

DGmax = 0.050 in

Calculation 4002000

TABLE 3-26

400# FLANGE GASKET STRESS, GROSS LEAK PRESSURE, AND LEAK RATE

INITIAL BOLT STRESS = 25000 psi

JOINT RELAXATION = 0%

Flange Diameter (in)	Eff Gasket Stress (psi)	Act Gasket Stress (psi)	Gasket Deflect (in)	Gross Leak Pressure (psi)	Leak Rate at GLP (mg/sec)	Leak Rate at .25GLP (mg/sec)	Leak Rate at .50GLP (mg/sec)	Leak Rate at .75GLP (mg/sec)	Leak Area at 1.25GLP (sq in)	Leak Area at 1.5GLP (sq in)	Leak Area at 1.75GLP (sq in)	Leak Area at 2.0GLP (sq in)	Bolt Stress at 2.0GLP (psi)
Flanges													
1-1/2	17906	17906	0.042	4245	0	0	0	0	0.22	0.45	0.67	0.89	44268
2	19150	19150	0.042	3575	0	0	0	0	0.33	0.66	0.98	1.31	44765
2-1/2	24301	24301	0.041	3904	0	0	0	0	0.43	0.87	1.30	1.74	45121
3	15778	15778	0.041	2700	0	0	0	0	0.61	1.22	1.84	2.45	45698
4	14567	12700	0.050	5787	0	0	0	0	2.00	5.43	10.89	21.52	71524
6	12272	9900	0.050	3761	2	0	0	1	2.96	5.91	11.09	18.78	62804
8	11192	10350	0.050	2919	1	0	0	1	4.12	8.24	13.42	22.73	59830
10	15978	14850	0.050	3229	0	0	0	0	3.52	8.95	14.37	24.71	56431
12	14529	14100	0.050	2657	0	0	0	0	0.83	7.00	13.14	19.28	51312
14	16673	16200	0.050	2522	0	0	0	0	0.05	3.21	9.59	15.97	46218
16	15046	15046	0.050	2387	0	0	0	0	0.06	3.70	11.25	18.81	46033
18	12356	11900	0.050	2212	1	0	0	0	0.06	3.95	12.67	21.39	45524
20	13563	10800	0.050	2224	1	0	0	0	0.08	4.91	15.13	25.34	45902
24	13219	12000	0.050	2008	1	0	0	0	0.10	6.73	20.13	33.53	46203

Bolt Yield Stress = 33,000 psi (SA193-B8)

DGmax = 0.050 in

Calculation 4002500

TABLE 3-27

400# FLANGE GASKET STRESS, GROSS LEAK PRESSURE, AND LEAK RATE

INITIAL BOLT STRESS = 30000 psi

JOINT RELAXATION = 0%

Flange Diameter (in)	Eff Gasket Stress (psi)	Act Gasket Stress (psi)	Gasket Deflect (in)	Gross Leak Pressure (psi)	Leak Rate at GLP (mg/sec)	Leak Rate at .25GLP (mg/sec)	Leak Rate at .50GLP (mg/sec)	Leak Rate at .75GLP (mg/sec)	Leak Area at 1.25GLP (sq in)	Leak Area at 1.5GLP (sq in)	Leak Area at 1.75GLP (sq in)	Leak Area at 2.0GLP (sq in)	Bolt Stress at 2.0GLP (psi)
Flanges													
1-1/2	21487	21487	0.050	13850	0	0	0	0	2.07	6.39	*	*	92871
2	22979	22800	0.050	12652	0	0	0	0	4.30	11.62	*	*	99790
2-1/2	29161	29161	0.050	14393	0	0	0	0	6.99	17.09	*	*	104178
3	18933	18933	0.050	9024	0	0	0	0	6.57	19.47	*	*	99174
4	17480	12700	0.050	6324	0	0	0	0	1.27	7.68	17.62	31.44	78159
6	14726	9900	0.050	4214	2	0	0	1	3.31	8.31	16.72	32.86	70371
8	13430	10350	0.050	3321	1	0	0	1	4.69	10.22	20.81	39.41	68051
10	19174	14850	0.050	3728	0	0	0	0	6.26	12.52	25.09	43.61	65157
12	17435	14100	0.050	3121	0	0	0	0	7.03	14.24	23.58	39.66	80274
14	20008	16200	0.050	3027	0	0	0	0	4.07	11.73	19.38	32.58	55462
16	18055	15100	0.050	2865	0	0	0	0	4.79	13.85	22.91	38.20	55240
18	14827	11900	0.050	2655	1	0	0	0	5.40	15.87	26.34	42.85	54628
20	16276	10800	0.050	2668	1	0	0	1	6.44	18.70	30.96	51.30	55082
24	15863	12000	0.050	2409	1	0	0	0	8.55	24.63	40.7[illegible]	0[illegible].39	55[illegible]3

* Bolt Ultimate Strength Exceeded

Bolt Ultimate Strength = 82,500 psi (SA193-B8)

Bolt Yield Stress = 33,000 psi (SA193-B8)

DGmax = 0.050 in

Calculation 4003000

TABLE 3-28

400# FLANGE GASKET STRESS, GROSS LEAK PRESSURE, AND LEAK RATE

INITIAL BOLT STRESS = 25000 psi

JOINT RELAXATION = 15%

Flange Diameter (in)	Eff Gasket Stress (psi)	Act Gasket Stress (psi)	Gasket Deflect (in)	oss Leak essure (psi)	Leak Rate at G' P (mg/sec)	Leak Rate at .25GLP (mg/sec)	Leak Rate at .50GLP (mg/sec)	Leak Rate at .75GLP (mg/sec)	Leak Area at 1.25GLP (sq in)	Leak Area at 1.5GLP (sq in)	Leak Area at 1.75GLP (sq in)	Leak Area at 2.0GLP (sq in)	Bolt Stress at 2.0G (psi)
Flanges													
1-1/2	15220	15220	0.042	6234	0	0	0	0	0.33	0.66	0.99	1.31	48549
2	16277	16277	0.042	5251	0	0	0	0	0.48	0.96	1.44	1.93	50279
2-1/2	20656	20656	0.041	5734	0	0	0	0	0.64	1.28	1.91	2.55	50803
3	13411	13411	0.041	3966	0	0	0	0	0.90	1.80	2.70	3.60	51651
4	14567	10795	0.050	5321	0	0	0	0	1.84	3.69	7.79	13.50	65772
6	12272	8415	0.050	3537	2	0	0	1	2.78	5.56	8.76	15.04	59038
8	11192	8798	0.050	2782	1	0	0	1	3.08	7.01	10.93	18.92	57021
10	15978	12623	0.050	3119	0	0	0	0	2.47	7.70	12.34	21.05	54511
12	14529	11985	0.050	2607	0	0	0	0	0.19	6.21	12.24	18.26	50337
14	16673	13770	0.050	2522	0	0	0	0	0.05	3.21	9.59	15.97	46218
16	15046	12789	0.050	2387	0	0	0	0	0.06	3.70	11.25	18.81	46033
18	12356	10115	0.050	2212	1	0	0	0	0.06	3.96	12.67	21.39	45524
20	13563	9180	0.050	2224	1	0	0	0	0.08	4.91	15.13	25.34	45902
24	13219	10200	0.050	2008	1	0	0	0	0.10	6.73	20.13	33.53	46203

Bolt Yield Stress = 33,000 psi (SA193-B8)

DGmax = 0.050 in

Calculation 4002515

TABLE 3-29

400# FLANGE GASKET STRESS, GROSS LEAK PRESSURE, AND LEAK RATE

INITIAL BOLT STRESS = 25000 psi

JOINT RELAXATION = 25%

Flange Diameter (in)	Eff Gasket Stress (psi)	Act Gasket Stress (psi)	Gasket Deflect. (in)	Gross Leak Pressure (psi)	Leak Rate at GLP (mg/sec)	Leak Rate at .25GLP (mg/sec)	Leak Rate at .50GLP (mg/sec)	Leak Rate at .75GLP (mg/sec)	Leak Area at 1.25GLP (sq in)	Leak Area at 1.5GLP (sq in)	Leak Area at 1.75GLP (sq in)	Leak Area at 2.0GLP (sq in)	Bolt Stress at 2.0GLP (psi)
Flanges													
1-1/2	13429	13429	0.042	7561	0	0	0	0	0.40	0.60	1.19	1.72	53070
2	14362	14362	0.042	6368	0	0	0	0	0.58	1.17	1.75	2.64	53956
2-1/2	18226	18226	0.041	6954	0	0	0	0	0.77	1.55	2.32	3.60	54591
3	11833	11833	0.041	4810	0	0	0	0	1.09	2.18	3.27	5.29	55619
4	14567	9525	0.050	5011	0	0	0	0	1.74	3.47	6.35	10.61	61937
6	12272	7425	0.050	3387	2	0	0	1	2.12	4.78	7.45	12.68	56561
8	11192	7763	0.050	2691	1	0	0	1	2.31	6.11	9.91	16.31	55149
10	15978	11138	0.050	3046	0	0	0	0	1.76	6.87	11.98	18.62	53230
12	14529	10575	0.050	2573	0	0	0	0	0.04	5.69	11.63	17.58	49687
14	16673	12150	0.050	2522	0	0	0	0	0.05	3.21	9.59	15.97	46218
16	15046	11284	0.050	2387	0	0	0	0	0.06	3.70	11.25	18.81	46033
18	12356	8925	0.050	2212	1	0	0	0	0.06	3.95	12.67	21.39	45524
20	13563	8100	0.050	2224	1	0	0	0	0.08	4.91	15.13	25.34	45902
24	13219	9000	0.050	2008	1	0	0	0	0.10	6.73	20.13	33.53	46203

Bolt Yield Stress = 33,000 psi (SA193 B8)

DGmax = 0.050 in

Calculation 4002525

TABLE 3-30

400# FLANGE GASKET STRESS, GROSS LEAK PRESSURE, AND LEAK RATE

INITIAL BOLT STRESS = 25000 psi

JOINT RELAXATION = 33%

Flange Diameter (in)	Eff Gasket Stress (psi)	Act Gasket Stress (psi)	Gasket Deflect. (in)	Gross Leak Pressure (psi)	Leak Rate at GLP (mg/sec)	Leak Rate at .25GLP (mg/sec)	Leak Rate at .50GLP (mg/sec)	Leak Rate at .75GLP (mg/sec)	Leak Area at 1.25GLP (sq in)	Leak Area at 1.5GLP (sq in)	Leak Area at 1.75GLP (sq in)	Leak Area at 2.0GLP (sq in)	Bolt Stress at 2.0GLP (psi)
Flanges													
1-1/2	11997	11997	0.042	7733	0	0	0	0	0.28	0.68	1.09	1.50	51853
2	12830	12830	0.042	7102	0	0	0	0	0.61	1.26	1.91	3.16	56014
2-1/2	16281	16281	0.041	7930	0	0	0	0	0.88	1.76	2.65	4.58	57821
3	10571	10571	0.041	5038	0	0	0	0	0.89	2.03	3.17	5.18	55372
4	14567	8509	0.050	4763	0	0	0	0	1.65	3.30	5.19	8.90	58870
6	12272	6633	0.050	3267	2	0	0	1	1.55	4.12	6.69	10	54564
8	11192	6935	0.050	2618	1	0	0	1	1.70	5.39	9.09	14.22	53451
10	15978	9950	0.050	2987	0	0	0	0	1.19	6.21	11.22	16.67	52206
12	14529	9447	0.050	2546	0	0	0	0	0.04	5.27	11.15	17.03	49167
14	16673	10854	0.050	2522	0	0	0	0	0.05	3.21	9.59	15.97	46218
16	15046	10081	0.050	2387	0	0	0	0	0.06	3.70	11.25	18.61	46033
18	12356	7973	0.050	2212	1	0	0	0	0.06	3.95	12.67	21.39	45524
20	13563	7236	0.050	2224	1	0	0	0	0.08	4.91	15.13	25.34	45902
24	13219	8040	0.050	2008	1	0	0	0	0.10	6.73	20.13	33.53	46203

Bolt Yield Stress = 33,000 psi (SA193-B8)

DGmax = 0.050 in

Calculation 4002533

TABLE 3-31

400# FLANGE GASKET STRESS, GROSS LEAK PRESSURE, AND LEAK RATE

INITIAL BOLT STRESS = 25000 psi

JOINT RELAXATION = 50%

Flange Diameter (in)	Eff Gasket Stress (psi)	Act Gasket Stress (psi)	Gasket Deflect. (in)	Gross Leak Pressure (psi)	Leak Rate at GLP (mg/sec)	Leak Rate at .25GLP (mg/sec)	Leak Rate at .50GLP (mg/sec)	Leak Rate at .75GLP (mg/sec)	Leak Area at 1.25GLP (sq in)	Leak Area at 1.5GLP (sq in)	Leak Area at 1.75GLP (sq in)	Leak Area at 2.0GLP (sq in)	Bolt Stress at 2.0GLP (psi)
Flanges													
1-1/2	8953	8953	0.042	5771	0	0	0	0	0.00	0.00	0.15	0.46	38696
2	9575	9575	0.042	5300	0	0	0	0	0.00	0.02	0.50	0.99	41801
2-1/2	12150	12150	0.041	5997	0	0	0	0	0.00	0.17	0.83	1.50	43407
3	7889	7889	0.041	3760	0	0	0	0	0.01	0.01	0.77	1.62	41322
4	14567	6350	0.050	4236	0	0	0	0	0.64	2.11	3.58	5.23	52351
6	12272	4950	0.050	3013	2	0	0	1	0.34	2.71	5.07	7.44	50318
8	11192	5175	0.050	2463	1	0	0	1	0.40	3.87	7.35	10.82	50468
10	15978	7425	0.050	2863	0	0	0	0	0.04	4.80	9.60	14.41	50029
12	14529	7050	0.050	2489	0	0	0	0	0.04	4.38	10.13	15.88	48063
14	16673	8100	0.050	2522	0	0	0	0	0.05	3.21	9.59	15.97	46218
16	15046	7523	0.050	2387	0	0	0	0	0.06	3.70	11.25	18.81	46033
18	12356	5950	0.050	2212	1	0	0	0	0.06	3.95	12.67	21.39	45524
20	13563	5400	0.050	2224	1	0	0	0	0.08	4.81	15.13	25.34	45902
24	13219	6000	0.050	2008	1	0	0	0	0.10	6.73	20.13	33.53	46203

Bolt Yield Stress = 33,000 psi (SA193-B8)

DGmax = 0.050 in

Calculation 4002550

TABLE 3-32
400# FLANGE GASKET STRESS, GROSS LEAK PRESSURE, AND LEAK RATE

INITIAL BOLT STRESS = 25000 psi

JOINT RELAXATION = 0%

Flange Diameter (in)	Eff Gasket Stress (psi)	Act Gasket Stress (psi)	Gasket Deflect. (in)	Gross Leak Pressure (psi)	Leak Rate at GLP (mg/sec)	Leak Rate at .25GLP (mg/sec)	Leak Rate at .50GLP (mg/sec)	Leak Rate at .75GLP (mg/sec)	Leak Area at 1.25GLP (sq in)	Leak Area at 1.5GLP (sq in)	Leak Area at 1.75GLP (sq in)	Leak Area at 2.0GLP (sq in)	Bolt Stress at 2.0GLP (psi)
Flanges													
1-1/2	17906	17906	0.042	1326	0	0	0	0	0.07	0.14	0.21	0.28	31021
2	19150	19150	0.042	1117	0	0	0	0	0.10	0.20	0.31	0.41	31176
2-1/2	24301	24301	0.041	1220	0	0	0	0	0.14	0.27	0.41	0.54	31288
3	15778	15778	0.041	844	0	0	0	0	0.19	0.38	0.57	0.76	31468
4	14567	12700	0.050	5787	0	0	0	0	3.73	10.47	23.12	35.76	71524
6	12272	9900	0.050	3761	2	0	0	1	2.96	9.08	19.02	37.66	62804
8	11192	10350	0.050	2919	1	0	0	1	4.12	10.85	22.00	43.98	59830
10	15978	14950	0.050	3229	0	0	0	0	5.42	11.50	23.55	43.99	56431
12	14529	14100	0.050	2657	0	0	0	0	6.14	12.26	21.48	36.12	51312
14	16673	16200	0.050	2522	0	0	0	0	3.40	9.77	16.15	27.18	46218
16	15046	15046	0.050	2387	0	0	0	0	3.99	11.54	19.09	31.86	46033
18	12356	11900	0.050	2212	1	0	0	0	4.50	13.23	21.95	35.75	45524
20	13563	10800	0.050	2224	1	0	0	0	5.37	15.58	25.80	42.79	45902
24	13219	12000	0.050	2008	1	0	0	0	7.13	20.5[illegible]	33.93	57.04	46203

Bolt Yield Stress = 27,500 psi (SA193-B8)

DGmax = 0.050 in

Calculation 4001250OY

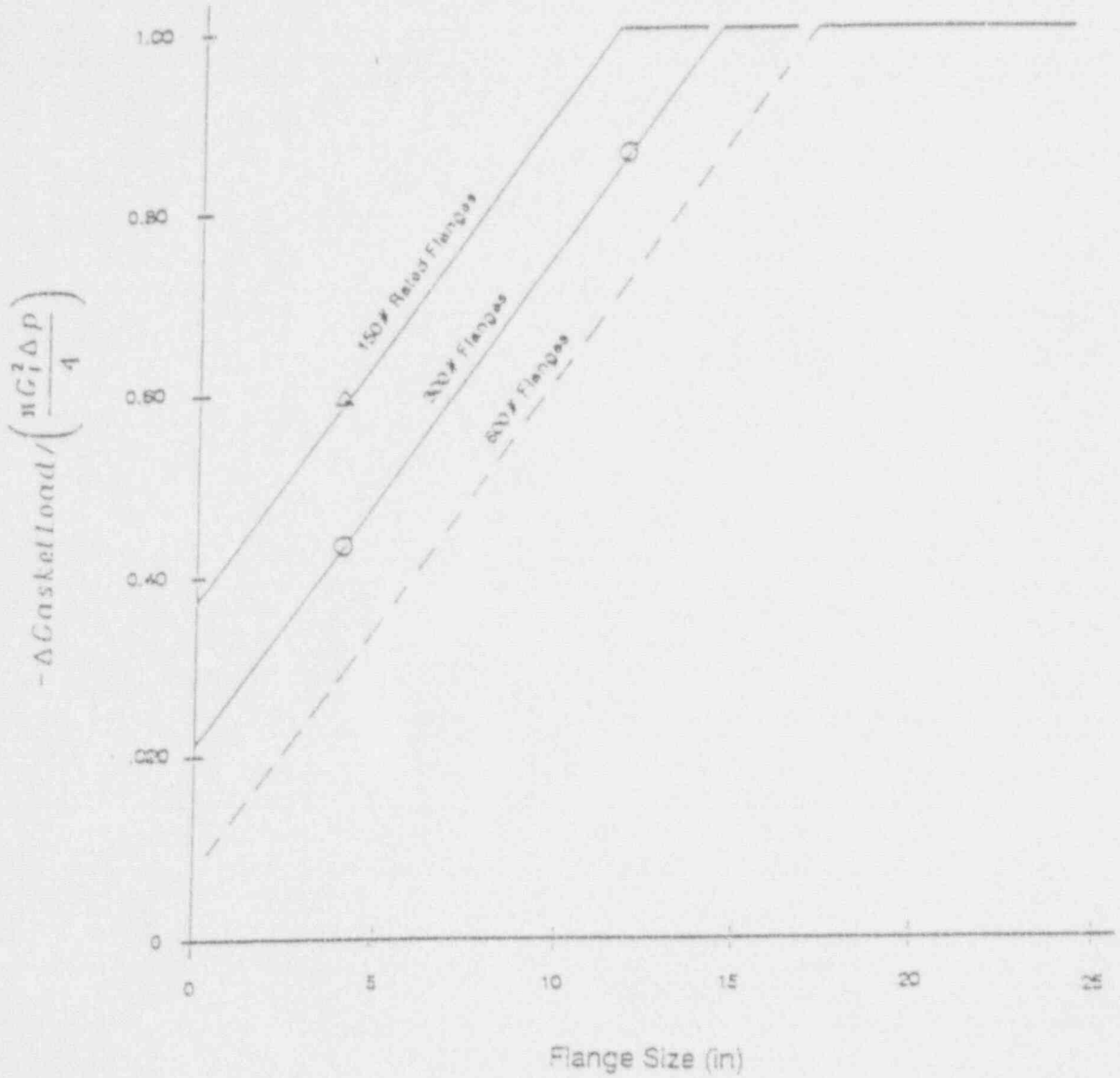

FIGURE 3-1

INCREMENTAL GASKET LOAD TO TOTAL PRESSURE LOAD RATIO
FOR 150 TO 600LB RATED FLANGES

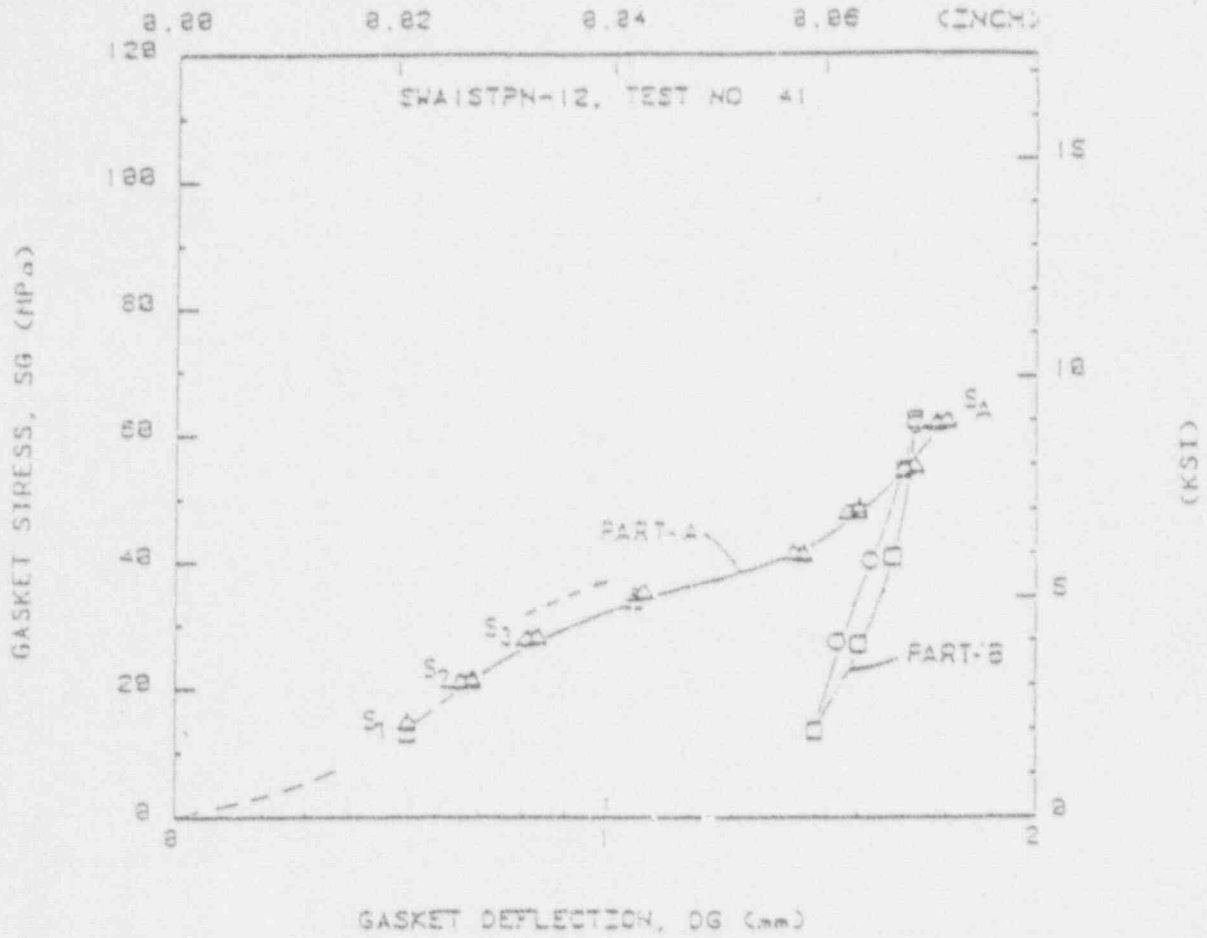

FIGURE 3-2

TYPICAL LOAD-DEFLECTION DIAGRAM SHOWING A STANDARD TEST SEQUENCE

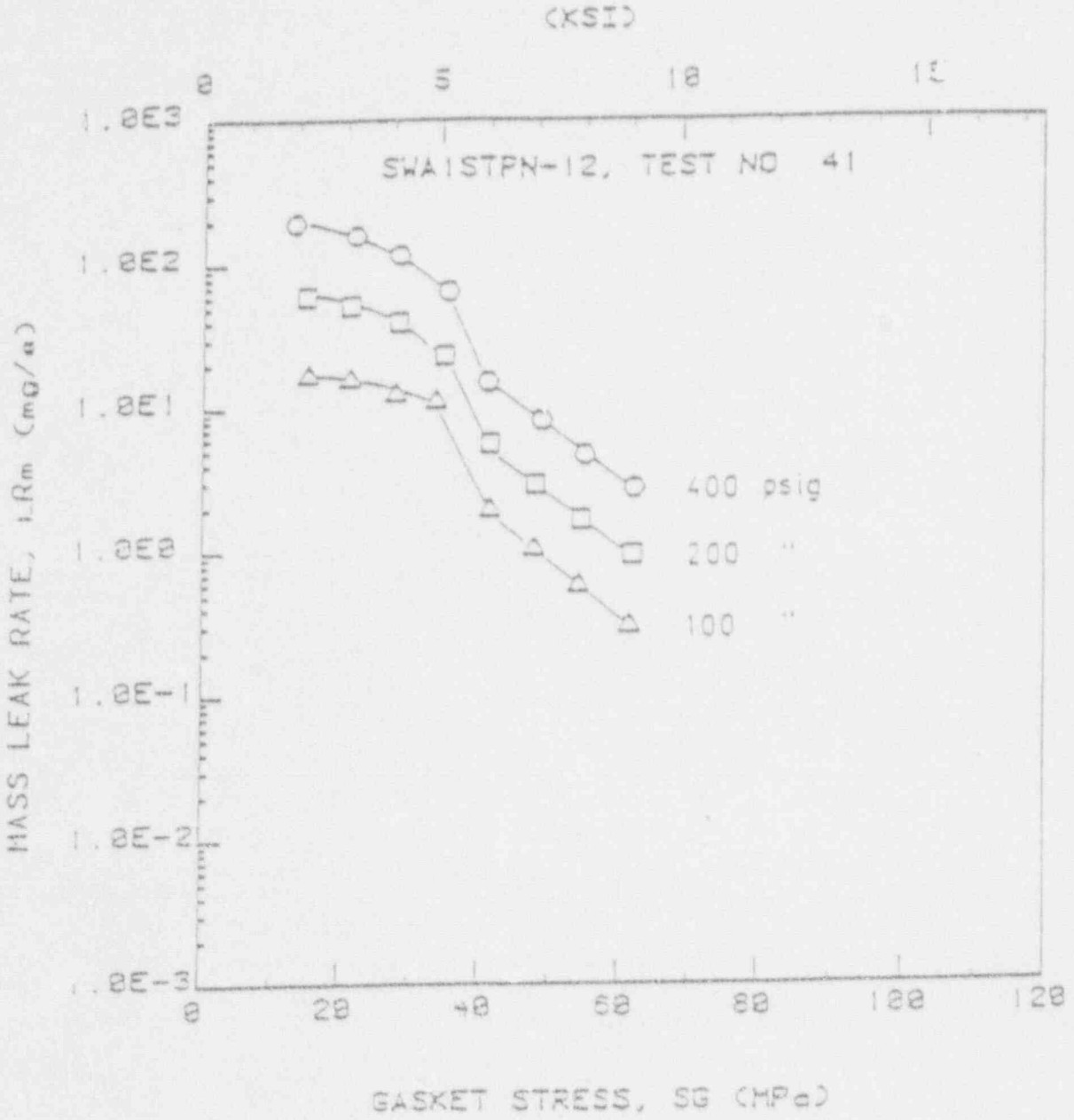

FIGURE 3-3

A TYPICAL MASS-LEAK-RATE VERSUS GASKET STRESS PLOT

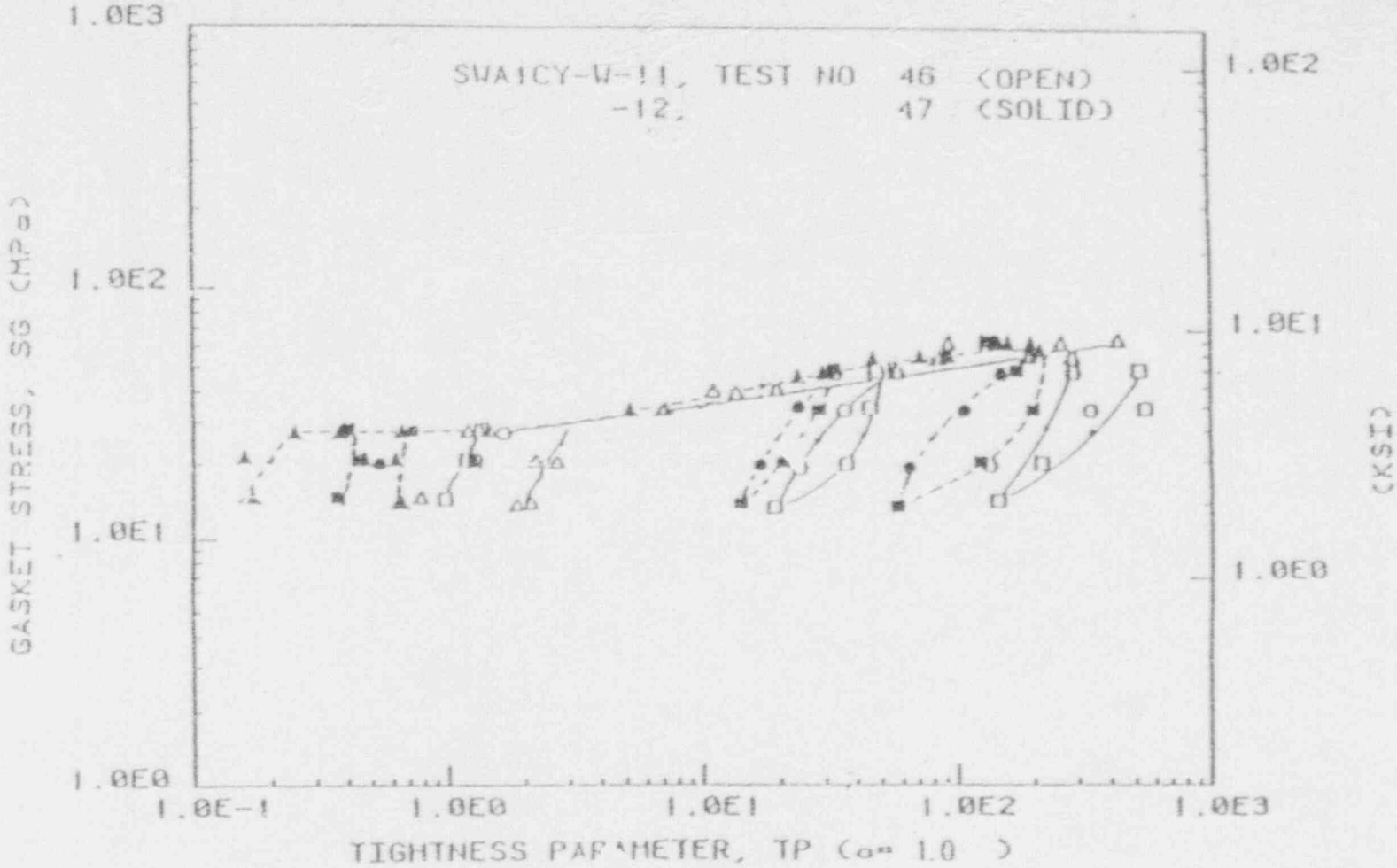

FIGURE 3-4

GASKET STRESS VERSUS TIGHTNESS PARAMETER FOR TWO SPIRAL-WOUND ASBESTOS GASKETS, CYCLIC TESTS WITH WATER

MV-4237-001-R004
Rev. 0

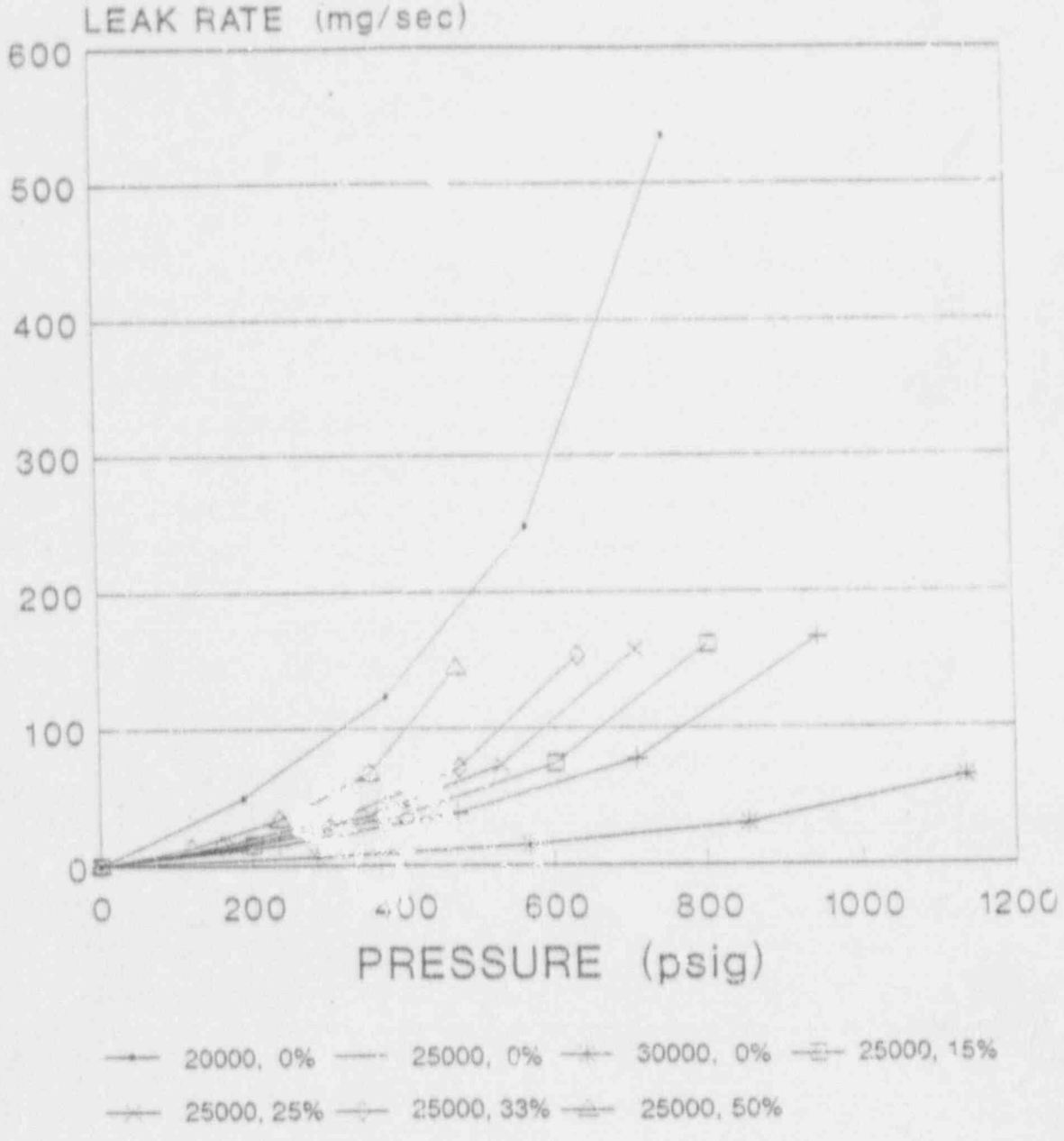

FIGURE 3-5

LEAK RATE VERSUS PRESSURE FOR 8"-150# FLANGE

4. VALVES

Three failure modes are postulated for the various valves present in the reference Combustion Engineering plant safety system under consideration. These include failure of the stem packing, failure of the bolted bonnet seal, and failure of the valve body. The types of valve stem packing currently used in most nuclear plants tend to compress under high pressure conditions providing greater leak resistance. Although it is possible that the stem packing for some valves could deteriorate in response to service conditions, it was judged that any resulting leak rate or leak area would be quite small and have a negligible effect on both valve and system operation. Failure of the bolted bonnet seal is a credible failure mode. However, information on the valve bolted bonnets was not available and, therefore, estimates of pressure capacities for this failure mode could not be made. Since the valve body thickness is typically greater than that for the adjacent piping, it was judged that failure of the adjacent piping will occur prior to the failure of the valve body. Table 4-1 lists the valves in the lines under consideration identified by EG&G.

A particular valve of interest is SI-107A(B), a valve that checks reverse flow from the suction side of the Low Pressure Safety Injection pump back into the Refueling Water Storage Pool. For this valve, the failure mode of interest is an internal failure allowing reverse flow into the Refueling Water Storage Pool. Adequate information on the dimensions of the internal hinged plates was not available. As a result, an evaluation of the pressure capacity for internal failure could not be made. However, based on the limited available information, it was judged that the pressure capacity for this failure mode would be high.

Table 4-1

Valves

SI-107A(B)	SI-208A
SI-201B	SI-216
SI-604B	SI-219A
SI-602B	SI-135A
SI-201A	SI-407A
SI-1071B	SI-405A
SI-108B	SI-133A
SI-109B	SI-138A
SI-410B	SI-226B
SI-122B	SI-244
SI-124B	SI-332B
SI-125B	SI-330B
SI-203A	SI-336B
SI-207A	

REFERENCES

1. Wesley, D. A., T. R. Kipp, D. K. Nakaki, and H. Hadidi-Tamjed, ***Pressure Dependent Fragilities for Piping Components - Pilot Study on Davis-Besse Nuclear Power Station***, prepared for EG&G Idaho, Inc. by ABB Impell Corporation, September 1990.

2. Harvey, P. D. Ed., ***Engineering Properties of Steel***, American Society for Metals, Metals Park, Ohio, 1985.

3. Weiss, V. and J. G. Sessler, Eds., ***Aerospace Structural Metals Handbook, Vol. I: Ferrous Alloys***, ASD-TDR-67-741, Air Force Materials Laboratory, Wright-Patterson Air Force Base, Ohio, March 1963.

4. Manjoine, M. H., ***Ductility Indices at Elevated Temperature***, J. Engineering Materials and Technology, Trans. ASME, Vol. 97, Series H, No. 2, 1975 pp. 156-161.

5. ***Metals Handbook, Vol. 1, Properties and Selection: Iron and Steel***, 8th Ed., American Society for Metals, Metals Park, Ohio, 1961.

6. General Torquing and Detensioning, Waterford 3 SES, Plant Operating Manual, Procedure No. MM-06-011, Rev. 4.

7. ***Response to INEL/USNRC Information Request, Bolt Type to Line Number from RWSP to LPSI Pump Suction to the MOV Isolation Valve***, Transmittal from Entergy Operations, Inc., to Dana Kelly, INEL, February 13, 1991.

8. ***Algor Finite Element System***, Algor Interactive Systems, Inc., Pittsburgh, PA, 1989.

9. Bazergui, A. and L. Marchand, ***PVRC Milestone Gasket Tests - First Results, Bulletin 292***, Welding Research Council, New York, NY, February 1984.

10. Bazergui, A., L. Marchand, and H. Raut, ***Development of A Production Test Procedure for Gaskets Bulletin 309***, Welding Research Council, New York, NY, November 1985.

11. Bazergui, A., L. Marchand, and H. Raut, ***Further Gasket Leakage Behavior Trends, Bulletin 325***, Welding Research Council, New York, NY, July 1987.

12. Bazergui, A., ***Short Term Creep and Relaxation Behavior of Gaskets, Bulletin 294***, Welding Research Council, New York, NY, May 1984.

13. MIL-G-21032E, ***Military Specification for Metallic-Asbestos, Spiral Wound Gaskets***, through Amendment 2, 18 May 1979.

NRC FORM 335 (2-89) NRCM 1102 3201, 3202

U.S. NUCLEAR REGULATORY COMMISSION

BIBLIOGRAPHIC DATA SHEET

(See instructions on the reverse)

1. REPORT NUMBER (Assigned by NRC, Add Vol., Supp., Rev., and Addendum Numbers, if any.)

NUREG/CR-5745
EGG-2650

2. TITLE AND SUBTITLE

Assessment of ISLOCA Risk-Methodology and Application to a Combustion Engineering Plant

3. DATE REPORT PUBLISHED

MONTH	YEAR
April	1992

4. FIN OR GRANT NUMBER

B5699

5. AUTHOR(S)

D. L. Kelly
J. L. Auflick
L. N. Haney

6. TYPE OF REPORT

Technical

7. PERIOD COVERED (Inclusive Dates)

8. PERFORMING ORGANIZATION – NAME AND ADDRESS (If NRC, provide Division, Office or Region, U.S. Nuclear Regulatory Commission, and mailing address; if contractor, provide name and mailing address.)

EG&G Idaho, Inc.
Idaho Falls, ID 83415

9. SPONSORING ORGANIZATION – NAME AND ADDRESS (If NRC, type "Same as above"; if contractor, provide NRC Division, Office or Region, U.S. Nuclear Regulatory Commission, and mailing address.)

Division of Safety Issue Resolution
Office of Nuclear Regulatory Research
U.S. Nuclear Regulatory Commission
Washington, D.C. 20555

10. SUPPLEMENTARY NOTES

11. ABSTRACT (200 words or less)

Inter-system loss-of-coolant accidents (ISLOCAs) have been identified as important contributors to offsite risk for some nuclear power plants. A methodology has been developed for identifying and evaluating plant-specific hardware designs, human factors issues, and accident consequence factors relevant to the estimation of ISLOCA core damage frequency and risk. This report presents a detailed description of the application of this analysis methodology to a Combustion Engineering plant.

12. KEY WORDS/DESCRIPTORS (List words or phrases that will assist researchers in locating the report.)

Inter-system loss-of-coolant accident
V-sequence
probabilistic risk assessment
core damage frequency

13. AVAILABILITY STATEMENT

Unlimited

14. SECURITY CLASSIFICATION

(This Page)
Unclassified

(This Report)
Unclassified

15. NUMBER OF PAGES

16. PRICE

NRC FORM 335 (2-89)

UNITED STATES
NUCLEAR REGULATORY COMMISSION
WASHINGTON, D.C. 20555

OFFICIAL BUSINESS
PENALTY FOR PRIVATE USE, $300

SPECIAL FOURTH-CLASS RATE
POSTAGE AND FEES PAID
USNRC
PERMIT NO. G-67

I2055513953I 1 1AN1R511SIPM
US NRC-OADM
DIV FOIA & PUBLICATIONS SVCS
TPS-PDR-NUREG
P-211
WASHINGTON DC 20555